ASPECTS OF PHENOMENOLOGY AND COSMOLOGY IN HETEROTIC M-THEORY

Rehan Deen

A DISSERTATION
in
Physics and Astronomy

Presented to the Faculties of the University of Pennsylvania
in
Partial Fulfillment of the Requirements for the
Degree of Doctor of Philosophy
2018

Supervisor of Dissertation

Burt A. Ovrut
Professor of Physics

Graduate Group Chairperson

Joshua R. Klein
Professor of Physics

Dissertation Committee:
Burt A. Ovrut, Professor of Physics
Justin Khoury, Professor of Physics
I. Joseph Kroll, Professor of Physics
Jonathan J. Heckman, Assistant Professor of Physics
Tom C. Lubensky, Christopher H. Browne Distinguished Professor of Physics

To my Mother, who made everything possible
And
To the memory of my Father

Acknowledgments

My work has been supported in part by DOE contract No. DE-SC0007901. I also wish to acknowledge a number of people who have assisted me throughout the course of my studies at the University of Pennsylvania.

First, I am deeply indebted to Autin Purves, whose computational framework for examining the B-L MSSM was central to the study of string thresholds and for the examining the phenomenology of high scale SUSY breaking. I am also indebted to Yong Cai, with whom the analysis of reheating in the Sneutrino-Higgs inflation model was carried out, and who undertook many of the necessary numerical computations. The exploration of effective brane actions was inspired in part by discussions with Anna Ijjas and Paul Steinhardt. Though the resulting work is not presented in this thesis, I have had many useful and enlightening conversations with Ling Lin regarding the construction of vector bundles on Calabi-Yau manifolds.

I would also like to thank a number of people for making my time at Penn an enjoyable one, including Ian Coulter, Nuno Barros, Eric Marzec and David Rivera. I am appreciative of stimulating discussions with Ben Elder at the early stages of my studies. I would be remiss not to mention the administrative help I have received from members of the department office, with special thanks to Millicent Minnick.

I am grateful for the continous support and encouragement of my advisor, Burt Ovrut, as well as for his infinite patience. His physical insight and clarity of thought will always be an example to me, and it has been a pleasure to have been his student.

Finally, I cannot express in words the thanks I owe to my family, who have trusted and believed in me from my youth.

ABSTRACT

ASPECTS OF PHENOMENOLOGY AND COSMOLOGY IN HETEROTIC M-THEORY

Rehan Deen
Burt Ovrut

We present an exploration of models of particle phenomenology and cosmology which arise from the $E_8 \times E_8$ heterotic string theory and its strong-coupled limit, known as heterotic M-theory. We first re-examine the B-L MSSM, a realistic supersymmetric extension of the Standard Model, in a more generic region of moduli space. We modify our previous analysis by demanding that the mass scales of the two Wilson lines be simultaneous, and we show that the resulting absence of gauge unification is consistent with string threshold corrections. Using these results, we build a realistic model of inflation where a scalar constructed from the fields of the B-L MSSM is taken to be the inflaton. The subsequent period of reheating is then investigated in detail. Finally, it is known that M-theory admits five-branes, which wrap holomorphic curves upon dimensional compactification. We construct an effective $N = 1$ supersymmetric action to describe the world-volume theory of the resulting three-branes, which live in the bulk space of heterotic M-theory.

Contents

List of Tables

List of Figures

Chapter 1

Introduction

1.1 Introduction

The discovery of the Higgs boson by the ATLAS and CMS groups at the LHC in 2012 marked the completion of half a century's worth of progress in the quest to understand the fundamental interactions which govern our universe. The so-called Standard Model of particle physics, with its three generations of matter and three gauge bosons of $SU(3)_C \times SU(2)_L \times U(1)_Y$, is now known to be accompanied by a scalar doublet H, which serves to break the electroweak interaction to $U(1)_{EM}$ at a scale of roughly ~ 100 GeV. To date, the Standard Model (SM) appears to be a valid description up to scales of ~ 1 TeV, i.e. no new physics has so far turned up at this energy scale.

This is puzzling. Though it is a tremendously useful description of the world, the Standard Model is in some ways unsatisfactory. Why are three generations of matter present? Why do the couplings of the gauge groups almost – but not quite – unify at some high scale? Why are there so many free parameters in the theory? These questions arise before one even addresses the elephant in the room: gravity. If one is to have a truly unified description of the interactions in our universe, it is natural to consider gravity on a level footing with interactions of the SM. However, even at the semi-classical level (where gravity is treated classically and the SM fields are treated quantized), we find problems. Why, if there is no new physics beyond the SM, is the scale of electroweak symmetry breaking $M_{\rm EW}$ so much smaller than the scale associated with gravitational interactions, M_P? Since gravity is universal, why is the observed value of the cosmological constant so much smaller than the value one expects from the SM vacuum energy? These questions have been raised before the Higgs discovery. Their persistence is both frustrating and inspiring, as it is clear that if there exists a consistent answer to all of them, its elegance and structure must be worthy of these years in the wilderness.

Though many of these problems have been individually addressed, a consistent framework in which solutions may arise is that of string theory. Originally constructed as a model of the strong interaction, two furious bursts of activity in the 1980s and 1990s have revealed a web of theories which can describe can provide a unified description of gravity and gauge interactions. Building on the key ingredients of Kaluza-Klein theory and supersymmetry, rich mathematical structures arise, which are highly constraining, yet have the potential to explain the issues raised above. String theory is not even just a theory about strings, with extended branes also becoming dynamical objects.

In the previous decade, progress has been made in obtaining the particle spectrum of the SM from one of the fundamental superstring theories, the $E_8 \times E_8$ heterotic string, compactified on a smooth Calabi-Yau manifold. This has been shown to give rise to a low-energy phenomenology which is consistent with LHC constraints. The construction of the SM spectrum addresses the number of generations of matter, and the origin of the low-energy gauge group, and (in principle) previously free parameters are now determined by algebro-geometric constraints – though in practice such calculations reach technical difficulties. It is now interesting to see if this particular string construction can address other problems in phenomenology and cosmology, and this is the general focus of the work discussed in this thesis.

1.2 The B-L MSSM and Simultaneous Wilson Lines

Within the context of the heterotic superstring and heterotic M-theory [141, 140, 139, 72], there have been a number of vacuum states whose four-dimensional low energy effective field theory [162] has the exact spectrum of the Minimally Supersymmetric Standard Model (MSSM)–with or without right-handed neutrino chiral multiplets–and, to prohibit rapid proton decay, contains R-parity [96, 148, 147]–either as a discrete symmetry or as a subgroup of an anomaly free $U(1)$ extension of the standard model gauge group [134, 13, 12, 14, 89, 95, 11, 108, 152, 149]. One such vacuum was presented in [37, 36, 7, 8] and will be referred to as the B-L MSSM . This is only the first step in finding a realistic heterotic string vacuum. Any such theory must also also be compatible with all presently observed low-energy phenomenology; that is, it must spontaneously break electroweak (EW) symmetry at the observed scale, must be compatible with the Higgs mass of ~ 125 GeV [1, 48], have all sparticle masses above the present observational lower bounds and–assuming R-parity is contained in an additional $U(1)$ symmetry–spontaneously break that Abelian group with an associated gauge boson mass in excess of the present experimental lower bound.

In a series of papers [159, 146, 145, 160, 161], the B-L MSSM was examined in detail–using a random statistical sampling of the initial set of soft supersymmetry (SUSY) breaking parameters–and the results confronted with these phenomenological requirements. It was shown, within *a restricted region of the compactification moduli space*, that the B-L

MSSM easily passed each of these requirements for a large and basically uncorrelated set of initial conditions.

Furthermore, this analysis led to a series of low energy predictions–for example, directly relating the lightest stop decay channels and branching ratios to the neutrino mass hierarchy and mixing angles–thus linking LHC experimental results to neutrino measurements. That is, the *B-L* MSSM is a possible candidate for a phenomenologically acceptable theory of the real world–a statement that will be directly testable as its structure and predictions are confronted with upcoming data from the LHC, neutrino experiments and cosmological observations.

However, despite these successes, the restricted region of moduli space is slightly unnatural, in the sense that it corresponds to compactifying the extra dimension on a Calabi-Yau manifold with "holes" that have different sizes. That is, the two-cycles associated with the symmetry breaking Wilson lines[1] differ in size by approximately an order of magnitude. Though this leads to the useful feature of unifying the gauge couplings at the standard GUT scale, our Calabi-Yau manifold is "non-generic". Further, raising the mass scale associated with supersymmetry breaking worsens this problem, as we must increase the size of the split if we continue to demand correct electroweak symmetry breaking. This can be an obstacle when considering possible models of cosmology constructed from the *B-L* MSSM .

We can avoid this problem by taking the mass scale associated with the two-cycles to be the same – that is, consider the scenario of simultaneous Wilson lines. The result is that the gauge couplings no longer unify but their values at the old unification scale are split by amount Δ. This splitting can be interpreted as arising from so-called "string threshold corrections", which, at least in the weakly-coupled heterotic string, arise due to heavy states on the genus-one string worldsheet. We recall that in string theory, the gauge couplings and Newton's constant unify at the string unification scale, which is typically lower than the four-dimensional Planck scale. By a similiar statistical examiniation to previous work [159, 146, 145, 160, 161], we determe the size of these thresholds and show that their values are consistent with the notion of string unification.

1.3 Inflation in the *B-L* MSSM

In typical inflationary models [107, 166, 138, 4][2], a (single) scalar field is used to generate an accelerated expansion in the early history of the universe as it traverses a path in field space, subsequently decaying into matter as it oscillates about its final vacuum state. Such an expansion was first proposed to solve a number of problems in early universe cosmology.

[1] As we will describe later, the *B-L* MSSM includes two Wilson lines which act like adjoint Higgses to break $SO(10)$ to the SM gauge group $SU(3)_C \times SU(2)_L \times U(1)_Y$

[2] See [136] for more details on the early literature of the inflationary scenario.

For instance, an accelerated phase can sufficiently dilute the effect of any primordial spatial curvature, explaining the remarkable flatness of the universe observed today. In order for inflation to take place– that is, for the scale-factor of a Friedman-Robertson-Walker metric $a(t)$ to obey $\ddot{a}(t) > 0$, the scalar field's kinetic energy is subdominant to the potential. The "chaotic" inflation scenario takes the scalar field to be displaced away from the minimum of the potential (which is usually taken to have vanishing or negligible vacuum energy) and "slowly rolls" towards the potential. The Hubble parameter H remains roughly constant until the very end of the inflaton's journey in field space. Defining the so-called slow-roll parameters ϵ and η,

$$\epsilon = \frac{1}{2M_P^2}\left(\frac{V'}{V}\right)^2 \qquad \eta = \frac{1}{M_P^2}\frac{V''}{V}, \tag{1.1}$$

where the derivatives are taken with respect to the inflaton field, it can be shown that as long as

$$\epsilon, |\eta| \ll 1\,, \tag{1.2}$$

inflation takes place, and one can define the end of inflation to occur when either parameter $= 1$.

The introduction of Higgs inflation [27, 23, 26, 17, 24, 25], emphasized the important idea that the inflaton might well be a fundamental scalar field in the Standard Model. In the non-supersymmetric case, this could only be the neutral Higgs scalar. A careful analysis of this possibility led to the result that an acceptable theory of inflation could potentially arise in this context–but only at the cost of assuming some unnatural features. For example, the square of the Higgs magnitude must necessarily be coupled to the curvature scalar in the Lagrangian density with an unnaturally large coupling parameter. Generalizing this idea to the supersymmetric standard model (MSSM), and some variants thereof, potentially extends this idea by introducing a large number of scalar fields into the theory, a subset of which might play the role of the inflaton. Although at first seeming promising, these models [78, 91, 115, 28] continued to exhibit further problems. In particular, it now becomes very difficult to obtain a potential for the inflaton that is stable with respect to the other field directions in field space. That is, the inflating field usually "rolls off" into another scalar direction, ending the inflationary period far short of the required 60 e-foldings.

Fortunately, as we will show, we can avoid this difficulty for an inflationary model constructed within the B-L MSSM . The reason for this is relatively straightforward. The potential energy of the scalar field has three contributions; the D-term potential $V_D = \frac{1}{2}\sum_a D_a^2$, the F-term potential V_F and contributions from the so-called soft supersymmetry breaking terms V_{soft}. As will be discussed below, the F-term potential essentially vanishes after the beginning of inflation. The essential feature of the B-L MSSM is that, for a precise combination–denoted by ϕ_1–of the right-handed sneutrino, the left-handed sneutrino and the neutral up Higgs field, all D_a contributions also vanish, rendering $V_D = 0$. This fact, which is due to the existence the right-handed sneutrino, lowers the entire D-flat potential into a "valley" that is stable[3], preventing the inflaton from rolling off into any other scalar direction.

As we will show, this particular potential can lead to an inflationary model which is consistent with Plank2015 cosmological data. This inflationary theory, which we have named "Sneutrino-Higgs inflation" was developed in detail in [63]. The model bears some similarity to the so-called "no scale" supergravity theory developed in a different context in [57, 83, 82, 79]. However, the distingushing feature of Sneutrino-Higgs inflation in the B-L MSSM is its relation to the observed low energy particle physics phenomenology, as we will show below. Central to this model is the raising of the soft SUSY breaking parameters, which are now of order 10^{13} GeV. Our previous discussion of simultaneous Wilson lines in the B-L MSSM becomes relevant, as we can now allow for upersymmetry breaking at this much higher scale. We show that this is consistent with electro-weak symmetry breaking and the measured Higgs mass.

Additionally, we move beyond the purely inflationary epoch and study the precise theory of reheating of the Sneutrino-Higgs theory. The subject of reheating in inflationary models has been studied extensively in [5, 2, 168, 132, 123, 133, 51, 20, 6, 9, 81][4]. As we will show, in the Sneutrino-Higgs theory, this reheating epoch is completely amenable to exact computation. The end result is that this theory also reheats in a technically determined manner and appears to be completely acceptable physically.

1.4 Brane Actions

As we will see, using right-handed sneutrino scalars instead of the Higgs boson as an inflaton within the context of the $N = 1$ supersymmetric B-L MSSM theory, can lead to a viable model of supersymmetric inflation. However, as with most inflationary scenarios, it suffers from the usual initial value and multiverse problems [119, 117], which we do not address here.

Generically, it appears natural to demand that any realistic theory of cosmology should 1) contain the standard model of particle physics, 2) naturally introduce the scalar or scalars associated with early universe dynamics and 3) imply the exact scalar self-couplings, as well as their explicit coupling to dynamical four-dimensional gravitation. While we

[3] Up to very small field displacements, as we will show.

[4] In this thesis, we will not explore so-called "pre-heating", but instead focus on the perturbative decay of the inflaton.

have tried to address these constraints in the model of Sneutrino-Higgs inflation, let us instead consider a different class of theories: the so-called "bouncing" theories of cosmology [55, 42, 31, 30, 131, 129, 77, 116, 118]. In these, a contracting Friedman-Robinson-Walker (FRW) geometry can bounce smoothly through the Big Bang to the present expanding spacetime. Natural versions of bouncing cosmologies should also satisfy criteria 1), 2) and 3). However, a fourth criterion must be be added; namely that 4) the theory naturally allow for the violation of the "null energy condition" (NEC). This is necessary for the derivative of the Hubble parameter $\dot{H}$ to be > 0 (if we imagine the stress-energy tensor to be sourced by a single component fluid), which is the statement that the universe has moved from a contracting to an expanding phase.

It is well-known that this fourth condition can naturally manifest itself in worldvolume theories of 3+1–dimensional branes. For example, it was shown in [54, 109] that the worldvolume theory of a three-brane embedded in an AdS_5 bulk space can, for the appropriate choice of coefficients, violate the NEC. It follows that co-dimension one bosonic branes embedded in various five-dimensional bulk spaces are potentially of interest in theories of cosmology. The generic form for the worldvolume action of such branes, subject to the restriction that the associated equations of motion have at most two derivatives, has been presented in[101, 100] for the maximally symmetric bulk spaces AdS_5, dS_5 and M_5. In these cases, the three-brane Lagrangians are potentially interesting in their own right. For example, the 3+1–dimensional bosonic brane embedded in AdS_5, when expanded into terms each containing the same number of derivatives, exactly reproduces the so-called "conformal Galileons" originally presented in [76, 155, 60]. These Galileon theories exhibit interesting non-linearly realized symmetries, inherited from the maximally symmetric bulk spaces used in their construction – e.g., the conformal Galileons are invariant under a specific set of transformations which are combined into $SO(4, 2)$, the symmetry group of AdS_5.

These theories, however, are not "naturally" associated with the standard model of particle physics. That is, these theories violate conditions 1) and 2) specified above. Additionally, theories of branes of varying dimensions embedded in higher-dimensional bulk spaces arise most naturally within the context of supersymmetric string theory and M-theory. Furthermore, whereas the spectrum and interactions of particle physics must simply be added in an ad hoc manner to bosonic cosmological scenarios, it is well-known that the Standard Model can arise as the spectrum of specific superstring vacua that simultaneously include various types of branes. A very concrete example is, of course, heterotic M-Theory. Naturally embedded within the five-dimensional bulk space are 3+1 branes (five-branes wrapped on a holomorphic curve), whose existence is required for anomaly cancellation and, hence, consistency [144]. In addition to this natural setting for particle physics and 3+1 brane worldvolume theories, there is a second, very significant, new ingredient. That is, these vacua, prior to possible spontaneous symmetry breaking, are all $N = 1$ supersymmetric.

These realistic vacua of supersymmetric three-branes embedded in heterotic M-theory led to the postulation of the "Ekpyrotic" theory of early universe cosmology [126]. In this theory, a relativistic three-brane embedded in the five-dimensional bulk space is attracted toward the observable wall via a potential energy, which arises from the exchange of M-theory membranes. This potential was explicitly computed in [137] and found to be a steep, negative exponential [5]. Hence, in this phase, the universe is contracting. The scalar fluctuations of the brane modulus evolving down this potential produce two-point quantum fluctuations that are nearly scale invariant. As discussed in [125], under certain conditions the NEC can be violated and the universe bounces to the expanding spacetime that we presently observe. Furthermore, it was shown in [21] that these fluctuations can pass through the bounce with almost no distortion and, hence, are consistent with observational data from the CMB.

An effective field theory for the 3+1 brane modulus in the exponential potential was constructed in [41]. However, the complete $N = 1$ supersymmetric worldvolume action of the three-brane has never been explicitly constructed. A first attempt to do this was carried out within the context of heterotic string theory in [10, 163]. However, based on previous non-supersymmetric work [46, 29], this was done by modelling the three-brane as a solitonic kink of a chiral superfield in the five-dimensional bulk space. Although some of the geometric terms, and particularly a computation of their coefficients, were found by these methods, the general theory of an $N = 1$ supersymmetric three-brane worldvolume theory was far from complete.

We present in this thesis another attempt to construct an $N = 1$ supersymmetric worldvolume theory for the three-brane. This time we use the formalism of the Galileon theories, adapted to the geometry of heterotic M-theory. By this construction, we end up with Lagrangians that give rise to second order equations of motion, which we then re-formulate in a well-motivated derivative expansion. The resulting theories are not supersymmetric, but we then extend them to $N = 1$ supersymmetry and supergravity by well-established means [171]. Interestingly, we find that these Lagrangians, which by construction involve terms that are higher-derivative, have an interesting new property. The auxiliary fields introduced to complete the various supersymmetry multiplets can no longer be integrated out, but instead become dynamical objects themselves. We do not show here whether we arrive at a viable cosmology with NEC violation, but by demonstrating that conditions 1), 2) and 3) are satisfied, and in principle being able to satisfy condition 4) in the manner of [54, 109], we hope to drive further work on this subject.

[5] Within this context, the lowest order kinetic energy for the 3+ 1 brane position modulus was presented in [65].

1.5 Outline

This thesis is structed as follows. First, we will give a very brief outline of heterotic M-theory in chapter 2, with the details limited to be relevant to the work which follows. Next, in chapter 3, we go into detail about the B-L MSSM in the case where Wilson lines are taken to be simultaneous, which is based on [64]. This scenario is more generic than that which has previously been investigated, and allows us to raise the supersymmetry breaking scale much higher than is usually considered. This allows to explore the theory of Sneutrino-Higgs inflation in chapter 4, which is based on work pursued in [63] and [43]. Finally, we discuss the supersymmetric world-volume actions of branes in chapter 5, which draws on [61] and [62]. We also include four appendices which add extra details to the work discussed in each of the chapters.

Chapter 2

Heterotic M-theory

2.1 The Heterotic String and M-theory

The heterotic string is so named since it is a hybrid of the closed bosonic string and the right-moving sector of superstring theory. The theory is tachyon free and has an effective description as a ten-dimensional Lagrangian that is $N = 1$ supersymmetric in spacetime, i.e., it is invariant under the action of 16 real supercharges, in contrast to the type II theories which are invariant under 32 supercharges.

One notices the mismatch between the 26 dimensions needed to make the bosonic string consistent, and the 10 dimensions required of the superstring. To be brief, the additional 16 dimensions of the bosonic sector are compactified on a torus. For reasons we will not discuss here, this torus must have the further property in that, viewed as $\mathbb{R}^{16}/\Gamma$, the 16-dimensional lattice Γ must be self-dual [106]. This property is highly restrictive, and in fact only two such lattices are allowed. The resulting isometries of the torus then give rise to two possible gauge symmetries in the ten-dimensional effective action: $SO(32)$[1] or $E_8 \times E_8$. Here, we will focus on the $E_8 \times E_8$ case.

To lowest order in the expansion of the heterotic string in the paramater α', we have an

[1]More precisely, $Spin(32)/\mathbb{Z}_2$

effective ten-dimensional Lagrangian given by[2] [104] :

$$
\begin{aligned}
e^{-1}\mathcal{L} \;=\;& -\frac{1}{2\kappa^2}R - \frac{1}{4g^2\phi}\sum_{l=1,2}\mathrm{tr}(F^{(l)\,2}_{MN}) - \frac{1}{\kappa^2}\left(\frac{\partial\phi}{\phi}\right)^2 - \frac{3\kappa^2}{8g^4\phi^2}H^2_{MNP} \\
& -\frac{1}{2}\bar{\psi}_M\Gamma^{MNP}\nabla_N\psi_P - \frac{1}{2}\bar{\lambda}\Gamma^M\nabla_M\lambda - \frac{1}{2}\sum_{l=1,2}\mathrm{tr}\left(\bar{\chi}^{(l)}\Gamma^M\nabla_M\chi^{(l)}\right) \\
& -\frac{1}{\sqrt{2}}\bar{\psi}_M\Gamma^N\Gamma^M\lambda\left(\frac{\partial_N\phi}{\phi}\right) + \frac{\kappa^2}{16g^2\phi}\sum_{l=1,2}\mathrm{tr}\left(\bar{\chi}^{(l)}\Gamma^{MNP}\chi^{(l)}\right)H_{MNP} \\
& -\frac{\kappa}{4g\sqrt{\phi}}\sum_{l=1,2}\mathrm{tr}\left[\bar{\chi}^{(l)}\Gamma^M\Gamma^{NP}(\psi_M + \frac{\sqrt{2}}{12}\Gamma_M\lambda)F^{(l)}_{NP}\right] \\
& +\frac{\kappa^2}{16g^2\phi}\left(\bar{\psi}_M\Gamma^{MNPQR}\psi_R + 6\bar{\psi}^N\Gamma^P\psi^Q - \sqrt{2}\bar{\psi}_M\Gamma^{NPQ}\Gamma^M\lambda\right)H_{NPQ} \\
& +\text{higher fermion terms}
\end{aligned}
\tag{2.1}
$$

The index $l = 1, 2$ labels each E_8 group. The fermions ψ_M, λ and $\chi^{(l),a}$ are respectively the gravitino, dilatino and gauginos of E_8. The field strength $F^{(l)}_{MN} = F^a_{MN}T^{(l),a}$, where the T^a are generators of each E_8 factor, and

$$F^a_{MN} = \partial_M A^a_N - \partial_N A^a_M + gf^a_{\ bc}A^b_M A^c_N \tag{2.2}$$

The three-form H_{MNP} is the field strength associated with the heterotic B-field, and ω_L, ω_Y are the Lorentz and Yang-Mills Chern-Simons forms:

$$
\begin{aligned}
H &= dB + \omega_L - \omega_Y \\
dH &= \mathrm{tr}R\wedge R - \mathrm{tr}F\wedge F
\end{aligned}
\tag{2.3}
$$

Of course, for a phenomenologically realistic model of our universe, this ten-dimensional description must be reduced to one which describes the observed four uncompactified dimensions and gives rise to the correct standard model matter spectrum. It is particularly useful to posit that the dimensionally reduced theory has $4d, N = 1$ supersymmetry, both to resolve experimental difficulties and in order to greatly simplify the technical framework of the reduction. Of course, supersymmetry must be broken as it is not observed at very low momenta but we will leave this mechanism unspecified as it will not be relevant to our present discussion.

Although both the ten- and (eventually) four-dimensional theories are $N = 1$ supersymmetric, in the former case, this involves invariance under the action of 16 real supercharges,

[2] We drop so-called Green-Schwarz terms in this expression for clarity.

while the later involves invariance under the action of four real supercharges. The supercharges of the four-dimensional theory are a subset of the 16 acting "upstairs", and so we see compactification ansatz must be chosen in such a ways as to preserve precisely these in the "downstairs" picture. To see this, and other conditions that are necessary to preserve $N=1$ supersymmetry in four dimensions, we must examine the conditions which are necessary to preserve $N=1$ supersymmetry in *ten* dimensions. It is sufficient [104] to look at the variations of the fermions in (2.1).

The variations of the ten-dimensional gravitino, dilatino and gaugino are:

$$\begin{aligned}
\delta_\eta \psi_M &= \frac{1}{\kappa}\nabla_M \eta + \frac{\kappa}{32 g^2 \phi}\left(\Gamma_M^{\ NPQ} - 9\delta_M^N \Gamma^{PQ}\right)\eta H_{NPQ} + \text{fermion terms} \\
\delta_\eta \lambda &= -\frac{1}{\sqrt{2}\phi}(\Gamma\cdot\partial\phi)\eta + \frac{\kappa}{8\sqrt{2}g^2\phi}\Gamma^{MNP}\eta H_{MNP} + \text{fermion terms} \\
\delta_\eta \chi^a &= -\frac{1}{4g\sqrt{\phi}}\Gamma^{MN}F^a_{MN}\eta + \text{fermion terms}
\end{aligned} \tag{2.4}$$

For the moment, we will drop the label (l) and focus on a single E_8 factor in the our analysis. In order that supersymmetry be preserved on a given compactification ansatz, all three variations in (2.4) must vanish.

Following [104], we will compactify our ten-dimensional theory on the product space $M^4 \times X$, where M^4 is four-dimensional Minkowski space, and X is a compact six-dimensional manifold. In addition, we will take

$$H = d\phi = 0 \tag{2.5}$$

which simplifies (2.4) [3]. Pure fermion terms are taken to vanish. Requiring that four-dimensional Poincaré invariance is preserved so that terms with a μ index are assumed to

[3]Condition (2.5) is actually restrictive given the definition of H in equation (2.3). Setting $H=0$ implies that we are taking the so-called "standard embedding", i.e. identifying the gauge connection with the spin connection. This leads to a holomorphic $SU(3)$ bundle. Since the commutant of $SU(3)$ in E_8 is E_6, this leads to an E_6 gauge sector in the four-dimensional effective theory. To construct more general bundles of different rank, leading to low energy gauge groups like $Spin(10)$, one must use the so-called "non-standard embedding". In this case, H is not taken to vanish, but then (2.4) must then be examined order by order in α'/R^2, where R is the average radius of the compactified space X. As we will shortly see, in the case of the standard embedding (2.4) will reduce to the Calabi-Yau condition for the internal space and the Hermitian Yang-Mills equations for the internal gauge connection. It can be shown that these equations still need to be satisfied even in the case of non-standard embeddings, though we will not demonstrate the analysis here - see for instance, [104].

vanish, we are left with

$$\begin{aligned}\delta_\eta \psi_\alpha &= \frac{1}{\kappa}\nabla_\alpha \eta \\ \delta_\eta \lambda &= 0 \\ \delta_\eta \chi^a &= -\frac{1}{4g\sqrt{\phi}}\Gamma^{\alpha\beta}F^a_{\alpha\beta}\eta \end{aligned} \tag{2.6}$$

The second equation automatically satisfies the condition for supersymmetry, while we must analyze the first and third terms in (2.6). The first equation in (2.6) can be shown to lead to condition that the compact six-dimensional manifold satisfy the so-called Calabi-Yau condition. That is, X is a Kähler manifold with vanishing first Chern class, $c_1(X) = 0$– this condition is equivalent to the manifold admitting a Ricci flat metric. To see that this has to be the case, the vanishing of the right hand side of the gravitino variation in (2.6) is tells us that we must allow for the non-trivial convariantly constant spinors on X, since η is a spinorial parameter and

$$\nabla_\alpha \eta = 0 \tag{2.7}$$

defines a convariantly constant spinor on X. For a six-dimensional manifold, $non-trival$ solutions to equation (2.7) exist if the holonomy group is reduced from the most general case of $SO(6)$. A manifold with the general holonomy group will have no covariantly constant spinors and can be shown not to preserve any supercharges upon compactification, leading to non-supersymmetric vacuum in four dimensions. Using the fact that the double cover of $SO(6)$ is $SU(4)$, it can be shown that to preserve exactly $N = 1$ supersymmetry in four dimensions, we must restrict ourselves to manifolds with $SU(3)$ holonomy group. Such a manifold can be shown to have vanishing first Chern class $c_1(X) = 0$ if it is Kähler. Kähler manifolds with $SU(3)$ holonomy admitting a Ricci flat metric are known as Calabi-Yau manifolds, after Calabi, who conjectured that a manifold of $SU(3)$ holonomy would have a unique metric with vanishing first Chern class, and Yau, who proved this conjecture.

Let us now focus on the third equation in (2.4). Setting $H = 0$, $\phi =$ constant, we find

$$\begin{aligned}\delta_\eta \chi^a &= -\frac{1}{4g\sqrt{\phi}}\Gamma^{\alpha\beta}F^a_{\alpha\beta}\eta \\ &= -\frac{1}{4g\sqrt{\phi}}\left(\Gamma^{ij}F^a_{ij} + \Gamma^{\bar{i}\bar{j}}F^a_{\bar{i}\bar{j}} + 2\Gamma^{i\bar{j}}F^a_{i\bar{j}}\right)\eta \end{aligned} \tag{2.8}$$

To set this variation to zero, we are led to the following set of equations

$$F^a_{ij} = F^a_{\bar{i}\bar{j}} = 0\,, \qquad g^{i\bar{j}}F^a_{i\bar{j}} = 0\,. \tag{2.9}$$

These are known as the Hermitian Yang-Mills equations. Finding non-trivial solutions to this set of differential equations for the gauge field A^a_α is a difficult problem which we will discuss in the next section. The first set of relations involving the purely holomorphic and anti-holomorphic part of the field strength F imply that a non-trivial solution to (2.9) involves the construction of a holomorphic vector bundle on the Calabi-Yau threefold. Thus, in order to arrive at a complete vacuum, we have to specify a Calabi-Yau manifold and then construct holomorphic vector bundles for both E_8 factors. The situation does not change for the strong-coupled case in which the the original theory is 11-dimensional.

We now briefly review some of the mathematical background that is needed in the study of string compactifications. For full details, we refer the reader to [104, 44, 45, 114, 105].

2.1.1 Calabi-Yau Manifolds

A Calabi-Yau manifold is a complex n-dimensional manifold which admits a Ricci flat metric, or alternatively whose first Chern class $c_1(X) = 0$. An elliptic curve or complex torus is an example of a one-dimensional (i.e. it has two real dimensions) Calabi-Yau manifold. The topologically unique two-dimensional Calabi-Yau manifold is known as the $K3$ surface. We will be interested in three-dimensional Calabi-Yau manifolds (threefolds), and we describe here how these can be constructed. First, we note that that although we can the theorem of Calabi and Yau guarantees a Ricci flat metric exists for a complex threefold with $SU(3)$ holonomy, in general one cannot write an explicit metric for these manifolds. Instead, we can must rely on the techniques of algebraic geometry to explore their properties. We define first the projective space $\mathbb{P}^n$ by taking the n-dimensional complex space $\mathbb{C}^{n+1}$, remove the origin and identify all the points which lie along complex lines through the origin. That is:

$$\mathbb{P}^n = (\mathbb{C}^{n+1} \setminus \{0\})/\mathbb{C}^* \,. \tag{2.10}$$

In each $\mathbb{P}^n$, we can define $n+1$ homogeneous coordinates $(z^1 : z^2 : \cdots : z^{n+1})$, where the z^i are not allowed to be simultaneously zero. We can define submanifolds in this complex space by looking athe vanishing locus of polynomials in the z^i. For instance, in the space $\mathbb{P}^4$ the vanishing of the polynomial

$$P = (z^1)^2 + (z^2)^2 + (z^3)^2 + (z^4)^2 + (z^5)^2 \tag{2.11}$$

defines a codimension one hypersurface Q which is actually a complex manifold. In fact, this is the so-called "Fermat quintic", a Calabi-Yau threefold. With this simple example we can illustrate how one explores the various properies of Calabi-Yau manifolds in general.

- We can perform a number of infinitesimal deformations of the polynomial (2.11) which preserve the complex structure of the manifold defined by the vanishing of P. These are characterized by a set of parameters known as the complex structure moduli, and their number is denoted by $h^{2,1}(Q)$. The notation is no accident - it is in fact the dimension of the cohomology group $H^{2,1}(Q)$. There are 101 such moduli, and these moduli appear as scalars in the four-dimensional effective action. Another set of parameters, the Kähler moduli, are denoted by $h^{1,1}(Q)$ (as they count the dimension of the cohomology group $H^{1,1}(Q)$) and are also relevant to our discussion. These moduli count the number of deformations which preserve the Kähler structure of the manifold $P = 0$.

- There is a freely acting $\mathbb{Z}_5 \times \mathbb{Z}_5$ discrete symmetry of the coordinates z^i. If we take the manifold and identify the points which are transformed by this symmetry ("modding" out the action of $\mathbb{Z}_5 \times \mathbb{Z}_5$), we can construct a new manifold which has a non-trivial homotopy group $\pi_1 = \mathbb{Z}_5 \times \mathbb{Z}_5$. This non-trivial homotopy describes "holes" in the new manifold, and their effect in the four-dimensional effective Lagrangian is to give rise a Wilson line for each abelian factor. The Wilson lines can then break the low-energy gauge group which arises after a vector bundle is constructed.

The Calabi-Yau threefold which is of particular interest to us is the Schoen manifold which is described by the vanishing locus of two polynomials in $\mathbb{P}^1 \times \mathbb{P}^1 \times \mathbb{P}^2$. This manifold has a $\mathbb{Z}_3 \times \mathbb{Z}_3$ symmetry, which we can mod out to define a new "downstairs" manifold X. It was shown in [35, 36] that X admits a holomorphic $SU(4)$ vector bundle which after the action of the two Wilson lines, gives rise to the Standard Model gauge group and particle spectrum, with the addition of right-handed neutrinos. We will give further details about this later, including an alternative definition of the construction of X.

2.1.2 Holomorphic Vector Bundles

As discussed previously, the preservation of $N = 1$ supersymmetry in four dimensions leads to the construction of a holomorphic vector bundle over the Calabi-Yau threefold X. More precisely, one constructs the vector bundle V_i, $i = 1, 2$ for each E_8 factor, which gives rise to the observable and hidden sector spectrum respectively.

A vector bundle E over a base manifold M looks *locally* like the product space $M \times F$, where the component F is a vector space. For an open set $U_\alpha \subset M$ we have the local trivialization of E as (p, f), where $p \in U_\alpha$, $f \in F$. We can define a projection operator $\pi : E \to M$, such that for $p \in M$, $f \in F$, $\pi : (p, f) \mapsto p$. Globally, obstructions prevent a description of E as $M \times F$. We can cover M with the open sets U_α covering M, and given two open sets U_α to U_β with overlap region $U_{(\alpha,\beta)} = U_\alpha \cap U_\beta$ via the transition functions $t_{\alpha\beta}$. Furthermore, one has the *structure group* of the vector bundle, G, which acts on the vector space F. Given a point $p \in U_{(\alpha,\beta)} \neq \emptyset$, it is required that $t_{\alpha\beta}(p) \in G$. A holomorphic vector bundle V on a complex manifold X has transition functions $t_{\alpha\beta}$ which are holomorphic. The fibre F is isomorphic to $\mathbb{C}^n$ and the bundle is said to be of "rank n" [4].

In dimensional reduction, the particle spectrum of the four-dimensional effective action consists of the zero modes of the Dirac operator on the internal Calabi-Yau space, $\not{D}_6$. The Atiyah-Singer index theorem relates the zero modes of the Dirac operator to certain cohomology groups associated withe the holomorphic vector bundle V. For instance, in the case of the heterotic Standard Models of [35, 36], where the observable vector bundle has structure group $SU(4)$, we have the decomposition of the adjoint E_8 under its maximal subgroup $SU(4) \times Spin(10)$:

$$\mathbf{248} = (\mathbf{1}, \mathbf{45}) \oplus (\mathbf{4}, \mathbf{16}) \oplus (\bar{\mathbf{4}}, \bar{\mathbf{16}}) \oplus (\mathbf{6}, \mathbf{10}) \oplus (\mathbf{15}, \mathbf{1}) \tag{2.12}$$

The fermions transforming as $(\mathbf{1}, \mathbf{45})$ representation corresponds to the gauginos of the low-energy four-dimensional gauge group, while $(\mathbf{15}, \mathbf{1})$ corresponds to fermionic partners of the "vector bundle moduli" - scalars which are singlets under the low-energy gauge group. The zero modes corresponding to each of the middle three representations of the right-hand side of (2.12) arise from the following cohomology groups:

$$H^1(X, V)\,, H^1(X, V^*)\,, H^1(X, \wedge^2 V)\,, \tag{2.13}$$

and the number of such fermions is counted by the dimension of these cohomology groups.

Hermitian Yang-Mills equations and the Donaldson-Uhlenbeck-Yau theorem

Having chosen our Yang-Mills connnection to be holomorphic – that is, we satisfy the the first relation in (2.9) – we now address the second relation in (2.9),

$$g^{i\bar{j}} F_{i\bar{j}} = 0\,, \tag{2.14}$$

where we have contracted $F^a_{i\bar{j}}$ with a generator T^a. This equation can be re-expressed in terms of differential forms in six dimensions and dualized to give

$$\omega \wedge \omega \wedge F = 0\,, \tag{2.15}$$

[4]Here, the rank is the dimension of the fibre of the vector bundle. This *should not* be confused with the rank of the Lie algebra of the associated structure group, which is also often enters these discussions. The rank of the Lie algebra is the dimension of its Cartan subalgebra, i.e. the number of commuting generators. In the literature we will often come across $SU(N)$ vector bundles, which are shorthand for rank n holomorphic vector bundles. Of course, the Lie algebra $\mathfrak{su}(N)$ has rank $N-1$.

where ω is the Kähler form on the Calabi-Yau three-fold. The above is now a special case of a more general equation,

$$\omega \wedge \omega \wedge F = 2\pi\mu \cdot \mathbf{1} \cdot d\mathrm{Vol}\,, \tag{2.16}$$

where, to begin with, μ is an arbitrary constant. We will describe (2.16) as the *general Hermitian Yang-Mills equation.*The factor dVol is needed on the RHS to match the degree of the form on the LHS. The constant μ can be found by integrating both sides of the equation to give:

$$\mu = \frac{1}{\mathrm{rk}\mathcal{V} \cdot \mathrm{Vol}} \int_X \omega \wedge \omega \wedge c_1(\mathcal{V})\,, \tag{2.17}$$

where $\mathcal{V}$ denotes the holomorphic vector bundle associated with the internal field strength F, and rk$\mathcal{V}$ denotes its rank. The constant μ is now identified as the *slope* of the vector bundle, and plays a crucial role in what follows.

Donaldson [74], in the case of complex surfaces, and Uhlenbeck and Yau [170], in higher dimensions, proved that there exists a unique solution to (2.16) under specific conditions: the holomorphic vector bundle must be slope *polystable*. To understand this condition, we must define slope stability. A vector bundle $\mathcal{V}$ is slope stable if for every subbundle $\mathcal{U} \subset \mathcal{V}$, it holds that

$$\mu(\mathcal{U}) < \mu(\mathcal{V}). \tag{2.18}$$

A polystable bundle is one which can be written as the direct sum of stable bundles, $\mathcal{V} = \oplus_{i=1}^{N} \mathcal{V}_i$, with the added condition that all the summand bundles have equal slope:

$$\mu(\mathcal{V}_i) = \mu(\mathcal{V}). \tag{2.19}$$

This definition indicates that a stability $\Rightarrow$ polystability, but the converse does not hold. In general, it appears easier to demonstrate the stability of a bundle $\mathcal{V}$ than its polystability.

2.1.3 The Strong Coupling Limit and Heterotic M-theory

In the picture of string dualities outlined above, an interesting question arises as to what theory is described by the strong coupling limit of the $E_8 \times E_8$ heterotic string. As noted by Witten [173], although compactifications of the weakly-coupled heterotic string gives rise to reasonable values of the four-dimensional effective α_{GUT}, predictions for the four-dimensional G_N do not agree with the observed value. Hořava and Witten [113, 112] showed that the strong-coupling limit is in fact 11-dimensional theory, with a particular topology: M-theory on $\mathbb{R}^{10} \times \mathbf{S}^1/\mathbb{Z}_2$. As mentioned previously, although the full description of M-theory is unknown, its low energy description is given by 11-dimensional supergravity, which is invariant under the action of 32 real supercharges. However, taking the 11th dimension to be the orbifold $\mathbf{S}^1/\mathbb{Z}_2$ results in breaking of half of the supersymmetry, leaving precisely the 16 supercharges necessary to match with the heterotic string. The orbifold has two special fixed points under the action of $\mathbb{Z}_2$, which define the location of two ten-dimensional "end-of-the-world" planes, and form the boundary of the 11-dimensional space. On each of these two orbifold fixed planes lives a ten-dimensional E_8 super-Yang-Mills theory. The bulk space bosonic sector consists of gravity $g_{\hat{M}\hat{N}}$ and an anti-symmetric three-form $C_{\hat{M}\hat{N}\hat{P}}$. To lowest order in κ_{11}, the 11-dimensional Newton's constant, the bosonic part of the action for this theory is given by

$$\begin{aligned}
S &= \int_{M^{11}} \sqrt{-g}\, \mathcal{L}_{SG} + \sum_{i=1}^{2} \int_{M_i^{10}} \sqrt{-g}\; \mathcal{L}_{YM}^{(i)} \\
\mathcal{L}_{SG} &= -\frac{1}{2\kappa_{11}^2} R - \frac{1}{48\kappa_{11}^2} G_{\hat{M}\hat{N}\hat{P}\hat{Q}} G^{\hat{M}\hat{N}\hat{P}\hat{Q}} \\
&\quad - \frac{1}{1728\sqrt{2}\kappa_{11}^2} \epsilon^{\hat{M}_1 \ldots \hat{M}_1 1} C_{\hat{M}_1\hat{M}_2\hat{M}_3} G_{\hat{M}_4\hat{M}_5\hat{M}_6\hat{M}_7} G_{\hat{M}_8\hat{M}_9\hat{M}_{10}\hat{M}_{11}} \\
\mathcal{L}_{YM}^{(i)} &= -\frac{1}{8\pi\kappa_{11}^2} \left(\frac{\kappa_{11}}{4\pi}\right)^{2/3} \operatorname{tr}(F^{(i)})^2
\end{aligned} \tag{2.20}$$

where G is the the four-form field strength associated with the three-form C. A schematic picture of this setup is given below in Figure 2.1.

It has been shown that by compactifying Hořava-Witten theory on a Calabi-Yau threefold (which has six real dimensions), one arrives at a five-dimensional theory that preserves four supercharges – the so-called "double domain-wall solution" [141, 140, 139]. Now, each E_8 sector lives on a *four*-dimensional boundary wall, separated by the fifth dimension. As in the weak coupling case, one can construct holomorphic vector bundles on the Calabi-Yau which reduce one or both of the E_8 factors into a group more amenable for model-building, and produce a chiral matter spectrum localized to one of the walls. Integrating out the fifth dimension then results in a four-dimensional, $N = 1$ supersymmetric theory with an "observable" sector descending from one of the E_8 factor. The other E_8 factor interacts only gravitationally with the observable sector and so is "hidden".

The low energy gauge group and particle spectrum on each four-dimensional orbifold surface is determined by the choice of this gauge connection [70], as well as by any locally flat Wilson lines. Finally, there can be a finite number of codimension-1 three branes located at various points within the 5-th dimension. These arise from topological five-branes in M-theory, each with two spatial dimensions wrapped on a holomorphic curve in the Calabi-Yau threefold, that must satisfy a specific homological constraint [143, 73]. It is important to note that since 1) the compactification manifold is a Calabi-Yau threefold, 2) the gauge connections each satisfy the traceless hermitian Yang-Mills equations and 3) that every five-brane is wrapped on a holomorphic curve, the low energy theory on each four-dimensional orbifold surface, as well as the worldvolume action on each three-brane, must be $N = 1$ *supersymmetric*.

It should be noted that Hořava-Witten theory, and the subsequent double-domain wall solution, are in fact constructed as an expansion in the 11-dimensional Newton's constant κ_{11}.

2.2 Constructing a Realistic Spectrum

There are clearly a very large number of heterotic M-theories that can be constructed, depending on the choice of the Calabi-Yau threefold as well as the specific gauge connections–that is, slope stable holomorphic vector bundles with vanishing slope–chosen on each orbifold surface. However, it was shown in a series of papers [38, 34, 35, 37, 36] that it is possible to pick both the compactification geometry and as well as the choice of vector bundles so that the low energy physics is phenomenologically realistic. This set of realistic vacua is called

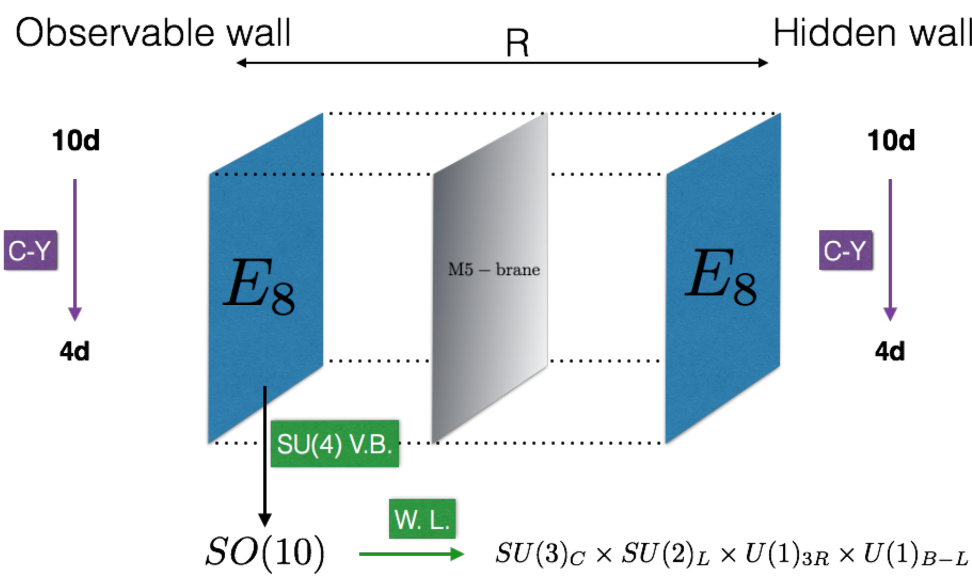

Figure 2.1: Schematic diagram of heterotic M-theory. The 11-dimensional theory is compactified on a Calabi-Yau of mean radius $\sim (10^{16}\text{GeV})^{-1}$. The two orbifold fixed planes are separated by a fifth dimension of length $R \sim (10^{15}\text{GeV})^{-1}$. The visible (observable sector) E_8 is reduced to $SO(10)$ by the construction of a holomorphic vector bundle, and Wilson lines further break this down to the gauge group of the B-L MSSM . Additionally, 3-branes wrapping holomorphic curves on the Calabi-Yau can fill the bulk between the two orbifold planes.

the *"heterotic standard model"*. To be specific, the Calabi-Yau threefold is chosen to be a quotient threefold of the form

$$X = \frac{\tilde{X}}{\mathbb{Z}_3 \times \mathbb{Z}_3} \ , \tag{2.21}$$

where

$$\tilde{X} = dP_9 \times_{P_1} dP_9 \tag{2.22}$$

is a "Schoen" threefold with isometry group $\mathbb{Z}_3 \times \mathbb{Z}_3$. That is, we first take the product of two dP_9 surfaces, which by definition have complex dimension 2. Each dP_9 can be thought of as an elliptic fibration over a base $\mathbb{P}^1$. We take this base P_1 to be the same for each dP_9. This restriction then means that the complex dimension of $\tilde{X}$ is $2 \times 2 - 1 = 3$, as required[5]. In the construction of $\tilde{X}$, it was required that the manifold exhibit a freely-acting $\mathbb{Z}_3 \times \mathbb{Z}_3$ isometry, and hence taking the quotient (2.21) does not give rise to singularities.

In [38] it was shown that X has three Kähler and three complex structure moduli, that is, $h^{1,1} = h^{1,2} = 3$, a specific set of intersection numbers d_{ijk} and homotopy group $\pi_1 = \mathbb{Z}_3 \times \mathbb{Z}_3$. It was then proven in [34, 35, 37, 36] that one can choose a slope-stable, holomorphic vector bundle with vanishing slope on X of the form

$$V = \frac{\tilde{V}}{\mathbb{Z}_3 \times \mathbb{Z}_3} \ , \tag{2.23}$$

where $\tilde{V}$ has structure group $SU(4) \subset E_8$ and is constructed by "extension" as

$$0 \longrightarrow V_1 \longrightarrow \tilde{V} \longrightarrow V_2 \longrightarrow 0 \ . \tag{2.24}$$

Each of V_1 and V_2 is a specific tensor product of a line bundle with a rank two bundle pulled back from a dP_9 factor of $\tilde{X}$. It was explicitly shown in [37, 36] that this bundle is $\mathbb{Z}_3 \times \mathbb{Z}_3$ "equivariant", as it must be. In the heterotic M-theory picture, we take this bundle to be associated to the observable sector.

In addition, non-trivial $\mathbb{Z}_3 \times \mathbb{Z}_3$ Wilson lines with specific actions on the representations R of $SU(4)$ are introduced. The particle spectrum on the quotient threefold X is obtained by tensoring the cohomology $H^1(\tilde{X}, U_R(\tilde{V}))$–where $U_R(\tilde{V})$ is the tensor product of the bundle associated the $SU(4)$ representation R–with the representation space of R and then taking the $\mathbb{Z}_3 \times \mathbb{Z}_3$ invariant part. That is, we start with the spectrum given by (2.12), and the associated cohomology groups $H^1(\tilde{X}, U_R(\tilde{V}))$. The elements of these cohomology groups are associated with $\mathbb{Z}_3 \times \mathbb{Z}_3$ actions. By acting with the Wilson lines, we project out those elements which transform non-trivially under $\mathbb{Z}_3 \times \mathbb{Z}_3$. It was shown in [36] that the

[5]This description is consistent with our earlier discussion describing $\tilde{X}$ as the vanishing locus of a set of polynomials.

resulting spectrum, given by

$$(H^1(\tilde{X}, U_R(\tilde{V}) \otimes R)^{\mathbb{Z}_3 \times \mathbb{Z}_3} \tag{2.25}$$

is *exactly* that of the MSSM with three right-handed neutrino chiral super-multiplets–one for each of the three families. Since the $\mathbb{Z}_3 \times \mathbb{Z}_3$ finite group is Abelian, it follows that the gauge group of the MSSM is

$$G = SU(3)_C \times SU(2)_L \times U(1)_Y \times U(1)_{B-L} \ . \tag{2.26}$$

That is, it is the standard model gauge group augmented by an extra gauged $U(1)_{B-L}$ factor. We explore the phenomenology of this spectrum in the next chapter.

Chapter 3

The B-L MSSM and Simultaneous Wilson Lines

3.1 Introduction

The B-L MSSM arises in the observable sector of heterotic M-theory compactified to four-dimensions on a Schoen Calabi-Yau (CY) threefold [38] with first homotopy group $\pi_1 = \mathbb{Z}_3 \times \mathbb{Z}_3$. This manifold admits a specific slope-stable holomorphic vector bundle [71] with structure group $SU(4) \subset E_8$, as well as two Wilson lines–each wrapped over a two-cycle associated with a different $\mathbb{Z}_3$ homotopy factor. This theory has three, in principle distinct, mass scales–M_U at which the gauge bundle spontaneously breaks E_8 to $SO(10)$ and two Wilson line mass scales, which we denote by $M_{\chi_{3R}}$ and $M_{\chi_{B-L}}$, associated with the inverse radii of their respective two-cycles. In previous work, we have assumed that the radius of one two-cycle is distinctly smaller than that of the other; that is, we chose $M_U \simeq M_{\chi_{B-L}} > M_{\chi_{3R}}$. By choosing the scale of separation of the two Wilson lines appropriately, one can exactly unify all gauge coupling parameters to a single value α_u at M_U. This hypothesis enhanced the specificity of the calculation, by (for instance) setting the boundary conditions in the renormalization group equations (RGEs) and determining $\sin^2\theta_R$ at the SUSY transition mass.

This specificity comes at the cost of introducing an *additional scaling regime*. Between $M_{\chi_{B-L}}$ and $M_{\chi_{3R}}$ the effective theory is that of the "left-right" model [159, 14, 92, 108] with gauge group $SU(3)_C \times SU(2)_L \times SU(2)_R \times U(1)_{B-L}$ and a specific particle spectrum that can be computed from string theory. It is only for energy-momentum below the lightest Wilson line mass $M_{\chi_{3R}}$ that one obtains the spectrum and $SU(3)_C \times SU(2)_L \times U(1)_Y \times U(1)_{B-L}$ gauge symmetry of the B-L MSSM .

Additionally, the splitting of the Wilson lines limits the analysis to a restricted region of CY moduli space where the associated two-cycles have considerably different radii. For soft

SUSY breaking masses in the TeV range, this constraint was reasonable since the separation between the Wilson line masses–and, hence, the difference in the two-cycle radii–was less than an order of magnitude. If one tries to take larger values for the soft SUSY breaking masses, the difference in the Wilson line masses grows rapidly. For example, for 10^4 TeV soft masses, the Wilson lines must be separated by a factor of 10^3–reducing the calculation to an extremely unnatural region of CY moduli space. For even larger values of the soft masses, the calculation breaks down completely. It follows that if one wishes to discuss the *B-L* MSSM for large soft SUSY breaking masses– a scenario we will discuss in the next chapter –then it becomes necessary to analyze the theory for the more natural case of simultaneous, or nearly simultaneous, Wilson lines.

In this chapter, we generalize and simplify the phenomenological analysis of the *B-L* MSSM by working in a *generic* region of CY moduli space where the radii of the two Wilson lines and the average radius of the CY manifold are all approximately equal: that is, with $M_U \simeq M_{\chi_{B-L}} \simeq M_{\chi_{3R}}$. This generalization is significant in that 1) *the region of moduli space is much larger and more "natural"* than that used previously and 2) *the "left-right" scaling region is eliminated*, with the *B-L* MSSM emerging immediately below the compactification scale–thus simplifying the scaling regimes. Of course, the four *B-L* MSSM gauge couplings will no longer unify near the scale of the CY radius. This does somewhat complicate the RG analysis. However, it opens the door for a discussion of unification of all gauge couplings with the gravitational coupling at the "string scale"–as has been discussed by many authors in [122, 121, 150, 67, 66, 127, 69, 157, 156, 98, 128, 59, 15]. More specifically, such unification should take place at tree level. However, at the one-loop (and higher) level one expects such unification to be split by "threshold" corrections. These are due to several effects, such as the inclusion of field theory thresholds at each of the SUSY, *B-L* and "unification" scales, and genus-one string theory corrections. Since in this analysis the latter is expected to be the largest, we will focus exclusively on them. By running the four *B-L* MSSM gauge parameters up to the string scale, we will 3) *statistically compute the heavy string threshold corrections for each gauge coupling.* Furthermore, we will statistically compute the hypercharge gauge threshold and, by subtracting various thresholds, analyze the moduli dependent sub-component of each. Finally, there is yet another important benefit of analyzing the *B-L* MSSM at the generic region of its CY moduli space–although we will not pursue this presently. In previous work and the present analysis, the scale of the soft SUSY breaking parameters is chosen to be in the TeV region. This is done in order for our low energy phenomenological predictions to be LHC accessible. However, unlike in the case of unified gauge couplings enforced by splitting the Wilson line masses discussed in [159, 146, 145, 160, 161]–which, for reasons elucidated above, is essentially restricted to the TeV region–for the simultaneous Wilson line masses discussed in this chapter, the SUSY breaking mass scale can be taken to be arbitrarily large. This has a number of important applications, both in particle phenomenology and in early universe cosmology [142]. We will pursue this in the next chapter.

This chapter is structured as follows. In section 3.2 we review the salient parts of the B-L MSSM theory, presenting the spectrum, the supersymmetric and the soft SUSY breaking Lagrangians, discussing the generic structure of spontaneous B-L and EW symmetry breaking and setting our notation. Section 3.3 is devoted to defining the exact meaning of the "simultaneous" Wilson line analysis presented in this chapter–as opposed to the "split" Wilson line approach in our previous work. It then discusses, in detail, the four relevant mass scales from "unification" to electroweak symmetry breaking. The statistical definitions of the "unification" mass and gauge coupling are given in our present context. In section 3.4, the three scaling regimes–for both the "right-side-up" and "upside-down" scenarios–along with the associated gauge coupling beta function parameters are presented. The RG running of the Yukawa couplings, including their transition at the SUSY scale, is discussed. Section 3.5 gives a brief review of the "statistical" approach to setting the initial soft supersymmetry breaking parameters at the "unification" scale presented in detail in our previous work. In section 3.6, the experimental constraints on the sparticle masses, the heavy vector boson mass and the lightest neutral Higgs mass are presented. We then solve the RGEs–for randomly chosen initial soft SUSY breaking parameters– sequentially from the "unification" scale down through the EW breaking scale subject to these constraints. Plots–and the exact number–of the initial points that sequentially satisfy the experimental constraints are given; ending with the robust number of phenomenologically "valid" black points that satisfy all experimental constraints. We relegate a brief analysis of both the LSP and non-LSP spectra to appendix A.

In section 3.7, we briefly discuss fine-tuning in the B-L MSSM . In section 3.8, we statistically calculate the heavy string threshold corrections for each of the four B-L MSSM gauge couplings, as well as the hypercharge gauge threshold, and analyze the moduli dependent differences of these quantities.

3.2 The Minimal SUSY B-L Model

In this section, we briefly review the minimal anomaly free extension of the MSSM with gauge group

$$SU(3)_C \times SU(2)_L \times U(1)_{3R} \times U(1)_{B-L} \ , \tag{3.1}$$

whose structure was motivated by heterotic string theory in [36] and by phenomenological considerations in [18, 85]. Although this model has been discussed in previous work [159, 146, 145, 160, 161], we outline its main features in this section for specificity and to set our notation. The Abelian gauge factors $U(1)_{3R} \times U(1)_{B-L}$ can be rotated into physically equivalent charge bases, such as $U(1)_Y \times U(1)_{B-L}$. However, as shown in [159], this comes at the cost of introducing kinetic mixing between the gauge fields. We therefore prefer to work in the basis $U(1)_{3R} \times U(1)_{B-L}$. The gauge covariant derivative is

$$D = \partial - ig_{3R} I_{3R} W_{3R} - ig_{BL} \frac{I_{BL}}{2} B' \ , \tag{3.2}$$

where I_{3R}, I_{BL} and g_{3R}, g_{BL} are the generators and couplings for the $U(1)_{3R}$ and $U(1)_{B-L}$ groups respectively. The gauge boson associated with $U(1)_{B-L}$ is denoted B' to distinguish it from the gauge boson associated with $U(1)_Y$, which is normally denoted B. The factor of $\frac{1}{2}$ in the last term is introduced by redefining the gauge coupling g_{BL}, thus simplifying many equations. A radiatively induced vacuum expectation value (VEV) of a right-handed sneutrino will break the Abelian factors $U(1)_{3R} \times U(1)_{B-L}$ to $U(1)_Y$, in analogy with the way the MSSM Higgs fields break $SU(2)_L \times U(1)_Y$ to $U(1)_{EM}$. This process is referred to as "*B-L* " symmetry breaking, although technically it breaks a specific combination of the groups generated from I_{3R} and I_{BL}, leaving invariant the usual hypercharge group generated by

$$Y = I_{3R} + \frac{I_{BL}}{2} \ . \tag{3.3}$$

The particle content of the model is simply that of the MSSM plus three right-handed neutrino chiral multiplets. This amounts to three generations of matter superfields

$$\begin{array}{llll} Q = \begin{pmatrix} u \\ d \end{pmatrix} \sim (\mathbf{3}, \mathbf{2}, 0, \frac{1}{3}) & \begin{array}{rl} u^c \sim & (\bar{\mathbf{3}}, \mathbf{1}, -1/2, -\frac{1}{3}) \\ d^c \sim & (\bar{\mathbf{3}}, \mathbf{1}, 1/2, -\frac{1}{3}) \end{array} & , \\ L = \begin{pmatrix} \nu \\ e \end{pmatrix} \sim (\mathbf{1}, \mathbf{2}, 0, -1) & \begin{array}{rl} \nu^c \sim & (\mathbf{1}, \mathbf{1}, -1/2, 1) \\ e^c \sim & (\mathbf{1}, \mathbf{1}, 1/2, 1) \end{array} & , \end{array} \tag{3.4}$$

along with the usual two Higgs supermultiplets

$$\begin{array}{lll} H_u = \begin{pmatrix} H_u^+ \\ H_u^0 \end{pmatrix} & \sim & (\mathbf{1}, \mathbf{2}, 1/2, 0) \ , \\ H_d = \begin{pmatrix} H_d^0 \\ H_d^- \end{pmatrix} & \sim & (\mathbf{1}, \mathbf{2}, -1/2, 0) \end{array} \tag{3.5}$$

where we have displayed their $SU(3)_C \times SU(2)_L \times U(1)_{3R} \times U(1)_{B-L}$ quantum numbers. The superpotential of the *B-L* MSSM is given by

$$W = Y_u Q H_u u^c - Y_d Q H_d d^c - Y_e L H_d e^c + Y_\nu L H_u \nu^c + \mu H_u H_d \ , \tag{3.6}$$

where both generational and gauge indices have been suppressed. In principle, the Yukawa couplings are three-by-three complex matrices. However, the observed smallness of the CKM mixing angles and CP-violating phase imply that the quark Yukawa matrices can be approximated as diagonal and real for the purposes of RG evolution in this chapter. The charged lepton Yukawa coupling can be made diagonal and real by moving the PMNS angles and phases into the neutrino Yukawa couplings. The small size of neutrino masses implies that the neutrino Yukawa couplings can be neglected for the purposes of RG evolution in our current discussion. The smallness of first- and second-generation fermion masses implies that first and second-generation Yukawa quark and charged lepton Yukawa couplings can also be neglected. The μ-parameter can be chosen to be real without loss of generality.

The soft supersymmetry breaking Lagrangian is

$$\begin{aligned}
-\mathcal{L}_{\text{soft}} = \Big(& \frac{1}{2} M_3 \tilde{g}^2 + \frac{1}{2} M_2 \tilde{W}^2 + \frac{1}{2} M_R \tilde{W}_R^2 + \frac{1}{2} M_{BL} \tilde{B'}^2 \\
& + a_u \tilde{Q} H_u \tilde{u}^c - a_d \tilde{Q} H_d \tilde{d}^c - a_e \tilde{L} H_d \tilde{e}^c + a_\nu \tilde{L} H_u \tilde{\nu}^c + b H_u H_d + h.c. \Big) \\
& + m_{\tilde{Q}}^2 |\tilde{Q}|^2 + m_{\tilde{u}^c}^2 |\tilde{u}^c|^2 + m_{\tilde{d}^c}^2 |\tilde{d}^c|^2 + m_{\tilde{L}}^2 |\tilde{L}|^2 + m_{\tilde{\nu}^c}^2 |\tilde{\nu}^c|^2 + m_{\tilde{e}^c}^2 |\tilde{e}^c|^2 \\
& + m_{H_u}^2 |H_u|^2 + m_{H_d}^2 |H_d|^2 \ ,
\end{aligned} \tag{3.7}$$

where generation and gauge indices have been suppressed. The a-parameters and sfermion soft-mass terms can, in principle, be hermitian matrices in family space. However, this tends to lead to unobserved CP violation. Therefore, we proceed assuming that they are diagonal and real. Furthermore, as discussed in section 3.5, we assume that the a-parameters are proportional to the Yukawa couplings. This implies that all the a-parameters can be neglected except for the (3,3) component of the quark and charged lepton a-parameters. The b-parameter can be chosen to be both real and positive without loss of generality. Although the gaugino soft masses can be complex in principle, this tends to lead to unobserved flavor and CP violation. Therefore, we proceed assuming that they are real.

The B-L symmetry is spontaneously broken by the VEV in a right-handed sneutrino, which carries the appropriate I_{3R} and I_{B-L} charges to break those symmetries while preserving hypercharge symmetry. This VEV is brought about by a sneutrino soft-mass term becoming tachyonic at the TeV scale due to the RGE evolution. As discussed in [152, 99, 19], this VEV will be purely in one of the three right-handed sneutrino generations – not in a linear combination of them. Furthermore, the three generations of right-handed sneutrinoes can be relabeled without loss of generality. Therefore, we henceforth assume that it is the third-generation right-handed sneutrino that acquires a VEV. Electroweak symmetry is broken by VEVs in the neutral components of the up and down Higgs multiplets. The electroweak breaking VEVs and the B-L breaking VEV together lead to small VEVs in all three generations of left-handed sneutrinos. The above VEVs will be denoted by

$$\langle\tilde{\nu}_3^c\rangle \equiv \frac{1}{\sqrt{2}}v_R, \quad \langle\tilde{\nu}_i\rangle \equiv \frac{1}{\sqrt{2}}v_{Li}, \quad \left\langle H_u^0\right\rangle \equiv \frac{1}{\sqrt{2}}v_u, \quad \left\langle H_d^0\right\rangle \equiv \frac{1}{\sqrt{2}}v_d, \tag{3.8}$$

where $i = 1, 2, 3$ is the generation index.

The neutral gauge boson that becomes massive due to B-L symmetry breaking is referred to as Z_R. Defining $v^2 = v_u^2 + v_d^2$, and assuming that $v^2 \ll v_R^2$, Z_R acquires to leading order a mass of

$$M_{Z_R}^2 = \frac{1}{4}\left(g_{3R}^2 + g_{BL}^2\right)v_R^2 \ . \tag{3.9}$$

The hypercharge gauge coupling is given by

$$g_Y = g_{3R}\sin\theta_R = g_{BL}\cos\theta_R \ , \tag{3.10}$$

where

$$\cos\theta_R = \frac{g_{3R}}{\sqrt{g_{3R}^2 + g_{BL}^2}} \ . \tag{3.11}$$

The smallness of the neutrino masses implies, first, that the neutrino Yukawa couplings are small and, second, that the left-handed sneutrino VEVs are much smaller than the electroweak scale. In this limit, the minimization conditions of the potential simplify to

$$v_R^2 = \frac{-8m_{\tilde{\nu}_3^c}^2 + g_{3R}^2\left(v_u^2 - v_d^2\right)}{g_{3R}^2 + g_{BL}^2} \ , \tag{3.12}$$

$$v_{Li} = \frac{\frac{v_R}{\sqrt{2}}(Y_{\nu i3}^*\mu v_d - a_{\nu i3}^* v_u)}{m_{\tilde{L}_i}^2 - \frac{g_2^2}{8}(v_u^2 - v_d^2) - \frac{g_{BL}^2}{8}v_R^2} \ , \tag{3.13}$$

$$\frac{1}{2}M_Z^2 = -\mu^2 + \frac{m_{H_u}^2\tan^2\beta - m_{H_d}^2}{1 - \tan^2\beta} \ , \tag{3.14}$$

$$\frac{2b}{\sin 2\beta} = 2\mu^2 + m_{H_u}^2 + m_{H_d}^2 \ . \tag{3.15}$$

Noting from above that $|v_u^2 - v_d^2| \ll |m_{\tilde{\nu}_3^c}^2|$, equations (3.9) and (3.12) can be combined to give

$$M_{Z_R}^2 = -2m_{\tilde{\nu}_3^c}^2 \ . \tag{3.16}$$

The VEV in the third-generation right-handed sneutrino induces spontaneous bilinear

R-parity violation through the operators

$$W \supset \epsilon_i \, L_i \, H_u - \frac{1}{\sqrt{2}} Y_{ei} \, v_{Li} \, H_d^- \, e_i^c \ , \tag{3.17}$$

where

$$\epsilon_i \equiv \frac{1}{\sqrt{2}} Y_{\nu i3} v_R \ . \tag{3.18}$$

Bilinear R-parity violation has been discussed extensively, including its relevance to neutrino masses. See, for example, some early works [154, 50, 49, 110]. The Lagrangian of this model contains additional bilinear terms due to the sneutrino VEVs:

$$\begin{aligned} \mathcal{L} \supset & -\frac{1}{2} v_{L_i^*} \left[g_2 \left(\sqrt{2} \, e_i \tilde{W}^+ + \nu_i \tilde{W}^0 \right) - g_{BL} \nu_i \tilde{B}' \right] \\ & -\frac{1}{2} v_R \left[-g_R \nu_3^c \tilde{W}_R + g_{BL} \nu_3^c \tilde{B}' \right] + \text{h.c.} \end{aligned} \tag{3.19}$$

The R-parity violating terms in this model have a variety of interesting consequences that have been studied in a number of different contexts. These include LHC studies [18, 85, 93, 94], predictions for neutrinos [152, 99, 19], and connections between the two [146, 145]. It has been shown that the R-parity violation can give rise to Majorana neutrino masses, with the lightest left-handed neutrino being massless. There is also a pair of sterile right-handed neutrinos that can have cosmological implications [94].

We now turn to connecting the phenomenology of the B-L MSSM to its high-scale origins. Specifically, we are considering the possibility that the B-L MSSM is the observable sector of the low-energy effective theory of an $E_8 \times E_8$ heterotic string theory. In this context, the B-L MSSM gauge group unifies into an $SO(10)$ gauge group, which is itself the commutant of the $SU(4)$ structure group of the observable sector E_8 vector bundle on the CY threefold. We have previously studied the B-L MSSM in this context [161]. In this chapter, however, we will study the effects of string threshold corrections on gauge unification. This requires a discussion of gauge unification–to which we now turn.

3.3 Journey From the “Unification” Scale

This section outlines the scales and scaling regimes associated with the evolution of the B-L MSSM from “unification” to the electroweak scale. Compactification to four dimensions yields a unified gauge group, $SO(10)$, at mass scale M_U. This unified gauge group is broken by two Abelian Wilson lines, denoted by χ_{3R} and χ_{B-L}. The mass scales associated with these Wilson lines, $M_{\chi_{3R}}$ and $M_{\chi_{B-L}}$ respectively, depend on the inverse radii of the 2-cycles over which they are wrapped. These, in turn, depend on the chosen point in the CY moduli space. Generically, one expects that the two Wilson line masses are approximately the same and close to the $SO(10)$ unification scale. That is, one "naturally" expects

$$M_U \simeq M_{\chi_{B-L}} \simeq M_{\chi_{3R}} \tag{3.20}$$

over a wide region of the CY moduli space. However, as one moves away from these generic points the Wilson line mass scales need not remain the same. This leads to an intermediate regime between the two scales associated with the Wilson lines. The particle content and gauge group in this intermediate regime depends on which Wilson line has a higher associated mass. If $M_U \simeq M_{\chi_{B-L}} > M_{\chi_{3R}}$, the particle content and gauge group of the intermediate regime is that of a "left-right" model. If $M_U \simeq M_{\chi_{3R}} > M_{\chi_{B-L}}$, the particle content and gauge group of the intermediate regime is similar to that of a"Pati-Salam" model.

In each case, the lower-mass Wilson line breaks the model in the intermediate regime to the *B-L* MSSM . In fact, it was shown in [159] that exact gauge coupling unification at one-loop *requires* that these scales be different. For specificity of the RGE calculation, it was convenient to *impose* precise gauge coupling unification. Hence, in [159] we studied the two cases with separated Wilson line masses–even though this can occur only in special regions of moduli space. Under the assumption that the soft SUSY breaking masses be of TeV order–to assure that sparticle masses potentially be LHC accessible–we found that gauge coupling unification dictates that the Wilson line scales must be separated by less than/approximately an order of magnitude in either case. Additionally, we found that both cases lead to similar low energy phenomenology. Hence, for specificity, we carried out our analysis using the first of these symmetry breaking patterns; that is, the intermediate regime containing the "left-right" model. We refer the reader to [159] for that analysis. Here, for concreteness, we simply show in Figure 3.1 the relationship of the $M_U \simeq M_{\chi_{B-L}}$ unification scale to that of the mass $M_{\chi_{3R}}$ of the second Wilson line in the "left-right" model case. This is plotted as a function of M_{SUSY} – defined below in equation (3.28). In this chapter, we turn to the analysis of the *generic* region of moduli space where equation (3.20), that is, $M_U \simeq M_{\chi_{B-L}} \simeq M_{\chi_{3R}}$, is satisfied, thereby *giving up exact gauge unification.* Be that as it may, to enable direct comparison of our new simultaneous Wilson line results with those from the split Wilson lines analyzed in [161], we continue to use the same notation for all quantities. In particular, it is important to use identical notation for the *B-L* gauge coupling. Thus far, we have discussed the gauge parameter g_{BL}, which couples to the $\frac{I_{BL}}{2}$ generator. However, as was discussed in [159], this gauge coupling has to be properly normalized so as to unify with the other gauge parameters in the split Wilson line scenarios. The appropriate coupling was denoted g'_{BL} and defined by

$$g'_{BL} = \sqrt{\frac{2}{3}} g_{BL} \ . \tag{3.21}$$

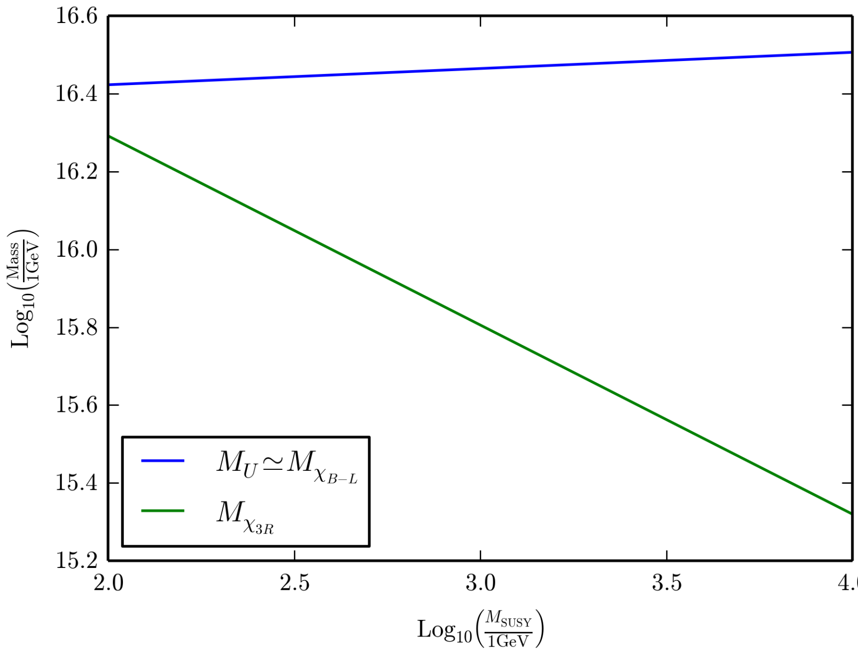

Figure 3.1: The $M_U \simeq M_{\chi_{B-L}}$ unification mass and $M_{\chi_{3R}}$ as functions of the SUSY scale in the "left-right" scenario.

Even though the four gauge couplings, including g'_{BL}, will not unify in the simultaneous Wilson line scenario, we will continue to use this parameter when appropriate. Note that g'_{BL} couples to the $\sqrt{\frac{3}{8}} I_{BL}$ generator and will appear in the RGEs. For quantities of physical interest, such as physical masses, g_{BL} will be used.

To fully understand the evolution of this model from "unification" to the electroweak scale, it should be noted that there are four relevant mass scales of interest. All four are described in the following:

M_U: the unification and the first and second Wilson lines mass scale.

Since, as discussed above, exact unification of the four gauge couplings no longer occurs for simultaneous Wilson lines, it is essential to give a justification–and an explicit definition–of what we mean by the "unification mass" in the present context. In [161], every phenomenologically valid point in the space of randomly chosen initial soft supersymmetry breaking parameters corresponds to an explicit unification mass M_U and unified coupling α_u. Both the unification scale and unification parameter vary for different valid points. The associated statistical histograms for these quantities are shown in Figures 3.2 and 3.3 respectively, along with their average values. These are found to be

$$\langle M_U \rangle = 3.15 \times 10^{16}\ \mathrm{GeV} \quad , \quad \langle \alpha_u \rangle = 0.0498\ . \tag{3.22}$$

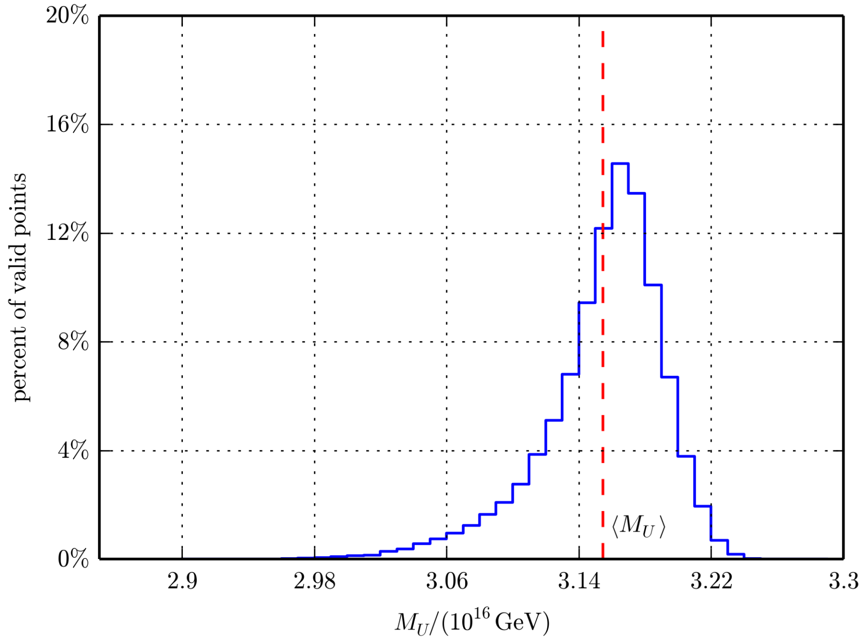

Figure 3.2: A histogram of the unification scale for the 53,512 phenomenologically valid points in the split Wilson line "left-right" unification scheme. The average unification scale is $\langle M_U \rangle = 3.15 \times 10^{16}$ GeV.

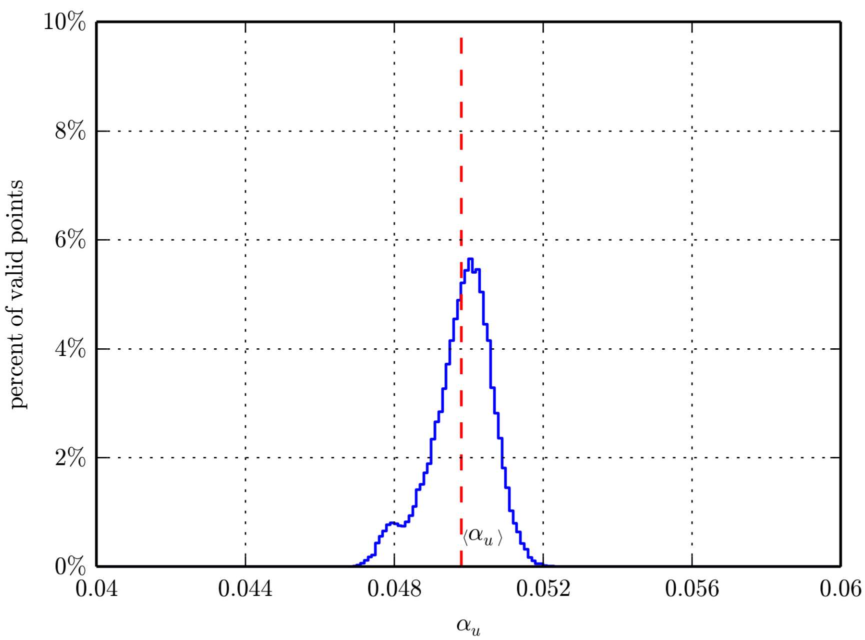

Figure 3.3: A histogram of the unification scale for the 53,512 valid points in the split Wilson line "left-right" unification scheme. The average value of the unified gauge coupling is $\langle \alpha_u \rangle = 0.0498$.

In this chapter, we will refer to the average values $\langle M_U \rangle$ and $\langle \alpha_u \rangle$ as the "unification" mass and "unified" gauge coupling–and RG scale the gauge parameters between this scale and the electroweak scale. The values of the four diverse couplings α_3, α_2, α_{3R} and α'_{BL} at $\langle M_U \rangle$ will be determined for each statistical choice of soft supersymmetry breaking parameters. Henceforth, for specificity, we will always take this unification scale and both Wilson line masses to be strictly identical; that is

$$\langle M_U \rangle = M_{\chi_{3R}} = M_{\chi_{B-L}} \ . \tag{3.23}$$

M_{B-L}: the mass at which the right-handed sneutrino VEV triggers $U(1)_{3R} \times U(1)_{B-L} \to U(1)_Y$ symmetry breaking.

Physically, this corresponds to the mass of the neutral gauge boson Z_R of the broken symmetry and, therefore, the scale of Z_R decoupling. Specifically

$$M_{Z_R} = M_{B-L}. \tag{3.24}$$

Note that M_{Z_R} itself depends on parameters evaluated at M_{B-L}. This results in a transcendental equation that can be solved using for M_{B-L} using numerical methods. The boundary condition relating the hypercharge coupling to the gauge couplings of $U(1)_{3R}$ and $U(1)_{B-L}$ at this scale is nontrivial. It is given by

$$g_1 = \sqrt{\frac{5}{3}} g_{3R} \sin\theta_R = \sqrt{\frac{5}{2}} g'_{BL} \cos\theta_R \ , \tag{3.25}$$

where

$$\cos\theta_R = \frac{g_{3R}}{\sqrt{g_{3R}^2 + \frac{3}{2} g'^2_{BL}}} \ . \tag{3.26}$$

As with the B-L gauge coupling, the hypercharge coupling has been rescaling to allow for unification in the split Wilson line scenarios. The rescaled hypercharge gauge coupling, g_1, is defined by

$$g_1 = \sqrt{\frac{5}{3}} g_Y \ . \tag{3.27}$$

M_{SUSY}: the soft SUSY breaking scale.

This is the scale at which all sparticles are integrated out, with the exception of the right-handed sneutrinos, which are associated with B-L breaking and, therefore, are integrated out at the B-L scale [161]. While the sparticles do not all have the same mass, we use the scale of stop decoupling as a representative scale associated with all sparticles. That is,

$$M_{\text{SUSY}} = \sqrt{m_{\tilde{t}_1}\ m_{\tilde{t}_2}}. \tag{3.28}$$

The scale of stop decoupling is the best choice for the SUSY scale since the stops give the dominant radiative corrections to phenomenologically important quantities such as the electroweak scale and the Higgs mass. See, for example, [97] for more details. Note that the physical stop masses depend on quantities evaluated at M_{SUSY}. Therefore, this equation must be solved using iterative numerical methods for the correct value of M_{SUSY}.

M_{EW}: the electroweak scale.

This is the well-known scale associated with the Z and W gauge bosons of the standard model (SM). We identify this scale with the mass of Z boson, as is conventional. That is,

$$M_{\text{EW}} = M_Z. \tag{3.29}$$

3.4 The Physical Regimes and the RG Scaling of the Supersymmetric Parameters

Having defined the relevant mass scales, we turn to a brief discussion of RG evolution that occurs between them. The gauge coupling RGEs are

$$\frac{d}{dt}\alpha_a^{-1} = -\frac{b_a}{2\pi}\ , \tag{3.30}$$

where a indexes the associated gauge groups. The slope factors b_a are different in the different scaling regimes.

- $\langle M_U \rangle$ – $\max(M_{\text{SUSY}}, M_{B-L})$: We refer to this regime as the "B-L MSSM regime" because the particle content and gauge group are the B-L MSSM . The b_a factors are

$$b_3 = -3,\ b_2 = 1,\ b_{3R} = 7,\ b_{BL'} = 6\ . \tag{3.31}$$

Note that the hierarchy between the SUSY and B-L scales depends on the point chosen in the initial parameter space. The remaining two regimes depend on which of the following two cases occurs: $M_{B-L} > M_{\text{SUSY}}$–the "right-side-up" hierarchy–and $M_{\text{SUSY}} > M_{B-L}$–the "upside-down" hierarchy.

right-side-up hierarchy:

- $M_{B-L} - M_{\mathrm{SUSY}}$: In this regime, the gauge group and particle content is that of the MSSM plus two right-handed neutrino supermultiplets. The gauge couplings in this regime evolve with the slope factors

$$b_3 = -3,\ b_2 = 1,\ b_1 = \frac{33}{5}\ . \tag{3.32}$$

We refer to this regime as the "MSSM" regime.

- $M_{\mathrm{SUSY}} - M_{\mathrm{EW}}$: In this regime, the sparticles are integrated out, leaving the SM with an additional two sterile neutrinos. It has the well-known slope factors

$$b_3 = -7,\ b_2 = -\frac{19}{6},\ b_1 = \frac{41}{10}\ . \tag{3.33}$$

We refer to this regime as the "SM" regime.

upside-down hierarchy:

- $M_{\mathrm{SUSY}} - M_{B-L}$: In this regime, sparticles, with the exception of the third-generation right-handed sneutrino, are integrated out. But B-L is still a good symmetry. This yields a non-SUSY $SU(3)_C \times SU(2)_L \times U(1)_{3R} \times U(1)_{B-L}$ model, which also includes three generations of right-handed sneutrinos–the third of which acts as the B-L Higgs. The slope factors are

$$b_3 = -7,\ b_2 = \frac{19}{6},\ b_{3R} = \frac{53}{12},\ b_{BL'} = \frac{33}{8}. \tag{3.34}$$

- $M_{B-L} - M_{\mathrm{EW}}$: This regime is identical to the SM regime with slope factors given in equation (3.33).

The boundary conditions imposed on the gauge couplings are that the three α_i coefficients of the SM take their experimental values at M_Z [164]:

$$\alpha_3(M_Z) = 0.118,\ \alpha_2(M_Z) = 0.0337,\ \alpha_1(M_Z) = 0.0170\ . \tag{3.35}$$

These experimental values will then be scaled up through the various regimes: $M_{EW} \to M_{SUSY}$, $M_{SUSY} \to M_{B-L}$ (for the right-side-up hierarchy) or $M_{EW} \to M_{B-L}$, $M_{B-L} \to M_{SUSY}$ (for the upside-down hierarchy), followed by scaling through the B-L MSSM regime to $\langle M_U \rangle$ using the beta functions listed above. The "splitting" of α_1 to α_{3R} and α'_{BL} at M_{B-L} is achieved using the boundary conditions (3.25), (3.26). In previous work [159], exact unification conveniently specified $\sin^2\theta_R \approx 0.6$. However, in the present scenario we are not requiring exact unification. Hence, this specificity is lost and $\sin^2\theta_R$ is a free

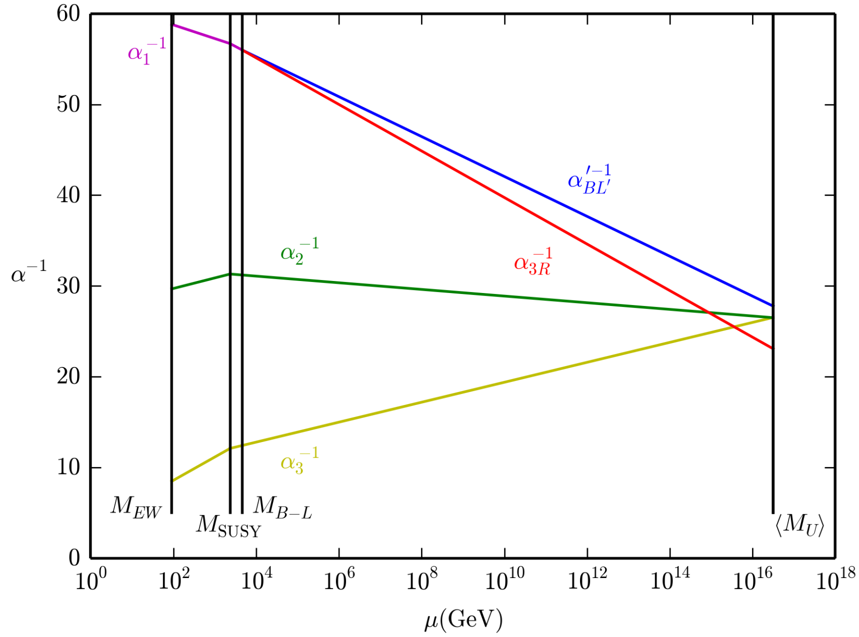

Figure 3.4: Running gauge couplings for one of the valid points in our main scan, discussed below, with $M_{\rm SUSY} = 2350$ GeV, $M_{B-L} = 4670$ GeV and $\sin^2\theta_R = 0.6$. In this example, $\alpha_3(\langle M_U\rangle) = 0.0377$, $\alpha_2(\langle M_U\rangle) = 0.0377$, $\alpha_{3R}(\langle M_U\rangle) = 0.0433$, and $\alpha_{BL'}(\langle M_U\rangle) = 0.0360$.

parameter. We proceed by simply setting

$$\sin^2\theta_R = 0.6 \tag{3.36}$$

in order to make the results of this chapter more directly comparable to those of [159]. An example of the running of the gauge couplings from the electroweak scale to $\langle M_U\rangle$, as well as the values of the couplings $\alpha_3(\langle M_U\rangle)$, $\alpha_2(\langle M_U\rangle)$, $\alpha_{3R}(\langle M_U\rangle)$ and $\alpha'_{BL}(\langle M_U\rangle)$, is presented in Figure 3.4 using a phenomenologically acceptable point in the space of initial soft SUSY breaking parameters.

Similarly to the gauge parameters, the Yukawa couplings run differently under the RG through each of the above scaling regimes. Before discussing them, we must first decide which Yukawa couplings are relevant to our analysis. As discussed in [161], we begin by inputting the experimentally determined Yukawa couplings derived from the fermion masses at the electroweak scale. For our present purposes, the SM Yukawa couplings, which are three-by-three matrices in flavor space, can all be approximated to be zero except for the three-three elements which give mass to the third-generation SM fermions. The experimentally determined initial conditions are

$$y_t = 0.955, \quad y_b = 0.0174, \quad y_\tau = 0.0102. \tag{3.37}$$

For details on relating fermion masses to Yukawa couplings, see [68]. We use lower case y to denote Yukawa couplings in the non-SUSY regime. The one-loop RGEs for these Yukawa couplings were presented in Appendix A of [161], to which we refer the reader.

3.5 The Soft Supersymmetry Breaking Parameters

The remaining parameters of the B-L MSSM are the massive coefficients appearing in equation (3.7) which are responsible for softly breaking supersymmetry. Their RGEs in each physical regime were presented in detail in [161] and won't be discussed in this chapter. Here, we simply note that flavor and CP-violation experimental results place well-known limits on these quantities. Generically, the implication of these constraints are, approximately, as follows:

- Soft sfermion mass matrices are diagonal.
- The first two generations of squarks are degenerate in mass.
- The trilinear a-terms are diagonal.
- The gaugino masses and trilinear a-terms are real.

It is typically assumed that the soft trilinear a-terms are proportional to the Yukawa couplings. That is, $a = YA$ for each fermions species. Each A is real and associated with the SUSY scale. Each Y factor is a dimensionless matrix in family space. This condition effectively makes all non-third-generation trilinear terms insignificant. The above constraints are summarized as

$$\begin{aligned}
&m_{\tilde{q}}^2 = \operatorname{diag}\left(m_{\tilde{q}_1}^2, m_{\tilde{q}_1}^2, m_{\tilde{q}_3}^2\right) \quad , \quad \tilde{q} = \tilde{Q},\, \tilde{u}^c,\, \tilde{d}^c \ , \\
&m_{\tilde{\ell}}^2 = \operatorname{diag}\left(m_{\tilde{\ell}_1}^2, m_{\tilde{\ell}_2}^2, m_{\tilde{\ell}_3}^2\right) \ , \quad \tilde{\ell} = \tilde{L},\, \tilde{e}^c \ , \tilde{\nu}^c \ , \\
&a_f = Y_f A_f \quad \ , \quad f = t,\, b,\, \tau \ .
\end{aligned} \tag{3.38}$$

These constraints can be implemented at the scale $\langle M_U \rangle$, since RG evolution to the SUSY scale will not spoil these relations. Note that we do not assume that the first and second generation slepton masses are degenerate, unlike the squark masses, since this is not required by experiments. The degeneracy or non-degeneracy of the first and second generation sleptons will not, however, greatly effect the results presented here.

We now turn to the input values for the SUSY breaking parameters. Unlike the cases of the gauge and Yukawa couplings, these soft SUSY breaking parameters are not experimentally determined. In [161], we introduced a novel way to analyze the initial parameter space of a SUSY model. We will follow the same approach in the present analysis of simultaneous

Wilson lines. Specifically, we run a statistical scan of input parameters at the scale $\langle M_U \rangle$. The randomly generated input parameters are then RG evolved to the SUSY scale. We conduct an analysis of which of these high-scale initial conditions lead to realistic physics. Although the soft SUSY breaking Lagrangian contains over 100 dimensionful parameters, the phenomenologically motivated assumptions discussed briefly above only allow significant values for 24 of them. These, along with $\tan\beta$ and the sign of certain parameters, are presented in the first column of Table 3.1.

The high-scale initial values of the 24 relevant dimensionful SUSY breaking parameters are determined as follows. We make the assumption that there is only one overall scale associated with SUSY breaking, requiring that these parameters be separated by no more than an order of magnitude, or so, from each other. To quantify this, we demand that any dimension one soft SUSY breaking parameter be chosen at random within the range

$$(\frac{M}{f}, Mf) \ , \tag{3.39}$$

where M is the overall scale of SUSY breaking and f is a dimensionless number satisfying $1 \leq f \lesssim 10$. We will further insist that any such parameter be evenly scattered around M; that is, that M be the average of the randomly generated values. In [161], we found that in the case of split Wilson line masses, the maximal number of phenomenologically acceptable "valid" initial points were obtained by statistically scattering within the interval defined by

$$M = 2700 \text{ GeV}, \ \ f = 3.3 \ . \tag{3.40}$$

To allow direct comparison of the results shown here to those of [161], we will continue to use these values in the present context. This is shown in the second column of Table 3.1, along with the scattering interval associated with tanβ and the allowed signs of various parameters.

Parameter	Range
$m_{\tilde{q}_1} = m_{\tilde{q}_2}, \ m_{\tilde{q}_3} : \quad \tilde{q} = \tilde{Q}, \tilde{u}^c, \tilde{d}^c$	(820, 8900) GeV
$m_{\tilde{\ell}_1}, m_{\tilde{\ell}_2}, \ m_{\tilde{\ell}_3} : \quad \tilde{\ell} = \tilde{L}, \tilde{e}^c, \tilde{\nu}^c$	(820, 8900) GeV
m_{H_u}, m_{H_d}	(820, 8900) GeV
$\lvert A_f \rvert : \quad f = t, b, \tau$	(820, 8900) GeV
$\lvert M_a \rvert : \quad a = 3R, BL', 2, 3$	(820, 8900) GeV
$\tan\beta$	(1.2, 65)
Sign of $\mu, a_f, M_a : \quad f = t, b, \tau \quad a = 3R, BL', 2, 3$	[-,+]

Table 3.1: The parameters and their ranges scanned in this study. The ranges for the soft SUSY breaking parameters are taken to be those of [161].

3.6 The Parameter Scan and Results

The technical details of our statistical scan over the interval of soft supersymmetry breaking parameters, the complete set of all RG equations, the evolution of all parameters under the RGEs and a discussion of the sparticle and the Higgs masses were presented in detail in both the text and Appendices of [161]. In this section, we will simply apply these methods to the more "natural" case of simultaneous Wilson lines satisfying equation (3.23). As in [161], we will perform a scan over 10 million random initial points, searching for those "valid" points that satisfy all present experimental lower bounds on the masses of the different types of SUSY particles and the B-L gauge boson. These lower bounds are presented in Table 3.2. In addition, we will impose the requirement that the Higgs mass be within the 2σ allowed

Particle(s)	Lower Bound
Left-handed sneutrinos	45.6 GeV
Charginos, sleptons	100 GeV
Squarks, except for stop or sbottom LSP's	1000 GeV
Stop LSP (admixture)	450 GeV
Stop LSP (right-handed)	400 GeV
Sbottom LSP	500 GeV
Gluino	1300 GeV
Z_R	2500 GeV

Table 3.2: The different types of SUSY particles and the lower bounds implemented in this chapter.

range from the value measured at the ATLAS experiment at the LHC [1, 48]:

$$m_{h^0} = 125.36 \pm 0.82 \text{ GeV}. \tag{3.41}$$

Since the initial soft SUSY breaking parameter space is 24-dimensional, graphically displaying the results is, in principle, very difficult. However, as was discussed in [161], much of the scaling behavior of the parameters is controlled by the two S-terms, $S_{BL'}$ and S_{3R}, defined by

$$S_{BL'} = \mathrm{Tr}\,(2m^2_{\tilde{Q}} - m^2_{\tilde{u}^c} - m^2_{\tilde{d}^c} - 2m^2_{\tilde{L}} + m^2_{\tilde{\nu}^c} + m^2_{\tilde{e}^c})\ , \tag{3.42}$$

$$S_{3R} = m^2_{H_u} - m^2_{H_d} + \mathrm{Tr}\ \left(-\frac{3}{2}m^2_{\tilde{u}^c} + \frac{3}{2}m^2_{\tilde{d}^c} - \frac{1}{2}m^2_{\tilde{\nu}^c} + \frac{1}{2}m^2_{\tilde{e}^c}\right)\ , \tag{3.43}$$

where "Tr" implies a sum over the three families. It follows that our results can be reasonably displayed in the two-dimensional $S_{BL'}(\langle M_U \rangle)$ - $S_{3R}(\langle M_U \rangle)$ plane.

We begin by presenting in Figure 3.5 all 10 million initial points in the $S_{BL'}(\langle M_U \rangle)$ - $S_{3R}(\langle M_U \rangle)$ plane in order to explore, sequentially, which points satisfy the first two funda-

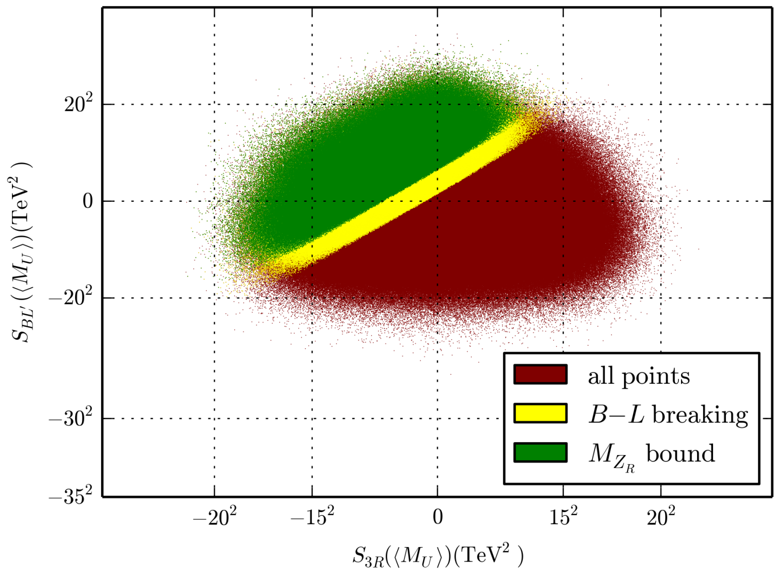

Figure 3.5: Points from the main scan in the $S_{BL'}(\langle M_U \rangle)$ - $S_{3R}(\langle M_U \rangle)$ plane. Red indicates no B-L breaking, in the yellow region B-L is broken but the Z_R mass is not above its 2.5 TeV lower bound, while green points have both B-L breaking and M_{Z_R} above this bound. The Figure expresses the fact that, despite there being 24 parameters at the UV scale scanned in our work, B-L physics is essentially dependent on only two combinations of them–the two S-terms. Note that the green points obscure some yellow and red points behind them. Similarly the yellow points obscure some red points.

mental checks that we require; that is, B-L breaking and the experimental Z_R mass lower bound. Points that do not break B-L are shown in red, points that satisfy B-L breaking but not the Z_R mass bound are in yellow, and points that break B-L symmetry and satisfy the Z_R mass bound are shown in green. We find that out of the 10 million initial points,

- 1,629,001 –the green and yellow points– break B-L symmetry.
- 697,886 –the green points–break B-L with $M_{Z_R} > 2.5$ TeV.

This plot shows that B-L breaking consistent with present experiments is a robust phenomena. Furthermore, it shows the strong dependence of B-L breaking and the Z_R mass on the values of the S-terms. There is a line in the $S_{BL'}$ - S_{3R} plane–between the yellow and red regions–below which B-L breaking is not possible. Note that this includes the origin, which corresponds to vanishing S-terms and, hence, universal soft masses. This shows that at least a small splitting from sparticle universality is required for B-L breaking. Another line exists–between the green and yellow regions–below which Z_R is always lighter than its experimental lower bound.

Proceeding sequentially, we present in Figure 3.6 the initial points in the $S_{BL'}(\langle M_U \rangle)$ - $S_{3R}(\langle M_U \rangle)$ plane that, in addition to breaking B-L with a Z_R mass above the experimental

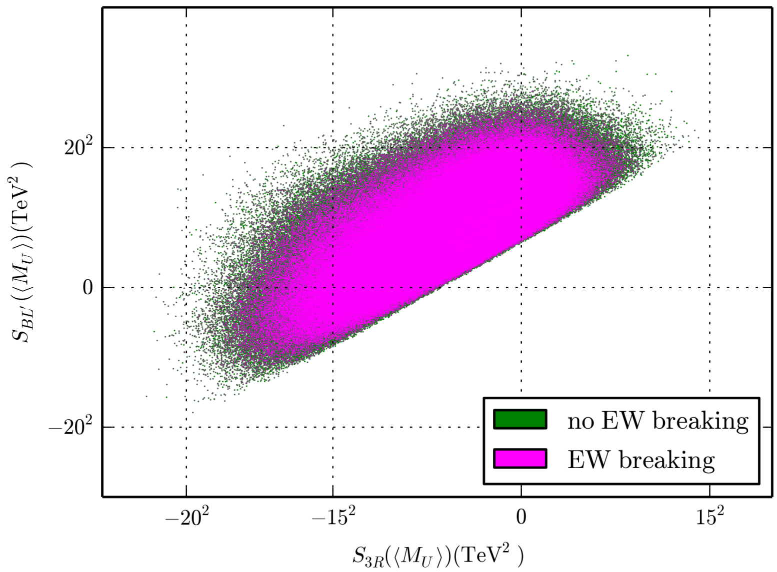

Figure 3.6: A plot encompassing the green region in Fig 3.5. The green points in this plot correspond to those which appropriately break B-L symmetry, but which do not break electroweak symmetry. However, the purple points, in addition to breaking B-L symmetry with an appropriate Z_R mass, also break EW symmetry. Note that a small density of green points that do not break EW symmetry are obscured by the purple points.

bound, also break EW symmetry. The entire colored region encompasses the green points shown in Figure 3.5. Those points that also break EW symmetry are displayed in purple. This plot indicates that most of the points that break B-L with a Z_R mass above the experimental bound, also break EW symmetry. Note that a small density of green points that do not break EW symmetry are obscured by the purple points. Specifically, we find that out of the 697,886 green points that break B-L with $M_{Z_R} > 2.5$ TeV,

- 485,952 – the purple points– also break EW symmetry.

In Figure 3.7, we reproduce Figure 3.6 but now, in addition, sequentially indicate the points that are consistent with the remaining checks–that is, all lower bounds on sparticles masses satisfied and, finally, that they reproduce the Higgs mass within the experimental uncertainty. Points that appropriately break B-L symmetry but do not satisfy electroweak symmetry breaking are still shown in green. Points that, additionally, do break electroweak symmetry are again shown in purple. Such points that also satisfy all lower bounds on sparticles masses, but do not match the known Higgs mass, are now indicated in cyan. Finally, points that satisfy all checks, including the correct Higgs mass, are shown in black. These are the "valid" points. The density of black points indicate that there is a surprisingly high number of initial parameters that satisfy all present low energy experimental constraints. Specifically, we find that out of the 485,952 purple points that appropriately

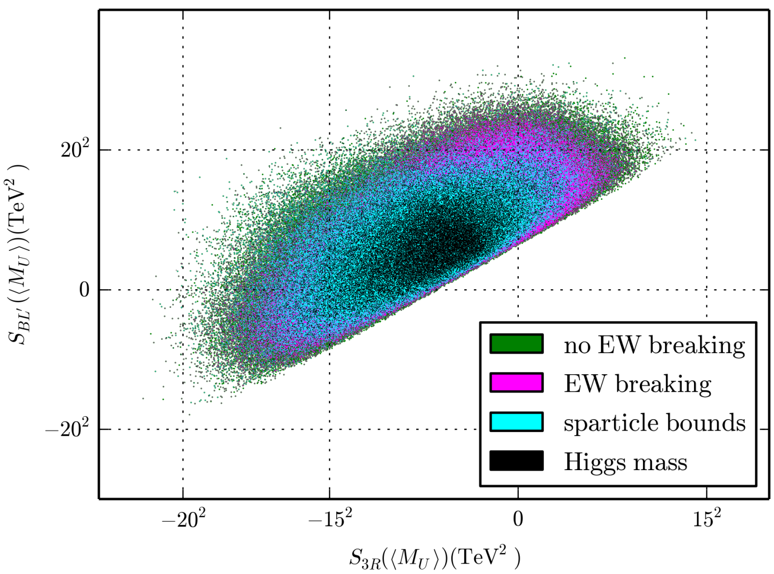

Figure 3.7: A plot of the "valid" points in our main scan. The green and purple points correspond to the green and purple points in Figure 3.6. The cyan points additionally satisfy all sparticle mass lower bounds. The black points are fully valid. That means that, in addition to satisfying all previous checks, they reproduce the correct Higgs mass within the stated tolerance. The distribution of points indicates that while B-L breaking prefers large S-terms, sfermion mass constraints prefer them to be not too large. Again, the cyan and black points may obscure a low density of other points not satisfying their constraint.

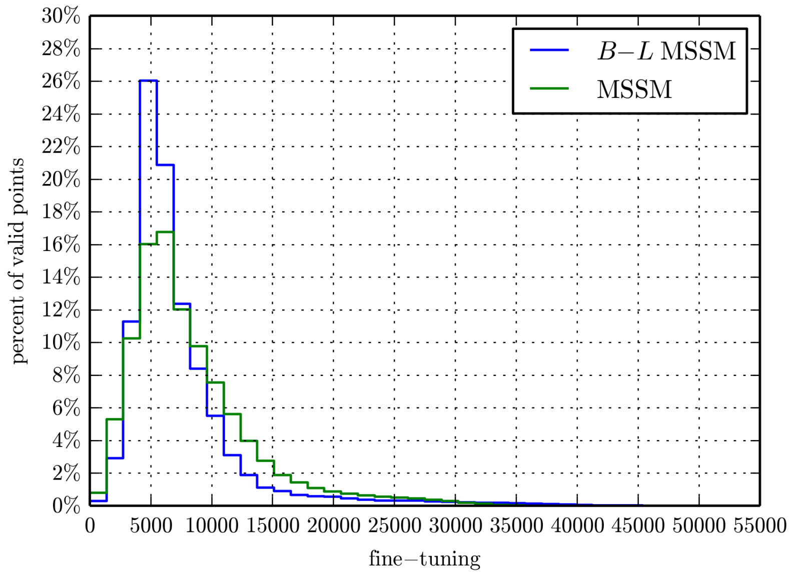

Figure 3.8: The blue line in the histogram shows the amount of fine-tuning required for valid points in the main scan of the simultaneous Wilson line B-L MSSM . Similarly, the green line specifies the amount of fine-tuning necessary for the valid points of the R-parity conserving MSSM–computed using the same statistical procedure as for the B-L MSSM with $M = 2700$ GeV and $f = 3.3$. The B-L MSSM shows slightly less fine-tuning, on average, than the MSSM.

break B-L symmetry as well as EW symmetry,

- 228,278 –the cyan points– also satisfy all sparticle lower mass bounds.
- 44,884 –the black points– satisfy all sparticle lower mass bounds and also give the measured value of the Higgs mass.

The distribution of black points can be explained from the fact that, while B-L breaking favors non-zero S-terms, very large S-terms can effect the RGE evolution of sfermion masses adversely. Since the effect of the S-terms depends on the charge of the sfermion in question, some sfermions will become quite heavy while others light or tachyonic. Therefore, in general, the valid points in our scan are a compromise between large S-terms, needed for a Z_R mass above its lower bound, and small S-terms needed to keep the sfermion RGEs under control.

Further discussion of the particle spectrum in this scenario is given in appendix A.

3.7 Fine-Tuning

A detailed discussion of the little hierarchy problem, fine-tuning and the Barbieri-Giudice (BG) method of quantifying the degree of fine-tuning was presented in [161]. Here, we simply give the results in the simultaneous Wilson line scenario discussed in this chapter. Unlike the quantitites presented above, which can differ substantially from the split Wilson line results in [161], the BG fine-tuning histogram for simultaneous Wilson lines in the B-L MSSM is very similar to that of the split Wilson line scenario. Be that as it may, for completeness, we present it here–along with the fine-tuning histogram for the R-parity conserving MSSM–in Figure 3.8. Note that the highest percentage of valid points require fine-tuning of the order of 1/4,000 – 1/5,000. However, there remain a small number of points with fine-tuning less than 1/1,000. As in the split Wilson line scenario, the simultaneous Wilson line B-L MSSM manifests somewhat less fine-tuning than the R-parity conserving MSSM.

3.8 String Threshold Corrections

As discussed in the introduction and section 3.3, and graphically illustrated for a valid initial point in Figure 3.4, the four gauge couplings of the B-L MSSM do not unify at $\langle M_U \rangle$ for simultaneous Wilson line masses; that is, when

$$\langle M_U \rangle = M_{\chi_{3R}} = M_{\chi_{B-L}} \ . \tag{3.44}$$

However, as described in the Introduction, the B-L MSSM arises on the observable orbifold plane of heterotic M-theory compactified on a Schoen Calabi-Yau threefold with $\pi_1 = \mathbb{Z}_3 \times \mathbb{Z}_3$ and a holomorphic vector bundle with $SU(4) \subset E_8$ structure group. That is, the B-L MSSM is a low energy effective theory of heterotic string theory. Hence, as discussed in numerous papers [122, 121, 150, 67, 66, 69, 127, 157, 156, 98, 128, 59, 15], it is expected that at *string tree level* all four gauge couplings, along with the dimensionless gravitational parameter

$$\sqrt{8\pi \frac{G_N}{\alpha'}} \tag{3.45}$$

where G_N is Newton's constant and α' is the string Regge slope, unify to a single parameter g_{string} at a "string unification" scale

$$M_{\text{string}} = g_{\text{string}} \times 5.27 \times 10^{17} \text{ GeV} \ . \tag{3.46}$$

The string coupling parameter g_{string} is set by the value of the dilaton, and is typically of $\mathcal{O}(1)$. A common value in the literature, see for example [66, 15, 156], is $g_{\text{string}} = 0.7$ which, for specificity, we will use henceforth. Therefore, we take α_{string} and the string unification scale to be

$$\alpha_{\text{string}} = \frac{g_{\text{string}}^2}{4\pi} = 0.0389, \quad M_{\text{string}} = 3.69 \times 10^{17} \text{ GeV} \tag{3.47}$$

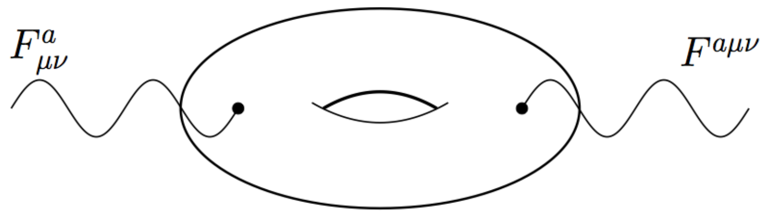

Figure 3.9: The worldsheet correlation function $\langle F^a_{\mu\nu} F^{a\mu\nu} \rangle$ on the genus-one string worldsheet is a typical example of heavy string threshold correction terms that need to be calculated.

respectively. Note that M_{string} is approximately an order of magnitude larger than $\langle M_U \rangle$. Below M_{string} however, the couplings begin to evolve according to the RGEs of effective field theory. This adds another–fourth– scaling regime to the three discussed at the beginning of section 3.4. This new regime is

- $M_{\text{string}} - \langle M_U \rangle$: The effective field theory in this regime remains that of the B-L MSSM with the couplings α_a, $a = 3, 2, 3R, BL'$ and the slope factors

$$b_3 = -3 \ , \ b_2 = 1 \ , \ b_{3R} = 7 \ , \ b_{BL'} = 6 \tag{3.48}$$

as in equation (3.31). However, the RGEs are now altered to become [1]

$$4\pi {\alpha_a}^{-1}(p) = 4\pi\alpha_{\text{string}}^{-1} - b_a \ln\big(\frac{p^2}{M_{\text{string}}^2}\big) + \tilde{\Delta}_a. \tag{3.49}$$

Note that the one-loop running couplings no longer unify exactly at M_{string}. Rather, they are "split" by dimensionless threshold effects. These arise predominantly from massive genus-one string modes that contribute to the correlation function $\left\langle F^a_{\mu\nu} F^{a\mu\nu} \right\rangle$ and, hence, to the α_a gauge couplings. This is depicted graphically in Figure 3.9.

Recall that we have found 44,884 valid initial points in the space of soft supersymmetry breaking dimensionful couplings– each of which satisfies all low energy phenomenological criteria. For *each* of these points, we can calculate–by scaling from the electroweak scale to $\langle M_U \rangle$– the four gauge couplings $\alpha_3(\langle M_U \rangle)$, $\alpha_2(\langle M_U \rangle)$, $\alpha_{3R}(\langle M_U \rangle)$ and $\alpha'_{BL}(\langle M_U \rangle)$. Note that in this analysis, we have defined an "average" SUSY scale M_{SUSY}, the B-L breaking scale M_{B-L}, as well as an "average" unification scale $\langle M_U \rangle$, in (28), (24) and (22)

[1]The RGE for the a-th gauge coupling generically contains the term $k_a \alpha_{\text{string}}^{-1}$ on the right-hand side, where k_a, $a = 3, 2, 3R, BL'$ are the associated string affine levels. However, these are all unity for the scaled gauge couplings of the B-L MSSM .

respectively. The RGEs have been scaled through the requisite intermediate regimes with the appropriate beta-function coefficients. That is, we have already taken into account the predominant threshold effects associated with each of these scales. For statistically "average" valid initial points–the vast majority of the phenomenologically acceptable initial soft SUSY breaking parameters–possible additional threshold effects arising from the "splitting" of particle masses around these scales are expected to be relatively small–and will be systematically ignored relative to the heavy string thresholds. That is, the $\tilde{\Delta}_a$, $a = 3, 2, 3R, BL'$ parameters in (50) will closely approximate the four heavy string gauge thresholds. With this input, using equation (3.48), $p = \langle M_U \rangle = 3.15 \times 10^{16}$ GeV and α_{string}, M_{string} given in (3.47), one can calculate the associated heavy string thresholds from (3.49); that is,

$$\tilde{\Delta}_a = 4\pi {\alpha_a}^{-1}(\langle M_U \rangle) - 4\pi\alpha_{\text{string}}^{-1} + b_a \ln\left(\frac{\langle M_U \rangle^2}{M_{\text{string}}^2}\right) . \tag{3.50}$$

for each $a = 3, 2, 3R, BL'$. Of course, these thresholds are expected to differ for each different valid initial point. It follows that one should analyze the thresholds statistically–graphing the dispersion of each as one runs over the 44,884 valid initial points. The histograms associated with each of these four thresholds are presented in Figure 3.10. To better understand the relationship of these different thresholds, we find it useful to plot all four of them in a single histogram. This is presented in Figure 3.11.

It is also useful to calculate the string threshold associated with the Abelian hypercharge coupling α_1 defined, using (3.25) and (3.26), by [2]

$$\alpha_1^{-1} = \frac{3}{5}\alpha_{3R}^{-1} + \frac{2}{5}\alpha_{BL'}^{-1} . \tag{3.51}$$

The associated statistical histogram is given in Figure 3.12. It is well-known [122, 66, 69, 150] that each string threshold breaks into two parts,

$$\tilde{\Delta}_a = \mathbb{Y} + \Delta_a , \tag{3.52}$$

where $\mathbb{Y}$ is a "universal" piece independent of the gauge group and Δ_a records the contributions of all massive string states as they propagate around the genus-one string worldsheet torus diagram shown in Figure 3.9. Note again that all string affine levels are unity in our normalization. As discussed in [66], an explicit calculation of the universal piece $\mathbb{Y}$ is difficult due to the presence of infrared divergences. However, the Δ_a threshold terms, although moduli dependent, can be directly calculated from string theory using a formulation given by V. Kaplunovsky in [122] and by Kaplunovsky and Louis in [121]. Such calculations are

[2]As with the other B-L MSSM gauge couplings, this scaled hypercharge coupling has string affine level $k_1 = 1$.

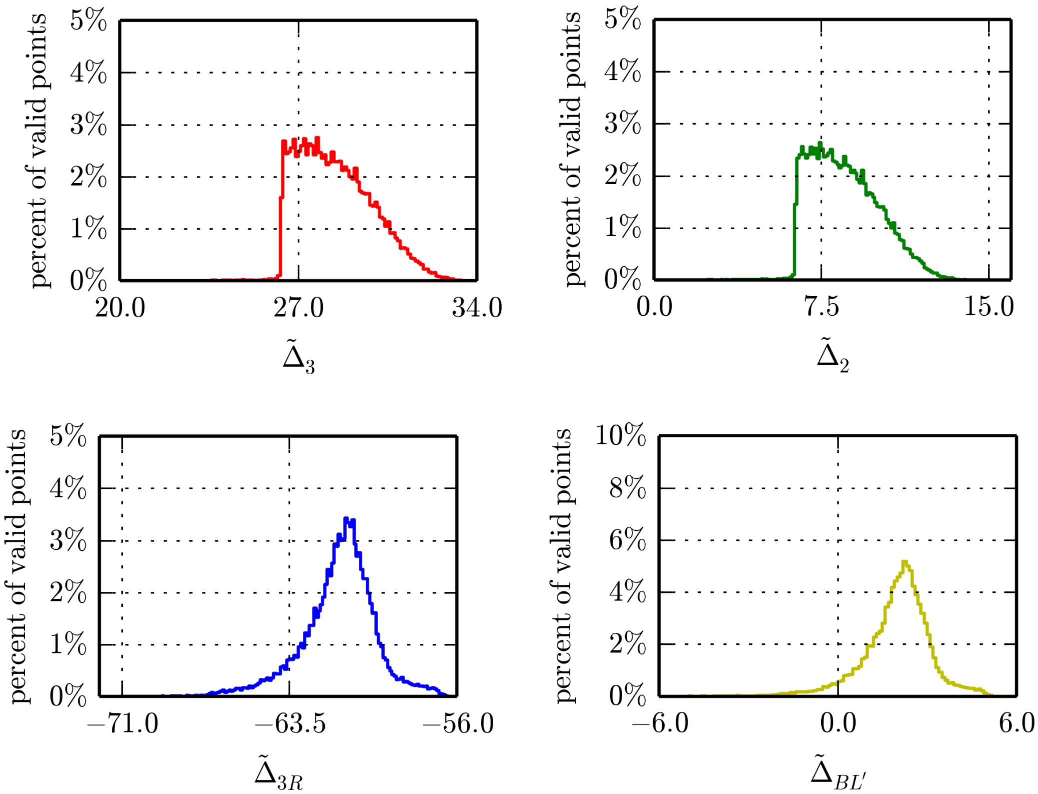

Figure 3.10: Histograms of each of the heavy string thresholds $\tilde{\Delta}_a$, $a = 3, 2, 3R, BL'$ arising from the $44,884$ phenomenologically valid points of our statistical survey. Each threshold value is plotted against the percentage of valid points giving rise to it. The bin width is 0.1.

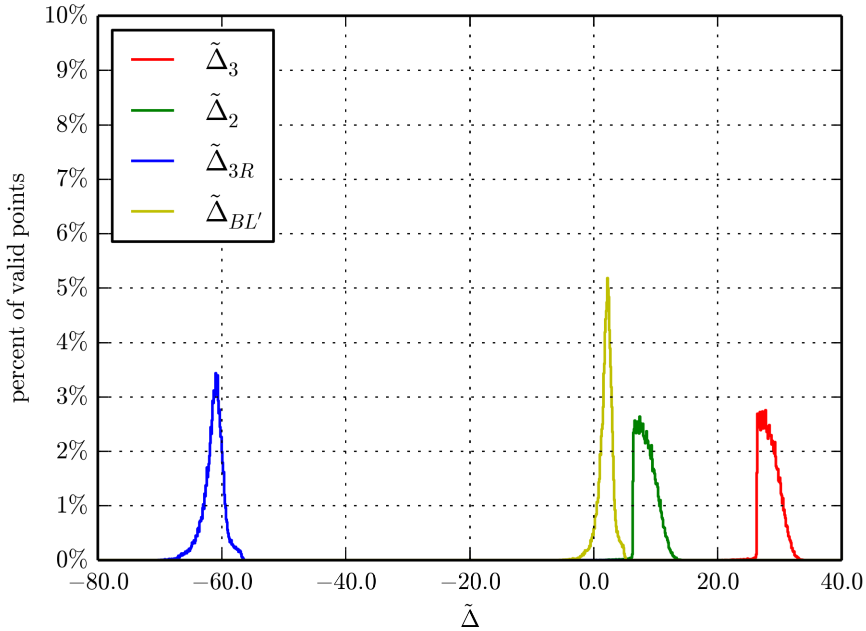

Figure 3.11: All four histograms in Figure 3.10 combined into a single graph to elucidate their relative occurrence and values.

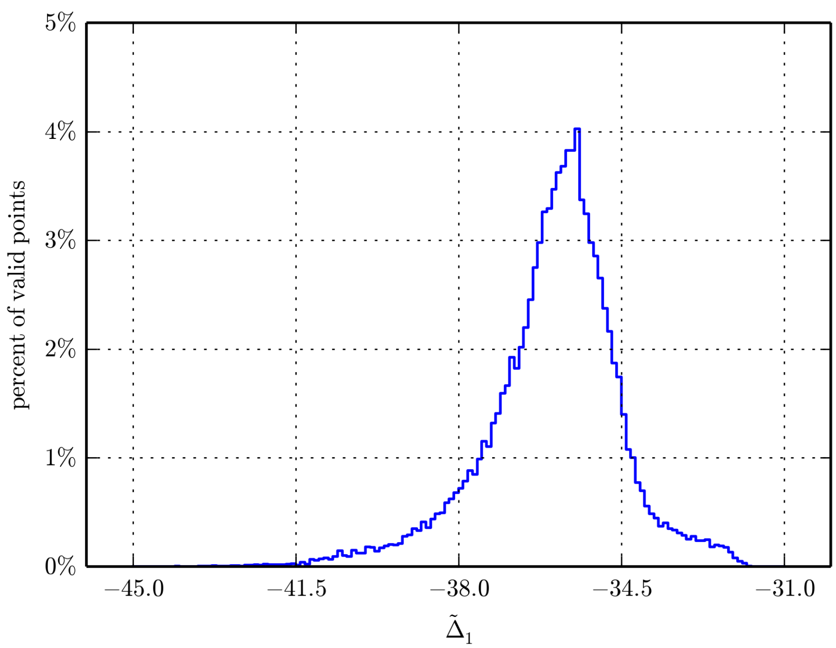

Figure 3.12: Histogram of the string hypercharge threshold $\tilde{\Delta}_1$ arising from the $44,884$ phenomenologically valid points of our statistical survey. Each threshold value is plotted against the percentage of valid points giving rise to it. The bin width is 0.1.

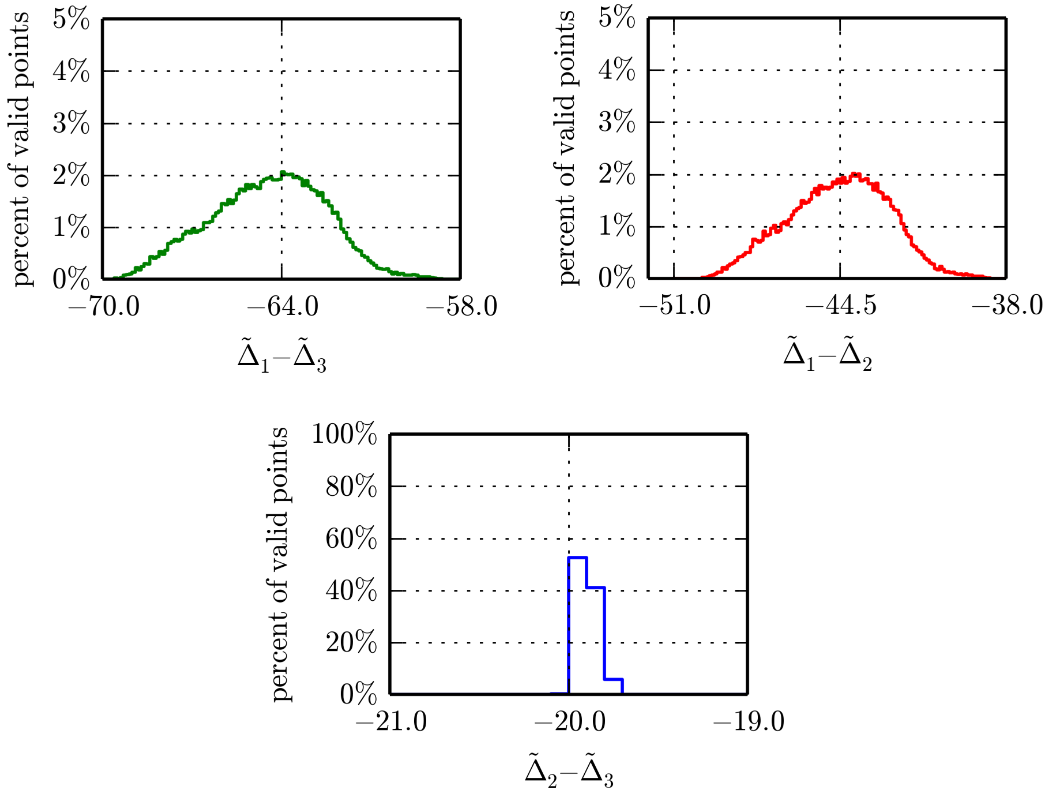

Figure 3.13: Histograms of our statistical predictions for the values of $\tilde{\Delta}_1 - \tilde{\Delta}_2$, $\tilde{\Delta}_1 - \tilde{\Delta}_3$, and $\tilde{\Delta}_2 - \tilde{\Delta}_3$. The third of these plots looks different because the quantity $\tilde{\Delta}_2 - \tilde{\Delta}_3$ falls in a very narrow range. The bin width in all three plots is 0.1.

heavily model dependent [67, 128, 15, 127] and, to date, have not been carried out in the B-L MSSM context. Be that as it may, it is useful to present our experimental predictions for $\tilde{\Delta}_1 - \tilde{\Delta}_2$, $\tilde{\Delta}_1 - \tilde{\Delta}_3$, and $\tilde{\Delta}_2 - \tilde{\Delta}_3$ –from which information about Δ_3, Δ_2 and Δ_1 can be inferred. The statistical results for these three quantities are presented in Figure 3.13. It would be very interesting to compare these results to direct calculations using [122, 121] in the B-L MSSM context.

Chapter 4

Sneutrino-Higgs Inflation

4.1 Introduction

In this chapter, we again consider the B-L MSSM theory; not, however, focussing on its realistic low energy phenomenology as in the previous chapter, but instead as a possible natural framework for a model of inflation, satisfying observational bounds from Planck2015 [3].

Specifically, we will do the following. In Section 4.2, we give review the Sneutrino-Higgs inflation model. We outline the basic formalism and present the specific parameters that lead to a successful theory of inflation–completely consistent with the Planck2015 data [3]. Using the statistical method for choosing the soft supersymmetry breaking parameters introduced in [161], we show in section 4.3 that there is a large and diverse set of phenomenologically valid initial conditions that are consistent with the appropriate cosmological parameters. We conclude this section by presenting a new result–specifically, we compute the range of values of the B-L breaking scale in this context and plot this as a histogram against the number of valid points at a given B-L scale. We find that the smallest B-L scale that one can attain in this formalism is $\simeq 2 \times 10^{12}$ GeV–and this for only a very small number of valid initial points. Although this is marginally acceptable, we would like to modify our formalism in such a way as to attain smaller values for the B-L scale. The reason is that we expect the reheating temperature to be of $\mathcal{O}(10^{13}$ GeV) and would, for simplicity, prefer that B-L breaking, and, hence, the breaking of baryon number, lepton number and R-parity, to occur at a much smaller scale. This allows one to separate the reheating epoch from the period of baryo- and lepto-genesis [169]. This is carried out in detail in appendix B, where we introduce an extension of our previous formalism that allows one to lower the B-L scale arbitrarily, while remaining completely phenomenologically realistic. In this appendix, we give an explicit example where the B-L scale is reduced to a range from a low of 10^6 GeV to well above 10^{13} GeV–all this occurring for phenomenologically acceptable initial conditions. We also give an explicit formula for the degree of fine-tuning required to set the B-L scale to any given value. Such a wide range is not required for cosmology. Hence, section 4.4 is devoted to explaining this new formalism, and then using it to alter the B-L scale to a more reduced range of values–namely from 10^{10} GeV to 10^{12} GeV. We find, in this context, that the greatest number of phenomenologically valid initial points occurs for a B-L scale of 10^{11} GeV and, hence, when specificity is required later in our analysis, we will choose this as the value of B-L symmetry breaking.

The remainder of this chapter concentrates on the post-inflationary epoch and reheating. In section 4.5, we give a detailed discussion of the classical behavior of both the inflaton and the Hubble parameter–ignoring for the time being the quantum mechanical decays of the inflaton into matter. We begin by calculating these quantities numerically and show that at a given time after the end of inflation, denoted by t_{osc}, the inflaton begins to oscillate around its minimum at zero. Then, using an iterative method, we analytically compute both the inflaton and Hubble parameter to a high degree of approximation. We show that this analytic solution becomes well-defined after a time, $t_{MD} > t_{osc}$, which marks the beginning of the period of matter-domination. The numerical and analytic results are plotted simultaneously and shown to very closely approximate each other for $t > t_{MD}$. In section 4.6, using these results, we compute the decay of the inflaton into matter and, hence, reheating. We show that there are four major decay channels–up-type standard model particles, charginos, neutralinos and gauge bosons–and analytically calculate the decay rates Γ of the inflaton into each of these species. We present the details of this analysis both in section 4.6 and in appendix C. In section 4.7, we analyze the full set of differential equations for the inflaton and Hubble parameter–now sourced by the decay rates and associated energy density of the matter species into which the inflaton decays–as well as the differential equations for the evolution of the matter itself. These equations are solved numerically for $t > t_{MD}$. The time-dependent behavior of the individual decay rates, as well as the behavior of the Hubble parameter, are plotted. Using these results, the fraction of the individual energy densities, $\frac{\rho_i}{\rho_{total}}$, including the inflaton density, are computed and plotted. The time of reheating, t_R, is defined to be the time at which the inflaton density vanishes–indicating that its energy has then been entirely transferred to matter. Finally, in section 4.8 we show that by t_R all the newly created matter species are in thermal equilibrium, and calculate the associated reheating temperature.

4.2 Sneutrino-Higgs Inflation

In this section, we review the theory of supersymmetric Sneutrino-Higgs inflation, first presented in [63], that arises within the context of the B-L MSSM [36, 18, 7, 85, 93, 159, 146, 145, 160, 161, 64] coupled to $N = 1$ supergravity.

To do this, we must begin by coupling the theory to $N = 1$ supergravity. The coupling of the four-dimensional observable sector of a generic M-theory compactification was carried out in [141]. This result is easily used to determine the explicit Lagrangian for the B-L MSSM coupled to $N = 1$ supergravity. The results are the following.

First, in the limit that the reduced Planck mass $M_P \to \infty$, the resulting theory is precisely the spectrum and Lagrangian of the flat space B-L MSSM –with an important addition. The compactification from eleven to four-dimensions potentially introduces "moduli" fields into the low energy theory. These correspond to the geometrical moduli of the Calabi-Yau threefold, the one geometrical radial modulus of the $S^1/\mathbb{Z}_2$ orbifold and the moduli of the $SU(4)$ vector bundle [73, 39, 40, 37]. It is expected that all moduli develop a non-perturbative potential energy which fixes their vacuum expectation values (VEVs) and gives them mass. In this chapter, we will assume that–with the exception of the two complex "universal" geometrical moduli– all of them are sufficiently heavy that they will not appear in the low energy theory. The real parts of the two universal moduli are the "breathing" modes of the CY and the orbifold respectively, and are formally defined to be the $a(x)$ and $c(x)$ fields in the 11-dimensional metric

$$ds^2 = g_{\mu\nu}dx^\mu dx^\nu + e^{2a(x)}\Omega_{AB}dx^A dx^B + e^{2c(x)}(dx^{11})^2 \ . \tag{4.1}$$

In the $M_P \to \infty$ limit, these universal moduli, although less massive, "decouple" from ordinary matter and can be ignored. However, for finite M_P this is no longer the case, and they must be included when we couple the B-L MSSM to supergravity. Specifically, when the B-L MSSM is coupled to $N = 1$ supergravity to order $\kappa^{2/3}$ in heterotic M-theory, the Kahler potential for the complex scalar fields is modified to become

$$K = -\ln(S + \bar{S}) - 3\ \ln(T + \bar{T} - \sum_i \frac{|C_i|^2}{M_P^2}) \ , \tag{4.2}$$

where the sum is over all complex scalar matter fields C_i in the B-L MSSM and

$$S = e^{6a} + i\sqrt{2}\sigma \ , \quad T = e^{2\hat{c}} + i\sqrt{2}\chi + \frac{1}{2}\sum_i \frac{|C_i|^2}{M_P^2} \tag{4.3}$$

with $\hat{c} = c + 2a$. The σ and χ fields arise as the duals of specific forms and are required by supersymmetry to extend a and c to the complex fields S and T respectively. The fact that the second term in (4.2) is a logarithm of a specific type will play a fundamental role in our analysis. Hence, it is important to note that the Kahler potential K in (4.2), as well as the specific field definitions given in (4.3), are identical to those found by Witten [172] within the context of the weakly coupled heterotic string. In addition, it was shown by a number of authors [47, 158, 135] that the off-shell structure of the $N = 1$ supergravity multiplet arising in heterotic string theory should be that of so-called "new minimal" supergravity. In [90], it was demonstrated that Kahler potentials of the above logarithmic form are consistent with this requirement. Finally, we find that to order $\kappa^{2/3}$ in heterotic M-theory, the gauge kinetic function in the observable sector is given by

$$f = S \ . \tag{4.4}$$

As with the Kahler potential, this form of the gauge kinetic function f is identical to that found in the weakly coupled heterotic string and is consistent with coupling to new minimal supergravity. Henceforth, unless otherwise specified, *we will work in units in which* $M_P = 1$.

Inserting the above expressions for K and f , as well as the superpotential W for the B-L MSSM [161], into the canonical expression for the Lagrangian of $N = 1$ matter/gauge fields coupled to supergravity [141], explicitly realizes our goal of coupling the B-L MSSM theory to $N = 1$ supergravity. Using this Lagrangian, we begin our analysis of the B-L MSSM as a potential framework for cosmological inflation. We first note that the moduli fields S and T, although appearing in the expressions for K and f, are assumed to have constant VEVs. One can then show that by appropriate rescaling of all matter fields, as well as all coupling parameters, that is, setting

$$C_i' = (\frac{3}{T+\bar{T}})^{1/2} C_i \ , \qquad g_a' = (\frac{2}{S+\bar{S}})^{1/2} g_a \ , \quad \text{for } a = 3, 2, 3R, BL' \ , \tag{4.5}$$

the S and T constants can be completely eliminated from the effective Lagrangian. Henceforth, we will drop the prime on all fields and couplings. It follows that the form of the effective Lagrangian is unaltered, but that the Kahler potential and the gauge kinetic function are now given by

$$K = -3 \ \ln(1 - \sum_i \frac{|C_i|^2}{3}) \ , \qquad f = 1 \ . \tag{4.6}$$

Recalling that the matter kinetic energy terms in the Lagrangian are $-K_{i\bar{j}} \partial_\mu C^i \partial^\mu C^{\bar{j}}$, it follows from (4.6) that for *small values of the fields* C_i the kinetic terms do not mix and are all canonically normalized. This is no longer true, however, for field values approaching the Planck scale. We continue by analyzing the remaining parts of the Lagrangian. To begin, we find that the pure gravitational action is simply given by

$$-\frac{1}{2} \int_{M_4} \sqrt{-g} R \ . \tag{4.7}$$

That is, in this analysis, *the pure gravitational action is canonical. We do not require any "non-canonical" coupling of matter to the curvature tensor* R.

Now consider the potential energy terms for the matter fields in the effective Lagrangian. These break into three types. The supersymmetric F-term and D-term potentials are given by

$$V_F = e^K \left(K^{i\bar{j}} D_i W \overline{D_{\bar{j}} W} - 3|W|^2 \right) \ , \qquad V_D = \frac{1}{2} \sum_a D_a^2 \tag{4.8}$$

respectively, where W is the B-L MSSM superpotential[1] [161],

$$W = Y_u Q H_u u_R^c - Y_d Q H_d d_R^c - Y_e L H_d e_R^c + Y_\nu L H_u \nu_R^c + \mu H_u H_d \ , \tag{4.9}$$

the D_a, $a = 3, 2, 3R, BL$ functions are

$$D_a^r = -g_a \frac{\partial K}{\partial C_i} [T_{(a)}^r]_i{}^j C_j = \frac{g_a}{\left(1 - \frac{1}{3}\sum_i |C_i|^2\right)} \mathcal{D}_{(a)}^r \ , \qquad \mathcal{D}_{(a)}^r = -\overline{C}^i [T_{(a)}^r]_i{}^j C_j \tag{4.10}$$

and $T_{(a)}^r$, $r = 1, \ldots, \dim G_a$ are the generators of the group G_a. For the B-L MSSM we find

$$\begin{aligned} -\mathcal{D}_{(3)}^r = (\overline{\tilde{u}_{R,\mathrm{f}}^c})^m [\Lambda^r]_m{}^n (\tilde{u}_{R,\mathrm{f}}^c)_n \quad &+ \quad (\overline{\tilde{d}_{R,\mathrm{f}}^c})^m [\Lambda^r]_m{}^n (\tilde{d}_{R,\mathrm{f}}^c)_n \\ +(\overline{\tilde{u}_{L,\mathrm{f}}})^m [\Lambda^r]_m{}^n (\tilde{u}_{L,\mathrm{f}})_n \quad &+ \quad (\overline{\tilde{d}_{L,\mathrm{f}}})^m [\Lambda^r]_m{}^n (\tilde{d}_{L,\mathrm{f}})_n \ , \end{aligned} \tag{4.11}$$

$$-\mathcal{D}_{(2)}^r = (\overline{H}_u)^k [\tau^r]_k{}^l (H_u)_l + (\overline{H}_d)^k [\tau^r]_k{}^l (H_d)_l + (\overline{\tilde{Q}}_\mathrm{f})^k [\tau^r]_k{}^l (\tilde{Q}_\mathrm{f})_l + (\overline{\tilde{L}}_\mathrm{f})^k [\tau^r]_k{}^l (\tilde{L}_\mathrm{f})_l \ , \tag{4.12}$$

$$\begin{aligned} -\mathcal{D}_{(3R)} \quad = \quad & \tfrac{1}{2} \left(|H_u^+|^2 + |H_u^0|^2 - |H_d^0|^2 - |H_d^-|^2 \right) \\ & -\tfrac{1}{2} |\tilde{\nu}_{R,\mathrm{f}}^c|^2 + \tfrac{1}{2} |\tilde{e}_{R,\mathrm{f}}^c|^2 - \tfrac{1}{2} |\tilde{u}_{R,\mathrm{f}}^c|^2 + \tfrac{1}{2} |\tilde{d}_{R,\mathrm{f}}^c|^2 \ , \end{aligned} \tag{4.13}$$

$$\begin{aligned} -\mathcal{D}_{(BL)} \quad = \quad & -|\tilde{\nu}_{L,\mathrm{f}}|^2 - |\tilde{e}_{L,\mathrm{f}}|^2 + \tfrac{1}{3} |\tilde{u}_{L,\mathrm{f}}|^2 + \tfrac{1}{3} |\tilde{d}_{L,\mathrm{f}}|^2 \\ & +|\tilde{\nu}_{R,\mathrm{f}}^c|^2 + |\tilde{e}_{R,\mathrm{f}}^c|^2 - \tfrac{1}{3} |\tilde{u}_{R,\mathrm{f}}^c|^2 - \tfrac{1}{3} |\tilde{d}_{R,\mathrm{f}}^c|^2. \end{aligned} \tag{4.14}$$

The subscript $\mathrm{f} = 1, 2, 3$ labels the families, the matrices Λ^r and τ^r are the generators of $SU(3)_C$ and $SU(2)_L$ respectively, while $m, n,$ are color indices and k, l are $SU(2)$ indices.

[1] Our notation defers slightly from the previous chapter; to emphasis the fact that the $SU(2)_L$ single fields u^c, d^c, e^c, ν^c correspond to "right-handed" fields, we add the subscript R, e.g. $e^c \to e_R^c$. Additionally, for clarity, in the remainder of this chapter we will continue to denote the rescaled gauge group as $U(1)_{B-L}$; that is, without the prime.

In addition, there is a soft supersymmetry breaking potential given by

$$
\begin{aligned}
V_{soft} &= m_{\tilde{Q}_{\rm f}}^2|\tilde{Q}_{\rm f}|^2 + m_{\tilde{u}^c_{R,{\rm f}}}^2|\tilde{u}^c_{R,{\rm f}}|^2 + m_{\tilde{d}^c_{R,{\rm f}}}^2|\tilde{d}^c_{R,{\rm f}}|^2 + m_{\tilde{L}_{\rm f}}^2|\tilde{L}_{\rm f}|^2 + m_{\tilde{\nu}^c_{R,{\rm f}}}^2|\tilde{\nu}^c_{R,{\rm f}}|^2 + m_{\tilde{e}^c_{R,{\rm f}}}^2|\tilde{e}^c_{R,{\rm f}}|^2 \\
&+ m_{H_u}^2|H_u|^2 + m_{H_d}^2|H_d|^2 \\
&+ \left(a_{u,{\rm f}}\tilde{Q}_{\rm f}H_u\tilde{u}^c_{R,{\rm f}} - a_{d,{\rm f}}\tilde{Q}_{\rm f}H_d\tilde{d}^c_{R,{\rm f}} - a_{e,{\rm f}}\tilde{L}_{\rm f}H_d\tilde{e}^c_{R,{\rm f}} + a_{\nu,{\rm f}}\tilde{L}_{\rm f}H_u\tilde{\nu}^c_{R,{\rm f}} + bH_uH_d + h.c.\right) ,
\end{aligned}
\tag{4.15}
$$

where the a_i are the cubic scalar terms, and we assume that each of these dimension one coefficients is proportional to the associated Yukawa coupling. In all three potentials, the sum over families is implicit.

It is possible to find solutions for which the D-term potential V_D vanishes, the so-called "D-flat" directions. Such a solution will be central to the construction of our inflationary potential. In this chapter, to satisfy the D-flatness condition, we restrict ourselves to fields that are not charged under $SU(3)_C$ or under $U(1)_{EM}$. Hence, we are naturally lead to the field space configuration

$$
H_u^0 = \tilde{\nu}^c_{R,3} = \tilde{\nu}_{L,3} \ , \tag{4.16}
$$

with all other fields set to zero. We note that only in a model such as the B-L MSSM with right-handed neutrino superfields would such a D-flat direction arise.

4.2.1 Inflationary Potential

From our preferred D-flat direction (4.16), we construct an inflationary potential as follows. First, define three new fields ϕ_i, $i = 1, 2, 3$ using

$$
\begin{aligned}
H_u^0 &= \tfrac{1}{\sqrt{3}}\left(\phi_1 - \phi_2 - \phi_3\right) , \\
\tilde{\nu}_{L,3} &= \tfrac{1}{\sqrt{3}}\phi_1 + \left(\tfrac{1}{2} + \tfrac{1}{2\sqrt{3}}\right)\phi_2 + \left(\tfrac{1}{2\sqrt{3}} - \tfrac{1}{2}\right)\phi_3, \\
\tilde{\nu}^c_{R,3} &= \tfrac{1}{\sqrt{3}}\phi_1 + \left(\tfrac{1}{2\sqrt{3}} - \tfrac{1}{2}\right)\phi_2 + \left(\tfrac{1}{2} + \tfrac{1}{2\sqrt{3}}\right)\phi_3.
\end{aligned}
\tag{4.17}
$$

Recall that all other fields have been set to zero. The field ϕ_1 corresponds to the D-flat field direction while ϕ_2 and ϕ_3 are two orthogonal directions. One may verify this by restricting attention to this three-dimensional subspace and noting that the D-term potential vanishes when $\phi_2 = \phi_3 = 0$ for any value of ϕ_1. For future reference, we note that

$$
\phi_1 = \tfrac{1}{\sqrt{3}}\left(H_u^0 + \tilde{\nu}_{L,3} + \tilde{\nu}^c_{R,3}\right) \ , \qquad m^2 = \frac{1}{3}(m_{H_u}^2 + m_{\tilde{L}_3}^2 + m_{\tilde{\nu}^c_{R,3}}^2) \ . \tag{4.18}
$$

where m^2 is the quadratic soft mass squared associated with ϕ_1. Setting all fields to zero with the exception of ϕ_1, the V_D potential vanishes and the Lagrangian becomes

$$\mathcal{L} = -\frac{1}{\left(1 - \frac{1}{3}|\phi_1|^2\right)^2}\partial_\mu \overline{\phi}_1 \partial^\mu \phi_1 - V_F(\phi_1) - V_{soft}(\phi_1) \ , \tag{4.19}$$

where

$$V_F(\phi_1) = \frac{3|\phi_1|^2\left(\mu^2 + Y_{\nu 3}^2|\phi_1|^2\right)}{\left(3 - |\phi_1|^2\right)^2} \ , \qquad V_{soft}(\phi_1) = m^2|\phi_1|^2 \ . \tag{4.20}$$

Here $Y_{\nu 3}$ is the third-family sneutrino Yukawa coupling and μ is the usual supersymmetric Higgs parameter[2].

Since this Lagrangian is symmetric under global $U(1)$ transformations, we choose our inflaton to be the real $\overline{\phi}_1 = \phi_1$ field, the potential for the imaginary part of ϕ_1 simply being flat. That is, the inflaton is a single real-valued field, which (somewhat abusing notation) we continue to denote by ϕ_1. We want to emphasize that

- *The inflaton is a linear combination of the real parts of H_u^0, $\nu_{L,3}$ and $\nu_{R,3}$ and, hence, is composed of fields already appearing in the B-L MSSM .*

In order to to canonically normalize the kinetic energy term, we make a field redefinition to a real scalar ψ given by

$$\phi_1 = \sqrt{3}\tanh\left(\frac{\psi}{\sqrt{6}}\right) . \tag{4.21}$$

In terms of the new field ψ, Lagrangian (4.19) now becomes

$$\mathcal{L} = -\frac{1}{2}\partial_\mu \psi \partial^\mu \psi - V_F(\psi) - V_{soft}(\psi) \ , \qquad V_{soft}(\psi) = 3m^2 \tanh^2\left(\frac{\psi}{\sqrt{6}}\right) \ , \tag{4.22}$$

where $V_F(\psi)$ is obtained from the first term in (4.20) using (4.21).

4.2.2 The Primordial Parameters

For an *arbitrary* potential function $V(\psi)$, one defines the "slow-roll" parameters to be $\epsilon = \frac{1}{2}\left(V'/V\right)^2$, $\eta = V''/V$. For there to be an interval of slow-roll inflation, these parameters must satisfy the conditions that $\epsilon, |\eta| \ll 1$. Assuming this to be the case for some range of ψ, one defines the end of the slow-roll period to be the smallest value of ψ for which $\epsilon = 1$. This will be denoted by ψ_{end}. To satisfy the CMB data, it is necessary that there be at least 60 e-foldings of inflation preceding ψ_{end}. The value of the field which precedes ψ_{end} by *exactly* 60 e-folds is found by integrating the function $1/\sqrt{2\epsilon}$, and will be denoted by ψ_*.

[2] Note that the contribution from the cubic soft SUSY breaking term to V_{soft} is negligible.

The spectral index n_s and the scalar-to-tensor ratio r are then defined to be

$$n_s \simeq 1 + 2\eta_* - 6\epsilon_* \ , \qquad r \simeq 16\epsilon_* \ , \tag{4.23}$$

where the label "$_*$", here and below, denotes quantities that are evaluated at ψ_*. In addition, the Planck2015 normalization of the CMB fluctuation amplitude requires that the energy scale of inflation satisfies

$$V_*^{1/4} = 1.88\left(\frac{r}{0.10}\right)^{1/4} \times 10^{16} \text{ GeV} \ , \tag{4.24}$$

where we have restored dimensionful units for clarity.

With this in mind, let us analyze our specific potential $V = V_F + V_{soft}$ presented above. We begin by considering V_{soft} in (4.22) alone, momentarily ignoring V_F. We find that the requirement of 60 e-folds of inflation leads to the results that

$$\psi_{end} = \ 1.21 \ , \qquad \psi_* = 6.23 \ . \tag{4.25}$$

It follows that the primordial quantities in (4.23) satisfy

$$n_s \simeq 0.967 \ , \qquad r \simeq 0.00326 \ , \tag{4.26}$$

which are consistent with the Planck2015 bounds [3] . Putting the value of the r parameter into (4.24), then implies

$$V_*^{1/4} = 7.97 \times 10^{15} \text{ GeV} \quad \Longrightarrow \quad m = 1.55 \times 10^{13} \text{ GeV} \ . \tag{4.27}$$

Recalling that m is typical of the soft mass parameters in the B-L MSSM then requires, within the context of this analysis, that

- *In order to be consistent with the Planck2015 cosmological data, supersymmetry must be broken at a high scale of* $\mathcal{O}(10^{13}$ GeV$)$.

The formalism of the B-L MSSM was extended to allow for an arbitrarily high SUSY breaking scale in [64]. In addition, note from (4.25) that ψ must be trans-Planckian at the start of inflation. It is straightforward to show, however, that the physical fields H_u^0, $\nu_{3,R}$ and $\nu_{3,L}$ are all sub-Planckian during the entire inflationary epoch.

The potential $V_{soft}(\psi)$ has already arisen in other contexts, such as supergravity models of inflaton chiral multiplets [167, 120, 82, 80]. Here, however, the inflaton is a fundamental component field in a theory of supersymmetric particle physics. Furthermore, note that

- *Our* V_{soft} *potential arises entirely from the associated soft supersymmetry breaking quadratic term, rescaled to canonically normalize the kinetic energy.*

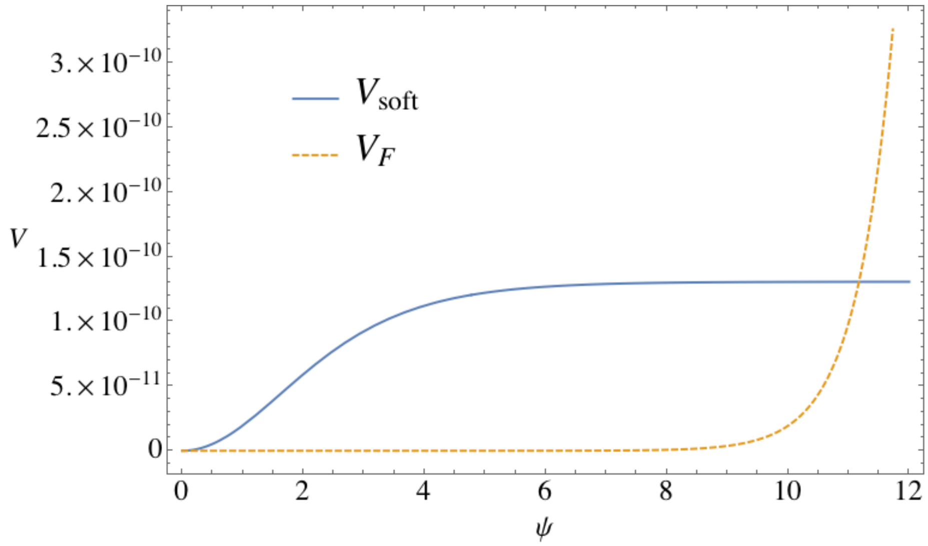

Figure 4.1: The blue line is a plot of V_{soft} for the soft mass value $m = 1.58 \times 10^{13}$ GeV in equation (4.31). The orange line is a graph of V_F for the parameters $Y_{\nu 3} \sim 10^{-12}$ and $\mu = \ 1.20 \times 10^{10}$ GeV in equation (4.28).

Reintroducing the F-term potential given in the first term of (4.20), we require that it makes at most a small correction to the above results–that is, it must be suppressed with respect to the soft mass potential[3]. In previous analyses [161], we found that the third family sneutrino Yukawa coupling $Y_{\nu 3}$ is typically very small, of order 10^{-12}. However, to achieve sufficient suppression of V_F, the μ parameter is now forced to be at least three orders of magnitude smaller than the soft mass scale; that is, $\mu \sim 10^{10}$ GeV. For specificity, we choose the value of μ to be close to its highest possible value:

$$\mu = \ 1.20 \times 10^{10} \text{ GeV} \ . \tag{4.28}$$

It follows that for 60 e-foldings of inflation

$$\psi_{end} \simeq 1.21 \ , \quad \psi_* \simeq 6.25 \tag{4.29}$$

and, hence, that

$$n_s \simeq 0.969 \ , \qquad r \simeq 0.00334 \ , \tag{4.30}$$

again consistent with the Planck2015 data. Attempting to take μ significantly larger than (4.28), will lead to values of n_s and r which are inconsistent with this data. It follows from

[3]We thus avoid the "η-problem" in supergravity models of inflation: that is, unless it is subdominant, the F-term potential would lead η to be of $\mathcal{O}(1)$, violating the slow-roll conditions.

(4.28) and (4.30) that

$$V_*^{1/4} = 8.07 \times 10^{15}\ \text{GeV}\ , \quad m = 1.58 \times 10^{13}\ \text{GeV}\ . \tag{4.31}$$

The potential $V_{soft}(\psi)$ is plotted as the blue line in Figure 1 for the parameter m in (4.31). Similarly, the F-term potential $V_F(\psi)$ is plotted as the dashed orange line in Figure 1 using parameter μ in (4.28). It follows from the first term in (4.20) that V_F has a pole for $\phi_1 = \sqrt{3}$ and, hence, using (4.21), that this function grows without bound as $\psi \to \infty$. Note that V_F is neglible compared to V_{soft} from $\psi = 0$ all the way up until $\psi \sim 8$, at which point V_F increases very rapidly. That is, the F-term potential acts as a natural "cut-off" for the inflationary potential V_{soft} for values of $\psi \gtrsim 8$. This gives a supersymmetric realization of the "Inflation without Selfreproduction" mechanism introduced in [153].

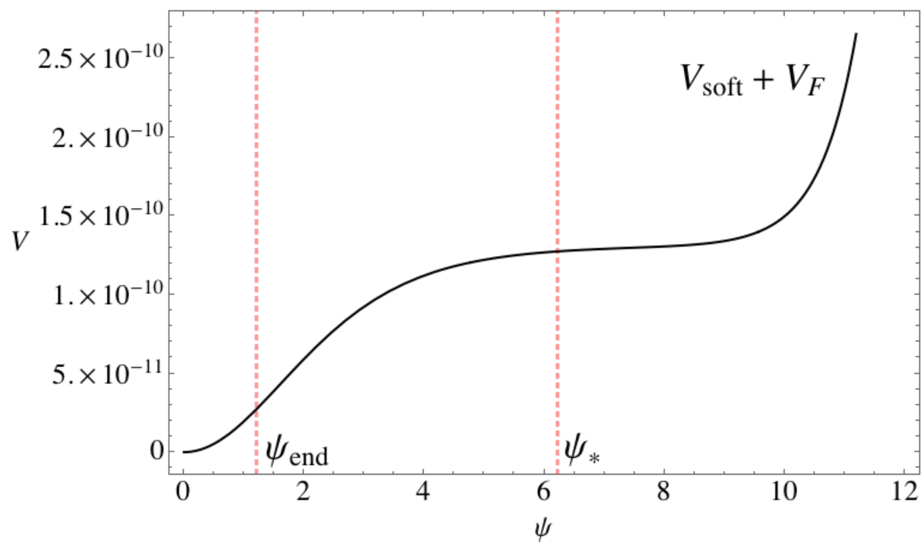

Figure 4.2: The black line is a graph of the potential $V_{soft} + V_F$ for the parameters $m = 1.58 \times 10^{13}$ GeV, $Y_{\nu 3} \sim 10^{-12}$ and $\mu =\ 1.20 \times 10^{10}$ GeV. For these values of the parameters, the vertical red dashed lines mark $\psi_{end} \simeq 1.21$ and $\psi_* \simeq 6.25$ respectively.

The complete potential in (4.22), that is, the sum of $V_{soft} + V_F$, is plotted in Figure 2. It will, for suitable values of couplings $Y_{\nu 3}, \mu$ and soft mass m, produce a period of inflation that is consistent with current cosmological bounds obtained by Planck2015.

To summarize, our inflationary potential is the sum of $V_{soft} + V_F$ for the field ϕ_1, with the parameters taken to be (restoring the usual mass parameters)

$$m = 1.58 \times 10^{13}\ \text{GeV}\ , \quad Y_{\nu 3} \sim 10^{-12}\ , \quad \mu = 1.20 \times 10^{10}\ \text{GeV}\,. \tag{4.32}$$

4.2.3 Stability

Within the B-L MSSM , our inflaton field ϕ_1 defines a single direction in a complicated, many-dimensional field space. For this to be a viable inflationary model, one must demonstrate that, during the inflationary epoch, this direction is safe from displacements in field directions orthogonal to ϕ_1. That is, no deviation away from our trajectory forces us to exit slow-roll inflation and continue down another direction in field space. However, we allow for displacements that lead to an orthogonal field attaining a VEV, provided this is small compared to the net field displacement of ϕ_1 during inflation–which is of $\mathcal{O}(1)$ in Planck units. This defines our criterion for the stability of the inflationary trajectory.

In order to show that our trajectory meets this criterion, we examine the second derivative matrix of the scalar potential evaluated at each value of ϕ_1, where the derivatives are with respect to the real and imaginary components of a given field in the B-L MSSM . For clarity we consider only the contributions due to the F- and D-term potentials. We first find that the second derivative matrix is block diagonal, with most of the blocks being four-by-four, involving a right-handed squark or slepton and their corresponding left-handed partner. Two exceptions arise: a six-by-six block involving the fields ϕ_2, ϕ_3 and H_d^0, and an eight-by-eight block involving the fields $e^c_{R,3}, e_{L,3}, H_u^+$ and H_d^-. It is clear why the larger blocks arise–any gauge invariant piece in the Lagrangian that involves the constituent fields of ϕ_1 must involve the fields in the six-by-six and eight-by-eight blocks.

All of the up-type squark blocks and the first and second family sneutrino blocks correspond to stable directions in field space; that is, once diagonalized, they have positive mass-squared eigenvalues. The down-type squarks and the first and second family selectron blocks each contain a pair of negative eigenvalues, corresponding to two unstable directions. Diagonalizing and examining these unstable directions, we are able to conclude that, while the inflaton may initially roll away, the D-term potential provides a sufficiently large positive contribution that the size of the resulting VEV is always of order 10^{-5} or less in Planck units. The eight-by-eight and six-by-six blocks also have positive eigenvalues. However, the fields in the six-by-six block grow a linear term for any non-zero value of ϕ_1. This results in a set of displacements, which are again at most order 10^{-5}. We thus conclude that the inflationary trajectory, ignoring roll-offs that are much smaller than the distance in field space traversed during inflation, is stable.

Finally, we have redone the above computations including the quadratic and cubic soft supersymmetry breaking terms in addition to the F- and D-term potentials. The result is that the above conclusions are not changed. That is, the inflationary trajectory, ignoring roll-offs that are much smaller–on the order of 10^{-5} or less–than the distance traversed by ϕ_1 during inflation, is stable.

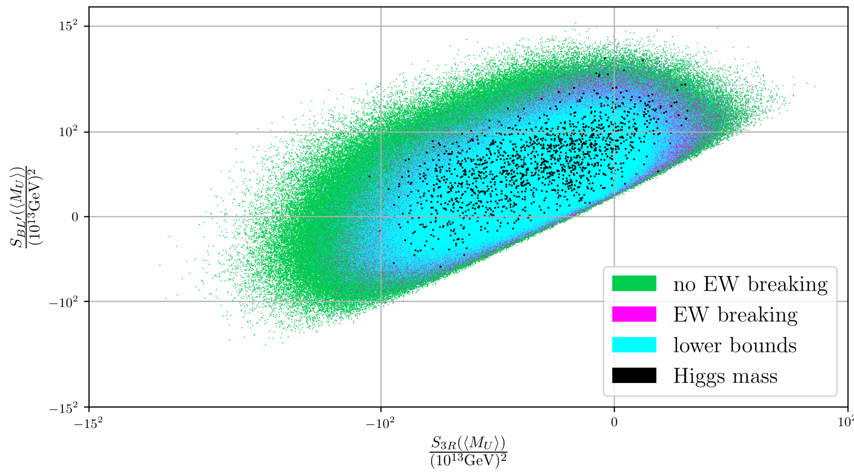

Figure 4.3: Results from generating 50 million sets of initial data where $m_{H_u}^2$ is fixed by the cosmological constraint. We find that 4,209,300 points break B-L but not electroweak symmetry, and 860,084 points appropriately break both B-L and electroweak symmetry. Of the latter, 545,753 points are consistent with current LHC bounds on sparticle searches. Finally, we have 1406 points which satisfy all these conditions and are within the 2σ window of the measured Higgs mass. The black points are enlarged for legibility.The axes are two dominant parameters of the renormalization group equations and are defined in [161].

4.3 The Search for Valid Low Energy Points

We now use the formalism presented in [161] to statistically search the space of initial soft supersymmetry breaking parameters for those points which 1) satisfy the Planck2015 data by using the parameters presented in (4.32) while 2) simultaneously being consistent with all present low energy phenomenological data–that is, appropriate B-L and EW breaking, all lower bounds on SUSY sparticles and the experimentally measured lightest neutral Higgs mass. Since the relevant phenomenological data is usually presented in GeV, we will work in these units for this analysis, including the discussion of lowering the B-L scale presented in the following section. Suffice it here to say that initial soft SUSY breaking parameters are analyzed by randomly scattering all of them, with the exception of m_{H_u}, in the interval $[m/f, fm]$, where $m = 1.58 \times 10^{13}$ GeV is the cosmologically consistent mass presented in (4.32) and $f = 3.3$. The parameter m_{H_u} is then fixed, for each initial throw, by demanding that it satisfy the cosmological constraint given by (4.18) and (4.32). In this chapter, to be consistent with the analysis below, we extend the results given in [64] by statistically throwing the initial parameters 50 million times instead of the 10 million times presented previously. The results satisfying both requirements 1) and 2) are shown as the "valid" black points in Figure 4.3.

It is of interest to use the formalism presented in [161] to compute the B-L breaking scale associated with each of the 1406 valid black points presented in Figure 4.3. As we will see below, knowledge of the B-L breaking scale is important in the discussion of reheating. Therefore, we have computed the B-L scales for all valid black points and present a statistical graph of the results in Figure 4.4. For completeness, we have indicated the percentage of points for which the B-L scale M_{BL} exceeds or is smaller than the supersymmetry breaking scale M_{SUSY} defined in [161]. This is referred to as "right-side-up" and "upside-down" B-L breaking respectively. We note that the smallest B-L scale associated with the valid

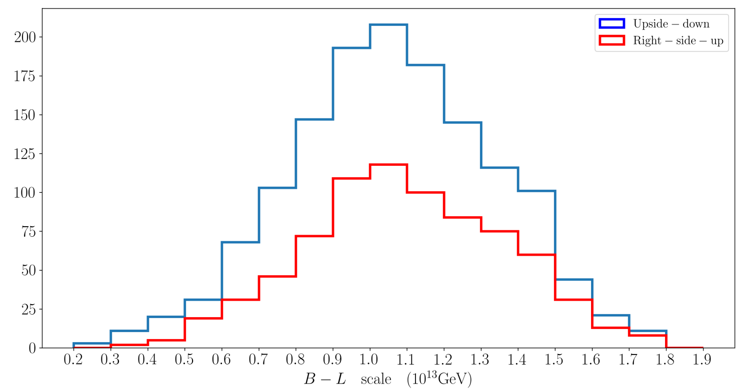

Figure 4.4: Plot of the $U(1)_{B-L}$ breaking scale for the 1406 valid black points shown in Figure 4.3. The B-L and supersymmetry breaking scales are computed using the formalism presented in [161]. We indicate what fraction of each bin consists of those cases in which $M_{BL} > M_{SUSY}$ (right-side-up), and in which $M_{BL} < M_{SUSY}$ (upside-down). For example, between 1.0 and 1.1 $\times 10^{13}$ GeV the number of right-side-up valid points is ≈ 120 whereas the number of upside-down valid points is $\approx 210 - 120 = 90$.

black points is approximately 2×10^{12} GeV. As we will see in the following, appropriate reheating will occur most naturally for values of $M_{BL} \lesssim 10^{12}$ GeV. It is important, therefore, to see if one can modify the initial statistical input of the soft breaking parameters so that one obtains physically realistic valid black points for which M_{BL} is substantially smaller than 10^{12} GeV. The answer is affirmative, as will be shown in the following section.

4.4 Lowering the B-L scale

We would like to arbitrarily lower the scale of B-L breaking for a given set of initial data so that the RGE evolution of this data is consistent with all phenomenological constraints; that is, 1) the electroweak scale is radiatively broken with the correct Z and W boson masses, 2) all sparticle masses exceed their present experimental lower bounds and 3) the Higgs mass is given to within 2σ of its measured value of 125 GeV. To accomplish this, we will no longer compute the scale of B-L breaking as an "output" of the initial class of data discussed in [161] and used in the previous section. Rather, we will input the B-L scale as an arbitrary parameter as part of the initial data.

To do this, we recall from [161] that the $U(1)_{B-L}$ symmetry breaks when the right-handed sneutrino $\tilde{\nu}_3^c$ obtains a non-vanishing vacuum expectation value. This occurs when the parameter $m^2_{\tilde{\nu}_3^c}$ turns negative as one runs down in energy-momentum from the unification scale $\langle M_U \rangle$ defined in [64]. Since natural reheating will require a lower value of M_{BL}, we will assume that our B-L scale will be less than the scale of SUSY breaking; that is, we will only consider the "upside-down" hierarchy where $M_{BL} < M_{SUSY}$. The B-L scale M_{BL} is defined in [161] via the recursive relation

$$M_{Z_R}(M_{BL}) = M_{BL}\,, \tag{4.33}$$

where M_{Z_R} is the mass of the Z' boson, which receives a mass when the right-handed sneutrino develops a vacuum expectation. We also have the relation

$$M_{Z_R} \simeq \sqrt{2}|m_{\tilde{\nu}_3^c}|\ . \tag{4.34}$$

It follows that

$$M^2_{BL} \simeq -2m^2_{\tilde{\nu}_3^c}(M_{BL})\,, \tag{4.35}$$

where $m^2_{\tilde{\nu}_3^c} < 0$ when B-L is broken. From this relation, we see that fixing M_{BL} at a particular value demands that $m^2_{\tilde{\nu}_3^c}(M_{BL})$ also be fixed. If we continue to randomly generate $m_{\tilde{\nu}_3^c}$ at the unification scale $\langle M_U \rangle$, as was done in all previous analyses, it is exceedingly improbable that, upon running the sneutrino mass down, we will arrive at our desired value of $m^2_{\tilde{\nu}_3^c}(M_{BL})$ and, hence, of M_{BL}. This problem is concretely expressed by the results shown in Figure 4.4.

We therefore change our approach from previous work, and no longer randomly generate the sneutrino mass $m^2_{\tilde{\nu}_3^c}$ at the unification scale. Instead, we specify the desired B-L breaking scale and use (4.35) and the relevant RGEs to *determine the required soft sneutrino mass parameter at* $\langle M_U \rangle$. Once this process is accomplished, we then have a complete set of initial data against which the phenomenological constraints 1), 2) and 3) above can be verified. To carry this out in detail relies heavily on a generalization of the formalism for the renormalization group equations of the B-L MSSM previously given in [161]. This is technically non-trivial and, hence, we present the mathematical details in appendix B of this thesis. In this section, we will simply use the results obtained in that appendix.

As discussed in subsection B.2, one can choose a range over which one wants to input the B-L scale and then, using the formalism presented there, determine the phenomenologically acceptable valid black points whose B-L scales lie in that range. In the appendix, we

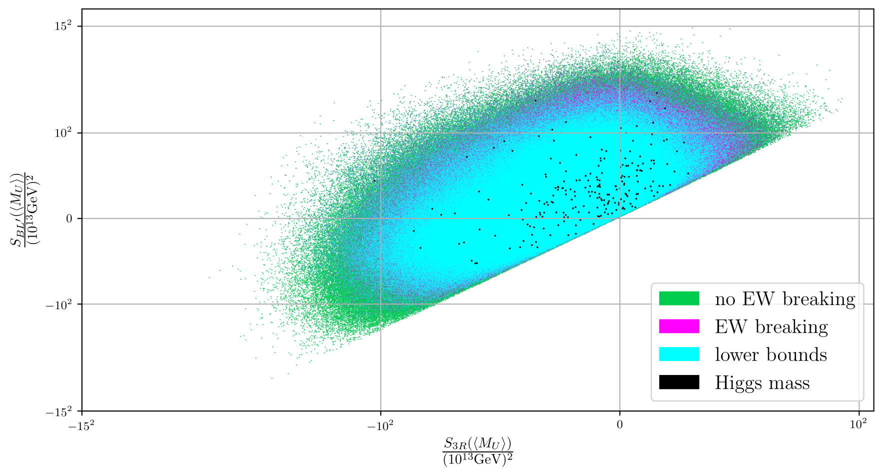

Figure 4.5: Results from generating 50 million sets of initial data where the B-L scale is chosen from a log-uniform distribution between 10^{10} GeV and 10^{12} GeV. We find that 5,949,281 points break B-L but not electroweak symmetry, and 1,937,174 points break B-L and electroweak symmetry. Of the latter 1,283,484 points are consistent with current LHC bounds on sparticle searches. Finally, we have 215 points which satisfy all these conditions and are within the 2σ window of the measured Higgs mass.

carried this out over a very wide range of B-L scales, specifically from 10^6 GeV to 10^{14} GeV. However, for the discussion of reheating in this chapter, such a wide range for M_{BL} is not required. Instead, we will limit our discussion in the text to B-L scales in the range 10^{10} GeV $\leq M_{BL} \leq 10^{12}$ GeV. Let us implement the procedure outlined in the appendix, now, however, for this restricted range of B-L scales. We will generate 50 million initial throws of the soft masses with the inputted scale of $U(1)_{B-L}$ breaking randomly generated from a log-uniform distribution between 10^{10} GeV and 10^{12} GeV. Carrying out our checks, we find that this ultimately leads to 215 sets of initial data which satisfy all phenomenological constraints. These physically valid black points are shown in Figure 4.5. The distribution of the B-L breaking scale for the black points in Figure 4.5 is given in Figure 4.6.

Finally, using the formalism discussed in subsection B.3, we compute the amount of fine-tuning required to lower the B-L scale into the 10^{10} GeV to 10^{12} GeV range. The results for the 215 valid black points are shown in Figure 4.7. Note that the degree of fine-tuning is of $\mathcal{O}(10^4 - 10^6)$ for B-L scale of order 10^{10} GeV and of $\mathcal{O}(10^2 - 10^3)$ for B-L scale of order 10^{12} GeV. We note in passing that all the black points in Figure 4.5 are in the so-called "upside-down" hierarchy, with $M_{BL} < M_{SUSY}$.

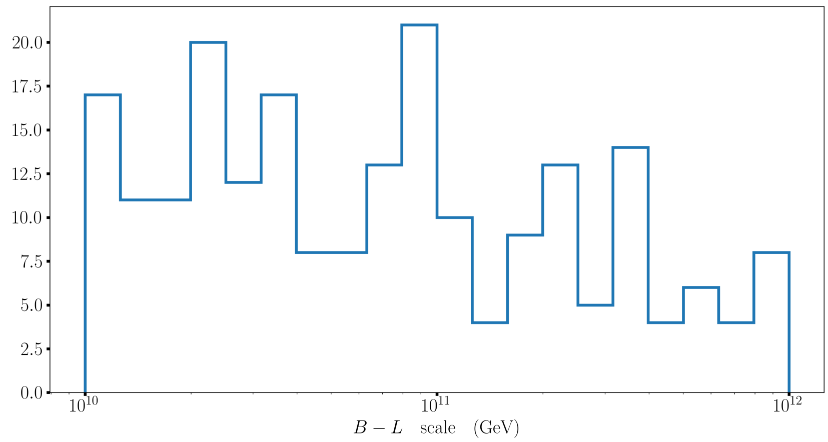

Figure 4.6: Distribution of the B-L breaking scale for the 215 black points displayed in Figure 4.5. The vertical axis labels the number of valid black points.

4.5 Post-Inflationary Epoch: Classical Behavior of ψ and H

In this section, we will begin our discussion of the post-inflationary epoch, assuming, for the time being, that the inflaton does *not* decay to normal matter. Within this context, we will calculate the classical behavior of the inflaton ψ and the Hubble parameter H numerically, and then present analytic solutions for both quantities which closely approximate the numerical results. Having achieved this, we will, in the next section, begin our discussion of the details of the inflaton decay to normal matter and reheating. For this analysis, it is far more convenient to work in units where $M_P = 1$.

In the inflationary and post-inflation epoch, the equations of motion for ψ and the Hubble parameter H are specified by

$$3H^2 = \frac{1}{2}\dot{\psi}^2 + V(\psi) \tag{4.36}$$

$$\dot{H} = -\frac{1}{2}\dot{\psi}^2 \tag{4.37}$$

$$\ddot{\psi} + 3H\dot{\psi} + V_{,\psi} = 0\,. \tag{4.38}$$

The values for the parameters m, $Y_{\nu 3}$ and μ will be chosen to be those given in (4.32) to ensure that the inflating epoch is consistent with all phenomenological data. As discussed above, for this choice of the $Y_{\nu 3}$ and μ the F-term potential satisfies $V_F \ll V_{soft}$ in both the inflationary and post-inflation regimes. Therefore, in this section, we can, to a high degree of accuracy, simply take the potential energy to be $V = V_{soft}$. Then the relevant equations

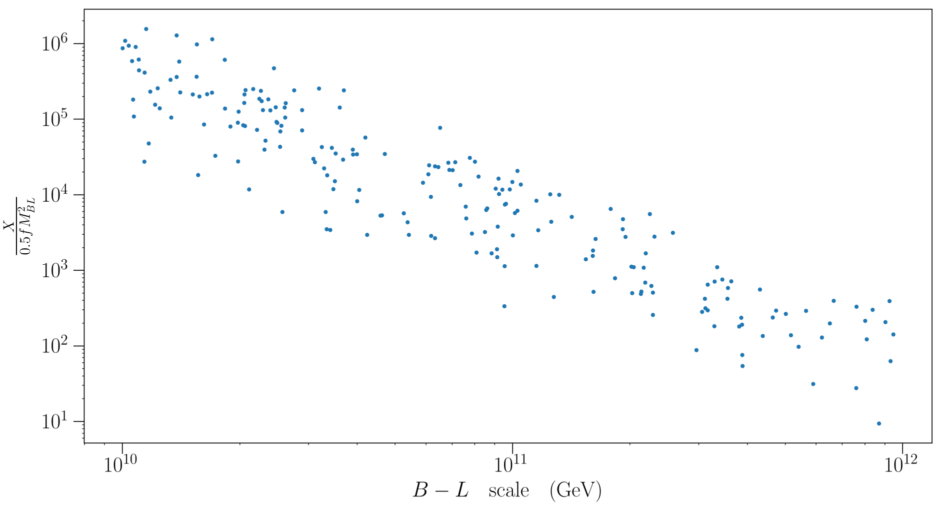

Figure 4.7: Log-log plot of $\frac{X}{\frac{1}{2} f M_{BL}^2}$ against the B-L scale, for the valid black points shown in Figure 4.5 from the scan of 50 million sets of initial conditions. The quantity $\frac{X}{\frac{1}{2} f M_{BL}^2}$ expresses the degree of fine-tuning required to achieve the associated value of the B-L scale. The expression for X is presented in appendix B.3.

of motion are given by

$$3H^2 = \frac{1}{2}\dot{\psi}^2 + V(\psi) \tag{4.39}$$

$$\dot{H} = -\frac{1}{2}\dot{\psi}^2 \tag{4.40}$$

$$\ddot{\psi} + 3H\dot{\psi} + V_{,\psi} = 0 \ , \tag{4.41}$$

where

$$V(\psi) = 3m^2 \tanh^2\left(\frac{\psi}{\sqrt{6}}\right) \ . \tag{4.42}$$

These equations can be solved numerically for both ψ and H as functions of time. The results for $\psi(t)$ and $H(t)$ starting 1) at the beginning of inflation at $t_* = 0$, 2) running through the inflationary epoch to $t_{end} \simeq 9.89 \times 10^6$, and then 3) continuing into the post-inflation epoch with for $t > t_{end}$, are shown in Figure 4.8 (a) and (b) respectively.

As is clear from Figure 4.8(a), shortly after the end of the inflationary period, the inflaton will begin to oscillate around the minimum of its potential at $\psi = 0$. Taylor expanding $V(\psi)$ in (4.42) around the origin, one obtains

$$V(\psi) = \frac{1}{2}m^2\psi^2 \left[1 - \left(\frac{\psi}{3}\right)^2 + \left(\frac{17\psi^4}{1620}\right) + \dots\right] . \tag{4.43}$$

When $\psi \ll 3$, $V \approx \frac{1}{2}m^2\psi^2$ and the mass of inflaton is $m_\psi = \sqrt{V_{\psi\psi}} \approx m$. Noting that $m =$

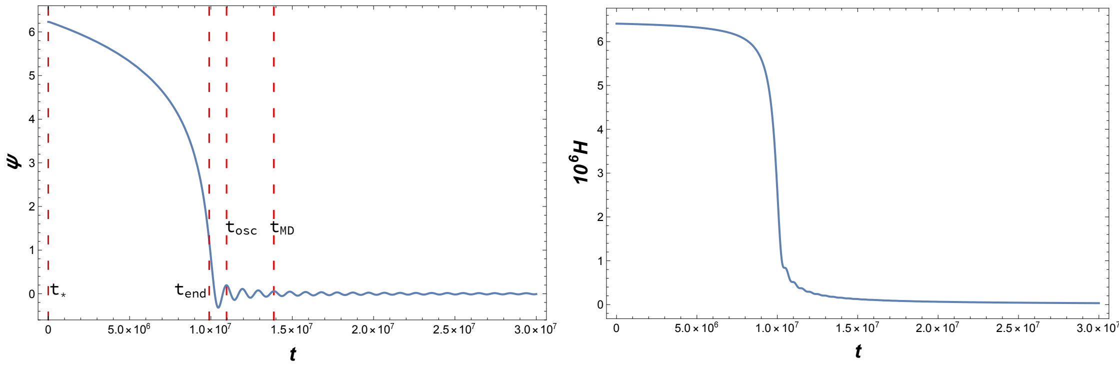

Figure 4.8: The numerical solutions for $\psi(t)$ and $H(t)$, where we have set $M_P = 1$. Note that $t_* = 0$ and $t_{end} \simeq 9.89 \times 10^6$ mark the beginning and end of the inflationary period. The times $t > t_{end}$ correspond to the post inflationary epoch. As defined in the text, $t_{osc} \simeq 1.096 \times 10^7$ marks the time at which the potential energy is well approximated by $V = \frac{1}{2}m\psi^2$ and $t_{MD} \simeq 1.387 \times 10^7$ is the time at which our analytic solutions for ψ and H become valid.

6.5×10^{-6}, it follows from Figure 4.8(b) that $m \gg H$ everywhere in the post-inflationary period. Hence, ψ will oscillate coherently around the minimum of V with a frequency $\omega = m_\psi$, although with decreasing amplitude. From Figure 4.8(a), we can numerically show that that the height of the first oscillatory peak corresponds to $\left(\frac{\psi}{3}\right)^2 \simeq 4.2 \times 10^{-3}$, which easily satisfies the above criterion that $\psi \ll 3$. Henceforth, for specificity, we consider this first peak as the beginning of the oscillatory phase and will denote the corresponding time, which we numerically compute, to be $t_{osc} \simeq 1.096 \times 10^7$. This time is indicated by a dashed red line in Figure 4.8(a). For all $t > t_{osc}$ we will, henceforth, take $V(\psi) = \frac{1}{2}m^2\psi^2$. During the oscillatory period, that is, when, $t > t_{osc}$, equations (4.39), (4.40) and (4.41) then become

$$3H^2 = \frac{1}{2}\dot{\psi}^2 + \frac{1}{2}m^2\psi^2\,, \tag{4.44}$$

$$\dot{H} = -\frac{1}{2}\dot{\psi}^2\,, \tag{4.45}$$

$$\ddot{\psi} + 3H\dot{\psi} + m^2\psi = 0\,. \tag{4.46}$$

We now want to find an approximate analytic solution to these equations for both H and ψ. To do this, we first neglect the effect of $3H\dot{\psi}$ in (4.46). That is, we will take the lowest order approximation to H to be $H_0 = 0$. Then the solution of ψ to this order is nothing but an harmonic oscillator. That is

$$\psi(t) \approx \psi_0(t) = A_0 \sin[m(t - c_1)]\,, \tag{4.47}$$

where A_0 and c_1 are constants. Using (4.47), we have

$$\frac{1}{2}\dot{\psi}_0^2 = \frac{1}{2}A_0^2 m^2 \cos^2[m(t-c_1)]\,, \tag{4.48}$$

$$V(\psi_0) = \frac{1}{2}A_0^2 m^2 \sin^2[m(t-c_1)]\,. \tag{4.49}$$

Plug these expressions into (4.44) and (4.45), yields

$$3H_1^2 = \frac{1}{2}A_0^2 m^2\,, \tag{4.50}$$

$$\dot{H}_1 = -\frac{1}{2}A_0^2 m^2 \cos^2[m(t-c_1)]\,, \tag{4.51}$$

where H_1 is the first order approximation to H. It then follows that

$$\frac{d}{dt}\left(\frac{1}{H_1}\right) = -\frac{\dot{H}_1}{H_1^2} = 3\cos^2[m(t-c_1)]\,. \tag{4.52}$$

Integrating this from t_{osc} to $t(> t_{osc})$ yields

$$\begin{aligned}
&\frac{1}{H_1(t)} - \frac{1}{H_1(t_{osc})} = 3\int_{t_{osc}}^{t} \cos^2[m(t'-c_1)]dt' \\
&= \frac{3}{2}\int_{t_{osc}}^{t} 1+\cos[2m(t'-c_1)]dt' \\
&= \frac{3}{2}(t-t_{osc}) + \frac{3}{4m}\left\{\sin[2m(t-c_1)] - \sin[2m(t_{osc}-c_1)]\right\}\,.
\end{aligned} \tag{4.53}$$

Clearly, for times t where $t - t_{osc} \gg 1/m$, we have

$$H \approx H_1(t) = \frac{2}{3(t-c_2)} \tag{4.54}$$

where

$$c_2 = t_{osc} - \frac{2}{3H(t_{osc})}\,. \tag{4.55}$$

By numerically evaluating $H(t_{osc})$ using the results displayed in Figure 4.8(b), we find that $c_2 \simeq 9.67 \times 10^6$.

Having found an approximate analytic expression for $H(t)$ beyond leading order, we now want to find the next order correction to ψ_0 given in (4.47). Due to the non-vanishing expansion of the Universe given by $H \approx H_1$, the amplitude of the oscillations of ψ will necessarily be damped. However, the frequency of the ψ oscillations will hardly be effected as long as $m \gg H$ which, as mentioned previously, will be true for all $t > t_{osc}$ and, hence, for $t - t_{osc} \gg 1/m$. Thus we can set

$$\psi(t) \approx \psi_1(t) = A_1(t) \sin[m(t - c_1)] \,, \tag{4.56}$$

where $A_1(t)$ can be obtained by inserting expressions (4.54) and (4.56) into equation (4.46). This gives

$$\left(\ddot{A}_1 + \frac{2}{t - c_2}\dot{A}_1\right) \sin[m(t - c_1)] + \left(2\dot{A}_1 m + \frac{2}{t - c_2} A_1 m\right) \cos[m(t - c_1)] = 0 \tag{4.57}$$

and, hence,

$$\ddot{A}_1 + \frac{2}{t - c_2}\dot{A}_1 = 0 \,, \tag{4.58}$$

$$\dot{A}_1 + \frac{1}{t - c_2} A_1 = 0 \,. \tag{4.59}$$

The solution is

$$A_1(t) = \frac{\mathcal{A}_1}{t - c_2} \,, \tag{4.60}$$

where $\mathcal{A}_1$ is a constant. Putting (4.54), (4.56) and (4.60) into (4.44), we find that

$$\frac{4}{3} = \mathcal{A}_1^2 \left(\frac{\sin^2 [m\,(t - c_1)]}{2\,(t - c_2)^{\,2}} - \frac{m \sin [m\,(t - c_1)] \cos [m\,(t - c_1)]}{t - c_2} + \frac{m^2}{2} \right) . \tag{4.61}$$

When $t - c_2 \gg 1/m$, which is automatically satisfied when $t - t_{osc} \gg 1/m$, we simply have

$$\mathcal{A}_1 = \sqrt{\frac{8}{3}} \frac{1}{m} \,. \tag{4.62}$$

Therefore, the next order analytic solution for $\psi(t)$, valid in the region where $t - t_{osc} \gg 1/m$, is given by

$$\psi(t) \approx \psi_1(t) = \sqrt{\frac{8}{3}} \frac{1}{m(t - c_2)} \sin[m(t - c_1)] \tag{4.63}$$

where $c_2 \simeq 9.67 \times 10^6$ was evaluated above. By matching (4.63) with the oscillations in the numerical solution of ψ, see Figure 4.8(a), we can find that $c_1 \simeq 9.78 \times 10^6$. For specificity, we note from the numerical calculation that the time associated with the fourth oscillatory peak in Figure 4.8(a) is given by $t \simeq 1.387 \times 10^7$ and satisfies $t - t_{osc} > 6\pi/m \gg 1/m$. Hence, to a high degree of approximation, the analytic solutions for H and ψ are both valid for any time larger than the time of the fourth oscillation peak. Since, as we will show below, this corresponds to the period of matter domination, we henceforth denote this time as t_{MD}

and indicated it by a red line in Figure 4.8(a). To summarize, when $t > t_{MD} \simeq 1.387 \times 10^7$

$$H(t) \approx H_1(t) = \frac{2}{3(t - c_2)}, \tag{4.64}$$

$$\psi(t) \approx \psi_1(t) = \sqrt{\frac{8}{3}} \frac{1}{m(t - c_2)} \sin[m(t - c_1)], \tag{4.65}$$

where $c_2 = t_{osc} - \frac{2}{3H(t_{osc})} \simeq 9.67 \times 10^6$ and $c_1 \simeq 9.78 \times 10^6$.

The numerical values of H and $(\psi(t)/3)^2$ at t_*, t_{end}, t_{osc} and t_{MD} are displayed in Table 4.1. The regimes of inflation and matter domination are shown as the yellow and blue

	$H(t)$	$\left(\frac{\psi(t)}{3}\right)^2$
$t_* = 0$	6.41×10^{-6}	4.31
$t_{end} \approx 9.89 \times 10^6$	3.29×10^{-6}	0.16
$t_{osc} \approx 1.096 \times 10^7$	5.16×10^{-7}	4.22×10^{-3}
$t_{MD} \approx 1.387 \times 10^7$	1.58×10^{-7}	3.93×10^{-4}

Table 4.1: The values for H and $\left(\frac{\psi}{3}\right)^2$ at the beginning and end of inflation, and at the beginning of both the oscillatory and matter dominated regimes respectively.

regions of Figure 4.9 respectively. The duration of the intermediate phase, that is, the gray area in Figure 4.9, is given by $\Delta t \simeq t_{MD} - t_{end} \simeq 3.97 \times 10^6$. As will be shown below, this is negligible compared with the duration of the reheating period. For that reason, this "transition" regime will, henceforth, be ignored. Finally, as a check on our approximate analytic solution for $H(t)$ in (4.64) and for $\psi(t)$ in (4.65), we compare them in Figure 4.10 (a) and (b) respectively against the exact numerical solutions for H and ψ in the region $t > t_{MD}$. It is clear that our analytic solution is a very accurate approximation.

4.6 Post Inflationary Epoch: Decay of ψ to Matter

In the previous section, we ignored the quantum mechanical decay of the inflaton into various species of matter, focussing instead on its purely classical behavior and the associated classical behavior of the Hubble parameter. However, ψ *does* decay into various species of matter, thus reheating the Universe. In this section we commence our discussion of these decays.

4.6.1 Dynamics of ψ and H During Particle Decay

Different decay processes can be occurring simultaneously, although they may have started at different times. In general, taking account of the decay of the inflaton, the ψ and H

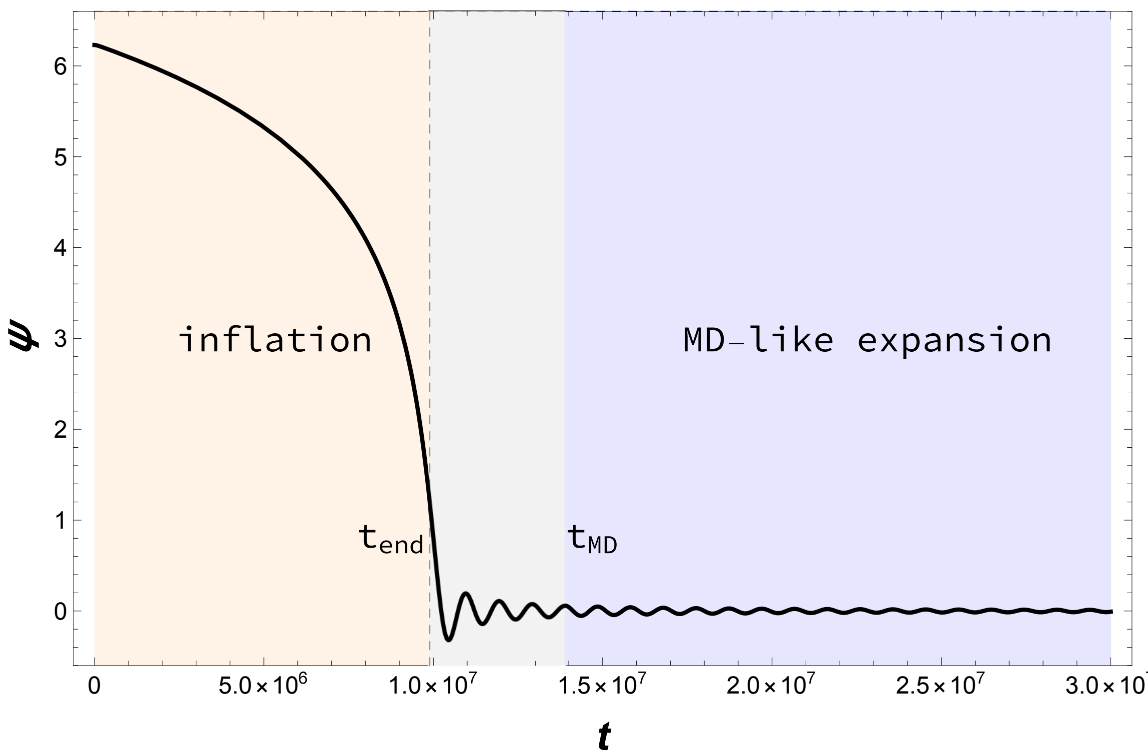

Figure 4.9: The inflationary, transition and matter dominated regimes are shown in yellow, grey and blue respectively. We have used $t_{MD} \simeq 1.387 \times 10^7$ and set $M_P = 1$.

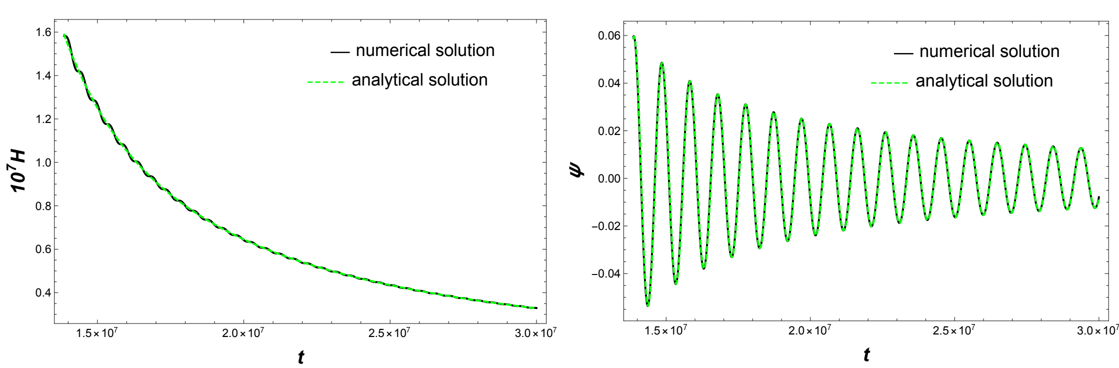

Figure 4.10: In (a), the black solid curve and the green dashed curve are the numerical solution and analytical solution (4.64) of $H(t)$, respectively. In (b), the black solid curve and the green dashed curve are the numerical solution and analytical solution (4.65) of $\psi(t)$, respectively. We have used $t_{MD} \simeq 1.387 \times 10^7$ and set $M_P = 1$.

equations (4.44), (4.45) and (4.46) are modified to become

$$3H^2 = \frac{1}{2}\dot{\psi}^2 + V(\psi) + \sum_i \rho_i \,, \tag{4.66}$$

$$\dot{H} = -\frac{1}{2}\dot{\psi}^2 - \frac{1}{2}\sum_i (\rho_i + p_i) \,, \tag{4.67}$$

$$\ddot{\psi} + \left(3H + \sum_i \Gamma_{d,i}\right)\dot{\psi} + V'(\psi) = 0 \,, \tag{4.68}$$

$$\dot{\rho}_i + 3\left(1 + w_i(t)\right) H\rho_i - \Gamma_{d,i}\dot{\psi}^2 = 0 \,, \tag{4.69}$$

where $\Gamma_{d,i}$ is the decay rate of ψ into the i-th matter species, and ρ_i and p_i are the energy density and pressure respectively of the i-th species in the decay products. The quantities ρ_i and p_i are related by the relation $p_i = w_i(t)\rho_i$, where $w_i = 0$ and $1/3$ respectively for matter and radiation. The initial conditions for ψ and H are set by their classical values at the end of the inflationary epoch, and can be determined from the results in the previous section. Additionally, we have $\rho_i = 0$ until the time at which the i-th decay process commences; that is, when $\Gamma_{d,i}$ becomes non-zero. For convenience, we define the fraction of energy density of the i-th species as

$$\Omega_i(t) = \frac{\rho_i(t)}{\rho_{total}} \,, \tag{4.70}$$

where, as follows from (4.66), the total energy density of the Universe is given by $\rho_{total} = 3H^2$. The fraction of energy density of the inflaton can be defined by $\Omega_\psi = \rho_\psi/\rho_{total}$ with $\rho_\psi = \frac{1}{2}\dot{\psi}^2 + V(\psi)$.

In our theory, the inflaton is defined in (4.18) to be

$$\phi_1 = \tfrac{1}{\sqrt{3}}\left(H_u^0 + \tilde{\nu}_{L,3} + \tilde{\nu}^c_{R,3}\right) \tag{4.71}$$

with the associated quadratic soft mass squared given in (4.18) by

$$m^2 = \frac{1}{3}(m^2_{H_u} + m^2_{\tilde{L}_3} + m^2_{\tilde{\nu}^c_{R,3}}) \,. \tag{4.72}$$

The value of m was fixed as

$$m = 6.49 \times 10^{-6} \tag{4.73}$$

to be consistent with the results of Planck2015 [3]. The relationship of H_u^0, $\tilde{\nu}_{L,3}$ and $\tilde{\nu}^c_{R,3}$ to ϕ_1 was presented in (4.17). Setting ϕ_2 and ϕ_3 to zero in those expressions–since their values vanish in the D-flat potential energy valley of the inflaton–gives

$$H_u^0 = \tilde{\nu}_{L,3} = \tilde{\nu}^c_{R,3} = \frac{1}{\sqrt{3}}\,\phi_1 \,. \tag{4.74}$$

Hence, each of these three fields can each be replaced by ϕ_1 in the Lagrangian density. However, as discussed above, ϕ_1 has a non-trivial Kähler potential and, hence, non-canonical kinetic energy. By performing the field redefinition in (4.21), that is

$$\phi_1 = \frac{1}{\sqrt{3}} \tanh\left(\frac{\psi}{\sqrt{6}}\right) \ , \tag{4.75}$$

we find that the ψ field is canonically normalized. We therefore used ψ in all our previous analysis. To analyze inflaton decay it is, therefore, essential that we re-express ϕ_1 in terms of ψ in the Lagrangian. Happily, expression (4.75) can be simplified in the post-inflationary regime. Taylor expanding (4.75) around $\psi = 0$, we find

$$\phi_1 = \frac{\psi}{\sqrt{2}} + \mathcal{O}((\psi)^2) \tag{4.76}$$

As can be seen from Figure 4.9(b), in the matter dominated period $t > t_{MD}$ we find $\psi \ll 1$. Hence, to a high degree of approximation, one can simply set

$$\phi_1 = \frac{\psi}{\sqrt{2}} \tag{4.77}$$

in the Lagrangian. We do this in the following analysis. It follows that the decay of H_u^0, $\tilde{\nu}^c_{R,3}$ and $\tilde{\nu}_{L,3}$ can be viewed as the decay of the canonical scalar field ψ. As will be shown in detail, ψ is coupled with different classes of particles; including the standard model particles, charginos, nuetralinos, gauge bosons and scalar particles.

A specific decay process can occur only when the total mass of the decay products is smaller than the mass of ψ. Since shortly after inflation, namely, when $t > t_{osc}$, ψ will oscillate around the minimum of its potential $V(\psi) = \frac{1}{2}m^2\psi^2$, the mass of the inflaton is

$$m_\psi = \sqrt{V''} = m. \tag{4.78}$$

The mass of potential decay products can have two origins; namely, from soft mass terms in the Lagrangian or from the non-zero expectation value of the inflaton ψ. In fact, as well as inducing mass terms, the expectation value of the inflaton will also give rise to mixing terms between different fields. For example, the coupling $\frac{1}{\sqrt{2}}g_2\psi\tilde{W}^-\tilde{\psi}_u^+$, which arises from a super-covariant derivative term, gives rise to mixing between the $\tilde{W}^-$ gaugino and the Higgsino ψ_u^+. This will be discussed in more detail below.

Given the essential role of the inflaton "expectation value" in determining the masses and couplings of its decay products, it is essential that this be carefully defined. Since ψ oscillates around 0 when $t > t_{osc}$, its "naive" expectation value will vanish. However, it is clear that this is not the physical expectation value effecting the inflaton decay. Rather, we will use the root mean squared value of ψ, that is, $\sqrt{\langle\psi^2\rangle}$, where $\langle\psi^2\rangle$ can be defined by

$$\langle\psi^2\rangle = \frac{1}{2\delta}\int_{t-\delta}^{t+\delta} \psi^2(\tilde{t})d\tilde{t} \tag{4.79}$$

with δ being the period of the oscillations of ψ. As long as the total decay rate $\sum_i \Gamma_{d,i} \ll m$, which as shown below will always be satisfied, then the frequency of the oscillations of ψ can accurately be taken to be $\delta = 2\pi/m_\psi$. Having defined this root mean squared VEV for the inflaton, we will henceforth expand ψ as

$$\psi = \sqrt{\langle\psi^2\rangle} + \delta\psi \ , \tag{4.80}$$

where $\delta\psi$ is a small fluctuation. As we will see below, using this expansion in the Lagrangian density will have two important ramifications; first, it will produce time dependent mass terms proportional to $\sqrt{\langle\psi^2\rangle}$ for each particle species and second, it will lead to a coupling of the inflaton fluctuation to matter–thus inducing quantum mechanical reheating of the universe. We will, for simplicity, often abuse notation and denote the fluctuation $\delta\psi$ simply as ψ. The correct meaning of the symbol will always be clear from the context.

4.6.2 A Useful Approximation

Consider the quantity

$$\langle\psi^2(t)\rangle = \frac{1}{2\delta}\int_{t-\delta}^{t+\delta} \psi^2(\tilde{t})d\tilde{t}\,, \tag{4.81}$$

where $\delta = 2\pi/m_\psi$ is the period of the oscillations of ψ. In order to remove of the integral in this expression, we use the approximation that $A(t)$ does not change much in the time interval $t-\delta$ to $t+\delta$. This is true since $\delta \ll H^{-1}$ as long as $m_\psi \gg H$. It follows that

$$\begin{aligned}\langle\psi^2(t)\rangle &= \frac{1}{2\delta}\int_{t-\delta}^{t+\delta} \psi^2(\tilde{t})d\tilde{t} \\ &\approx \frac{A^2(t)}{2\delta}\int_{t-\delta}^{t+\delta} \sin^2\left[m_\psi(\tilde{t}-t_{osc})\right]d\tilde{t} \\ &= \frac{A^2(t)}{2}\,.\end{aligned} \tag{4.82}$$

4.6.3 Decay Classes

In this subsection, we present a detailed analysis of the different types of matter into which the inflaton can decay. These are

1. up type standard model particles ($\psi \to t\bar{t}, c\bar{c}, u\bar{u}$);

2. charginos ($\psi \to \tilde{C}_1^+ \tilde{C}_1^-$, $\psi_u^- \tau_R$);

3. neutralino ($\psi \to \tilde{N}_2 \tilde{N}_2$).

4. gauge bosons ($\psi \to W_0^\mu W_{0\mu}, W_{R\mu} W_R^\mu, W^{-\mu} W_\mu^+, B^\mu B_\mu$).

These classes are distinguished by whether the decay products are fermions or bosons, and whether their masses must be determined by diagonalizing a mass matrix which arises due to mixing terms from the inflaton VEV.

Up-Type Standard Model Fermions

Note from (4.18) that the inflaton contains H_u^0 as a component field. It follows that the inflaton is able to decay via the Yukawa interactions directly into up-type standard model fermions. Since, as we will discuss below, the up-type leptons, that is, the neutrinos, can also mix with Higgsinos, we will treat these separately. Here, we consider only up-type quarks, since they cannot mix with other fermions. If we denote by F any of the u, c and t quarks then

$$\mathcal{L} \supset y_{HF} H F \bar{F} = y_{\psi F} \psi F \bar{F} \,, \tag{4.83}$$

where y_{HF} is the usual Yukawa parameter for coupling to the Higgs and, using (4.74) and (4.77), the Yukawa parameter for coupling to ψ is

$$y_{\psi F} = \frac{y_{HF}}{\sqrt{6}} \,. \tag{4.84}$$

The values for y_{HF} depend on the energy scale at which they are evaluated, and can be determined at any given scale using the renormalization group analysis presented in [161]. As discussed in subsection 4.7.4, an appropriate scale in the interior of the reheating interval is 5.8×10^{13} GeV. The values for y_{HF} at this energy are found to be

$$y_{Hu} = 6.47 \times 10^{-6} \quad , \; y_{Hc} = 3.77 \times 10^{-3} \quad , \; y_{Ht} = 6.07 \times 10^{-1} \,. \tag{4.85}$$

That is, the inflaton can decay, in the order of the coupling strength, as $\psi \to t\bar{t}$, $\psi \to c\bar{c}$ and $\psi \to u\bar{u}$.

Consider the process $\psi \to t\bar{t}$ as an example. Since

$$\mathcal{L} \supset -y_{\psi t} \psi (t_L t_R^c + t_L^\dagger t_R^{c\,\dagger}) \,, \tag{4.86}$$

ψ can decay into $t\bar{t}$ (see Figure 4.11) where we define the four component Dirac spinors

$$t = \begin{pmatrix} t_L \\ t_R^{c\,\dagger} \end{pmatrix} , \qquad \bar{t} = \begin{pmatrix} t_R^c \\ t_L{}^\dagger \end{pmatrix} . \tag{4.87}$$

The decay rates of ψ to $t\bar{t}$, $c\bar{c}$ and $u\bar{u}$ all have the following form. Noting that $m_F = m_{\bar{F}}$,

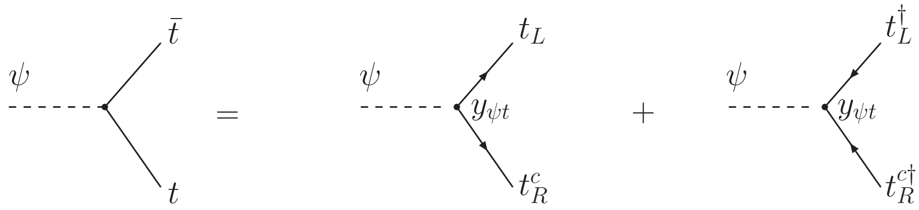

Figure 4.11: $\psi \to t\bar{t}$

we find

$$\Gamma_d(\psi \to F\bar{F}) = \frac{y_{\psi F}^2 m_\psi}{8\pi} \left[1 - 4\left(\frac{m_F}{m_\psi}\right)^2\right]^{\frac{3}{2}} , \tag{4.88}$$

where the mass of the fermion is given by

$$m_F = y_{\psi F}\sqrt{\langle\psi^2\rangle} \tag{4.89}$$

and $m_\psi = m = 6.49 \times 10^{-6}$. It is important to note that the decay can only occur once $2m_F < m_\psi$. Since m_F is determined by $\sqrt{\langle\psi^2\rangle}$, m_F can initially be larger than $m_\psi/2$. In this case, $\Gamma_d = 0$. With the expansion of the Universe, the amplitude of the oscillations of ψ will decrease. When $\sqrt{\langle\psi^2\rangle}$ becomes sufficiently small, the decay $\psi \to F\bar{F}$ will become non-zero at some specific time, which we denote by t_{F*}. For $t > t_{F*}$, Γ_d will increase as $\sqrt{\langle\psi^2\rangle}$ continues to get smaller. Eventually, when $m_F \ll m_\psi$, it follows from (4.88) that Γ_d will approach a constant. That is,

$$\Gamma_d \longrightarrow \frac{y_{\psi F}^2 m_\psi}{8\pi} \equiv \Gamma_d^{\max} , \tag{4.90}$$

which is the maximal value of Γ_d. Using (4.73) and (4.85) we find that

$$\Gamma_{d,u}^{\max} = 1.801 \times 10^{-18} \ , \ \Gamma_{d,c}^{\max} = 6.116 \times 10^{-13} \ , \ \Gamma_{d,t}^{\max} = 1.585 \times 10^{-8} \tag{4.91}$$

Therefore, a species with a smaller Yukawa coupling constant will be produced earlier, but with a relatively smaller maximal decay rate than a species with a larger Yukawa coupling.

The equation of state for $F\bar{F}$ is given by $p_{F\bar{F}} = w_{F\bar{F}}\rho_{F\bar{F}}$, where

$$w_{F\bar{F}} = \frac{1}{3}\left[1 - 4\left(\frac{m_F}{m_\psi}\right)^2\right] \tag{4.92}$$

for $2m_F \leq m_\psi$. When $2m_F \simeq m_\psi$, the decay products F and $\bar{F}$ are highly non-relativistic and $w_{F\bar{F}} \approx 0$. However, when $2m_F \ll m_\psi$, F and $\bar{F}$ are relativistic and, hence, $w_{F\bar{F}} \approx 1/3$. In the regime where $\Gamma_d \simeq \Gamma_d^{\max} \ll H$, it is possible to give an approximate analytic solution for $\rho_{F\bar{F}}$ using equations (4.66)-(4.69). However, this condition can only be satisfied for the up and charm quarks since their Yukawa parameters are relatively small. For the top quark, its Yukawa parameter is sufficiently large that $\Gamma_d^{\max} > H$. Therefore, *the results in the remainder of this subsection apply to u and c quark decays only.* The density function $\rho_{t\bar{t}}$ for the top quark can only be computed numerically. This will be carried out in section 4.7.

To lowest order, one can ignore $\rho_{F\bar{F}}$ and, hence, $p_{F\bar{F}}$ in (4.66) and (4.67), as well as Γ_d in (4.68). It follows that H can still be approximated by

$$H(t) = \frac{2}{3(t-c_2)} \tag{4.93}$$

as in (4.64), where $c_2 \simeq 9.67 \times 10^6$. Putting this back into (4.68) and taking $\Gamma_d = \Gamma_d^{\max}$, one can solve this equation for ψ. We find that

$$\psi(t) = \sqrt{\frac{8}{3}} \frac{1}{\omega(t-c_2)} \cdot \exp\left[-\frac{\Gamma_d^{\max}}{2}(t-c_2)\right] \sin\left[\omega(t-c_1)\right] , \tag{4.94}$$

where $c_1 \simeq 9.78 \times 10^6$ and

$$\omega = \sqrt{m_\psi^2 - \left(\frac{\Gamma_d^{\max}}{2}\right)^2} . \tag{4.95}$$

Note that in the limit $\Gamma_d^{\max} \to 0$, this expression reproduces the result in (4.65). Putting expressions (4.90), (4.92), (4.93) and (4.94) into (4.69), we find that

$$\rho_{F\bar{F}} \approx \frac{4\Gamma_d^{\max}}{5(t-c_2)} \left[1 - \left(\frac{t-c_2}{t_{F*}-c_2}\right)^{-5/3}\right] . \tag{4.96}$$

Note that as $t \to t_{F*}$, this expression for $\rho_{F\bar{F}} \to 0$. That is, although derived in the in the regime where $\Gamma_d = \Gamma_d^{\max}$, we find that it remains a good approximation to the density for any $t \geq t_{F*}$ since physically one knows that

$$\rho_{F\bar{F}}(t \leq t_{F*}) = 0 . \tag{4.97}$$

After t_{F*}, that is, when $2m_F < m_\psi$, $\rho_{F\bar{F}}$ will initially increase with time and reach a maximum value of

$$\rho_{F\bar{F}}^{\max} \approx \frac{0.28\Gamma_d^{\max}}{t_{F*}-c_2} \tag{4.98}$$

at $t \approx c_2 + 1.8(t_{F*}-c_2)$. Then, $\rho_{F\bar{F}}$ will decrease with time as $\rho_{F\bar{F}} \sim (t-c_2)^{-1}$. It follows from (4.70) and (4.96) that the fraction of energy density of species $F\bar{F}$ is given by

$$\Omega_{F\bar{F}} \approx \frac{2}{5}\frac{\Gamma_d^{\max}}{H}\left[1-\left(\frac{t-c_2}{t_{F*}-c_2}\right)^{-5/3}\right] < \frac{2}{5}\frac{\Gamma_d^{\max}}{H} \ll 1\,. \tag{4.99}$$

It is interesting to note that for $\Gamma_d^{\max} \ll H$, by using the approximation in 4.6.2, we find that

$$t_{F*} = t_{osc} + \frac{2\sqrt{2}y_{HF}}{3m_\psi^2} - \frac{2}{3H(t_{osc})}\,. \tag{4.100}$$

As we will determine below, the time at which reheating is finalized is given by $t_R \simeq 8\times 10^9$. It then follows from (4.93) and (4.99) that

$$\Omega_{u\bar{u}}(t_R) < 8.636\times 10^{-9}\ ,\ \ \Omega_{c\bar{c}}(t_R) < 2.932\times 10^{-3}\ . \tag{4.101}$$

Similarly, using $t_{osc} \simeq 1.096\times 10^7$ from Figure 4.8, $H(t_{osc}) \simeq 5.16\times 10^{-7}$ from Table 4.1 and (4.73), (4.85) we find that

$$t_{u*} = 9.726\times 10^6 < t_{osc}\ \ ,\ t_{c*} = 4.413\times 10^7 > t_{MD}\ . \tag{4.102}$$

with $t_{MD} \simeq 1.387\times 10^7$. We conclude that although up-type fermions with small Yukawa coupling constants, that is, u and c, can be produced relatively early, their contribution to the background evolution of H and the final decay products of ψ are actually negligible. Physically, this is true because if $\Gamma_d \ll H$, the decay products will be diluted by the expansion of the Universe, thus barely effecting the evolution of H and ψ. As a proof of this, one can compare, for example, $\Omega_{c\bar{c}}(t_R) < 2.932\times 10^{-3}$ against the smallest $\Omega(t_R)$ computed numerically in section 4.7. This is found to be $\Omega_{BB}(t_R) = 4\times 10^{-3}$. Noting that the value of $\Omega_{c\bar{c}}(t_R)$ is actually dramatically reduced relative to its value in (4.101) by the decay of the inflaton into the other species discussed below, we conclude that reheating into charm quarks, and therefore, into up quarks is negligibly small. They will, henceforth, be ignored. Only when a Yukawa parameter is large enough that the decay rate becomes comparable and then larger than H, will that species play an important role in reheating. As we will see below, this will be the case for the top quark.

Charginos

As mentioned previously, the non-zero expectation value of the inflaton–more precisely, the RMS value $\sqrt{\langle\psi^2\rangle}$–gives rise to effective mass terms for fields, as well as to mixing between different particle species. By diagonalizing the mass matrix for such species, one can determine the correct mass eigenstates into which the inflaton decays. We now examine the first class of such mass eigenstates, which we will label “charginos”, in direct analogy with the mass eigenstates associated with dynamical electroweak symmetry breaking in the B-L MSSM [148, 161].

The mixing terms can arise from two sources; 1) the superpotential and 2) the"super-covariant derivative" of the H_u Higgs doublet superfield. The former set are parameterized by $y_{Hi}\sqrt{\langle\psi^2\rangle}$, while the latter have the parameters $g_a\sqrt{\langle\psi^2\rangle}$, where y_{Hi}, g_a denote Higgs coupled Yukawa parameters and gauge couplings respectively. We give an explicit description of where these terms arise from in appendix C. Since the third family Yukawa coupling parameters are the largest, we will, for simplicity, assume that

1. All Yukawa coupling matrices are diagonal.
2. Only the third family quark and lepton Yukawa coupling parameters need be considered.
3. Since the third family neutrino Yukawa coupling parameter is also negligible, it can be dropped as well.

Dropping all terms which have a neutrino Yukawa coupling y_ν and examining the effective mass Lagrangian for the "charginos", we find that one set of fields which are mixed due to the non-zero value of $\sqrt{\langle\psi^2\rangle}$ are

$$\tilde{W}^+, \tilde{\psi}_u^+, \tau_R^c, \tilde{W}^-, \psi_d^-, \tau_L \,. \tag{4.103}$$

In order to construct the inflaton potential given described above, we have previously taken the supersymmetric μ parameter to be of $\mathcal{O}(10^{10}\mathrm{GeV})$. This value is much smaller than the soft masses of the W-gauginos, as well as the initial values of the mixing terms $y_{H\tau}\sqrt{\langle\psi^2\rangle}$ and $g_2\sqrt{\langle\psi^2\rangle}$. We can, therefore, simplify this system further by working in the "small μ" limit, and drop terms involving μ. Of course, as the value of $\sqrt{\langle\psi^2\rangle}$ decreases, the value of μ will eventually exceed that of other terms we have not dropped. However, this effect is not significant since it will only occur very near the end of the reheating period. Hence we can, to a good approximation, take μ to be negligible.

In this limit, we are able to decouple the τ_R^c, ψ_d^- states since there is no longer any mixing between ψ_d^- and ψ_u^+. Examining the effective mass Lagrangian in equation (C.8), we see that

$$\mathcal{L}_{mass} \quad \supset \quad y_{H\tau}\,\langle\tilde{\nu}_{3,L}\rangle\,\tau_R^c\psi_d^- + \text{h.c.} \tag{4.104}$$

where, using the formalism presented in [161], we find that the value of $y_{H\tau}$ at 5.8×10^{13} GeV is given by

$$y_{H\tau} = 3.88\times10^{-2} \,. \tag{4.105}$$

Note that (4.104) is a mass term for a Dirac mass

$$\Psi' = \begin{pmatrix} \psi_d^- \\ \tau_R \end{pmatrix} \tag{4.106}$$

with mass

$$m_{\psi_d\tau} = y_{\psi_d\tau}\sqrt{\langle\psi^2\rangle} \quad , \quad y_{\psi_d\tau} = \frac{y_{H\tau}}{\sqrt{6}} \tag{4.107}$$

The decay rate to the ψ_d^- and τ_R^c states is, therefore, analogous to the decay of the inflaton to top quarks, and takes the form

$$\Gamma_d(\psi \to \psi_d^- \tau_R^c) \quad = \quad \frac{y_{\psi_d\tau}^2 m_\psi}{8\pi}\left[1 - 4\frac{m_{\psi_d\tau}^2}{m_\psi^2}\right]^{3/2} \tag{4.108}$$

The equation of state parameter for $\psi_d\tau$ is

$$w_{\psi_d\tau} = \frac{1}{3}\left[1 - 4\frac{m_{\psi_d\tau}^2}{m_\psi^2}\right] . \tag{4.109}$$

The remaining fermions,

$$\tilde{W}^+, \tilde{\psi}_u^+, \tilde{W}^-, \tau_L \tag{4.110}$$

remain mixed and form the new mass eigenstates $\tilde{C}_1^\pm$ and $\tilde{C}_2^\pm$, where

$$\begin{pmatrix} \tilde{C}_1^+ \\ \tilde{C}_2^+ \end{pmatrix} = V\begin{pmatrix} \tilde{W}^+ \\ \tilde{\psi}_u^+ \end{pmatrix} , \qquad \begin{pmatrix} \tilde{C}_1^- \\ \tilde{C}_2^- \end{pmatrix} = U\begin{pmatrix} \tilde{W}^- \\ \tau_L \end{pmatrix} . \tag{4.111}$$

Determining the matrices U, V is straightforward. The explicit form of both are given in appendix C.1. The states $\tilde{C}_1^\pm$ and $\tilde{C}_2^\pm$ form Dirac fermions with masses $m_{\tilde{C}_1}$ and $m_{\tilde{C}_2}$ respectively. These are also presented in appendix C.1. We find that the large value of $m_{\tilde{C}_2}$ makes the decay of the inflaton to $\tilde{C}_2^\pm$ kinematically impossible. Hence, only $\tilde{C}_1^\pm$ are produced. The decay rate of the inflaton to the mass eigenstates $\tilde{C}_1^\pm$ is then given by

$$\begin{aligned} \Gamma_d(\psi \to \tilde{C}_1^+\tilde{C}_1^-) \quad &= \quad \gamma^2\frac{(m_\psi^2 - 4m_{\tilde{C}_1}^2)^{3/2}}{8\pi m_\psi^2} \\ &= \quad \frac{\gamma^2 m_\psi}{8\pi}\left[1 - 4\frac{m_{\tilde{C}_1}^2}{m_\psi^2}\right]^{3/2} \quad , \end{aligned} \tag{4.112}$$

where

$$\gamma = \frac{g_2}{\sqrt{6}}(U_{1W}V_{iu} + U_{1\tau}V_{1W}) \, , \; m^2_{\tilde{C}_1} = \frac{1}{2}\left((x_1)^2 + 2(x_2)^2 - \sqrt{(x_1)^4 + 4(x_1)^2(x_2)^2}\right) \tag{4.113}$$

and $x_1 = M_2$, $x_2 = g_2\sqrt{\langle\psi^2\rangle}/\sqrt{6}$. The elements of U, V are given in appendix C.1. The equation of state parameter for $\tilde{C}^{\pm}_1$ is

$$w_{\tilde{C}^{\pm}_1} = \frac{1}{3}\left[1 - 4\frac{m^2_{\tilde{C}_1}}{m^2_\psi}\right] . \tag{4.114}$$

It is important to note that the rate and equation of state for the inflaton decay into $\tilde{C}^{\pm}_1$ depend on the soft $SU(2)_L$ gaugino mass M_2. However, this will vary statistically over the interval $[m/f, fm]$, where $m = 1.58 \times 10^{13}$ GeV and $f = 3.3$. Generically, it will be different for each of the 215 valid black points discussed in section 4.4. To avoid having to do a separate analysis for each of these 215 black points, we will, instead, note that one expects their average value, denoted by M, to be near the center of the interval. Furthermore, for concreteness, we will henceforth assume that

$$M = m = 1.58 \times 10^{13} \text{ GeV} . \tag{4.115}$$

Looking ahead, we note that inflaton decays into different species will depend on the gaugino soft masses M_R and M_{B-L}, as well as on M_2. Therefore, for concreteness, we will henceforth make the generic assumption that

$$M_2 \simeq M_R \simeq M_{B-L} = M = m = 1.58 \times 10^{13}\text{GeV} . \tag{4.116}$$

Secondly, we note that the rate and equation of state for the inflaton decay into $\tilde{C}^{\pm}_1$ also depend on the $SU(2)_L$ gauge parameter g_2. This quantity is evaluated, as are all the other gauge couplings, by running it from its measured value at the electroweak scale up to the scale of reheating at $\sim 5.8 \times 10^{13}$ GeV. Hence, its value will essentially be the same for all 215 valid black points. Using the formalism developed in [161], we find that at 5.8×10^{13} GeV

$$g_2 = 0.57 . \tag{4.117}$$

Again, looking ahead we find that inflaton decays into different species will depend on the gauge couplings g_R and g_{BL} as well as on g_2, all evaluated at the reheating scale of 5.8×10^{13} GeV. Using the formalism developed in [161], we find that at 5.8×10^{13} GeV

$$g_3 = 0.60 \; , \quad g_2 = 0.57 \; , \quad g_R = 0.56 \; , \quad g_{BL} = 0.56 \tag{4.118}$$

Mass	Degeneracy	State
0	1	$\tilde{N}_1$
$\frac{1}{2}(M - \sqrt{M^2 + 12u^2})$	2	$\tilde{N}_{2a}$, $\tilde{N}_{2b}$
M	1	$\tilde{N}_3$
$\frac{1}{2}(M + \sqrt{M^2 + 12u^2})$	2	$\tilde{N}_{4a}$, $\tilde{N}_{4b}$

Table 4.2: Mass eigenstates of the neutralino mass matrix $M_{\tilde{N}}$.The masses M and u are defined in (4.115) and (4.121) respectively

with an average value of $g = 0.57$. Therefore, for simplicity of calculation, we will henceforth make the generic assumption that

$$g_2 \simeq g_R \simeq g_{BL} = g = 0.57 \,. \tag{4.119}$$

As with the top quark, the expressions for the energy densities $\rho_{\psi\tau}$ and the $\rho_{\tilde{C}\tilde{C}}$ charginos can only be computed numerically. We will carry this out in section 4.7.

Neutralinos

We now turn to the second set of particles which mix due to the non-zero inflaton VEV. We refer to these as "neutralinos", in analogy with states described by the B-L MSSM . Again, we will ignore all terms multiplied by a neutrino Yukawa coupling parameter $y_{H\nu}$. Making the same assumptions about Yukawa couplings as before, the effective mass Lagrangian for the "neutralinos" is such that the states that mix are

$$\tilde{B}, \tilde{W}_R, \tilde{W}^0, \psi_d^0, \psi_u^0, \nu_{3L}, \nu_{3R}^c \,. \tag{4.120}$$

Once again, we take μ to be negligible compared to other terms in the effective mass Lagrangian. In this limit, the state ψ_d^0 decouples. It follows that the effective mixed state mass matrix, $M_{\tilde{N}}$, is six-by-six. To proceed, this must be diagonalized. We leave the details of this to appendix C, but note that to simplify our expressions we again make the assumptions given in (4.116) and (4.119). Additionally, we define

$$u \equiv \frac{1}{\sqrt{6}} \sqrt{\langle \psi^2 \rangle} \ . \tag{4.121}$$

Diagonalizing the mass matrix $M_{\tilde{N}}$, we find the six mass eigenstates given in Table 4.2. Of the six eigenstates, only $\tilde{N}_1$ and $\tilde{N}_{2a}$, $\tilde{N}_{2b}$ are kinematically accessible to the decay of the inflaton. The decay processes and rates are

$$\Gamma(\psi \to \tilde{N}_{2a}\tilde{N}_{2a}) = \frac{\gamma_a^2 m_\psi}{16\pi}\left[1 - 4\frac{m_{\tilde{N}_2}^2}{m_\psi^2}\right]^{3/2} ,$$
$$\Gamma(\psi \to \tilde{N}_{2b}\tilde{N}_{2b}) = \frac{\gamma_b^2 m_\psi}{16\pi}\left[1 - 4\frac{m_{\tilde{N}_2}^2}{m_\psi^2}\right]^{3/2} ,$$
$$\Gamma(\psi \to \tilde{N}_{2a}\tilde{N}_{2b}) = \frac{\gamma_c^2 m_\psi}{8\pi}\left[1 - 4\frac{m_{\tilde{N}_2}^2}{m_\psi^2}\right]^{3/2} , \tag{4.122}$$

where $\tilde{N}_{2a}$ and $\tilde{N}_{2b}$ have the same mass presented in Table 4.2 and

$$\gamma_a = \left(\frac{7g}{2\sqrt{3}}\right)\frac{\frac{1}{2}u(M+\sqrt{M^2+12u^2})}{M^2+12u^2+M\sqrt{M^2+12u^2}} ,$$
$$\gamma_b = \left(\frac{9g}{2}\right)\frac{u\sqrt{u^2+\frac{1}{6}(M^2+M\sqrt{M^2+12u^2})}}{M^2+12u^2+M\sqrt{M^2+12u^2}} , \tag{4.123}$$
$$\gamma_c = \left(\frac{\sqrt{3}g}{2}\right)\frac{u\sqrt{u^2+\frac{1}{6}(M^2+M\sqrt{M^2+12u^2})}}{M^2+12u^2+M\sqrt{M^2+12u^2}} - \left(\frac{g}{4}\right)\frac{u(M+\sqrt{M^2+12u^2})}{M^2+12u^2+M\sqrt{M^2+12u^2}} .$$

Since $\tilde{N}_{2a}$ and $\tilde{N}_{2b}$ have the same mass, their equations of states parameters are given by the same form

$$w_{N_2} = \frac{1}{3}\left[1 - 4\frac{m_{\tilde{N}_2}^2}{m_\psi^2}\right] . \tag{4.124}$$

As with the top quark and the charginos, the expressions for the energy densities $\rho_{\tilde{N}\tilde{N}}$ for the neutralinos can only be computed numerically. We will carry this out in section 4.7.

Gauge Bosons

The covariant derivatives of H_u^0, $\tilde{\nu}_{3L}$ and $\tilde{\nu}_{3R}^c$ couple the inflaton ψ to the associated gauge bosons and, furthermore, give an effective mass to these bosons. This occurs via the following terms in the Lagrangian

$$\begin{aligned}
& \mathcal{L}_{gauge-coupling} \\
\supset\ & -\frac{g_2^2}{4}\left(|H_u^0|^2 + |\tilde{\nu}_{3L}|^2\right)W^{0\mu}W_\mu^0 - \frac{g_2^2}{2}\left(|H_u^0|^2 + |\tilde{\nu}_{3L}|^2\right)W^{+\mu}W_\mu^- \\
& -g_R^2\left(q_{R_u}^2|H_u^0|^2 + q_{R_\nu}^2|\tilde{\nu}_{3R}^c|\right)W_R^\mu W_{R\mu} - g_R^2\left(q_{BL_\nu}^2|\tilde{\nu}_{3R}^c| + q_{BL_L}^2|\tilde{\nu}_{3L}|^2\right)B^\mu B_\mu \\
=\ & -\frac{g_2^2}{12}\psi^2 W^{0\mu}W_\mu^0 - \frac{g_2^2}{6}\psi^2 W^{+\mu}W_\mu^- - \frac{g_R^2}{12}\psi^2 W_R^\mu W_{R\mu} - \frac{g_{BL}^2}{3}\psi^2 B^\mu B_\mu .
\end{aligned} \tag{4.125}$$

To find the mass for each species of vector boson, as well as to determine their coupling parameter to the inflaton, we expand the inflaton around its root mean squared VEV as in (4.80). Inserting this into the final expression in (4.125) and, as previously discussed, denoting $\delta\psi$ simply as ψ, we find that

$$
\begin{aligned}
\mathcal{L}_{gauge-coupling} \supset\; & -\frac{1}{2}m_{W^0}^2 W^{0\mu}W_\mu^0 - m_{W^\pm}^2 W^{+\mu}W_\mu^- - \frac{1}{2}m_{W_R}^2 W_R^\mu W_{R\mu} - \frac{1}{2}m_{W_B}^2 B^\mu B_\mu \\
& -\frac{g_2^2}{6}\sqrt{\langle\psi^2\rangle}\psi W^{0\mu}W_\mu^0 - \frac{g_2^2}{3}\sqrt{\langle\psi^2\rangle}\psi W^{+\mu}W_\mu^- \\
& -\frac{g_R^2}{6}\sqrt{\langle\psi^2\rangle}\psi W_R^\mu W_{R\mu} - \frac{2g_{BL}^2}{3}\sqrt{\langle\psi^2\rangle}\psi B^\mu B_\mu \;,
\end{aligned}
\tag{4.126}
$$

where the masses are given by

$$
m_{W^0} = m_{W^\pm} = \frac{g_2\sqrt{\langle\psi^2\rangle}}{\sqrt{6}},\; m_{W_R} = \frac{g_R\sqrt{\langle\psi^2\rangle}}{\sqrt{6}},\; m_{W_B} = \sqrt{\frac{2}{3}}g_{BL}\sqrt{\langle\psi^2\rangle}\;. \tag{4.127}
$$

For a generic coupling $G_i\psi W_i^\mu W_{i\mu}$ with identical W-bosons, the decay rate and the equation of state parameter are given by

$$
\Gamma_d(\psi \to W_i^\mu W_{i\mu}) = \frac{G_i^2}{32\pi m_\psi}\left[1 - 4\frac{m_{W_i}^2}{m_\psi^2}\right]^{1/2}\;, \tag{4.128}
$$

$$
w_{W_i} = \frac{1}{3}\left(1 - 4\frac{m_{W_i}^2}{m_\psi^2}\right) \tag{4.129}
$$

respectively. For decays into two different W-bosons, one multiplies expression (4.128) by 2. It then follows from (4.126) that the decay rates of the inflaton to the four gauge bosons, and the associated equation of state parameters, are

$$
\begin{aligned}
\Gamma_d(\psi \to W_0^{\mu} W_{0\mu}) &= \frac{g_2^4 \langle \psi^2 \rangle}{1152 \pi m_\psi} \left[1 - 4 \frac{m_{W_0}^2}{m_\psi^2} \right]^{1/2} , && (4.130) \\
w_{W_0} &= \frac{1}{3} \left[1 - 4 \frac{m_{W_0}^2}{m_\psi^2} \right] , && (4.131) \\
\Gamma_d(\psi \to W^{-\mu} W_\mu^+) &= \frac{g_2^4 \langle \psi^2 \rangle}{144 \pi m_\psi} \left[1 - 4 \frac{m_{W_\pm}^2}{m_\psi^2} \right]^{1/2} , && (4.132) \\
w_{W_\pm} &= \frac{1}{3} \left[1 - 4 \frac{m_{W_\pm}^2}{m_\psi^2} \right] , && (4.133) \\
\Gamma_d(\psi \to W_{R\mu} W_R^{\mu}) &= \frac{g_2^4 \langle \psi^2 \rangle}{1152 \pi m_\psi} \left[1 - 4 \frac{m_{W_R}^2}{m_\psi^2} \right]^{1/2} , && (4.134) \\
w_{W_R} &= \frac{1}{3} \left[1 - 4 \frac{m_{W_R}^2}{m_\psi^2} \right] , && (4.135) \\
\Gamma_d(\psi \to B^{\mu} B_\mu) &= \frac{g_{BL}^4 \langle \psi^2 \rangle}{72 \pi m_\psi} \left[1 - 4 \frac{m_B^2}{m_\psi^2} \right]^{1/2} , && (4.136) \\
w_B &= \frac{1}{3} \left[1 - 4 \frac{m_B^2}{m_\psi^2} \right] . && (4.137)
\end{aligned}
$$

where the gauge boson masses are given in (4.127).

As with the top quark, charginos and neutralinos, the expressions for the energy densities ρ_{WW} and ρ_{BB} for the gauge fields can only be computed numerically. We will carry this out in section 4.7. To simplicity the calculations, we will again use the approximation for the gauge couplings presented in (4.119).

Scalars

The inflaton can couple to other scalar fields via the supersymmetric F-term and D-term potentials, as well as the soft supersymmetry breaking terms. These couplings give rise to a potential three-body decay vertex, as well as mass terms and mixing terms. To find out the mass eigenstates into which the inflaton can decay, one must examine the mass matrix $\mathcal{M}$ whose elements are

$$
\mathcal{M}_{ij} = \left. \frac{\partial^2 V}{\partial \phi_i \partial \phi_j^*} \right|_{\psi = \sqrt{\langle \psi^2 \rangle}} , \tag{4.138}
$$

where i, j run over all scalars other than the inflaton and

$$
V = V_F + V_D + V_{soft} \, . \tag{4.139}
$$

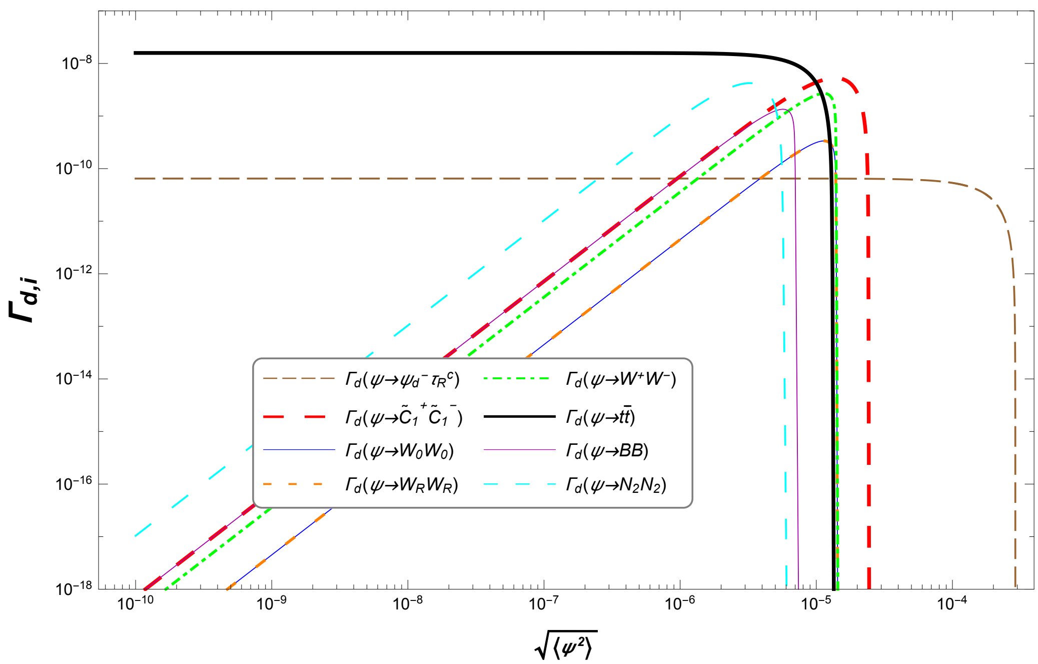

Figure 4.12: The rates $\Gamma_{d,i}$ for different decay processes plotted with respect to $\sqrt{\langle\psi^2\rangle}$. The Yukawa couplings are all evaluated at the reheating scale of 5.8×10^{13} GeV. Since $\sqrt{\langle\psi^2\rangle}$ will decrease with time, $\psi \to \psi_d^- \tau_R^c$ will be the first decay process to become non-zero, whereas the decay $\psi \to \tilde{N}_2\tilde{N}_2$ will be turned on last.

To simplify our calculations, we assume that all scalars have identical soft masses given by

$$m = 1.58 \times 10^{13}\text{GeV} \tag{4.140}$$

and take the gauge couplings to have their average value at order 5.8×10^{13} GeV, as discussed above. That is,

$$g_3 \simeq g_2 \simeq g_R \simeq g_{BL} \simeq g = 0.57\,. \tag{4.141}$$

Diagonalizing $\mathcal{M}$, we find that the eigenvalues of $\mathcal{M}$ are either m^2 or larger. It follows that there are no decays of the inflaton to scalars.

4.7 Numerical Calculation

As discussed in previous sections, the inflaton can decay into different species with different time dependent decay rates. The root mean squared value of ψ, that is, $\sqrt{\langle\psi^2\rangle}$, decreases with the decrease of the oscillatory amplitude of ψ due to the expansion of the Universe and the decay of the inflaton. Thus, different decay processes will begin at different times since the masses of the decay products depend on $\sqrt{\langle\psi^2\rangle}$. We plot the decay rates for different processes with respect to $\sqrt{\langle\psi^2\rangle}$ in Figure 4.12. We did not plot the decay rates for $u\bar{u}$ and $c\bar{c}$ because, as discussed above, they are too small to have any substantial effect. The values of $\sqrt{\langle\psi^2\rangle}$ at which each relevant process is turned on can be found in Table 4.3. Even though we have simplified the computations by ignoring the u and c quark decays, it remains impossible to find analytical solutions for (4.66)-(4.69) to account for all the relevant decay processes simultaneously. Therefore, in this section, we will numerically solve (4.66)-(4.69) to find the solutions for H, ψ and ρ_i. From this, one can determine the relative energy densities of the different species at the end of the reheating epoch, as well as the reheating temperature.

Decay processes	Value of $\sqrt{\langle\psi^2\rangle}$ at turn on ($M_P = 1$)	Value of $\sqrt{\langle\psi^2\rangle}$ at turn on (GeV)
$\psi \to \psi_d^- \tau_R^c$	2.05×10^{-4}	4.99×10^{14} GeV
$\psi \to \tilde{C}_1^+ \tilde{C}_1^-$	2.41×10^{-5}	5.88×10^{13} GeV
$\psi \to W_0^\mu W_{0\mu}$, $W_{R\mu} W_R^\mu$, $W^{-\mu} W_\mu^+$	1.39×10^{-5}	3.39×10^{13} GeV
$\psi \to t\bar{t}$	1.31×10^{-5}	3.19×10^{13} GeV
$\psi \to B^\mu B_\mu$	6.97×10^{-6}	1.70×10^{13} GeV
$\psi \to \tilde{N}_{2a} \tilde{N}_{2a}$, $\tilde{N}_{2b} \tilde{N}_{2b}$, $\tilde{N}_{2a} \tilde{N}_{2b}$	5.69×10^{-6}	1.39×10^{13} GeV

Table 4.3: Values of $\sqrt{\langle\psi^2\rangle}$ at which each decay process is turned on. We use the Yukawa couplings evaluated at the reheating scale of order 5.8×10^{13} GeV.

4.7.1 Initial Conditions

To find the solutions for H, ψ and ρ_i by numerically solving (4.66)-(4.69), one needs the initial conditions for H, ψ and ρ_i. In principle, one can solve these equations starting from the beginning of inflation. However, such an approach would take a great deal of computing time due to the severe oscillations of ψ after t_{osc}. Furthermore, ignoring the u and c quark decays, it follows from Table 4.3 that the first decay process to turn on is $\psi \to \psi_d^- \tau_R^c$. The time at which this decay commences can be computed from the expression

$$t_{\psi_d^- \tau_R^c *} = t_{osc} + \frac{2\sqrt{2} y_{H\tau}}{3 m_\psi^2} - \frac{2}{3H(t_{osc})} \ , \tag{4.142}$$

where $t_{osc} \simeq 1.096 \times 10^7$ from Figure 4.8, $H(t_{osc}) \simeq 5.16 \times 10^{-7}$ from Table 4.1 and $y_{H\tau}$ was given in (4.105). This expression was first presented in (4.100) for top-quark decays, but can be used here since both u and c are being neglected. The result is

$$t_{\psi_d^- \tau_R^c *} \simeq 8.78 \times 10^8 \tag{4.143}$$

which is much later than t_{osc}, thus exacerbating the computing time even more. Therefore, to save computing time, we will start our calculation from an arbitrarily chosen time $t =$

t_{I}, where t_{I} is close to, but smaller than, $t_{\psi_d^- \tau_R^c *}$. The exact value of t_{I} is for technical convenience only. We will set $t_{\mathrm{I}} = 8 \times 10^8$. When $t \leq t_{\psi_d^- \tau_R^c *}$, we can neglect all decay effects. Thus, we can approximately set $\rho_i = 0$ at t_{I} for all decay products. Using (4.65) and (4.64), one can obtain the initial conditions for ψ and H at t_{I}, respectively. Of course, the decay rates for each process are zero until the corresponding process is turned on.

As can be ascertained from Figure 4.12 and Table 4.3, the second decay to turn on is $\psi \to \tilde{C}_1^+ \tilde{C}_1^-$. It is clear from this data that the associated time, $t_{\tilde{C}_1 *}$, will be much later than $t_{\psi_d^- \tau_R^c *}$. As we will see below,

$$t_{\tilde{C}_1 *} \simeq 6.45 \times 10^9 \ . \tag{4.144}$$

Therefore, to further reduce the time for computation, we will divide the numerical calculations into two parts. First, we will numerically compute from $t = t_{\mathrm{I}}$ to some time $t = t_{\mathrm{II}} < t_{\tilde{C}_1 *}$ by using the iterative method described in next subsection. Again, the choice of the value of t_{II} is for technical convenience only, which will not make any physical difference as long as $t_{\mathrm{II}} < t_{\tilde{C}_1 *}$. We will choose $t_{\mathrm{II}} = 5 \times 10^9$. Second, we numerically compute, also using the iterative method, from $t = t_{\mathrm{II}}$ to the time t_R where reheating has been completed. The initial conditions for ψ, H and ρ_i at $t = t_{\mathrm{II}}$ will be set by the numerical solutions of the first part; that is, for $t_{\mathrm{I}} < t < t_{\mathrm{II}}$.

4.7.2 Iterative Method

In (4.66)-(4.69), the equation of state parameters w_i and the decay rates $\Gamma_{d,i}$ depend on the root mean square value of ψ, that is, $\sqrt{\langle \psi^2 \rangle}$. This makes these background equations very difficult to solve–even numerically–especially when the $\sqrt{\langle \psi^2 \rangle}$-dependence becomes complicate after t_{I}. Hence, we will solve them by iteration. We accomplish this by using Eq. (4.65), which is the solution for ψ without considering any decay, as the first input ψ for $\sqrt{\langle \psi^2 \rangle}$ in w_i and $\Gamma_{d,i}$. Then, we treat w_i and $\Gamma_{d,i}$ simply as some time-dependent functions so that we can find solutions for (4.66)-(4.69) numerically. This gives the first output $\psi(t)$. The first output $\psi(t)$ will be identical with the first input $\psi(t)$ until some observable decay processes are turned on. Once $\sum_i \Gamma_{d,i}$ becomes effectively nonzero, the oscillations of ψ will be damped more quickly. From then on, the output $\sqrt{\langle \psi^2 \rangle}$ will be smaller than that of the input.

Next, we use this first output $\psi(t)$ as a second input ψ for $\sqrt{\langle \psi^2 \rangle}$ in w_i and $\Gamma_{d,i}$ and numerically solve (4.66)-(4.69) again. This then leads to the second output $\psi(t)$ that is closer to the final solution. By repeating this method, the output $\psi(t)$ will become closer and closer to the real solution of ψ. We repeat this method iteratively multiple times until the output $\psi(t)$ is almost identical with the input $\psi(t)$, which means we have found the correct solution for ψ. Using this method also leads to solutions for H and ρ_i to some reasonable accuracy.

Additionally, since the inflaton will oscillate rapidly around the minimum of its potential during the reheating phase, the oscillations of ψ are too dense to be easily handled in the numerical calculation. The amplitude of the oscillations of ψ will decrease with time. However, the frequency of the oscillations is almost a constant as long as $\sum_i \Gamma_{d,i} \ll m_\psi$, as we will demonstrate in the numerical results. Hence, as a good approximation we can set

$$\psi(t) = A(t) \sin\left[m_\psi (t - c_1)\right] , \tag{4.145}$$

where $c_1 \simeq 9.78 \times 10^6$. This is very useful in getting rid of the obstacles described above. Then, by using the discussion in section 4.6.2, we can simply replace $\sqrt{\langle\psi^2\rangle}$ in w_i and $\Gamma_{d,i}$ with $A(t)/\sqrt{2}$. Therefore, for every input $\psi(t)$ in the iterative calculation, we can focus on $A(t)$ instead of $\psi(t)$. We apply this iterative method to both the first part of the calculation, where $t_{\rm I} < t < t_{\rm II}$, and to the second part, where $t > t_{\rm II}$, which we respectively denote as part I and part II. Eventually, when the input $A(t)$ and the output oscillatory amplitude are almost same, we can conclude that we have found the correct solution for $A(t)$ (or equivalently $\psi(t)$), $H(t)$ (or equivalently $a(t)$) and $\rho_i(t)$ (or equivalently $\Omega_i(t)$).

The possible corrections to $\sum_i \Omega_i$ from the accuracy of the solution of ψ can be defined as

$$\Delta\Omega_\psi = \frac{\rho_{\psi\rm out} - \rho_{\psi\rm in}}{3M_P^2 H^2} , \tag{4.146}$$

where $\rho_{\psi\rm in} = 1/2\dot{\psi}_{\rm in}^2 + V(\psi_{\rm in})$, $\rho_{\psi\rm out} = 1/2\dot{\psi}_{\rm out}^2 + V(\psi_{\rm out})$ and $\psi_{\rm in}$, $\psi_{\rm out}$ are the input and the output ψ, respectively. Note that Eq. (4.145) should be used when we transform between ψ and A.

4.7.3 Numerical Results

After several iterations, we obtained the final solution for $A(t)$ (or, equivalently, for $\psi(t)$). For the last round of n such iterations, we plot the input $A(t)$ (let us denote it by $A_n(t)$), the corresponding output $\psi(t)$ or $A(t)$ (let us denote it by $\psi_{n+1}(t)$ or $A_{n+1}(t)$, respectively) and the solution of H in Figure 4.13. $A_n(t)$ is actually the numerical output $A(t)$ of the $(n-1)$th round of iteration. Note that the oscillations of ψ are too dense to be plotted completely. Instead, we simply plot 5000 random points from the curve of $\psi_{n+1}(t)$ for both part I and part II. Thus A_{n+1} corresponds to the upper boundaries of the magenta points in Figure 4.13, while A_n is the black curves in Figure 4.13. We can see that A_n and A_{n+1} are almost same. We can, therefore, treat ψ_{n+1} as the actual solution of ψ. We have verified that their deviation is sufficiently small for our present interests.[4]

We plot the decay rates $\Gamma_{d,i}$ and the Hubble parameter H in Figure 4.14. Obviously,

[4]In fact, we find that the maximum of $\Delta\Omega_\psi$ in the final iteration is smaller than 10^{-4}.

$\sum_i \Gamma_{d,i} \ll m_\psi = 6.49 \times 10^{-6} (= 1.58 \times 10^{13}$ GeV) throughout. Thus the decay of ψ cannot significantly effect its oscillatory frequency. As can be seen in Figure 4.14, the decay process $\psi \to \psi_d^- \tau_R^c$ turns on much earlier than the other species, as was quantified above. Its decay rate reaches its maximal value and then becomes a constant. This is comparable to, but smaller than, H prior to the other species in Figure 4.14 turning on. Thus the backreaction from $\psi \to \psi_d^- \tau_R^c$ cannot be neglected. The decay rate of $\psi \to t\bar{t}$ is similar to that of $\psi \to \psi_d^- \tau_R^c$, but turns on later and with a much larger maximal value. The decay rates of other species in Figure 4.14 first increase with time after they are turned on. However, since they are proportional to $\langle \psi^2 \rangle$, when $\langle \psi^2 \rangle$ is small enough they achieve a maximum and then decrease with time. Note that $\Gamma(\psi \to \tilde{N}_2 \tilde{N}_2)$ is the total decay rate for the three processes $\psi \to \tilde{N}_{2a}\tilde{N}_{2a}$, $\tilde{N}_{2b}\tilde{N}_{2b}$, $\tilde{N}_{2a}\tilde{N}_{2b}$.

The evolutions of Ω_i and Ω_ψ are displayed in Figure 4.15. $\Omega_{N_2 N_2}$ includes the decay products for all three processes $\psi \to \tilde{N}_{2a}\tilde{N}_{2a}$, $\tilde{N}_{2b}\tilde{N}_{2b}$, $\tilde{N}_{2a}\tilde{N}_{2b}$. We did not specify them individually because even their sum is very small. Note that $\sum_i \Omega_i = 1 - \Omega_\psi$ by definition. Eventually, $\sum_i \Omega_i \to 1$, since $\Omega_\psi \to 0$. We can define the end of the reheating epoch as the time, t_R, when $\Omega_\psi \to 0$, which means that all of the energy of the inflaton has been converted to relativistic species of matter. It is clear from Figure 4.15 that

$$t_R \simeq 8 \times 10^9 \ . \tag{4.147}$$

However, due to numerical imprecision, we may find that $\sum_i \Omega_i \approx 0.9999$ at t_R, which is more than sufficient for our purposes. Note that the values of the Ω_i in Figure 4.15(b) have been rounded to three decimal places. When added together, we find that they sum to

$$\sum_i \Omega_i = 1.000 \ . \tag{4.148}$$

When $t \simeq t_R$, we find $H(t_R) \simeq 7.8 \times 10^{-11} (\simeq 1.9 \times 10^8$ GeV). Since the Universe is now dominated by relativistic particle species, that is, $3M_P^2 H^2 = \rho_{\text{rel}}$, one can, assuming the Universe is in thermal equilibrium, find the reheating temperature from the expression

$$\rho_{\text{rel}} = \frac{\pi^2}{30} g_* T_R^4 \,, \tag{4.149}$$

where g_* is the (effectively) massless degrees of freedom and T_R is the temperature. It follows that the reheating temperature for the Sneutrino-Higgs theory is

$$T_R = g_*^{-\frac{1}{4}} \sqrt{\frac{\sqrt{90} M_P H(t_R)}{\pi}} \approx \frac{3.74}{g_*^{1/4}} \times 10^{13}\,\text{GeV} \ , \tag{4.150}$$

Since reheating takes place to a mixture of standard model particles (such as the top quark and various W-bosons) and lighter supersymmetric sparticles (such as $\tilde{C}_1^{\pm}$), the counting of the degrees of freedom is complicated. However, all of these species will eventually decay to the standard model particles with right-handed neutrinos, which has $g_* = 118$. Hence, it is sufficient for our purposes to make a crude approximation and take this as the number of degrees of freedom at the reheating temperature. It follows that

$$T_R \simeq 1.13 \times 10^{13} \text{ GeV} . \tag{4.151}$$

In this discussion, we are requiring that the B-L breaking scale be well separated from the scale at which reheating takes place; that is B-L breaking occurs at a scale $\ll 10^{13}$ GeV. This simplifies the reheating calculations and, more importantly, allows reheating to occur prior to the breaking of baryon and lepton number. As discussed in B.3, the B-L scale can be made arbitrarily small, albeit at the expense of some fine-tuning. Clearly, the above requirement will be fulfilled for the B-L scales between 10^{10} GeV and 10^{12} GeV discussed in section 4.4. As a concrete example, we see from Figure 4.6 that of the 215 phenomenologically valid black points, the maximal number (≈ 20) occur at a B-L scale of 10^{11} GeV. Henceforth, as an example, let us choose this to be the B-L scale. It follows that the associated energy density is $\rho_{BL} = 10^{44}$ GeV^4. Hence

$$3M_P^2 H(t_{BL})^2 = \rho_{BL} \Rightarrow H(t_{BL}) \simeq 2.371 \times 10^3 \text{ GeV} . \tag{4.152}$$

Thus $H(t_R) \gg H(t_{BL})$, which indicates that B-L breaking will occur much later than the end of the reheating epoch.

4.7.4 The Reheating Interval

The entire analysis of reheating discussed above depends on inputting the numerical values of specific Yukawa parameters and all of the gauge couplings. However, these quantities all "run" with energy scale, changing their values to satisfy the renormalization group equations. We have made two important assumptions that drastically simplify, and clarify, the calculations of reheating. 1) As we will see below, the interval of active reheating to matter is less than one order of magnitude in GeV units. Hence, these parameters vary only minimally over this small energy range. It is therefore a good approximation to choose a point in the interior of the reheating interval and to evaluate all Yukawa and gauge couplings at this fixed scale. 2) We find a point in the interior of the reheating interval as follows. We choose an arbitrary energy scale within an order of magnitude of where we expect to find the end of reheating. Using all Yukawa and gauge couplings evaluated at this energy, we numerically compute $t_{\psi_d^- \tau_R^{c*}}$ and t_R and the Hubble parameters associated with them. We then take the average of the Hubble parameters, H_{avg}, and convert it to a "matter" energy

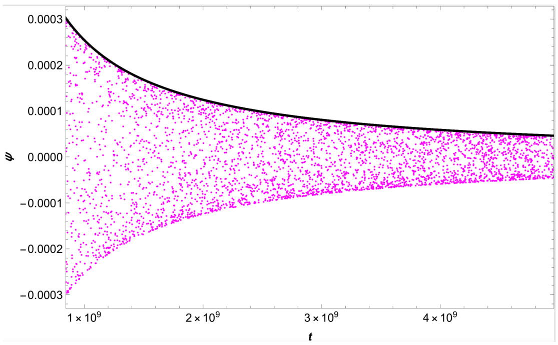

(a) $t_{\mathrm{I}} \le t \le t_{\mathrm{II}}$

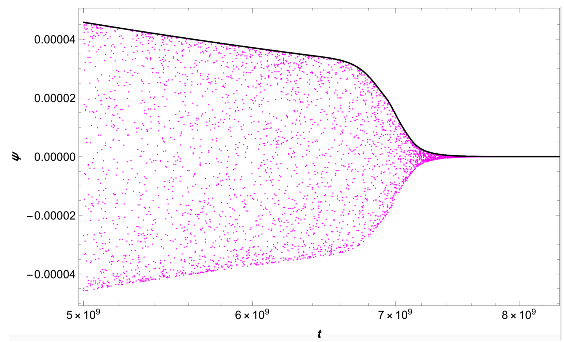

(b) $t \ge t_{\mathrm{II}}$

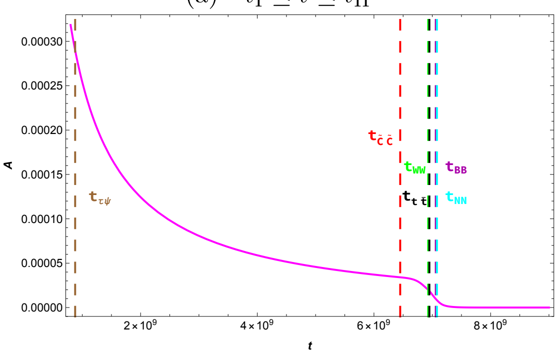

(c) $t \ge t_{\mathrm{I}}$

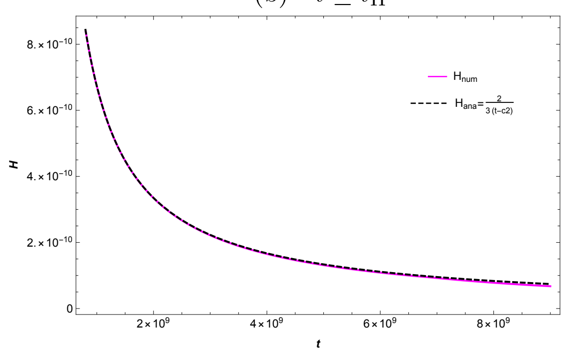

(d) $t \ge t_{\mathrm{I}}$

Figure 4.13: In both (a) and (b), the 5000 magenta points are randomly chosen from the curve of the output $\psi(t)$, in the last (nth) round of iteration, during the time intervals $t_{\mathrm{I}} \le t \le t_{\mathrm{II}}$ and $t \ge t_{\mathrm{II}}$ respectively. Their upper boundaries are identical to the input $A(t)$ in the last round of iteration, that is, A_n, which is the black curves in (a) and (b). In (c), we plot the upper boundaries of the magenta points, that is, A_{n+1}, from t_{I} to sometime after reheating. In addition, the time at which each specie is turned on is marked with a vertical line, where $t_{\tau\psi *} = 8.78 \times 10^8$, $t_{\tilde{C}\tilde{C}*} = 6.45 \times 10^9$, $t_{WW*} = 6.93 \times 10^9$, $t_{t\bar{t}*} = 6.95 \times 10^9$, $t_{BB*} = 7.06 \times 10^9$ and $t_{NN*} = 7.08 \times 10^9$. In (d), we plot the solution for H in the last round of iteration, that is, H_{num}, and also (4.64) as a reference, from t_{I} to sometime after reheating. We always set $t_{\mathrm{I}} = 8 \times 10^8$ and $t_{\mathrm{II}} = 5 \times 10^9$ in our numerical calculations for technical convenience and everywhere set $M_P = 1$.

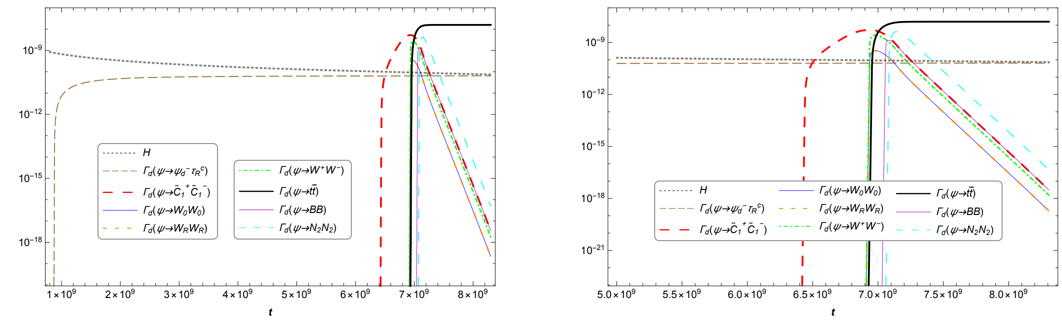

(a) $t \geq t_{\rm I}$ (b) $t \geq t_{\rm II}$

Figure 4.14: In (a), we plot the evolutions of H and the decay rates $\Gamma_{d,i}$ from $t_{\rm I}$ to sometime after the end of reheating. In (b), we plot H and $\Gamma_{d,i}$ from $t_{\rm II}$ to sometime after the end of reheating. Note that $\Gamma_d(\psi \to \psi_d^- \tau_R^c)$ is very close to H when $t > t_{\rm II}$. We set $t_{\rm I} = 8 \times 10^8$ and $t_{\rm II} = 5 \times 10^9$. In both (a) and (b), $\Gamma(\psi \to \tilde{N}_2 \tilde{N}_2)$ is the total decay rate for three processes $\psi \to \tilde{N}_{2a}\tilde{N}_{2a}$, $\tilde{N}_{2b}\tilde{N}_{2b}$, $\tilde{N}_{2a}\tilde{N}_{2b}$.

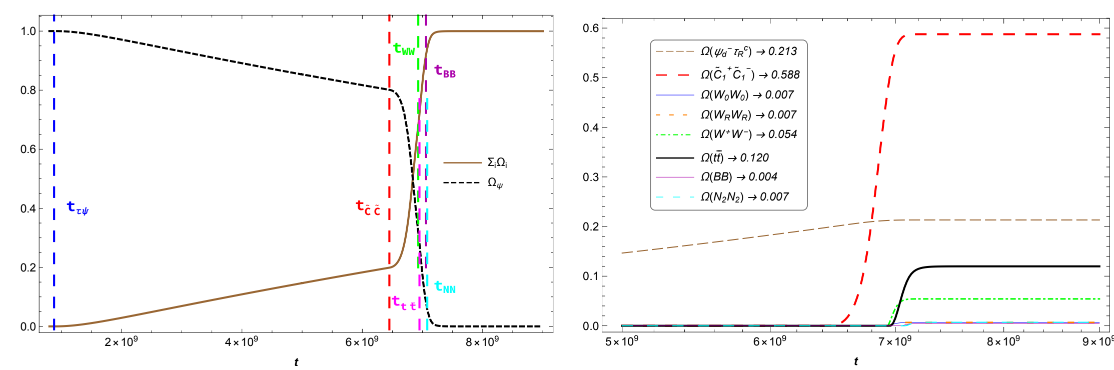

(a) $t \geq t_{\rm I}$ (b) $t \geq t_{\rm II}$

Figure 4.15: In (a), we plot the evolutions of Ω_ψ and $\sum_i \Omega_i$ from $t_{\rm I}$ to sometime after the end of reheating. The time at which each specie is turned on is marked with a vertical line, where $t_{\tau\psi *} = 8.78 \times 10^8$, $t_{\tilde{C}\tilde{C}*} = 6.45 \times 10^9$, $t_{WW*} = 6.93 \times 10^9$, $t_{t\bar{t}*} = 6.95 \times 10^9$, $t_{BB*} = 7.06 \times 10^9$ and $t_{NN*} = 7.08 \times 10^9$. In (b), we plot each Ω_i from $t_{\rm II}$ to sometime after the end of reheating. Note that $\Omega(\psi_d^- \tau_R^c) = 0.183$ at $t_{\rm II}$.

density using $3H^2M_P^2 = \rho_{avg}$. The interior energy scale is then chosen to be the fourth root of ρ_{avg}. Further iteration shows that this interior point remains a good approximation for characterizing the reheating interval.

Specifically, we do the following. First consider 2). We begin by choosing the arbitrary scale to be 10^{12} GeV and use the RGE's to compute all Yukawa and gauge parameters at this energy. The numerical calculation of Γ_i, Ω_i and H, as well as $t_{\psi_d^- \tau_R^{c}*}$ and t_R, are carried out as described previously in this section. We find that the associated Hubble parameters are

$$H(t_{\psi_d^- \tau_R^{c}*}) \simeq 1.6 \times 10^9 \text{ GeV} , \; H(t_R) \simeq 1.6 \times 10^8 \text{ GeV} \tag{4.153}$$

and, hence,

$$H_{avg} \simeq 8.0 \times 10^8 \text{ GeV} \quad \Rightarrow \quad \rho_{avg}^{1/4} \simeq 5.8 \times 10^{13} \text{ GeV} . \tag{4.154}$$

It then follows from assumption 1) that all Yukawa and coupling parameters used in our reheating calculations will be evaluated at 5.8×10^{13} GeV.

4.8 Attaining Equilibrium

In order to define a reheating temperature for the plasma of decay products, one must determine that they have attained equilibrium [151]. In this section, we will show that this is indeed the case prior to $t_R \simeq 8 \times 10^9$. Thermal equilibrium occurs when the interaction rate of the i-th decay product, which we denote by Γ^i_{int}, is sufficiently large for all species i. Specifically, one requires that

$$\Gamma^i_{int} > H , \; \forall \; i . \tag{4.155}$$

This implies that the mean interaction length, $1/\Gamma^i_{int}$, is within the causal horizon $1/H$.

To demonstrate that (4.155) is indeed satisfied by the end of reheating, let us consider the elastic scattering of the charginos, $\tilde{C}_1^{\pm}$, mediated by gauge bosons. As we have shown in Figure 4.15(b), these comprise the largest fraction of inflaton decay products by the end of reheating. We argue that all other interaction processes involving different species present in the plasma will have similar interaction rates – since these will also involve gauge boson mediated scattering, all with similarly large values of gauge couplings. Therefore, if condition (4.155) is satisfied for one species, it is safe to assume that it is satisfied for all of them by the time that reheating is completed.

For simplicity, let us determine the rate for the process $\tilde{C}_1^+ \tilde{C}_1^- \to \tilde{C}_1^+ \tilde{C}_1^-$, where, for simplicity, we take the mediating gauge boson to be W^0_μ. This process is also mediated by $W_{R\mu}$ and B_μ, but since at this energy scale the gauge couplings are all of similar value, see (4.141), the results will be very similar. Feynman diagrams which contribute to this process are shown in Figure 4.16. The differential cross-section for this interaction is

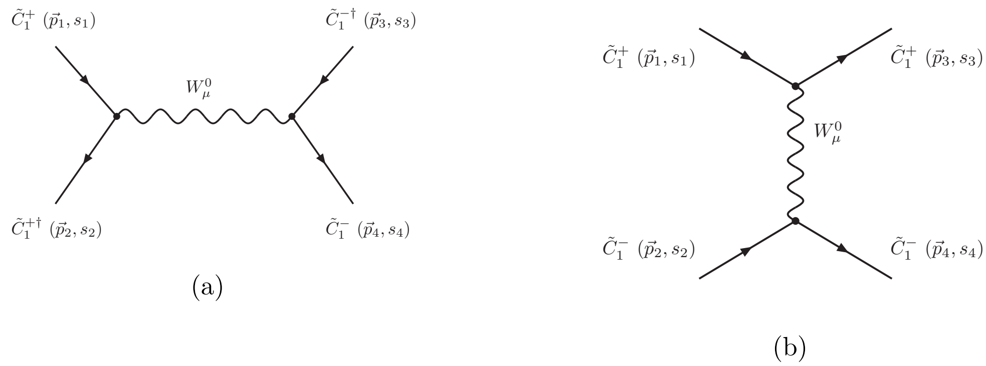

Figure 4.16: Subfigures (a) and (b) show some of the s- and t-channel diagrams respectively contributing to the $\tilde{C}_1^+\tilde{C}_1^- \to \tilde{C}_1^+\tilde{C}_1^-$ scattering process exchanging a W_μ^0 boson.

$$\frac{d\sigma}{dt}(\tilde{C}_1^+\tilde{C}_1^- \to \tilde{C}_1^+\tilde{C}_1^-) \quad = \quad \frac{\mathcal{O}_a^4}{8\pi s^2}\left[\left(\frac{s}{t}\right)^2 + u^2\left(\frac{1}{s}+\frac{1}{t}\right)^2 + \left(\frac{t}{s}\right)^2\right] \tag{4.156}$$

where the coupling $\mathcal{O}_a$ is given by

$$\mathcal{O}_a \quad = \quad g_2\left(\frac{1}{2}|V_{1u}|^2 + |V_{1W}|^2\right) . \tag{4.157}$$

The matrix elements V_{1u}, V_{1W} are given in appendix C.1. We have used the fact that

$$V_{1u} = U_{1\tau}\,, \quad V_{1W} = U_{1W} \tag{4.158}$$

in this calculation. Here, as in the rest of this chapter, we follow the conventions and notation outlined in [75]. In the center-of-mass frame, the Mandelstam variables s, t and u are

$$\begin{aligned} s &= -(p_1+p_2)^2 = E_{cm}^2 \\ t &= -(p_3-p_1)^2 = -\frac{1}{2}(E_{cm}^2 - 4m_{\tilde{C}_1}^2)(1-\cos\theta) \\ u &= -(p_4-p_1)^2 = -\frac{1}{2}(E_{cm}^2 - 4m_{\tilde{C}_1}^2)(1+\cos\theta)\,, \end{aligned} \tag{4.159}$$

where we have assumed that the incoming states carry energy $E_{cm}/2$, with

$$E_{cm} = m_\psi. \tag{4.160}$$

In deriving equation (4.156), we have ignored the mass of the gauge boson, which quickly becomes negligible as the inflaton VEV decreases. The total cross section is then given by integrating

$$\sigma = \int_{t_-}^{t_+} \frac{d\sigma}{dt} \,, \quad t_- = t|_{\cos\theta=-1} \,, \quad t_+ = t|_{\cos\theta=1-\delta} \,, \tag{4.161}$$

where the cutoff δ must be introduced to remove the collinear divergence. We use the standard result that

$$\delta = \frac{2m^2_{\tilde{C}_1}}{s} \,. \tag{4.162}$$

In Figure 4.17, we plot the resulting cross-section as a function of the parameter $x_2 = g_2\sqrt{\langle\psi^2\rangle}/\sqrt{6}$, which is proportional to the inflaton expectation value. The interaction rate is given by

$$\Gamma_{int}(\tilde{C}_1^+\tilde{C}_1^- \to \tilde{C}_1^+\tilde{C}_1^-) \quad = \quad n\sigma v \,, \tag{4.163}$$

where n is the number density of $\tilde{C}_1^\pm$ and v is the average particle velocity, which we take to be $v \sim c = 1$. For a given particle species with average energy $\langle E\rangle$, the number density can be approximated by the expression

$$n = \frac{\rho}{\langle E\rangle} \,, \tag{4.164}$$

The rate $\Gamma_{int}(\tilde{C}_1^+\tilde{C}_1^- \to \tilde{C}_1^+\tilde{C}_1^-)$ is plotted as a function of time along with the Hubble parameter in Figure 4.18. It is clear that condition (4.155) is satisfied well before the completion of reheating. Since the self-scattering interactions of other decay products involve similarly sized gauge couplings, we expect analogous rates for these species–for example, top quarks and W bosons–to also satisfy condtion (4.155) by the end of reheating, despite their smaller number density.

Strictly speaking, we have determined that the particles above have attained *kinetic* equilibrium, one of two necessary conditions to ensure that the decay products of the inflaton have thermalized [84, 58, 151]. The second condition, the achievement of *chemical* equilibrium, requires the analysis of number-violating $2 \to 3$ interactions. An example of such a process is given in Figure 4.19. Naively, these interactions may be suppressed by an extra factors of perturbative couplings and hence their rates may be smaller than the number conserving $2 \to 2$ scattering - although this is not always the case. Without going into the full details of such processes, we will simply argue that their rates are still sufficiently high. That is, a $2 \to 3$ scattering rate involving the charginos could at worse be

$$\Gamma_{2\to 3}(\tilde{C}_1^+\tilde{C}_1^-) \sim 10^{-2}\,\Gamma_{int}(\tilde{C}_1^+\tilde{C}_1^- \to \tilde{C}_1^+\tilde{C}_1^-) \,. \tag{4.165}$$

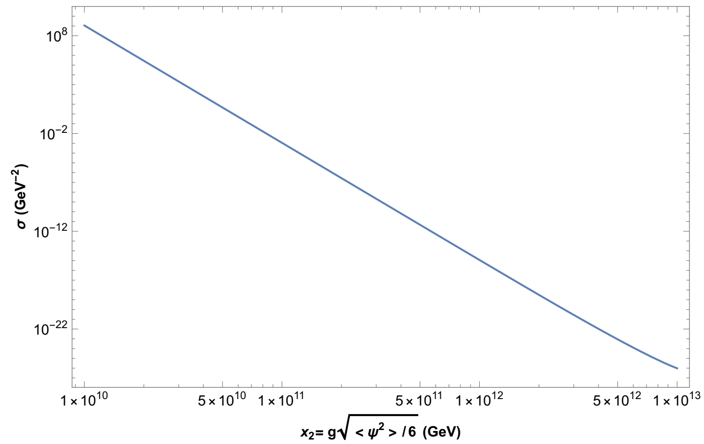

Figure 4.17: A log-log plot of the cross section for the process $\tilde{C}_1^+\tilde{C}_1^- \to \tilde{C}_1^+\tilde{C}_1^-$ plotted against the inflaton expectation value $x_2 = g\sqrt{\langle\psi^2\rangle}/\sqrt{6}$, where $g = 0.57$ as in the rest of this text.

Under this assumption, from Figure 4.18, we can see that the condition

$$\Gamma_{2\to3}(\tilde{C}_1^+\tilde{C}_1^-) > H \tag{4.166}$$

is also attained before the end of reheating. We expect that this holds for all other decay products as well.

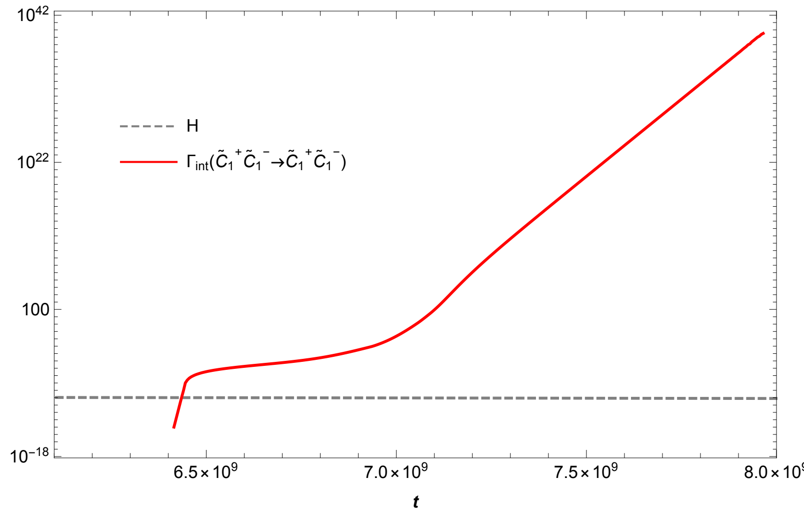

Figure 4.18: The rate Γ_{int} for the process $\tilde{C}_1^+\tilde{C}_1^- \to \tilde{C}_1^+\tilde{C}_1^-$ plotted against time (shown in units where $M_P = 1$). The rate almost immediately becomes larger than the Hubble parameter H, which is approximately 7.8×10^{-11} at the very end of the plot. The time at the end of reheating, $t_R \simeq 8 \times 10^9$.

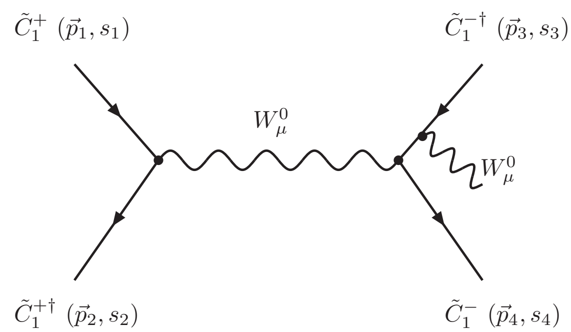

Figure 4.19: Example of a Feynman diagram for $2 \to 3$ inelastic scattering involving the charginos.

Chapter 5

Effective Brane Actions

5.1 Introduction

Heterotic M-theory consists of a five-dimensional manifold of the form $\mathbf{S}^1/\mathbb{Z}_2 \times M_4$. It has been shown that one of the two orbifold planes, the "observable" sector, can have a low energy particle spectrum which is precisely the $N = 1$ supersymmetric standard model with three right-handed neutrino chiral supermultiplets. The other orbifold plane constitutes a "hidden" sector which, since its communication with the observable sector is suppressed, will be ignored in this chapter. However, the finite fifth-dimension allows for the existence of three-brane solitons which, in order to render the vacuum anomaly free, must appear. That is, heterotic M-theory provides a natural framework for brane-world cosmological scenarios coupled to realistic particle physics.

The complete worldvolume action of such three-branes is unknown. Here, treating these solitons as probe branes, we construct their scalar worldvolume Lagrangian as a derivative expansion of the heterotic DBI action. In analogy with similar calculations in the M_5 and AdS_5 context, this leads to the construction of "heterotic Galileons". However, realistic vacua of heterotic M-theory are necessarily $N = 1$ supersymmetric in four dimensions. Hence, we proceed to supersymmetrize the three-brane worldvolume action, first in flat superspace before extending the results to $N = 1$ supergravity. Such a worldvolume action may lead to interesting cosmology, such as "bouncing" universe models, by allowing for the violation of the Null Energy Condition (NEC).

The plan of this chapter is as follows. We briefly review the properties of five-branes in heterotic M-theory in section 5.2, before describing specific properties of the five-dimensional heterotic M-theory geometry in secion 5.3. In section 5.4 we discuss the construction of (non-supersymmetric) co-dimension one probe brane actions embedded in a generic five-dimensional bulk space. For later comparison, we present the action of such probe branes when the bulk space is taken to be AdS_5, as well as the organization of the relevant Lagrangians under a derivative expansion into the so-called "conformal galileons" in section 5.5. We then move onto the more relevant case where the bulk space is taken to be the heterotic M-theory background presented in 5.3, and derive the "heterotic galileon" Lagrangians in section 5.6.

As mentioned above, these Lagrangians must be extended into $N = 1$ supersymmetry, and we do this first in flat or rigid superspace in section 5.7 by embedding the brane position modulus in a chiral multiplet. Applying some reasonable physical constraints, we describe the elimination of the auxiliary field in section 5.8. We then extend the Lagrangians in to curved superspace–i.e. $N = 1$ supergravity–in section 5.9. Details of computing higher derivative supergravity expressions are presented in D. Finally, we present a "cosmological" limit of the resulting action in 5.10.

5.2 Inclusion of Branes in Heterotic M-theory

The complete heterotic M-theory vacuum requires that one specify a slope stable, holomorphic vector bundle with vanishing slope on the Calabi-Yau threefold associated with the hidden sector. This choice is far from unique, only being restricted by the requirement that the homological constraint

$$c_2(V^{(observable)}) + c_2(V^{(hidden)}) + W - c_2(TX) = 0 \tag{5.1}$$

be satisfied. Here, c_2 specifies the second Chern class and TX is the tangent bundle of the quotient Calabi-Yau threefold X. W specifies the homology class associated with the three-branes in the finite 5-th dimensional interval–henceforth, referred to as the "bulk space". For the relevant case where X and $V^{(observable)}$ are the Calabi-Yau and vector bundle giving rise to the B-L MSSM described previously, an explicit example of a hidden sector bundle $V^{(hidden)}$ which satisfies condition (5.23) for an "effective" homology class W is given in [33]. However, we expect there to be many such hidden sector bundles. Since their spectrum is connected to our observable world only by gravitational suppressed interactions, we, henceforth, ignore the hidden sector. What is important to this chapter, however, is the existence of an effective homology class W, which contains holomorphic curves on which two spatial dimensions of a bulk space five-brane can be wrapped. We will, henceforth, assume that there is only a *single* five-brane wrapped on a holomorphic curve in W. That is, our heterotic M-theory vacuum contains a single, isolated three-brane in the bulk space. Since the curve is holomorphic, the worldvolume theory of this three-brane must be $N = 1$ supersymmetric. The possible intrinsic fields on the three-brane worldvolume were discussed in detail in [143]. In general, for a specific gauge choice, the worldvolume contains two real scalar fields–π, which specifies its embedding in the bulk space and χ, which is the dual to an antisymmetric tensor on the brane surface. These combine together to form a complex "universal" scalar, which is the lowest component of a chiral superfield. Additionally, if the genus of the holomorphic curve is g, there can also exists g vector superfields on the three-brane worldvolume. Henceforth, for simplicty, we will assume that the holomorphic curve has genus zero and, therefore, these vector supermultiplets do not arise.

5.3 The Five-dimensional Heterotic Metric

Before continuing to the construction of supersymmetric heterotic three-brane actions, there remains one more important issue that must be discussed; namely, the form of the five-dimensional bulk space metric in heterotic M-theory. This was worked out in a number of different contexts in [139]. Choosing a flat foliation of the bulk space, the general form of the five-dimensional metric is given by

$$ds^2 = a(y)^2 \eta_{\mu\nu} dx^\mu dx^\nu + b(y)^2 dy^2 \ , \tag{5.2}$$

where $y \in [0, \pi\rho]$ is the coordinate of the finite 5-th dimension and the functions $a(y)$ and $b(y)$ are determined by solving the equations of motion derived from the five-dimensional heterotic M-theory Lagrangian. This is straightforward for Calabi-Yau threefold compactifications with $h^{1,1} = 1$ [139, 32]. However, for compactifications where $h^{1,1} > 1$, this is considerably more difficult. Be that as it may, the solutions for the heterotic standard model, where $h^{1,1} = 3$, were presented in a "linearized" approximation in [139] . In this case, *assuming there is no three-brane in the bulk space*, one finds

$$a^2(y) = a_0^2 h(y) \ , \ b^2(y) = b_0^2 h(y)^4 \ , \tag{5.3}$$

where

$$h(y) = -\frac{2}{3}(\alpha y + c_0) \tag{5.4}$$

and a_0, b_0 and c_0 are dimensionless constants. The dimension one parameter α is defined by

$$\alpha = \frac{\pi}{\sqrt{2}} \left(\frac{\kappa}{4\pi}\right)^{2/3} \frac{1}{v^{2/3}} \beta \ , \tag{5.5}$$

with κ the 11-dimensional Planck constant and v is the Calabi-Yau "reference" volume, with mass dimensions $-9/2$ and -6 respectively, and

$$\beta = \frac{1}{v^{1/3}} \int_X \left(c_2(V^{(observable)}) - \frac{1}{2} c_2(TX) \right) \wedge \omega \ , \tag{5.6}$$

where ω the Kähler form on X. For the case of a single three-brane located at the point $Y \in [0, \pi\rho]$, it was shown in [32, 10] that this solution for $h(y)$ generalizes to

$$h(y) = -\frac{2}{3}((\alpha + \alpha^{(3)})y - \alpha^{(3)}Y + c_0) \ , \tag{5.7}$$

where the three-brane charge $\alpha^{(3)}$ is

$$\alpha^{(3)} = \left(\frac{\pi}{\sqrt{2}}\left(\frac{\kappa}{4\pi}\right)^{2/3}\frac{1}{v^{2/3}}\right)\frac{1}{v^{1/3}}\int_X W \wedge \omega \ . \tag{5.8}$$

Here, W is the two-form associated with the wrapped three-brane and satisfies homology condition (5.1). Clearly, the dimension one parameter $\alpha^{(3)}$ depends explicitly on the choice of the hidden sector gauge bundle. For different hidden sector bundles, $\alpha^{(3)}$ can be either smaller or larger than the observable sector parameter α. Since, in this chapter, we are ignoring any discussion of the hidden sector, we will simply use the *"probe brane"* approximation; that is, we assume the three-brane does not back-react on the geometry and, hence, does not effect the five-dimensional metric presented in (5.3) and (5.4). We expect this to be a good approximation for certain choices of the hidden sector bundle. In any case, we will, for simplicity, use the "probe brane" approximation in the remainder of this chapter. Finally, it was shown in [163] that, after a coordinate transformation to a new variable z with the same range $[0, \pi\rho]$ as y, as well as further restrictions on the coefficients, the metric can be expressed simply as

$$ds^2 = a(z)^2 \eta_{\mu\nu} dx^\mu dx^\nu + dz^2 \ , \tag{5.9}$$

where

$$a^2(z) = (1 - 2\alpha z)^{1/3} \ . \tag{5.10}$$

This is the form of the five-dimensional bulk space metric that we will use in the remainder of this chapter.

Finally, this metric has two important properties that will be essential in our analysis of the heterotic three-brane worldvolume action. First, note that the only mass scale entering the metric and, hence, the curvature of the bulk space is α–given in (5.5),(5.6). Second, in order to avoid metric (5.9) becoming singular, it follows from (5.10) that

$$\alpha z < \frac{1}{2}, \quad z \in [0, \pi\rho] \ . \tag{5.11}$$

Furthermore, as shown in [139], the "linearized" approximation necessitated by the fact that $h^{1,1} = 3$, strengthens this inequality to become

$$\alpha z \ll 1 \ . \tag{5.12}$$

For the heterotic M-theory standard model discussed above, we find that $1/\pi\rho \sim 10^{15}$ GeV and, using (5.5) and (5.6), that

$$\alpha \simeq 10^{14}\,\text{GeV} \ , \tag{5.13}$$

thus satisfying the inequality (5.12).

5.4 Co-Dimension One Brane Action

In this section, we review the formalism [101, 100] for constructing the worldvolume action of a 3-brane in a 4+1–dimensional bulk space. Denote the bulk space coordinates by X^A, $A = 0, 1, 2, 3, 5$ and the associated metric by $G_{AB}(X)$, where $A = 0$ is the time-like direction. The coordinates X^A have dimensions of length. We begin by defining a foliation of the bulk space composed of time-like slices. Following [101, 100], one chooses coordinates X^A so that the leaves of the foliation are the surfaces associated with X^5 =constant, where the constant runs over a continuous range which depends on the choice of bulk space. It follows that the coordinates on an arbitrary leaf of the foliation are given by X^μ, $\mu = 0, 1, 2, 3$. Note that we have denoted the four coordinate indices $A = 0, 1, 2, 3$ as $\mu = 0, 1, 2, 3$ to indicate that these are the coordinates on the leaves of a time-like foliation. Now, further restrict the foliation so that it is 1) Gaussian normal with respect to the metric $G_{AB}(X)$ and 2) the extrinsic curvature on each of the leaves of the foliation is proportional to the induced metric. Under these circumstances, X^5 is the transverse normal coordinate and the metric takes the form

$$G_{AB}(X)dX^A dX^B = (dX^5)^2 + f(X^5)^2 g_{\mu\nu}(X)dX^\mu dX^\nu \ , \tag{5.14}$$

where $g_{\mu\nu}(X)$ is an arbitrary metric on the foliation and is a function of the four leaf coordinates X^μ, $\mu = 0, 1, 2, 3$ only. The function $f(X^5)$ and the intrinsic metric $g_{\mu\nu}(X)$ are dimensionless and will depend on the specific bulk space and foliation geometries of interest. It is important to notice that the coordinates X^A satisfying the above conditions and, in particular, the location of their origin, have not been uniquely specified. Although this could be physically important in some contexts, for any bulk space of maximal symmetry, such as the AdS_5 geometry we will discuss shortly, the origin of such a coordinate system is completely arbitrary and carries no intrinsic information.

Now consider a physical 3+1 brane embedded in the bulk space. Denote a set of intrinsic worldvolume coordinates of the brane by σ^μ, $\mu = 0, 1, 2, 3$. The worldvolume coordinates also have dimensions of length. The location of the brane in the bulk space is specified by the five "embedding" functions $X^A(\sigma)$ for $A = 0, 1, 2, 3, 5$, where any given five-tuplet $(X^{(0)}(\sigma), \ldots X^{(5)}(\sigma))$ on the brane is a point in the bulk space written in X^A coordinates. The induced metric and extrinsic curvature on the brane worldvolume are then given by

$$\bar{g}_{\mu\nu} = e^A_{\ \mu} e^B_{\ \nu} G_{AB}(X), \quad K_{\mu\nu} = e^A_{\ \mu} e^B_{\ \nu} \nabla_A n_B \tag{5.15}$$

where $e^A_{\ \mu} = \frac{\partial X^A}{\partial \sigma^\mu}$ are the tangent vectors to the brane and n_A is the unit normal vector. One expects the worldvolume action to be composed entirely of the geometrical tensors associated with the embedding of the brane into the target space; that is, $\bar{g}_{\mu\nu}$ and $K_{\mu\nu}$ defined in (5.15), as well as $\bar{\nabla}_\mu$ and the curvature $\bar{R}^\alpha_{\beta\mu\nu}$ constructed from $\bar{g}_{\mu\nu}$. It follows that the worldvolume action must be of the form

$$S = \int d^4\sigma \ \mathcal{L}\left(\bar{g}_{\mu\nu}, K_{\mu\nu}, \bar{\nabla}_\mu, \bar{R}^\alpha_{\mu\beta\nu}\right) = \int d^4\sigma \sqrt{-\bar{g}} \mathcal{F}\left(\bar{g}_{\mu\nu}, K_{\mu\nu}, \bar{\nabla}_\mu, \bar{R}^\alpha_{\mu\beta\nu}\right) , \tag{5.16}$$

where $\mathcal{F}$ is a scalar function. Furthermore, the brane action, and, hence, $\mathcal{F}$, must be invariant under arbitrary diffeomorphisms of the worldvolume coordinates σ^μ. Infinitesimal diffeomorphisms are of the form

$$\delta X^A(\sigma) = \xi^\mu \partial_\mu X^A(\sigma) \tag{5.17}$$

for arbitrary local gauge parameters $\xi^\mu(\sigma)$. Although, naively, there would appear to be five scalar degrees of freedom on the 3-brane worldvolume, it is straightforward to show that one can use the gauge freedom (5.17) to set

$$X^\mu(\sigma) = \sigma^\mu \ , \quad \mu = 0, 1, 2, 3 \ . \tag{5.18}$$

Inverting this expression, it is clear that the worldvolume coordinates σ^μ are, in this gauge, fixed to be the bulk coordinates X^μ of the foliation. The function $X^5(\sigma)$, however, is completely unconstrained by this gauge choice. Henceforth, we will always work in the gauge specified by (5.18) and define

$$X^5(\sigma) \equiv \pi(\sigma) = \pi(X^\mu). \tag{5.19}$$

That is, there is really only a single scalar function of the transverse foliation coordinates X^μ, $\mu = 0, 1, 2, 3$ that defines the location of the 3+1 brane relative to the choice of origin of the X^A coordinates. We reiterate that, although in some contexts the specific choice of the coordinate origin could be physically important, in a bulk space of maximal symmetry, such as AdS_5 space, the location of the coordinate origin is completely arbitrary and carries no intrinsic information. Note that $\pi(X^\mu)$ has dimensions of length.

For clarity, let us relate our notation to that which often appears in the literature [101, 100]. With this in mind, we will denote the four foliation coordinates and the transverse Gaussian normal coordinate by $X^\mu \equiv x^\mu, \mu = 0, 1, 2, 3$ and $X^5 \equiv \rho$ respectively. It follows that the generic bulk space metric appearing in (5.14) can now be written as

$$G_{AB}(X)dX^A dX^B = d\rho^2 + f(\rho)^2 g_{\mu\nu}(x)dx^\mu dx^\nu \ . \tag{5.20}$$

Using (5.18)and (5.19), one notes that the scalar field specifying the 3+1 brane location relative to a chosen origin can be expressed as $\rho(x) = \pi(x)$. Therefore, the metric (5.20) restricted to the brane worldvolume becomes

$$G_{AB}(X)dX^A dX^B = d\rho^2 + f(\pi(x))^2 g_{\mu\nu}(x)dx^\mu dx^\nu \ . \tag{5.21}$$

It then follows that the induced metric and the extrinsic curvature on the brane are given by

$$\bar{g}_{\mu\nu} = f(\pi)^2 g_{\mu\nu} + \nabla_\mu\pi\nabla_\nu\pi, \qquad K_{\mu\nu} = \gamma\Big(- \nabla_\mu\nabla_\nu\pi + ff' g_{\mu\nu} + 2\frac{f'}{f}\nabla_\mu\pi\nabla_\nu\pi\Big) \tag{5.22}$$

respectively, where $' = \partial/\partial\pi$ and

$$\gamma = \frac{1}{\sqrt{1 + \frac{1}{f^2}(\nabla\pi)^2}} \ . \tag{5.23}$$

An action of the form (5.16) will generically lead to equations of motion for the physical scalar field $\pi(x)$ that are higher than second order in derivatives and, hence, possibly propagate extra ghost degrees of freedom. Remarkably, this can be avoided [60, 101, 100] if one restricts the Lagrangian to be of the form

$$\mathcal{L} = \Sigma_{i=1}^5 \ c_i \mathcal{L}_i, \tag{5.24}$$

where the c_i are constant real coefficients,

$$\begin{aligned}
\mathcal{L}_1 &= \sqrt{-g}\int^\pi d\pi' f(\pi')^4, \\
\mathcal{L}_2 &= -\sqrt{-\bar{g}}, \\
\mathcal{L}_3 &= \sqrt{-\bar{g}}\ K, \\
\mathcal{L}_4 &= -\sqrt{-\bar{g}}\ \bar{R}, \\
\mathcal{L}_5 &= \frac{3}{2}\sqrt{-\bar{g}}\ K_{GB}
\end{aligned} \tag{5.25}$$

with $K = \bar{g}^{\mu\nu} K_{\mu\nu}$, $\bar{R} = \bar{g}^{\mu\nu} \bar{R}^{\alpha}_{\mu\alpha\nu}$ and $\mathcal{K}_{GB}$ is a Gauss-Bonnet boundary term given by

$$\mathcal{K}_{GB} = -\frac{1}{3}K^3 + K^2_{\mu\nu}K - \frac{2}{3}K^3_{\mu\nu} - 2\Big(\bar{R}_{\mu\nu} - \frac{1}{2}\bar{R}\bar{g}_{\mu\nu}\Big)K^{\mu\nu} \ . \tag{5.26}$$

All indices are raised and traces taken with respect to $\bar{g}^{\mu\nu}$. It has been shown [60, 101, 100] that Lagrangian (5.24), for any choices of coefficients c_i, leads to an equation of motion for $\pi(X^\mu)$ that is only second order in derivatives. In this chapter, we will assume that both (5.16) and (5.24),(5.25) are satisfied.

Evaluating each of the Lagrangians in (5.25) for an arbitrary metric of the form (5.20) is arduous and has been carried out in several papers [60, 101, 100]. The $\mathcal{L}_5$ term is particularly long and not necessary for the work to be discussed here. Hence, we will ignore it in the rest of this chapter. The remaining four Lagrangians are found to be

$$\begin{aligned}
\mathcal{L}_1 &= \sqrt{-g}\int^{\pi} d\pi' f^4(\pi') \\
\mathcal{L}_2 &= -\sqrt{-g} f^4 \sqrt{1 + \frac{1}{f^2}(\nabla\pi)^2} \\
\mathcal{L}_3 &= \sqrt{-g}\Big[f^3 f'(5-\gamma^2) - f^2[\Pi] + \gamma^2[\pi^3]\Big] \\
\mathcal{L}_4 &= -\sqrt{-g}\Big\{\frac{1}{\gamma}f^2 R - 2\gamma R_{\mu\nu}\nabla^\mu\pi\nabla^\nu\pi + \gamma\Big[[\Pi]^2 - [\Pi^2] + 2\gamma^2\frac{1}{f^2}\big(-[\Pi][\pi^3] + [\pi^4]\big)\Big] \\
&\quad + 6\frac{f^3 f''}{\gamma}(-1+\gamma^2) + 2\gamma f f'\Big[-4[\Pi] + \frac{\gamma^2}{f^2}\big(f^2[\Pi] + 4[\pi^3]\big)\Big] \\
&\quad - 6\frac{f^2(f')^2}{\gamma}(1 - 2\gamma^2 + \gamma^4)\Big\}
\end{aligned} \tag{5.27}$$

In these expressions, all covariant derivatives and curvatures are with respect to the foliation metric $g_{\mu\nu}$. We follow the notation common in the literature. Defining $\Pi_{\mu\nu} \equiv \nabla_\mu\nabla_\nu\pi$, the bracket $[\Pi^n]$ denotes the trace of n-powers of $[\Pi]$ with respect to $g^{\mu\nu}$. For example, $[\Pi] = \nabla_\mu\nabla^\mu\pi$, $[\Pi^2] = \nabla_\mu\nabla_\nu\pi\nabla^\mu\nabla^\nu\pi$ and so on. Similarly, we also define contractions of powers of Π with $\nabla\pi$ using the notation $[\pi^n] \equiv \nabla\pi\Pi^{n-2}\nabla\pi$. For example, $[\pi^2] = \nabla_\mu\pi\nabla^\mu\pi$, $[\pi^3] = \nabla_\mu\pi\nabla^\mu\nabla^\nu\pi\nabla_\nu\pi$ and so on. Note that the Lagrangians $\mathcal{L}_1, \mathcal{L}_2, \mathcal{L}_3$ and $\mathcal{L}_4$ in (5.27) have mass dimensions $-1, 0, 1$ and 2 respectively. Hence, the constant coefficients c_1, c_2, c_3, c_4 in action (5.24) have mass dimensions $5, 4, 3$ and 2.

5.5 A Flat 3-Brane in AdS_5: Conformal Galileons

As an warm-up exercise, let us consider the case where the target space is the "maximally symmetric" five-dimensional anti-de Sitter space AdS_5 with isometry algebra $so(4,2)$ and the foliation leaves are "flat"–that is, have Poincaré isometry algebra $p(3,1)$ [1]. This geometry is easily shown to satisfy the above two assumptions that the foliations are Gaussian normal with respect to the target space metric and the extrinsic curvature is proportional to the induced metric. It then follows that the AdS_5 metric written in the X^A coordinates subject to gauge choice (5.17) and definition (5.19) is of the form (5.21). More specifically, if we denote the AdS_5 radius of curvature by $\mathcal{R}(>0)$, and denote the flat metric on the foliations by $\eta_{\mu\nu}$, one finds that the target space metric is given by

$$G_{AB}dX^A dX^B = d\rho^2 + f(\pi)^2\eta_{\mu\nu}dx^\mu dx^\nu, \tag{5.28}$$

where

$$f(\pi) = e^{-\frac{\pi}{\mathcal{R}}}. \tag{5.29}$$

It follows that the four Lagrangians given in (5.27) become

$$\begin{aligned}
\mathcal{L}_1 &= -\frac{\mathcal{R}}{4}e^{-\frac{4\pi}{\mathcal{R}}} \\
\mathcal{L}_2 &= -e^{-\frac{4\pi}{\mathcal{R}}}\sqrt{1+e^{\frac{2\pi}{\mathcal{R}}}(\partial\pi)^2} \\
\mathcal{L}_3 &= \gamma^2[\pi^3] - e^{-\frac{2\pi}{\mathcal{R}}}[\Pi] + \frac{1}{\mathcal{R}}e^{-\frac{4\pi}{\mathcal{R}}}(\gamma^2-5) \\
\mathcal{L}_4 &= -\gamma([\Pi]^2-[\Pi^2]) - 2\gamma^3 e^{\frac{2\pi}{\mathcal{R}}}([\pi^4]-[\Pi][\pi^3]) \\
&\quad + \frac{6}{\mathcal{R}^2}e^{-\frac{4\pi}{\mathcal{R}}}\frac{1}{\gamma}(2-3\gamma^2+\gamma^4) + \frac{8}{\mathcal{R}}\gamma^3[\pi^3] - \frac{2}{\mathcal{R}}e^{-\frac{2\pi}{\mathcal{R}}}\gamma(4-\gamma^2)[\Pi]
\end{aligned} \tag{5.30}$$

respectively, where

$$\gamma = \frac{1}{\sqrt{1+e^{\frac{2\pi}{\mathcal{R}}}(\partial\pi)^2}} \tag{5.31}$$

and $[\Pi^n]$, $[\pi^n]$ are defined as above with $\nabla \to \partial$. These are precisely the conformal DBI Galileons, first presented in [60, 101, 100]. It can be shown that each of the terms in (5.30) is invariant, up to a total divergence, under the transformations

$$\delta\pi = \mathcal{R} - x^\mu\partial_\mu\pi \ , \qquad \delta_\mu\pi = 2x_\mu + (\mathcal{R}e^{\frac{2\pi}{\mathcal{R}}} + \frac{1}{\mathcal{R}}x^2)\partial_\mu\pi - \frac{2}{\mathcal{R}}x_\mu x^\nu\partial_\nu\pi \ . \tag{5.32}$$

[1] The case of the five-dimensional Poincaré space, leading to the "Poincaré" Galileons, and their extension to supersymmetry has been discussed in [86].

Defining the dimensionless field and the AdS_5 mass scale by

$$\hat{\pi} = \frac{\pi}{\mathcal{R}} \ , \qquad \mathcal{M} = 1/\mathcal{R} \tag{5.33}$$

respectively, it is clear that each of the four conformal DBI Lagrangians in (5.30) admits an expansion in powers of $(\frac{\partial}{\mathcal{M}})^2$. Performing this expansion and combining terms with the same power of $(\frac{\partial}{\mathcal{M}})^2$ arising in different Lagrangians (5.30), one can, up to total derivatives, re-express the action $\mathcal{L} = \Sigma_{i=1}^4 c_i \mathcal{L}_i$ as

$$\mathcal{L} = \Sigma_{i=1}^4 \bar{c}_i \bar{\mathcal{L}}_i \tag{5.34}$$

where

$$\begin{aligned}
\bar{c}_1 &= \frac{c_1}{\mathcal{M}} + 4c_2 + 16\mathcal{M}c_3, \\
\bar{c}_2 &= \frac{c_2}{\mathcal{M}^2} + 6\frac{c_3}{\mathcal{M}} + 12c_4, \\
\bar{c}_3 &= \frac{c_3}{\mathcal{M}^3} + 6\frac{c_4}{\mathcal{M}^2}, \\
\bar{c}_4 &= \frac{c_4}{\mathcal{M}^4}
\end{aligned} \tag{5.35}$$

are real constants and

$$\begin{aligned}
\bar{\mathcal{L}}_1 &= -\frac{1}{4}e^{-4\hat{\pi}} \\
\bar{\mathcal{L}}_2 &= -\frac{1}{2}e^{-2\hat{\pi}}(\frac{\partial\hat{\pi}}{\mathcal{M}})^2 \\
\bar{\mathcal{L}}_3 &= \frac{1}{2}(\frac{\partial\hat{\pi}}{\mathcal{M}})^2\frac{\Box\hat{\pi}}{\mathcal{M}^2} - \frac{1}{4}(\frac{\partial\hat{\pi}}{\mathcal{M}})^4 \\
\bar{\mathcal{L}}_4 &= e^{-2\hat{\pi}}(\frac{\partial\hat{\pi}}{\mathcal{M}})^2\Big[-\frac{1}{2}(\frac{\Box\hat{\pi}}{\mathcal{M}^2})^2 + \frac{1}{2}(\frac{\partial_\mu\partial_\nu\hat{\pi}}{\mathcal{M}^2})(\frac{\partial\mu\partial^\nu\hat{\pi}}{\mathcal{M}^2}) \\
&\quad -\frac{1}{5}(\frac{\partial\hat{\pi}}{\mathcal{M}})^2\frac{\Box\hat{\pi}}{\mathcal{M}^2} + \frac{1}{5}(\frac{\partial_\mu\hat{\pi}}{\mathcal{M}})(\frac{\partial_\nu\hat{\pi}}{\mathcal{M}})(\frac{\partial^\mu\partial^\nu\hat{\pi}}{\mathcal{M}^2}) - \frac{3}{20}(\frac{\partial\hat{\pi}}{\mathcal{M}})^4\Big]
\end{aligned} \tag{5.36}$$

We have chosen each Lagrangian in (5.36) to be dimensionless and, hence, each coefficient $\bar{c}_i$ has dimension 4. Note that (5.36) are precisely the first four conformal Galileons. Since the original coefficients $c_i, \ i = 1 \dots 4$ are arbitrary, it follows from (5.35) that the coefficients $\bar{c}_i, \ i = 1 \dots 4$ are also unconstrained. We find from (5.32) and (5.33) that, in this expansion, each Lagrangian in (5.36) is invariant under the conformal Galileon symmetry

$$\delta\hat{\pi} = 1 - x^\mu\partial_\mu\hat{\pi}, \qquad \delta_\mu\hat{\pi} = 2x_\mu + x^2\partial_\mu\hat{\pi} - 2x_\mu x^\nu\partial_\nu\hat{\pi} \ . \tag{5.37}$$

We conclude that, expanded up to sixth-order in $(\partial/\mathcal{M})$, the worldvolume Lagrangian for a flat 3-brane embedded in AdS_5 is given by

$$\mathcal{L} = \Sigma_{i=1}^{4} \bar{c}_i \bar{\mathcal{L}}_i \ , \tag{5.38}$$

where each Lagrangian $\bar{\mathcal{L}}_i$ and each constant coefficient $\bar{c}_i$ have mass dimensions 0 and 4 respectively. As discussed previously, we are, for simplicity, ignoring the fifth Galileon which is eighth-order in $(\partial/\mathcal{M})$–since it is not necessary for our present discussion. However, it can easily be included without changing any of our results. Note that all terms of order greater than 8 in the derivative expansion of the DBI conformal Galileons can be shown to be a total divergence [155, 56] and, hence, do not contribute to the theory.[2]

5.6 Heterotic Bosonic Brane Action

The formalism and results described thus far are valid for a probe three-brane in any background five-dimensional bulk space. We now apply this generic formalism to the case of a probe three-brane embedded in the five-dimensional bulk space of heterotic M-theory. It follows from the metric (5.31), (5.32) presented in section 2 that

$$f(\pi) = (1 - 2\alpha\pi)^{1/6} \tag{5.39}$$

and, hence,

$$\gamma = \frac{1}{\sqrt{1 + (1 - 2\alpha\pi)^{-1/3}(\partial\pi)^2}} \ . \tag{5.40}$$

The total Lagrangian then becomes

$$\mathcal{L} = \sum_{i=1}^{4} \mathcal{L}_i \tag{5.41}$$

[2] A more complete discussion of the $(\frac{\partial}{\mathcal{M}})^2$ expansion is the following. Unlike the discussion in this section, let us here include the Lagrangian $\mathcal{L}_5$ in the sum $\mathcal{L} = \Sigma_{i=1}^{5} \ c_i \mathcal{L}_i$ as in (5.24). Now perform the derivative expansion of the $\mathcal{L}_i$ for $i = 1 \ldots 5$ to all orders in $(\frac{\partial}{\mathcal{M}})^2$. It is well-known [155, 56] that all terms with $(\frac{\partial}{\mathcal{M}})^{2p}$ for $p > 4$ form a total divergence and, hence, can be ignored in the action. Therefore, this expansion is exact and does not require that one demand that $(\frac{\partial}{\mathcal{M}})^2 \ll 1$. This is unique to the case of the conformal Galileons that we are discussing.

where the geometric Lagrangians presented in (5.27) are given by

$$
\begin{aligned}
\mathcal{L}_1 &= -\frac{3}{10\alpha}(1-2\alpha\pi)^{5/3} \\
\mathcal{L}_2 &= -(1-2\alpha\pi)^{2/3}\sqrt{1+(1-2\alpha\pi)^{-1/3}(\partial\pi)^2} \\
\mathcal{L}_3 &= -\frac{\alpha}{3}(1-2\alpha\pi)^{-1/3}[5-\gamma^2]-(1-2\alpha\pi)^{1/3}\Box\pi+\gamma^2[\pi^3] \\
\mathcal{L}_4 &= -\gamma\Big([\Pi]^2-[\Pi^2]+2\gamma^2(1-2\alpha\pi)^{-1/3}\big[-[\Pi][\pi^3]+[\pi^4]\big]\Big) \\
&\quad +\frac{10}{3}\frac{\alpha^2}{\gamma}(1-2\alpha\pi)^{-4/3}(-1+\gamma^2) \\
&\quad +\frac{2}{3}\alpha\gamma(1-2\alpha\pi)^{-2/3}\Big(-4\Box\pi+\gamma^2\big[\Box\pi+4(1-2\alpha\pi)^{-1/3}[\pi^3]\big]\Big) \\
&\quad +\frac{2}{3}\frac{\alpha}{\gamma}(1-2\alpha\pi)^{-4/3}(1-2\gamma^2+\gamma^4)\,. \qquad (5.42)
\end{aligned}
$$

Note that, unlike the Poincaré and conformal DBI Galileons, these Lagrangians do not exhibit a non-linearly realized global symmetry. The reason is that the Poincaré and conformal symmetries arise from those Killing vectors of the bulk space which are not parallel to the surfaces of foliation. While such Killing vectors are present in the maximally symmetric M_5 and AdS_5 spaces, there are none in the heterotic bulk space. Hence, the absence of an analogous symmetry in the heterotic DBI Galileons. We emphasize that since the Lagrange densities in (5.42) arise from those presented in (5.25), the associated equations of motion all contain at most two derivatives.

5.6.1 The Derivative Expansion

For the case of heterotic M-theory, the mass scale associated with the curvature of the five-dimensional bulk space is α, as discussed in section 2. Hence, the appropriate expansion parameter in the heterotic case will be $(\partial/\alpha)^2$. As discussed above, there is no special symmetry inherent in heterotic geometry. One might think, therefore, that a derivative expansion of the Lagrangians in (5.42) would require one to keep terms to all order in $(\partial/\alpha)^2$. However, this is not the case. Heterotic M-theory is only valid for momenta that are small compared to, not only the Planck mass M_P and the Calabi-Yau scale of order 10^{16} GeV, but also with respect to the scale associated with the curvature of the fifth-dimension. As discussed above, for the heterotic standard model this is found to be of order 10^{14} GeV. Therefore, it is necessary to restrict $(\partial/\alpha)^2$ to be small and, hence, one can truncate the derivative expansion at a small finite order in this expansion parameter.

We begin by defining the dimensionless field

$$\hat{\pi} = \alpha\pi \,. \tag{5.43}$$

Let us also scale the individual Lagrangians $\mathcal{L}_i$ and coefficients c_i as follows

$$\mathcal{L}_i \to \alpha^{2-i}\mathcal{L}_i \,, \qquad c_i \to \alpha^{i-2}c_i \tag{5.44}$$

for $i = 1, 2, 3, 4$. This ensures that the c_i, while still arbitrary, now have mass dimension 4, while each Lagrangian density $\mathcal{L}_i$ is dimensionless. We now expand the total Lagrangian $\mathcal{L}$ in powers of

$$(\partial/\alpha)^2 \ll 1. \tag{5.45}$$

Collecting terms up to order $(\partial/\alpha)^6$, and using integration by parts, we can then express our total Lagrangian (5.41) as

$$\mathcal{L} \;=\; \sum_{i=1}^{4} \bar{\mathcal{L}}_i \tag{5.46}$$

where

$$\begin{aligned}
\bar{\mathcal{L}}_1 &= -\frac{3}{10}c_1(1-2\hat{\pi})^{5/3} - c_2(1-2\hat{\pi})^{2/3} - \frac{4}{3}c_3(1-2\hat{\pi})^{-1/3} \\
\bar{\mathcal{L}}_2 &= \left(-\frac{1}{2}c_2(1-2\hat{\pi})^{1/3} - c_3(1-2\hat{\pi})^{-2/3} - \frac{2}{3}c_4(1-2\hat{\pi})^{-5/3}\right)\left(\frac{\partial\hat{\pi}}{\alpha}\right)^2 \\
\bar{\mathcal{L}}_3 &= \left(-\frac{1}{2}c_3 - c_4(1-2\hat{\pi})^{-1}\right)\left(\frac{\partial\hat{\pi}}{\alpha}\right)^2\frac{\Box\hat{\pi}}{\alpha^2} + \left(\frac{1}{8}c_2 + \frac{1}{3}c_3(1-2\hat{\pi})^{-1} - \frac{1}{3}c_4(1-2\hat{\pi})^{-2}\right)\left(\frac{\partial\hat{\pi}}{\alpha}\right)^4 \\
\bar{\mathcal{L}}_4 &= -\frac{1}{4}c_4(1-2\hat{\pi})^{-1/3}\frac{\partial_\mu}{\alpha}\left(\frac{\partial\hat{\pi}}{\alpha}\right)^2\frac{\partial^\mu}{\alpha}\left(\frac{\partial\hat{\pi}}{\alpha}\right)^2 + c_4(1-2\hat{\pi})^{-1/3}\frac{\Box\hat{\pi}}{\alpha^2}\frac{\hat{\pi}^{,\mu}}{\alpha}\frac{\hat{\pi}_{,\mu\nu}}{\alpha^2}\frac{\hat{\pi}^{,\nu}}{\alpha} \\
&- \frac{19}{6}c_4(1-2\hat{\pi})^{-4/3}\left(\frac{\partial\hat{\pi}}{\alpha}\right)^4\frac{\Box\hat{\pi}}{\alpha^2} \\
&+ \left(-c_3(1-2\hat{\pi})^{-1/3} - \frac{11}{3}c_4(1-2\hat{\pi})^{-4/3}\right)\left(\frac{\partial\hat{\pi}}{\alpha}\right)^2\frac{\hat{\pi}^{,\mu}}{\alpha}\frac{\hat{\pi}_{,\mu\nu}}{\alpha^2}\frac{\hat{\pi}^{,\nu}}{\alpha} \\
&+ \left(-\frac{1}{16}c_2(1-2\hat{\pi})^{-1/3} - \frac{1}{3}(1-2\hat{\pi})^{-4/3} - \frac{9}{4}c_4(1-2\hat{\pi})^{-7/3}\right)\left(\frac{\partial\hat{\pi}}{\alpha}\right)^6 .
\end{aligned} \tag{5.47}$$

Up to now, we have discussed the derivative expansion of the DBI heterotic Lagrangian using the necessary restriction that $(\partial/\alpha)^2 \ll 1$. However, there is an additional physical restriction that must be taken into account. It follows from (5.12) that the dimensionless field $\hat{\pi}$ must satisfy

$$\hat{\pi} \ll 1 \,. \tag{5.48}$$

While the DBI expressions given in (5.42) can be considered accurate as far as the expansion in $(\partial/\alpha)^2$ is concerned, we must now additionally expand all functions of $\hat{\pi}$ derived from $f(\hat{\pi})$ and its derivatives to *linear order* in $\hat{\pi}$. This expansion must terminate at linear order since higher powers of $\hat{\pi}$ cannot arise in the metric deduced from the dimensional reduction of M-theory to leading order in κ. Performing this expansion in (5.47), we find that the worldvolume Lagrangian of a probe three-brane in five-dimensional heterotic M-theory is given by

$$\mathcal{L} = \sum_{i=1}^{4} \bar{\mathcal{L}}_i \tag{5.49}$$

where

$$\begin{aligned}
\bar{\mathcal{L}}_1 &= -\frac{3}{10}c_1 - c_2 - \frac{4}{3}c_3 + \big(c_1 + \frac{4}{3}c_2 - \frac{8}{9}c_3\big)\hat{\pi} \\
\bar{\mathcal{L}}_2 &= \left(-\frac{1}{2}c_2 - c_3 - \frac{2}{3}c_4 + (\frac{1}{3}c_2 - \frac{4}{3}c_3 - \frac{20}{9}c_4)\hat{\pi}\right)\left(\frac{\partial\hat{\pi}}{\alpha}\right)^2 \\
\bar{\mathcal{L}}_3 &= \left(-\frac{1}{2}c_3 - c_4 - 2c_4\hat{\pi}\right)\left(\frac{\partial\hat{\pi}}{\alpha}\right)^2\frac{\Box\hat{\pi}}{\alpha^2} + \left(\frac{1}{8}c_2 + \frac{1}{3}c_3 - \frac{1}{3}c_4 + (\frac{2}{3}c_3 - \frac{4}{3}c_4)\hat{\pi}\right)\left(\frac{\partial\hat{\pi}}{\alpha}\right)^4 \\
\bar{\mathcal{L}}_4 &= -\left(\frac{1}{4}c_4 + \frac{1}{6}c_4\hat{\pi}\right)\frac{\partial_\nu}{\alpha}\left(\frac{\partial\hat{\pi}}{\alpha}\right)^2\frac{\partial^\nu}{\alpha}\left(\frac{\partial\hat{\pi}}{\alpha}\right)^2 + \left(c_4 + \frac{2}{3}c_4\hat{\pi}\right)\frac{\Box\hat{\pi}}{\alpha^2}\frac{\hat{\pi}^{,\mu}}{\alpha}\frac{\hat{\pi}_{,\mu\nu}}{\alpha^2}\frac{\hat{\pi}^{,\nu}}{\alpha} \\
&\quad -\left(\frac{19}{6}c_4 + \frac{76}{9}c_4\hat{\pi}\right)\left(\frac{\partial\hat{\pi}}{\alpha}\right)^4\frac{\Box\hat{\pi}}{\alpha^2} + \left(-c_3 - \frac{11}{3}c_4 + (-\frac{2}{3}c_3 - \frac{88}{9}c_4)\hat{\pi}\right)\left(\frac{\partial\hat{\pi}}{\alpha}\right)^2\frac{\hat{\pi}^{,\mu}}{\alpha}\frac{\hat{\pi}_{,\mu\nu}}{\alpha^2}\frac{\hat{\pi}^{,\nu}}{\alpha} \\
&\quad +\left(-\frac{1}{16}c_2 - \frac{1}{3}c_3 - \frac{9}{4}c_4 + (-\frac{1}{24}c_2 - \frac{8}{9}c_3 - \frac{21}{2}c_4)\hat{\pi}\right)\left(\frac{\partial\hat{\pi}}{\alpha}\right)^6 .
\end{aligned} \tag{5.50}$$

Again, we note the absence of a non-linearly realized global symmetry in the worldvolume Lagrangian. In the small derivative limit, this means that, unlike in the conformal case, one cannot re-express the c_i coefficients in terms of new constants $\bar{c}_i$ such that the total Lagrangian is of the form $\sum_{i=1}^{4}\bar{c}_i\bar{\mathcal{L}}_i$. This feature of the parameters will be helpful when the formalism is used in a cosmological context–such as to ensure the appearance of NEC violation. Be that as it may, since the expressions in (5.50) arise from those in (5.42), they give rise to second order equations of motion and make up the worldvolume action for a probe brane in a five-dimensional heterotic M-theory geometry. Therefore, we will refer to them as “heterotic Galileons”.

5.7 Supersymmetric Heterotic Galileons

We now extend the scalar Lagrangians given in (5.50) to d=4, $N = 1$ global supersymmetry, as is required by heterotic M-theory. To do this, we employ the formalism of $N = 1$ superspace [171], whose coordinates are x^μ, $\mu = 0, 1, 2, 3$, an anti-commuting two component Weyl spinor θ and its hermitian conjugate $\bar{\theta}$. These coordinates have mass dimensions 0, -1/2 and 1/2 respectively. Following [62, 124], we begin by defining a dimensionless complex scalar field A, whose real part is the brane position modulus $\hat{\pi}$. That is,

$$A(x) \equiv \frac{1}{\sqrt{2}}(\hat{\pi}(x) + i\chi(x)) \ , \tag{5.51}$$

where χ is a second real scalar field. We now take the scalar field A to be the lowest component of a dimensionless chiral superfield $\Phi(x^\mu, \theta, \bar{\theta})$. Expressing this as an expansion in the anti-commuting spinor coordinates, one finds that there are two new fields in the chiral multiplet in addition to A. These are a complex two-component Weyl spinor ψ and a complex scalar field F, with mass dimensions 1/2 and 1 respectively. Abusing notation, we can simply write

$$\Phi = (A, \psi, F) \, . \tag{5.52}$$

Using the superspace formalism, one can construct manifestly supersymmetric Lagrangians as the $\theta\theta\bar{\theta}\bar{\theta}$ component of a *real combination* of Φ and $\Phi^\dagger$ (such as $\Phi\Phi^\dagger$), or the $\theta\theta$ (or $\bar{\theta}\bar{\theta}$) component of a *complex, holomorphic* function of Φ (or $\Phi^\dagger$) alone (such as Φ^2). Henceforth, since it is not required in this chapter, we will drop all terms involving the fermion ψ and focus on the bosonic fields only.

5.7.1 Supersymmetric $\bar{\mathcal{L}}_2$

We start by defining a manifestly hermitian Kähler potential by

$$K(\Phi, \Phi^\dagger) \;=\; \frac{(c_2 + 2c_3 + \frac{4}{3}c_4)}{\alpha^2}\Phi\Phi^\dagger + \frac{1}{\sqrt{2}}\frac{(-\frac{1}{3}c_2 + \frac{4}{3}c_3 + \frac{20}{9}c_4)}{\alpha^2}(\Phi^2\Phi^\dagger + \Phi\Phi^{\dagger 2}) \, . \tag{5.53}$$

Note that K is a real superfield. The supersymmetric extension of the $\bar{\mathcal{L}}_2$ Lagrangian in (5.50) is then the highest (that is, $\theta\theta\bar{\theta}\bar{\theta}$) component of $K(\Phi, \Phi^\dagger)$, given by

$$\begin{aligned} \bar{\mathcal{L}}_2^{\mathrm{SUSY}} &= K(\Phi, \Phi^\dagger)\Big|_{\theta\theta\bar{\theta}\bar{\theta}} = -\frac{\partial^2 K}{\partial A \partial A^*}\partial A \cdot \partial A^* + \frac{\partial^2 K}{\partial A \partial A^*} F F^* \\ &= \Big(-\frac{1}{2}c_2 - c_3 - \frac{2}{3}c_4 + (\frac{1}{3}c_2 - \frac{4}{3}c_3 - \frac{20}{9}c_4)\hat{\pi} \Big) \Big((\frac{\partial \hat{\pi}}{\alpha})^2 + (\frac{\partial \chi}{\alpha})^2 - 2\frac{FF^*}{\alpha^2} \Big) \, . \end{aligned} \tag{5.54}$$

It is important to note that the dimension one auxiliary field F that appears here is everywhere suppressed by α, in the same manner as the derivatives $\partial\hat{\pi}$. To simplify the notation, for the remainder of this section, unless explicitly stated otherwise, we will set $\alpha = 1$.

5.7.2 Supersymmetric $\bar{\mathcal{L}}_3$

The supersymmetric extension of the $\bar{\mathcal{L}}_3$ Lagrangian given in (5.50) can be constructed from two terms,

$$
\begin{aligned}
\overline{\mathcal{L}}^{\rm SUSY}_{3,\text{1st term}} &= \frac{1}{16}\Big(-\frac{1}{\sqrt{2}}c_3 - \frac{\sqrt{2}}{3}c_4 - 2c_4(\Phi+\Phi^\dagger)\Big)\Big(D\Phi D\Phi \overline{D}^2\Phi^\dagger + \text{h.c.}\Big)\Big|_{\theta\theta\bar{\theta}\bar{\theta}} \\
&= \Big(-\frac{1}{\sqrt{2}}c_3 - \frac{\sqrt{2}}{3}c_4 - 2c_4(A+A^*)\Big)\Big((\partial A)^2\Box A^* + (\partial A^*)^2\Box A - FF^*(\Box A + \Box A^*) \\
&\qquad + F^*\partial F\cdot(\partial A - \partial A^*) - F\partial F^*\cdot(\partial A - \partial A^*)\Big) \\
&+ 4c_4\Big((FF^*)^2 - FF^*\partial A\cdot\partial A^*\Big)
\end{aligned} \tag{5.55}
$$

and

$$
\begin{aligned}
\overline{\mathcal{L}}^{\rm SUSY}_{3,\text{2nd term}} &= \frac{1}{4}\Big(\frac{1}{8}c_2 + \frac{1}{3}c_3 - \frac{1}{3}c_4 + \frac{1}{\sqrt{2}}(\frac{2}{3}c_3 - \frac{4}{3}c_4)(\Phi+\Phi^\dagger)\Big)\Big(D\Phi D\Phi\bar{D}\Phi^\dagger\bar{D}\Phi^\dagger\Big)\Big|_{\theta\theta\bar{\theta}\bar{\theta}} \\
&= \Big(\frac{1}{8}c_2 + \frac{1}{3}c_3 - \frac{1}{3}c_4 + \frac{1}{\sqrt{2}}(\frac{2}{3}c_3 - \frac{4}{3}c_4)(A+A^*)\Big) \\
&\qquad \times\Big(4(FF^*)^2 - 8FF^*\partial A\cdot\partial A^* + 4(\partial A)^2(\partial A^*)^2\Big)
\end{aligned} \tag{5.56}
$$

In terms of the real scalar fields $\hat{\pi}$ and χ, as well as the complex auxiliary field F, we find that the complete supersymmetrization of $\bar{\mathcal{L}}_3$ is given by

$$
\begin{aligned}
\overline{\mathcal{L}}^{\rm SUSY}_{3} &= \Big(-\frac{1}{2}c_3 - c_4 - 2c_4\hat{\pi}\Big)\Big((\partial\hat{\pi})^2\Box\hat{\pi} + (\partial\chi)^2\Box\hat{\pi} + 2\partial\hat{\pi}\cdot\partial\chi\Box\chi - 2FF^*\Box\hat{\pi} \\
&\qquad + 2iF^*\partial F\cdot\partial\chi - 2iF\partial F^*\cdot\partial\chi\Big) \\
&+ 4c_4\Big((FF^*)^2 + \frac{1}{2}FF^*(\partial\hat{\pi})^2 + \frac{1}{2}FF^*(\partial\chi)^2\Big) \\
&+ \Big(\frac{1}{8}c_2 + \frac{1}{3}c_3 - \frac{1}{3}c_4 + (\frac{2}{3}c_3 - \frac{4}{3}c_4)\hat{\pi}\Big)\Big((\partial\hat{\pi})^4 + (\partial\chi)^4 - 2(\partial\hat{\pi})^2(\partial\chi)^2 + 4(\partial\hat{\pi}\cdot\partial\chi)^2 \\
&\qquad - 4FF^*(\partial\hat{\pi})^2 - 4FF^*(\partial\chi)^2 + 4(FF^*)^2\Big)\,.
\end{aligned} \tag{5.57}
$$

We note the appearance of derivatives of F, as well as a term proportional to $(FF^*)^2$. In the conformal Galileon case arising from the AdS_5 bulk space, the first type of term occurred at the level of $\overline{\mathcal{L}}_3^{\rm SUSY}$, but a serendipitous cancellation removed the latter type at this order.

5.7.3 Supersymmetric $\bar{\mathcal{L}}_4$

In order to supersymmetrize the fourth order heterotic Galileon, we have to consider each of the five terms in (5.50) that comprise $\bar{\mathcal{L}}_4$ separately. Let us begin with the term involving $\partial_\mu(\partial\hat{\pi})^2\partial^\mu(\partial\hat{\pi})^2$. To extend this to $N=1$ supersymmetry, we construct

$$
\begin{aligned}
\overline{\mathcal{L}}^{\rm SUSY}_{4,\,\rm 1st\,term} &= \frac{1}{32}\left(\frac{1}{4}c_4+\frac{1}{6\sqrt{2}}c_4(\Phi+\Phi)\right)\{D,\bar{D}\}(D\Phi D\Phi)\{D,\bar{D}\}(\bar{D}\Phi^\dagger\bar{D}\Phi^\dagger)\Big|_{\theta\theta\bar{\theta}\bar{\theta}}\\
&= \left(-\frac{1}{4}c_4-\frac{1}{6\sqrt{2}}c_4(A+A^*)\right)\\
&\quad\times\left(4\partial_\mu(\partial A)^2\partial^\mu(\partial A^*)^2-8\partial_\mu(FA_{,\nu})\partial^\mu(F^*A^{*,\nu})+16FF^*\partial F\cdot\partial F^*\right)\\
&= \left(-\frac{1}{4}c_4-\frac{1}{6}c_4\hat{\pi}\right)\Big(\partial_\mu(\partial\hat{\pi})^2\partial^\mu(\partial\hat{\pi})^2+\partial_\mu(\partial\chi)^2\partial^\mu(\partial\chi)^2-2\partial_\mu(\partial\hat{\pi})^2\partial^\mu(\partial\chi)^2\\
&\qquad+4\partial_\mu(\partial\hat{\pi}\cdot\partial\chi)\partial^\mu(\partial\hat{\pi}\cdot\partial\chi)-4\partial_\mu(F\hat{\pi}_{,\nu})\partial^\mu(F^*\hat{\pi}^{,\nu})\\
&\qquad-4\partial_\mu(F\chi_{,\nu})\partial^\mu(F^*\chi^{,\nu})+16FF^*\partial F\cdot\partial F^*\Big)\,. \qquad (5.58)
\end{aligned}
$$

In addition to the desired term $\partial_\mu(\partial\hat{\pi})^2\partial^\mu(\partial\hat{\pi})^2$, as well as related terms containing both scalars $\hat{\pi}$ and χ, we encounter terms involving two derivatives of F in this expression; for example, $FF^*\partial F\cdot\partial F^*$. These will occur throughout the supersymmetrization of $\bar{\mathcal{L}}_4$.

Next, we consider the term involving $\Box\hat{\pi}\partial^\mu(\partial\hat{\pi})^2\hat{\pi}_{,\mu}$. It is given by

$$
\begin{aligned}
\overline{\mathcal{L}}^{\rm SUSY}_{4,\,\rm 2nd\,term} &= \frac{1}{128}\left(c_4+\frac{2}{3\sqrt{2}}c_4(\Phi+\Phi^\dagger)\right)\left(\{D,\bar{D}\}(\Phi+\Phi^\dagger)\{D,\bar{D}\}(D\Phi D\Phi)\bar{D}^2\Phi^\dagger+\text{h.c.}\right)\Big|_{\theta\theta\bar{\theta}\bar{\theta}}\\
&= \left(c_4+\frac{2}{3\sqrt{2}}c_4(A+A^*)\right)\Big((A+A^*)^{,\mu}\big(\partial_\mu(\partial A)^2\Box A+\partial_\mu(\partial A^*)^2\Box A^*\big)\\
&\qquad-(A+A^*)^{,\mu}\big(\partial_\mu(FA_{,\nu})F^{*,\nu}+\partial_\mu(F^*A^*_{,\nu})F^{,\nu}\big)\\
&\qquad-(A+A^*)^{,\mu}\big(\partial_\mu(F\Box A-\partial F\cdot\partial A)F^*+\partial_\mu(F^*\Box A^*-\partial F^*\cdot\partial A^*)F\big)\\
&\qquad-\partial_\mu\partial_\nu(A-A^*)\big(\partial^\mu(FA^{,\nu})F^*-\partial^\mu(F^*A^{*,\nu})F\big)-4FF^*\partial F\cdot\partial F^*\Big)\\
&- \frac{32}{3\sqrt{2}}c_4(A-A^*)^{,\nu}(A+A^*)_{,\mu}\big(\partial^\mu(FA_\nu)F^*-\partial^\mu(F^*A^*_\nu)F\big)\\
&- \frac{32}{3\sqrt{2}}c_4FF^*(A+A^*)_{,\mu}\big(\partial^\mu(\partial A)^2+\partial^\mu(\partial A^*)^2\big)\\
&+ \frac{64}{3\sqrt{2}}c_4\left(F(F^*)^2(A+A^*)_{,\mu}F^{,\mu}+F^*F^2(A+A^*)_{,\mu}F^{*,\mu}\right) \qquad (5.59)
\end{aligned}
$$

Expressed in terms of the fields $\hat{\pi}$ and χ, as well as the auxiliary field F, this becomes

$$
\begin{aligned}
&\overline{\mathcal{L}}^{\rm SUSY}_{4,\,\rm 2nd\ term} \\
= \quad & \left(c_4+\frac{2}{3}c_4\hat{\pi}\right)\Bigg(\Box\hat{\pi}\partial^\mu(\partial\hat{\pi})^2\hat{\pi}_{,\mu}-\Box\hat{\pi}\partial^\mu(\partial\chi)^2\hat{\pi}_{,\mu}-2\Box\chi\partial^\mu(\partial\hat{\pi}\cdot\partial\chi)\hat{\pi}_{,\mu} \\
&\quad -\hat{\pi}^{,\mu}\partial_\mu(F\hat{\pi}_{,\nu})F^{*,\nu}-\hat{\pi}^{,\mu}\partial_\mu(F^*\hat{\pi}_{,\nu})F^{,\nu}-i\hat{\pi}^{,\mu}\partial_\mu(F\chi_{,\nu})F^{*,\nu}+i\hat{\pi}^{,\mu}\partial_\mu(F^*\chi_{,\nu})F^{,\nu} \\
&\quad -\hat{\pi}^{,\mu}\partial_\mu(F\Box\hat{\pi})F^*-\hat{\pi}^{,\mu}\partial_\mu(F^*\Box\hat{\pi})F-\hat{\pi}^{,\mu}\partial_\mu(\partial F\cdot\partial\hat{\pi})F^*-\hat{\pi}^{,\mu}\partial_\mu(\partial F^*\cdot\partial\hat{\pi})F \\
&\quad -i\hat{\pi}^{,\mu}\partial_\mu(F\Box\chi)F^*+i\hat{\pi}^{,\mu}\partial_\mu(F^*\Box\chi)F+i\hat{\pi}^{,\mu}\partial_\mu(\partial F\cdot\partial\chi)F^*-i\hat{\pi}^{,\mu}\partial_\mu(\partial F^*\cdot\partial\chi)F \\
&\quad -i\chi_{,\mu\nu}\partial^\mu(F\hat{\pi}^{,\nu})F^*+i\chi_{,\mu\nu}\partial^\mu(F^*\hat{\pi}^{,\nu})F+\chi_{,\mu\nu}\partial^\mu(F\chi^{,\nu})F^*+\chi_{,\mu\nu}\partial^\mu(F^*\chi^{,\nu})F \\
&\quad -4FF^*\partial F\cdot\partial F^*\Bigg) \\
+ \quad & \frac{32}{3}c_4\left(i\hat{\pi}^{,\mu}\partial_\mu(F\hat{\pi}_{,\nu})\chi^{,\nu}F^*-i\hat{\pi}^{,\mu}\partial_\mu(F^*\hat{\pi}_{,\nu})\chi^{,\nu}F-\hat{\pi}^{,\mu}\partial_\mu(F\chi_{,\nu})\chi^{,\nu}F^*-\hat{\pi}^{,\mu}\partial_\mu(F^*\chi_{,\nu})\chi^{,\nu}F\right) \\
- \quad & \frac{32}{3}c_4\left(FF^*\hat{\pi}^{,\mu}\partial_\mu(\partial\hat{\pi})^2+FF^*\hat{\pi}^{,\mu}\partial_\mu(\partial\chi)^2\right)+\frac{64}{3}c_4\left(F(F^*)2\partial F\cdot\partial\hat{\pi}+F^*F^2\partial F^*\cdot\partial\hat{\pi}\right)
\end{aligned}
\tag{5.60}
$$

The remaining three terms, which involve $(\partial\hat{\pi})^4\Box\hat{\pi}$, $(\partial\hat{\pi})^2\hat{\pi}_{,\mu}\hat{\pi}_{\mu\nu}\hat{\pi}^{,\nu}$ and $(\partial\hat{\pi})^4$respectively, have the following supersymmetric extensions.

$$
\begin{aligned}
&\overline{\mathcal{L}}^{\rm SUSY}_{4,\,\rm 3rd\ term} \\
= \quad & \frac{1}{32\sqrt{2}}\left(\frac{19}{6}c_4+\frac{76}{9\sqrt{2}}c_4(\Phi+\Phi^\dagger)\right)D\Phi D\Phi\bar{D}\Phi^\dagger\bar{D}\Phi^\dagger\{D,\bar{D}\}\{D,\bar{D}\}(\Phi+\Phi^\dagger)\Big|_{\theta\theta\bar{\theta}\bar{\theta}} \\
= \quad & 2\sqrt{2}\left(-\frac{19}{6}c_4-\frac{76}{9\sqrt{2}}c_4(A+A^*)\right)\Box(A+A^*)\left((\partial A)^2(\partial A^*)^2-2FF^*\partial A\cdot\partial A^*+(FF^*)^2\right) \\
= \quad & \left(-\frac{19}{6}c_4-\frac{76}{9}c_4\hat{\pi}\right)\Bigg((\partial\hat{\pi})^4\Box\hat{\pi}+(\partial\chi)^4\Box\hat{\pi}-2(\partial\hat{\pi})^2(\partial\chi)^2\Box\hat{\pi}+(\partial\hat{\pi}\cdot\partial\chi)^2\Box\hat{\pi} \\
&\qquad -2FF^*((\partial\hat{\pi})^2+(\partial\chi)^2)\Box\hat{\pi}+4(FF^*)^2\Box\hat{\pi}\Bigg),
\end{aligned}
\tag{5.61}
$$

$$
\begin{aligned}
\bar{\mathcal{L}}^{\rm SUSY}_{4,\,\rm 4th\ term} &= -\frac{1}{128\sqrt{2}}\Big(-c_3-\frac{11}{3}c_4+\frac{1}{\sqrt{2}}(-\frac{2}{3}c_3-\frac{88}{9}c_4)(\Phi+\Phi^\dagger)\Big) \\
&\quad \Big(\{D,\bar{D}\}D\Phi D\Phi\bar{D}\Phi\bar{D}\Phi^\dagger\{D,\bar{D}\}\Phi+\text{h.c.}\Big)\Big|_{\theta\theta\bar{\theta}\bar{\theta}} \\
&= \frac{1}{\sqrt{2}}\Big(-c_3-\frac{11}{3}c_4+\frac{1}{\sqrt{2}}(-\frac{2}{3}c_3-\frac{88}{9}c_4)(A+A^*)\Big) \\
&\quad \Big(\partial_\mu\big((\partial A)^2(\partial A^*)^2\big)-2\partial_\mu(FF^*\partial A\cdot\partial A^*)+\partial_\mu(FF^*)^2\Big)(A+A^*)^{,\mu} \\
&= \Big(-c_3-\frac{11}{3}c_4+(-\frac{2}{3}c_3-\frac{88}{9}c_4)\hat{\pi}\Big)\Big((\partial\hat{\pi})^2\hat{\pi}_{,\mu}\hat{\pi}_{\mu\nu}\hat{\pi}^{,\nu}-(\partial\hat{\pi})^2\hat{\pi}_{,\mu}\hat{\pi}_{\mu\nu}\hat{\pi}^{,\nu} \\
&\quad -(\partial\hat{\pi})^2\hat{\pi}_{,\mu}\chi_{\mu\nu}\chi^{,\nu}+(\partial\chi)^2\hat{\pi}_{,\mu}\chi_{\mu\nu}\chi^{,\nu}+4\partial_\mu\big(\partial\hat{\pi}\cdot\partial\chi\big)^2\hat{\pi}^{,\mu}-\partial_\mu(FF^*(\partial\hat{\pi})^2)\hat{\pi}^{,\mu} \\
&\quad -\partial_\mu(FF^*(\partial\chi)^2)\hat{\pi}^{,\mu}+\partial_\mu(FF^*)\hat{\pi}^{,\mu}\Big)\,, \qquad (5.62)
\end{aligned}
$$

$$
\begin{aligned}
&\bar{\mathcal{L}}^{\rm SUSY}_{4,\,\rm 5th\ term} \\
&= \frac{1}{16}\Big(-\frac{1}{16}c_2-\frac{1}{3}c_3-\frac{9}{4}c_4+\frac{1}{\sqrt{2}}(-\frac{1}{24}c_2-\frac{8}{9}c_3-\frac{21}{2}c_4)(\Phi+\Phi^\dagger)\Big) \\
&\quad \times D\Phi D\Phi\bar{D}\Phi^\dagger\bar{D}\Phi^\dagger\{D,\bar{D}\}\Phi\{D,\bar{D}\}\Phi^\dagger\Big|_{\theta\theta\bar{\theta}\bar{\theta}} \\
&= \Big(-\frac{1}{16}c_2-\frac{1}{3}c_3-\frac{9}{4}c_4+\frac{1}{\sqrt{2}}(-\frac{1}{24}c_2-\frac{8}{9}c_3-\frac{21}{2}c_4)(A+A^*)\Big) \\
&\quad \Big((\partial A)^2(\partial A^*)^2-2FF^*\partial A\cdot\partial A^*+(FF^*)^2\Big)\partial A\cdot\partial A^* \\
&= \Big(-\frac{1}{16}c_2-\frac{1}{3}c_3-\frac{9}{4}c_4+(-\frac{1}{24}c_2-\frac{8}{9}c_3-\frac{21}{2}c_4)\hat{\pi}\Big)\Big((\partial\hat{\pi})^2+(\partial\chi)^2\Big) \\
&\quad \Big((\partial\hat{\pi})^4+(\partial\chi)^4-2(\partial\hat{\pi})^2(\partial\chi)^2+4(\partial\hat{\pi}\cdot\partial\chi)^2-4FF^*\big((\partial\hat{\pi})^2-(\partial\chi)^2\big)+4(FF^*)^2\Big)\,. \\
&\qquad (5.63)
\end{aligned}
$$

5.7.4 Supersymmetric $\bar{\mathcal{L}}_1$

Thus far, we have ignored the first scalar Lagrangian density $\bar{\mathcal{L}}_1$ given in (5.50). Since $\bar{\mathcal{L}}_1$ is a function of $\hat{\pi}$ only, without any derivatives, it is logical to treat it as a potential energy term for $\hat{\pi}$. In $N = 1$ supersymmetry, one specifies a potential by constructing a holomorphic function of chiral superfields, $W(\Phi)$, known as a superpotential. We then choose

$$\overline{\mathcal{L}}_1^{\mathrm{SUSY}} \quad = \quad W(\Phi)\Big|_{\theta\theta} + W(\Phi^\dagger)\Big|_{\bar\theta\bar\theta} = F\frac{\partial W}{\partial A} + F^*\frac{\partial W^*}{\partial A^*}\,, \tag{5.64}$$

where we have not yet specified the form of W. In order to do this, and complete the supersymmetrization of $\bar{\mathcal{L}}_1$, one must eliminate the auxiliary field F using its equation of motion. We now address this issue, returning to the final component field expression for $\overline{\mathcal{L}}_1^{\mathrm{SUSY}}$ at the end of the next subsection.

5.8 Elimination of the F-field

Let us first collect all those terms from the supersymmetric action that contain the complex auxiliary field F. Denoting this subset of the Lagrangian by $\overline{\mathcal{L}}_F^{\text{SUSY}}$, we find that

$$
\begin{aligned}
&\overline{\mathcal{L}}_F^{\text{SUSY}} \\
= \;& F\frac{\partial W}{\partial A} + F^*\frac{\partial W^*}{\partial A^*} + \Big(\gamma + 2\sqrt{2}\delta\hat{\pi}\Big)FF^* \\
+ \;& \Big(-\frac{1}{2}c_3 - c_4 - 2c_4\hat{\pi}\Big)\Big(-2FF^*\Box\hat{\pi} + 2iF^*\partial F\cdot\partial\chi - 2iF\partial F^*\cdot\partial\chi\Big) \\
+ \;& 4c_4\Big((FF^*)^2 - \frac{1}{2}FF^*(\partial\hat{\pi})^2 - \frac{1}{2}FF^*(\partial\chi)^2\Big) \\
+ \;& \Big(\frac{1}{8}c_2 + \frac{1}{3}c_3 - \frac{1}{3}c_4 + (\frac{2}{3}c_3 - \frac{4}{3}c_4)\hat{\pi}\Big)\Big(-4FF^*(\partial\hat{\pi})^2 - 4FF^*(\partial\chi)^2 + 4(FF^*)^2\Big) \\
- \;& \Big(\frac{1}{4}c_4 + \frac{1}{6}c_4\hat{\pi}\Big)\Big(-4\partial_\mu(F\hat{\pi}_{,\nu})\partial^\mu(F^*\hat{\pi}^{,\nu}) - 4\partial_\mu(F\chi_{,\nu})\partial^\mu(F^*\chi^{,\nu}) + 16FF^*\partial F\cdot\partial F^*\Big) \\
+ \;& \Big(c_4 + \frac{2}{3}c_4\hat{\pi}\Big) \\
& \times\Big(-\hat{\pi}^{,\mu}\partial_\mu(F\hat{\pi}_{,\nu})F^{*,\nu} - \hat{\pi}^{,\mu}\partial_\mu(F^*\hat{\pi}_{,\nu})F^{,\nu} - i\hat{\pi}^{,\mu}\partial_\mu(F\chi_{,\nu})F^{*,\nu} + i\hat{\pi}^{,\mu}\partial_\mu(F^*\chi_{,\nu})F^{,\nu} \\
& \quad -\hat{\pi}^{,\mu}\partial_\mu(F\Box\hat{\pi})F^* - \hat{\pi}^{,\mu}\partial_\mu(F^*\Box\hat{\pi})F - \hat{\pi}^{,\mu}\partial_\mu(\partial F\cdot\partial\hat{\pi})F^* - \hat{\pi}^{,\mu}\partial_\mu(\partial F^*\cdot\partial\hat{\pi})F \\
& \quad -i\hat{\pi}^{,\mu}\partial_\mu(F\Box\chi)F^* + i\hat{\pi}^{,\mu}\partial_\mu(F^*\Box\chi)F + i\hat{\pi}^{,\mu}\partial_\mu(\partial F\cdot\partial\chi)F^* - i\hat{\pi}^{,\mu}\partial_\mu(\partial F^*\cdot\partial\chi)F \\
& \quad -i\chi_{,\mu\nu}\partial^\mu(F\hat{\pi}^{,\nu})F^* + i\chi_{,\mu\nu}\partial^\mu(F^*\hat{\pi}^{,\nu})F + \chi_{,\mu\nu}\partial^\mu(F\chi^{,\nu})F^* + \chi_{,\mu\nu}\partial^\mu(F^*\chi^{,\nu})F \\
& \quad -4FF^*\partial F\cdot\partial F^*\Big) \\
+ \;& \frac{32}{3}c_4\Big(i\hat{\pi}^{,\mu}\partial_\mu(F\hat{\pi}_{,\nu})\chi^{,\nu}F^* - i\hat{\pi}^{,\mu}\partial_\mu(F^*\hat{\pi}_{,\nu})\chi^{,\nu}F - \hat{\pi}^{,\mu}\partial_\mu(F\chi_{,\nu})\chi^{,\nu}F^* - \hat{\pi}^{,\mu}\partial_\mu(F^*\chi_{,\nu})\chi^{,\nu}F\Big) \\
- \;& \frac{32}{3}c_4\Big(FF^*\hat{\pi}^{,\mu}\partial_\mu(\partial\hat{\pi})^2 + FF^*\hat{\pi}^{,\mu}\partial_\mu(\partial\chi)^2\Big) + \frac{64}{3}c_4\Big(F(F^*)2\partial F\cdot\partial\hat{\pi} + F^*F^2\partial F^*\cdot\partial\hat{\pi}\Big) \\
+ \;& \Big(-\frac{19}{6}c_4 - \frac{76}{9}c_4\hat{\pi}\Big)\Big(-2FF^*((\partial\hat{\pi})^2 + (\partial\chi)^2)\Box\hat{\pi} + 4(FF^*)^2\Box\hat{\pi}\Big) \\
+ \;& \Big(-c_3 - \frac{11}{3}c_4 + (-\frac{2}{3}c_3 - \frac{88}{9}c_4)\hat{\pi}\Big) \\
& \qquad\qquad \times\Big(-\partial_\mu(FF^*(\partial\hat{\pi})^2)\hat{\pi}^{,\mu} - \partial_\mu(FF^*(\partial\chi)^2)\hat{\pi}^{,\mu} + \partial_\mu(FF^*)\hat{\pi}^{,\mu}\Big) \\
+ \;& \Big(-\frac{1}{16}c_2 - \frac{1}{3}c_3 - \frac{9}{4}c_4 + (-\frac{1}{24}c_2 - \frac{8}{9}c_3 - \frac{21}{2}c_4)\hat{\pi}\Big) \\
& \qquad\qquad \times\Big((-4FF^*\big((\partial\hat{\pi})^2 - (\partial\chi)^2\big) + 4(FF^*)^2)\big((\partial\hat{\pi})^2 + (\partial\chi)^2\big)\Big),
\end{aligned}
\tag{5.65}
$$

where, for convenience, we have defined two parameters, γ and δ, of mass dimension 2 as

$$\gamma \equiv \frac{(c_2 + 2c_3 + \frac{4}{3}c_4)}{\alpha^2}\,, \qquad \delta \equiv \frac{1}{\sqrt{2}}\frac{(-\frac{1}{3}c_2 + \frac{4}{3}c_3 + \frac{20}{9}c_4)}{\alpha^2}\,. \tag{5.66}$$

As mentioned previously, this Lagrangian not only contains terms that are cubic or higher order polynomials in F and F^*, but also terms which involve derivatives of F; including terms with two derivatives on F, such as $FF^*\partial F \cdot \partial F^*$. The question then arises as to whether or not F can legitimately be considered an auxiliary field–which can be eliminated via an algebraic equation of motion–or is, instead, a dynamical scalar which propagates in the same manner as $\hat{\pi}$ and χ. This issue is typical of higher derivative theories of supersymmetry and supergravity–see, for example, [124, 130]. Of course, a propagating complex scalar F is not necessarily a problem for supersymmetry, since it can be be associated with two extra propagating degrees of freedom in the Weyl spinor ψ.

A method for addressing this issue in the case of the supersymmetric conformal Galileons is known [62]. We now adapt this method to the supersymmetric heterotic Lagrangians. To begin, we observe that after restoring α in the supersymmetric Lagrangians given above, the mass dimension 1 scalar F always appears in the ratio F/α. This mirrors the structure of the derivative $\partial\hat{\pi}$, which always appears in the form $\partial\hat{\pi}/\alpha$. Since we are restricting the derivative terms to be small so as to limit the derivative expansion to the four heterotic Galileons discussed above, it is natural to demand that in the supersymmetric extension, F/α, be small as well. To be explicit, we henceforth require that

$$\left|\frac{F}{\alpha}\right|^2 \ll 1\,. \tag{5.67}$$

This condition means that (5.65) is composed of terms which are suppressed by successively higher powers of α^2, as were the heterotic Galileons in (5.50). Therefore, higher order terms in F and those involving derivatives of F, which arise in the supersymmetrization of $\bar{\mathcal{L}}_3$ and $\bar{\mathcal{L}}_4$, will be small compared to the linear and quadratic terms from $\overline{\mathcal{L}}_1^{\mathrm{SUSY}}$ and $\overline{\mathcal{L}}_2^{\mathrm{SUSY}}$. This allows us to treat F as an auxiliary field, since the terms that would "propagate" it are heavily suppressed. We can then solve for F perturbatively and substitute the result into Lagrangian (5.65). The perturbative expansion for F will be of the form

$$F = F^{(0)} + F^{(1)} + \dots\,, \tag{5.68}$$

where $F^{(0)}$ arises from solving the F equation of motion using $\overline{\mathcal{L}}_1^{\mathrm{SUSY}}$ and $\overline{\mathcal{L}}_2^{\mathrm{SUSY}}$ only, $F^{(1)}$ is then computed by adding the contribution of $\overline{\mathcal{L}}_3^{\mathrm{SUSY}}$ to the F equation of motion, and so on. Let us write (5.68) in the form.

$$F = F^{(0)}(1 + \frac{F^{(1)}}{F^{(0)}} + \ldots) \ . \tag{5.69}$$

It is clear from the above discussion that

$$\frac{F^{(1)}}{F^{(0)}} \sim (\frac{\partial}{\alpha})^2 \ll 1 \tag{5.70}$$

and, hence, F is very well approximated by $F^{(0)}$. Therefore, in the remainder of this chapter we will always take $F = F^{(0)}$ and ignore higher order corrections. In doing so, it will become clear that the coefficients c_i, which arose from the construction of the DBI action (5.42), can no longer be arbitrary and must satisfy certain specific constraints. As stated above, the largest terms in (5.65) arise from $\overline{\mathcal{L}}_1^{\mathrm{SUSY}}$ and $\overline{\mathcal{L}}_2^{\mathrm{SUSY}}$, and are given by

$$\overline{\mathcal{L}}_F^{\mathrm{SUSY}(0)} = F^{(0)}\frac{\partial W}{\partial A} + F^{*(0)}\frac{\partial W^*}{\partial A^*} + (\gamma + 2\sqrt{2}\delta\hat{\pi})F^{(0)}F^{*(0)} \,, \tag{5.71}$$

where the dimension 2 constants γ and δ are the linear combinations of the coefficients c_i given in (5.66). Solving the equation of motion for $F^{(0)}$, we find that

$$F^{(0)} = -\frac{1}{(\gamma + 2\sqrt{2}\delta\hat{\pi})}\frac{\partial W^*}{\partial A^*} \ . \tag{5.72}$$

For the holomorphic function, $W(A)$, we choose

$$W(A) = \beta_1 A + \beta_2 A^2 \,, \tag{5.73}$$

where the constant coefficients β_1, β_2 each have mass dimension 3. Furthermore, it will be sufficient to take each of the β_i coefficients to be real numbers. As we will demonstrate below, superpotential (5.73) leads to the correct scalar Lagrangian $\bar{\mathcal{L}}_1$ presented in (5.50)– and appears to be the minimal holomorphic superpotential which can do so. Hence, although more complicated superpotentials might be possible, we will, for simplicity, take $W(A)$ to be the quadratic function given in (5.73). It then follows from (5.72) and (5.73) that, to linear order in $\hat{\pi}$,

$$F^{(0)} \quad = \quad -\frac{\beta_1}{\gamma} + \sqrt{2}\Big(2\frac{\beta_1}{\gamma}\Big(\frac{\delta}{\gamma}\Big) - \frac{\beta_2}{\gamma}\Big)\hat{\pi} + i\sqrt{2}\frac{\beta_2}{\gamma}\chi - i4\frac{\beta_2}{\gamma}\Big(\frac{\delta}{\gamma}\Big)\hat{\pi}\chi \,. \tag{5.74}$$

Note from the denominator in (5.72) that to consistently work to first order in $\hat{\pi}$ only, we have to constrain δ and γ to satisfy

$$|\frac{\delta}{\gamma}| \lesssim 1 \ . \tag{5.75}$$

It then follows from (5.66) that the coefficients c_i, $i = 1, 2, 3, 4$ must satisfy the constraint that

$$|-\frac{1}{3}c_2 + \frac{4}{3}c_3 + \frac{20}{9}c_4| \lesssim \sqrt{2}|c_2 + 2c_3 + \frac{4}{3}c_4| \ . \tag{5.76}$$

Before discussing the conditions under which $|F^{(0)}/\alpha|^2 \ll 1$, one must first compute $\overline{\mathcal{L}}_F^{\mathrm{SUSY}(0)}$ and determine whether or not it is consistent with $\bar{\mathcal{L}}_1$ in (5.50). Putting expression (5.74) into (5.71), we find that the complete scalar potential energy is given by

$$\begin{aligned} V(\hat{\pi}, \chi) &= -\overline{\mathcal{L}}_F^{\mathrm{SUSY}(0)} \\ &= \frac{\beta_1^2}{\gamma} + \frac{2\sqrt{2}}{\gamma^2}\big(-\beta_1^2\delta + \beta_1\beta_2\gamma\big)\hat{\pi} + \frac{2}{\gamma}\beta_2^2\chi^2 \\ &- \frac{4\sqrt{2}}{\gamma^2}\beta_2^2\delta\hat{\pi}\chi^2 \ . \end{aligned} \tag{5.77}$$

Setting $\chi = 0$ in expression (5.77), and demanding that the result reproduce $-\bar{\mathcal{L}}_1$ in (5.50) exactly, necessitates the imposition of two constraints on β_1 and β_2. These are

$$\beta_1^2 = \gamma\Big(\frac{3}{10}c_1 + c_2 + \frac{4}{3}c_3\Big) , \qquad -\beta_1^2\delta + \beta_1\beta_2\gamma = -\frac{\gamma^2}{2\sqrt{2}}\Big(c_1 + \frac{4}{3}c_2 - \frac{8}{9}c_3\Big) . \tag{5.78}$$

Note that the first constraint immediately implies that

$$\gamma\Big(\frac{3}{10}c_1 + c_2 + \frac{4}{3}c_3\Big) > 0 \ . \tag{5.79}$$

We conclude that choosing the quadratic superpotential (5.72) leads to the appropriate $N = 1$ supersymmetrization $\overline{\mathcal{L}}_F^{\mathrm{SUSY}(0)}$ of the scalar $\bar{\mathcal{L}}_1$ heterotic Galileon as long as the two coefficients β_i, $i = 1, 2$ of $W(A)$ satisfy the constraints in (5.78).

Having determined this, we must now ensure that $F^{(0)}$ presented in (5.74) satisfies the constraint given in (5.67); that is, that $|F^{(0)}/\alpha|^2 \ll 1$. It is clear from expression (5.74) and (5.75) that this will be the case as long as

$$|\frac{\beta_i}{\gamma}| \ll 1, \quad i = 1, 2 \ . \tag{5.80}$$

Solving these inequalities subject to the constraints given in (5.78), leads to two conditions on the coefficients c_i, $i = 1, 2, 3, 4$. First, demanding that $|\beta_1/\gamma| \ll 1$ and using the first expression in (5.78), leads to the inequality

$$\frac{3}{10}c_1 + c_2 + \frac{4}{3}c_3 \ll c_2 + 2c_3 + \frac{4}{3}c_4 \ . \tag{5.81}$$

Second, the constraint $|\beta_2/\gamma| \ll 1$ and the second expression in (5.78) implies that

$$|-c_1 - \frac{4}{3}c_2 + \frac{8}{9}c_3| \ll 2\sqrt{2}|\beta_1| \ . \tag{5.82}$$

Before continuing, we note that having chosen the form of the superpotential $W(A)$ in (5.73), one can now write the expression for $\bar{\mathcal{L}}_1^{\rm SUSY}$ in (5.64) in terms of component fields. It is given by

$$\bar{\mathcal{L}}_1^{\rm SUSY} = \beta_1(F+F^*) + \sqrt{2}\beta_2(F+F^*)\hat{\pi} + i\sqrt{2}\beta_2(F-F^*)\chi \ . \tag{5.83}$$

5.8.1 Physical Requirements

We will impose that our Lagrangian admit a solution of the equations of motion for which, if we take both $\chi = 0$ and $\partial_\mu\chi = 0$ initially, then $\chi = \partial_\mu\chi = 0$ remains unchanged as time evolves. That is, any dynamical motion is purely in the $\hat{\pi}$ direction in field space. This requires an analysis of the potential (5.77). For this to be the case, it is necessary that

$$m_\chi^2 = \frac{\partial^2 V}{\partial\chi^2}\bigg|_{\chi=0} \geq 0 \tag{5.84}$$

for all values of $\hat{\pi}$, where

$$\frac{\partial^2 V}{\partial\chi^2}\bigg|_{\chi=0} \quad = \quad \frac{4\beta_2^2}{\gamma}(1 - 2\sqrt{2}(\frac{\delta}{\gamma})\hat{\pi}) \ . \tag{5.85}$$

Using (5.75), it follows that (5.84) will be satisfied as long as one chooses the c_i coefficients such that $\gamma > 0$. It then follows from (5.66) that

$$c_2 + 2c_3 + \frac{4}{3}c_4 > 0 \tag{5.86}$$

Note that putting this result back in (5.79), simplifies that constraint to become

$$\frac{3}{10}c_1 + c_2 + \frac{4}{3}c_3 > 0 \tag{5.87}$$

Of course, condition (5.84) will lead to the solution $\chi = \partial_\mu\chi = 0$ only if one assumes a non-ghost like kinetic energy for χ. To ensure that this is the case, let us combine the kinetic terms for χ which arise from (5.54) and (5.65). That is

$$\Big[-\frac{1}{2}c_2 - c_3 - \frac{2}{3}c_4 + (\frac{1}{3}c_2 - \frac{4}{3}c_3 - \frac{20}{9}c_4)\hat{\pi}$$
$$+\Big(-\frac{1}{2}c_2 - \frac{4}{3}c_3 - \frac{2}{3}c_4 + (-\frac{8}{3}c_3 + \frac{16}{3}c_4)\hat{\pi}\Big) F^{(0)}F^{*(0)}$$
$$+\Big(-\frac{1}{4}c_2 - \frac{4}{3}c_3 - 9c_4 + (-\frac{1}{6}c_2 - \frac{32}{9}c_3 - 42c_4)\hat{\pi}\Big) (F^{(0)}F^{*(0)})^2\Big] (\partial\chi)^2 \,, \quad (5.88)$$

where $F^{(0)}$ is given by (5.74). This kinetic energy will be ghost free if and only if the coefficient of $(\partial\chi)^2$ is negative for any value of $\hat{\pi}$. It follows that the c_i coefficients must satisfy

$$(-\frac{1}{2}c_2 - c_3 - \frac{2}{3}c_4) + (-\frac{1}{2}c_2 - \frac{4}{3}c_3 - \frac{2}{3}c_4)|F^{(0)}|^2 + (-\frac{1}{4}c_2 - \frac{4}{3}c_3 - 9c_4)|F^{(0)}|^4 < 0 \quad (5.89)$$

and

$$(\frac{1}{3}c_2 - \frac{4}{3}c_3 - \frac{20}{9}c_4) + (-\frac{8}{3}c_3 + \frac{16}{3}c_4)|F^{(0)}|^2 + (-\frac{1}{6}c_2 - \frac{32}{9}c_3 - 42c_4)|F^{(0)}|^4 < 0 \quad (5.90)$$

This imposes two additional extra conditions on the coefficients c_i. It is important to note that the kinetic energy term for $\hat{\pi}$ is identical to that of χ; one simply replaces $(\partial\chi)^2$ in equation (5.88) with $(\partial\hat{\pi})^2$. By requiring χ be ghost free, we thus ensure that $\hat{\pi}$ is ghost-free as well; that is, requiring $(\partial\hat{\pi})^2$ to be ghost free imposes no additional constraints.

Finally, there are two additional "physical" constraints that we impose on the supersymmetric three-brane action. The first is that we require the three-brane "tension" to be positive. It is straightforward to show that this will be the case if and only if

$$c_2 > 0 \,. \quad (5.91)$$

Second, on physical grounds we would like the three-brane to be attracted to the *observable* orbifold plane by the potential energy in the worldvolume action. It then follows from (5.77) that

$$-c_1 - \frac{4}{3}c_2 + \frac{8}{9}c_3 > 0 \quad (5.92)$$

Note that this simplifies (5.82) to become

$$-c_1 - \frac{4}{3}c_2 + \frac{8}{9}c_3 \ll 2\sqrt{2}|\beta_1| \,. \quad (5.93)$$

5.8.2 Summary of Constraints on the Coefficients

The complete set of constraints on the coefficients c_i, $i = 1, 2, 3, 4$ determined above are the following:

1. $|-\frac{1}{3}c_2 + \frac{4}{3}c_3 + \frac{20}{9}c_4| \lesssim \sqrt{2}(c_2 + 2c_3 + \frac{4}{3}c_4)$
2. $\frac{3}{10}c_1 + c_2 + \frac{4}{3}c_3 > 0$
3. $\frac{3}{10}c_1 + c_2 + \frac{4}{3}c_3 \ll c_2 + 2c_3 + \frac{4}{3}c_4$
4. $-c_1 - \frac{4}{3}c_2 + \frac{8}{9}c_3 \ll 2\sqrt{2}|\beta_1|$
5. $c_2 + 2c_3 + \frac{4}{3}c_4 > 0$
6. $c_2 > 0$
7. $-c_1 - \frac{4}{3}c_2 + \frac{8}{9}c_3 > 0$
8. $(-\frac{1}{2}c_2 - c_3 - \frac{2}{3}c_4) + (-\frac{1}{2}c_2 - \frac{4}{3}c_3 - \frac{2}{3}c_4)|F^{(0)}|^2 + (-\frac{1}{4}c_2 - \frac{4}{3}c_3 - 9c_4)|F^{(0)}|^4 < 0$
9. $(\frac{1}{3}c_2 - \frac{4}{3}c_3 - \frac{20}{9}c_4) + (-\frac{8}{3}c_3 + \frac{16}{3}c_4)|F^{(0)}|^2 + (-\frac{1}{6}c_2 - \frac{32}{9}c_3 - 42c_4)|F^{(0)}|^4 < 0$

where β_1 is defined in (5.78).

In this chapter, we will make no attempt to present a complete set of solutions to these conditions. Instead, we will perform a numerical scan over four-dimensional c_i-space to demonstrate that there exist reasonable values of the coefficients (c_1, c_2, c_3, c_4) which satisfy the constraints given above. We will restrict the values of the c_i's so that, in units of $\alpha = 1$, their absolute value is bounded by

$$|c_i| \leq 10\,, \tag{5.94}$$

which is a physically realistic assumption. We first set up a four-dimensional grid with an incremental step size Δc, and evaluate every point in the grid to see if they satisfy the required inequalities. Let us be precise about the numerical definition of the $\ll$ symbol appearing in inequalities 3. and 4. in the summary of constraints. We will, in this analysis, take it to mean that the ratio of the two quantities given is less than 1/25; that is

$$a \ll b \Rightarrow \frac{a}{b} < \frac{1}{25}\ . \tag{5.95}$$

Furthermore, we will work in a restricted region of *field* space, such that the magnitude of both $\hat{\pi}$ and χ cannot exceed 1/10. Note that for $\hat{\pi}$ this is consistent with condition (5.48). This enables us to evaluate inequalities involving the field dependent quantity $F^{(0)}$. We do so by replacing $\hat{\pi}$ and χ with their maximum value, that is, 1/10, in the expression for $F^{(0)}$.

A preliminary search reveals that c_1 must be negative for there to be any satisfactory points. Taking c_1 to be a *fixed* negative value, we perform a more refined scan over the remaining c_i's by taking $\Delta c = 0.01$. The results for $c_1 = -1$ and $c_1 = -10$ are presented in Figures 5.1 and 5.2 respectively. We note that taking c_1 to be more negative, as in Figure 5.2, means that more points can satisfy the constraints. This is clear from the larger "volume" of valid points in Figure 5.2, as opposed to those of Figure 5.1. Finally, we find that $|F^{(0)}|^2$ is indeed small for all of the valid points displayed in Figures 5.1 and 5.2; as is required for the perturbative expansion of F to be valid. At its largest, $|F^{(0)}|^2 \simeq 0.04$ in both cases, but is generically smaller, as can be seen in Figure 5.3.

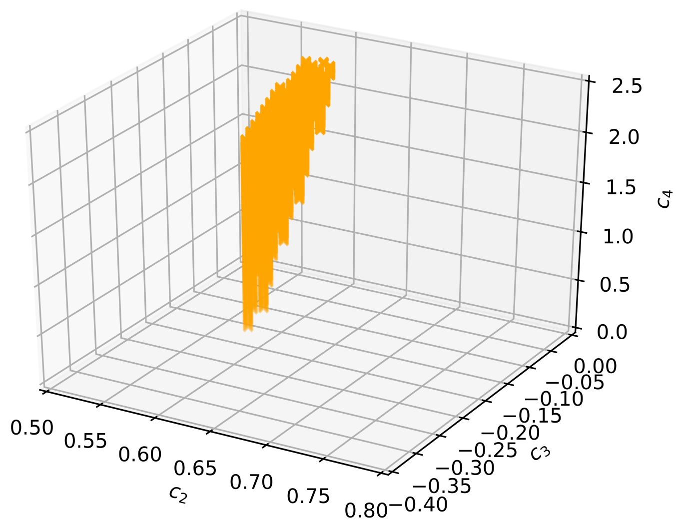

Figure 5.1: Numerical scan over $-10 \leq c_i \leq 10$ for $i = 2, 3, 4$, taking $c_1 = -1.0$ and with step size $\Delta c = 0.01$. Points which satisfy all inequalities in the "summary of constraints" are labelled by an orange $\times$.

5.9 Extension of Heterotic Galileons to $N = 1$ Supergravity

We now proceed to extend the heterotic Galileons in equation (5.50) to local supersymmetry; that is, to $N = 1$ supergravity. This is essential if we are to explore the cosmological implications of three-branes in heterotic M-theory. We continue to use the superspace formalism described in [171], where the global anti-commuting θ^α coordinates are now replaced by local superspace coordinates Θ^α. These now define the superfield expansions.

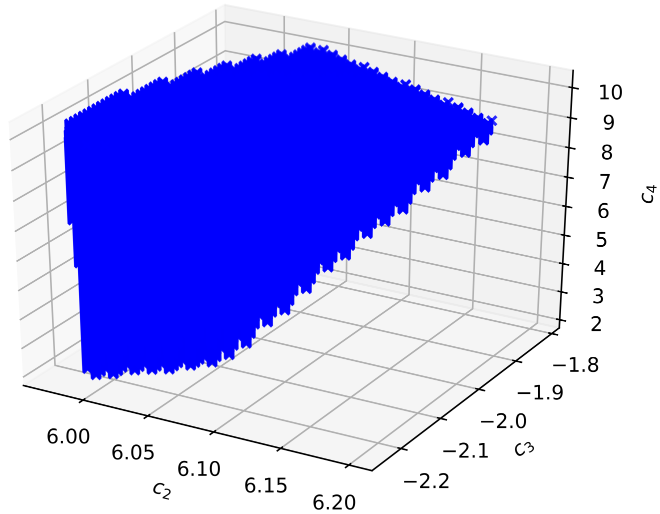

Figure 5.2: Numerical scan over $-10 \leq c_i \leq 10$ for $i = 2, 3, 4$, taking $c_1 = -10.0$ and with step size $\Delta c = 0.01$. Points which satisfy all inequalities given in the "summary of constraints" are labelled by a blue $\times$.

As above, we will embed the real scalar field $\hat{\pi}$ appearing in (5.50) in a complex scalar field $A = \frac{1}{2}(\hat{\pi} + \chi)$, which is taken to be the lowest component of a chiral superfield

$$\Phi = A + \sqrt{2}\Theta\psi + \Theta\Theta F \ . \tag{5.96}$$

As in the flat superspace case, this chiral superfield contains, in addition to A, a two component Weyl spinor ψ and a complex scalar auxiliary field F. With the exception of the supergravity extension of $\bar{\mathcal{L}}_1$, our $N = 1$ locally supersymmetric Lagrangians are all of the form

$$\int d^2\Theta\, 2\mathcal{E}(\overline{\mathcal{D}}^2 - 8R)\mathcal{O}(\Phi, \Phi^\dagger) + \text{h.c.}\,, \tag{5.97}$$

where $\mathcal{O}(\Phi, \Phi^\dagger)$ is a Lorentz scalar involving Φ and $\Phi^\dagger$. The integral is over half of superspace, where the chiral projection operator $\overline{\mathcal{D}}^2 - 8R$, involving the curvature *chiral superfield* R, acts on $\mathcal{O}$ so as to make the combination $(\overline{\mathcal{D}}^2 - 8R)\mathcal{O}$ a chiral superfield. The geometrical *chiral density* $\mathcal{E}$ ensures that the Lagrangian has the appropriate transformation properties under local $N = 1$ supersymmetry.

Local $N = 1$ supersymmetry necessitates the introduction of a supergravity multiplet

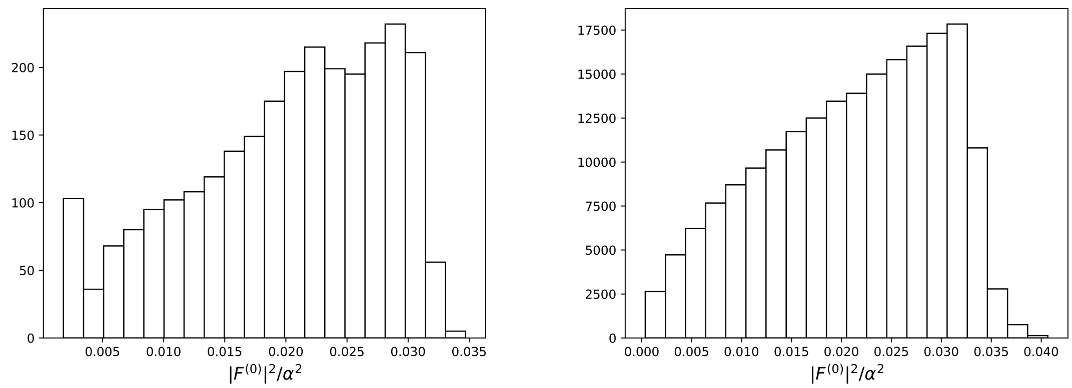

(a) (b)

Figure 5.3: Histograms of $|F^{(0)}|^2/\alpha^2$ for (a) $c_1 = -1$ and (b) $c_1 = -10$. The data are from the same numerical scans as in Figures 5.1 and 5.2. Plots (a) and (b) each represent a total of 2,701 and 198,903 points respectively.

containing the spin 2 graviton $e_\mu{}^a$ and the spin 3/2 gravitino $\psi_\mu{}^\alpha$. However, the off-shell superspace formalism that we are using requires the addition of two new auxiliary fields, a complex scalar M and a real vector field b_μ, to the supergravity multiplet. Both M and b_μ have mass dimension one, and appear in the Θ expansions of the chiral superfield R and the geometrical chiral density $\mathcal{E}$. Explicitly, one finds that

$$\begin{aligned} R &= -\tfrac{1}{6}M + \Theta^2\left(\tfrac{1}{12}\mathcal{R} - \tfrac{1}{9}MM^* - \tfrac{1}{18}b^\mu b_\mu + \tfrac{1}{6}ie_a{}^\mu\mathcal{D}_\mu b^a\right) \\ \mathcal{E} &= \tfrac{1}{2}e - \tfrac{1}{2}\Theta^2 eM^* \ , \end{aligned} \tag{5.98}$$

where $\mathcal{R}$ is the four-dimensional Ricci scalar (not to be confused with the similar notation for the radius of curvature in the AdS_5 case) and $e = \det e_\mu{}^a$. For more details on the construction of $N = 1$ supergravity Lagrangians using the superspace formalism, we refer the reader to [62, 171], as well as to [130, 53, 22]. Higher-derivative Lagrangians in $N = 1$ supergravity have been examined in [130, 53, 22, 87, 88, 86, 52]. Therefore, in addition to the auxiliary field F of the chiral supermultiplet Φ, one must now examine the behaviour of the supergravity auxiliary fields M and b_μ.

Let us first consider the supergravity extension of $\bar{\mathcal{L}}_1$, $\bar{\mathcal{L}}_2$ and $\bar{\mathcal{L}}_3$, deferring the discussion of $\bar{\mathcal{L}}_4$ to the end of this section. For simplicity, we will set $\alpha = 1$ unless otherwise stated. However, to explicitly demonstrate where effects due to gravitation arise, we will exhibit the factors of the Planck mass, M_P, wherever they occur in our expressions. As above, we will not present terms which involve fermions, since these are not relevant for this discussion. Therefore, in addition to dropping terms involving the Weyl fermion ψ, we will also exclude terms which containing the gravitino $\psi_\mu{}^\alpha$. The appropriate supergravity extensions of $\bar{\mathcal{L}}_1$

and $\bar{\mathcal{L}}_2$ are given, in terms of superfields, by

$$\bar{\mathcal{L}}_1^{\rm SUGRA} = \int d^2\Theta\, 2\mathcal{E}\, W(\Phi) + \text{h.c.} \tag{5.99}$$

$$\bar{\mathcal{L}}_2^{\rm SUGRA} = M_P^2 \int d^2\Theta\, 2\mathcal{E}\Big(-\frac{3}{8}(\overline{\mathcal{D}}^2 - 8R) e^{-K(\Phi,\Phi^\dagger)/3M_P^2}\Big) + \text{h.c} \tag{5.100}$$

To be consistent with the flat supersymmetry results of the previous section, it follows from (5.53) and (5.73) that one must take

$$K(\Phi,\Phi^\dagger) = \gamma\Phi\Phi^\dagger + \delta(\Phi^2\Phi^\dagger + \Phi(\Phi^\dagger)^2)\,, \qquad W(\Phi) = \beta_1\Phi + \beta_2\Phi^2\,, \tag{5.101}$$

where γ, δ are defined in equation (5.66) and β_1, β_2 are real coefficients. Written in terms of components fields, we find that (5.99) and (5.100) become

$$\begin{aligned}
\frac{1}{e}\bar{\mathcal{L}}_1^{\rm SUGRA} &= \frac{\partial W}{\partial A}F + \frac{\partial W^*}{\partial A^*}F^* - WM^* - W^*M\ , \\
\frac{1}{e}\bar{\mathcal{L}}_2^{\rm SUGRA} &= M_P^2 e^{-\frac{1}{3}\frac{K}{M_P^2}}\Big(-\frac{1}{2}\mathcal{R} - \frac{1}{3}MM^* + \frac{1}{3}b^\mu b_\mu\Big) + 3M_P^2\frac{\partial^2 e^{-\frac{1}{3}\frac{K}{M_P^2}}}{\partial A\partial A^*}(\partial A\cdot\partial A^* - FF^*) \\
&+ iM_P^2 b^\mu(\partial_\mu A\frac{\partial e^{-\frac{1}{3}\frac{K}{M_P^2}}}{\partial A} - \partial_\mu A^*\frac{\partial e^{-\frac{1}{3}\frac{K}{M_P^2}}}{\partial A^*}) + M_P^2(MF\frac{\partial e^{-\frac{1}{3}\frac{K}{M_P^2}}}{\partial A} + M^*F^*\frac{\partial e^{-\frac{1}{3}\frac{K}{M_P^2}}}{\partial A^*})
\end{aligned} \tag{5.102}$$

respectively.

The extension to $N=1$ supergravity of $\bar{\mathcal{L}}_3$ is constructed from two terms,

$$\begin{aligned}
\bar{\mathcal{L}}_{3,\rm I} &= -\frac{1}{64}\int d^2\Theta\, 2\mathcal{E}\,(\overline{\mathcal{D}}^2 - 8R)\Big(-\frac{1}{\sqrt{2}}c_3 - \frac{\sqrt{2}}{3}c_4 - 2c_4(\Phi+\Phi^\dagger)\Big)\mathcal{D}\Phi\mathcal{D}\Phi\overline{\mathcal{D}}^2\Phi^\dagger + \text{h.c.} \\
&= \Big(-\frac{1}{\sqrt{2}}c_3 - \frac{\sqrt{2}}{3}c_4 - 2c_4(A+A^*)\Big)\Big((\partial A)^2\big(\nabla_\mu\partial^\mu A^* + \frac{2}{3}ib^\mu\partial_\mu A + \frac{2}{3}M^*F^*\big) \\
&\qquad +(\partial A^*)^2\big(\nabla_\mu\partial^\mu A + \frac{2}{3}ib^\mu\partial_\mu A^* + \frac{2}{3}MF\big) - \frac{4}{3}MF^2F^* - \frac{4}{3}M^*(F^*)^2F \\
&\qquad +2F^*\partial F\cdot\partial A + 2F\partial F^*\cdot\partial A^* + \frac{1}{6}iFF^*b^\mu(\partial_\mu A - \partial_\mu A^*)\Big) \\
&+ 2c_4\Big(2(FF^*)^2 - 4FF^*\partial A\cdot\partial A^* - FF^*\big((\partial A)^2 + (\partial A^*)^2\big)\Big) \\
&- \Big(-\frac{1}{\sqrt{2}}c_3 - \frac{\sqrt{2}}{3}c_4 - 2c_4(A+A^*)\Big) \\
&\quad \times\Big((\partial A)^2F^*M^* + (\partial A^*)^2FM - \frac{1}{3}MF^2F^* - \frac{1}{3}M(F^*)^2F\Big)
\end{aligned} \tag{5.103}$$

and

$$
\begin{aligned}
&\overline{\mathcal{L}}_{3,\mathrm{II}} \\
= \quad & -\frac{1}{32}\int d^2\Theta\, 2\mathcal{E}\,(\overline{\mathcal{D}}^2-8R)\bigg(\frac{1}{8}c_2+\frac{1}{3}c_3-\frac{1}{3}c_4+\frac{1}{\sqrt{2}}(\frac{2}{3}c_3-\frac{4}{3}c_4)(\Phi+\Phi^\dagger)\bigg)\mathcal{D}\Phi\mathcal{D}\Phi\overline{\mathcal{D}}\Phi^\dagger\overline{\mathcal{D}}\Phi^\dagger \\
& \quad +\mathrm{h.c.} \\
= \quad & \bigg(\frac{1}{8}c_2+\frac{1}{3}c_3-\frac{1}{3}c_4+\frac{1}{\sqrt{2}}(\frac{2}{3}c_3-\frac{4}{3}c_4)(A+A^*)\bigg) \\
& \quad \times\bigg(4(\partial A)^2(\partial A^*)^2-8FF^*\partial A\cdot\partial A^*+4(FF^*)^2\bigg)\ .
\end{aligned}
\tag{5.104}
$$

Then

$$
\overline{\mathcal{L}}_3^{\mathrm{SUGRA}}=\overline{\mathcal{L}}_{3,\mathrm{I}}+\overline{\mathcal{L}}_{3,\mathrm{II}}\,. \tag{5.105}
$$

Ignoring, for the time being the contribution of $\overline{\mathcal{L}}_4^{\mathrm{SUGRA}}$, let us take the $N=1$ supergravity Lagrangian for the worldvolume action of a probe brane in heterotic M-theory to be

$$
\overline{\mathcal{L}} \quad = \quad \overline{\mathcal{L}}_1^{\mathrm{SUGRA}}+\overline{\mathcal{L}}_2^{\mathrm{SUGRA}}+\overline{\mathcal{L}}_3^{\mathrm{SUGRA}}. \tag{5.106}
$$

To ensure that this Lagrangian has the appropriate non-linear sigma model kinetic energy, that is, so that gravity is canonically normalized, one must perform a Weyl rescaling of the vielbein

$$
e_\mu{}^a \to e_\mu{}^a e^{\frac{1}{6}\frac{K}{M_P^2}}\ . \tag{5.107}
$$

This induces transformations on the Ricci scalar $\mathcal{R}$ and on all covariant derivatives and Christoffel symbols in the component field Lagrangian. To proceed, one must now eliminate the auxiliary fields M and b_μ using their equations of motion. The procedure is straightforward but tedious, and the essential steps were outlined in [62], Therefore, in this chapter, we simply present the results. For compactness, we use the notation

$$
\begin{aligned}
&D_A=\frac{\partial}{\partial A}+\frac{\partial K}{\partial A}\,, \qquad \bar{D}_{A^*}=\frac{\partial}{\partial A^*}+\frac{\partial K}{\partial A^*}, \qquad K_{,A}=\frac{\partial K}{\partial A}\,, \qquad K_{,A^*}=\frac{\partial K}{\partial A^*} \\
&\mu_1=-\frac{1}{64}\bigg(-\frac{1}{\sqrt{2}}c_3-\frac{\sqrt{2}}{3}c_4\bigg)\,, \quad \lambda_1=\frac{c_4}{32}, \quad \mu_2=-\frac{1}{32}\bigg(\frac{1}{8}c_2+\frac{1}{3}c_3-\frac{1}{3}c_4\bigg) \\
&\lambda_2=-\frac{1}{32\sqrt{2}}(\frac{2}{3}c_3-\frac{4}{3}c_4)\,, \quad f(A,A^*)=\frac{64}{3}\bigg(\mu_1+\lambda_1(A+A^*)\bigg)\ .
\end{aligned}
\tag{5.108}
$$

Using this notation, we find that, after Weyl rescaling, the auxiliary field b_μ is given by

$$b_\mu = -\frac{3}{2}\Big(j_\mu - \frac{1}{4M_P^2}(\mu_1 + \lambda_1(A + A^*))h_\mu\Big) \tag{5.109}$$

where

$$\begin{aligned} j_\mu &= -\frac{i}{M_P^2}\Big(K_{,A}\partial_\mu A - K_{,A^*}\partial_\mu A^*\Big) \\ h_\mu &= i\Big(\partial_\mu A(\frac{512}{3}(\partial A)^2 + \frac{128}{3}e^{\frac{1}{3}\frac{K}{M_P^2}}FF^*) - \partial_\mu A^*(\frac{512}{3}(\partial A^*)^2 + \frac{128}{3}e^{\frac{1}{3}\frac{K}{M_P^2}}FF^*)\Big) \ . \end{aligned} \tag{5.110}$$

To remove the auxiliary field M, it is conventional to perform the following redefinition to another complex scalar N defined by

$$M = N - \frac{1}{M_P^2}\frac{\partial K}{\partial A^*}F^* \ . \tag{5.111}$$

This, of course, leads to additional terms in (5.106) which depend on F and A alone. Solving for N, we find that

$$N = \frac{3}{M_P^2}e^{-\frac{1}{3}\frac{K}{M_P^2}}\Big(-e^{\frac{2}{3}\frac{K}{M_P^2}}W + fe^{\frac{1}{3}\frac{K}{M_P^2}}(\partial A)^2F^* + 3fe^{\frac{2}{3}\frac{K}{M_P^2}}(F^*)^2F\Big) \ . \tag{5.112}$$

Inserting these results back into Lagrangian (5.106), gives

$$
\begin{aligned}
&\frac{\bar{\mathcal{L}}'}{e} \\
= \;& -\tfrac{1}{2}M_P^2\mathcal{R} - K_{,AA^*}\partial A\cdot\partial A^* + e^{\frac{1}{3}\frac{K}{M_P^2}}K_{,AA^*}FF^* + e^{\frac{2}{3}\frac{K}{M_P^2}}(D_AWF + \bar{D}_{A^*}W^*F^*) \\
&+\frac{3}{M_P^2}e^{\frac{K}{M_P^2}}|W|^2 \\
&-\frac{1}{4}\Big(\mu_1+\lambda_1(A+A^*)\Big)\Big(16(\partial A)^2\big(16\nabla^2A^* + 32\partial_\mu e^{\frac{1}{6}\frac{K}{M_P^2}}\partial^\mu A^*\big) \\
&\qquad\qquad +16(\partial A^*)^2\big(16\nabla^2 A + 32\partial_\mu e^{\frac{1}{6}\frac{K}{M_P^2}}\partial^\mu A\big)\Big) \\
&-128e^{\frac{1}{3}\frac{K}{M_P^2}}\Big(\mu_1+\lambda_1(A+A^*)\Big)\Big(F^*\nabla F\cdot\nabla A + F\nabla F^*\cdot\nabla A^*\Big) \\
&+\Big(\mu_2+\lambda_2(A+A^*)\Big)\Big(-128(\partial A)^2(\partial A^*)^2 + 256e^{\frac{1}{3}\frac{K}{M_P^2}}\partial A\cdot\partial A^*FF^* - 128e^{\frac{2}{3}\frac{K}{M_P^2}}(FF^*)^2\Big) \\
&+\lambda_1\Big(128e^{\frac{2}{3}\frac{K}{M_P^2}}(FF^*)^2 - 256e^{\frac{1}{3}\frac{K}{M_P^2}}\partial A\cdot\partial A^*FF^* - 64e^{\frac{1}{3}\frac{K}{M_P^2}}\big((\partial A)^2+(\partial A^*)^2\big)FF^*\Big) \\
&-\frac{f}{M_P^2}e^{\frac{1}{3}\frac{K}{M_P^2}}FF^*\big(K_{,A}(\partial A)^2 + K_{,A^*}(\partial A^*)^2\big) - 3\frac{f}{M_P^2}e^{\frac{2}{3}\frac{K}{M_P^2}}(FF^*)^2\big(K_{,A}+K_{,A^*}\big) \\
&+\frac{3}{8}\Big(\mu_1+\lambda_1(A+A^*)\Big)j_\mu h^\mu - \frac{3}{64M_P^2}\Big(\mu_1+\lambda_1(A+A^*)\Big)^2 h_\mu h^\mu \\
&+\frac{3}{M_P^2}\Big(f^2e^{\frac{2}{3}\frac{K}{M_P^2}}(\partial A)^2(\partial A^*)^2FF^* + 9f^2e^{\frac{4}{3}\frac{K}{M_P^2}}(FF^*)^3 + 3f^2e^{\frac{K}{M_P^2}}(\partial A)^2(FF^*)^2 \\
&\qquad +3f^2e^{\frac{K}{M_P^2}}(\partial A^*)^2(FF^*)^2 - fe^{\frac{K}{M_P^2}}\big(W^*(\partial A)^2F^* + W(\partial A^*)^2F^*\big) \\
&\qquad -3fe^{\frac{4}{3}\frac{K}{M_P^2}}\big(W^*(F^*)^2F^* + W(F)^2F^*\big)\Big), \qquad (5.113)
\end{aligned}
$$

where j_μ, h_μ are given in (5.110). The prime on $\bar{\mathcal{L}}'$ indicates that both Weyl rescaling and the elimination of the supergravity auxiliary fields have been performed. An important check on this result is the following. Taking the limit in which $M_P^2 \to \infty$, and $g_{\mu\nu} \to \eta_{\mu\nu}$, we find that

$$
\begin{aligned}
\overline{\mathcal{L}'} \;=\;& \frac{\partial W}{\partial A}F + \frac{\partial W^*}{\partial A^*}F^* - \frac{\partial^2 K}{\partial A\partial A^*}(\partial A\cdot\partial A^* - FF^*) \\
+\;& \Big(-\frac{1}{\sqrt{2}}c_3 - \frac{\sqrt{2}}{3}c_4 - 2c_4(A+A^*)\Big) \\
&\quad\times\Big((\partial A)^2(\Box A^*) + (\partial A^*)^2(\Box A) + 2F^*\partial F\cdot\partial A + 2F\partial F^*\cdot\partial A^*\Big) \\
+\;& 2c_4\Big(2(FF^*)^2 - 4FF^*\partial A\cdot\partial A^* - FF^*\big((\partial A)^2 + (\partial A^*)^2\big)\Big) \\
+\;& \Big(\frac{1}{8}c_2 + \frac{1}{3}c_3 - \frac{1}{3}c_4 + \frac{1}{\sqrt{2}}(\frac{2}{3}c_3 - \frac{4}{3}c_4)(A+A^*)\Big) \\
&\quad\times\Big(4(\partial A)^2(\partial A^*)^2 - 8FF^*\partial A\cdot\partial A^* + 4(FF^*)^2\Big)\;. \qquad (5.114)
\end{aligned}
$$

After an integration by parts, this is *precisely* the sum of the flat superspace Lagrangians presented in (5.64), (5.54) and (5.57)–as it must be.

5.9.1 $\overline{\mathcal{L}}_4^{\mathrm{SUGRA}}$

The $N=1$ supergravity extension of $\bar{\mathcal{L}}_4$ is given by

$$\overline{\mathcal{L}}_4^{\mathrm{SUGRA}} = \overline{\mathcal{L}}_{4,\mathrm{I}} + \overline{\mathcal{L}}_{4,\mathrm{II}} + \overline{\mathcal{L}}_{4,\mathrm{II}} + \overline{\mathcal{L}}_{4,\mathrm{IV}} + \overline{\mathcal{L}}_{4,\mathrm{V}}\,, \tag{5.115}$$

where

$$\begin{aligned}
\overline{\mathcal{L}}_{4,\mathrm{I}} &= \frac{-1}{256}\int d^2\Theta\, 2\mathcal{E}\,(\overline{\mathcal{D}}^2-8R)\Big(\frac{1}{4}c_4+\frac{1}{6\sqrt{2}}(\Phi+\Phi^\dagger)\Big)\{\mathcal{D},\overline{\mathcal{D}}\}(\mathcal{D}\Phi\mathcal{D}\Phi)\{\mathcal{D},\overline{\mathcal{D}}\}(\overline{\mathcal{D}}\Phi^\dagger\overline{\mathcal{D}}\Phi^\dagger)\\
&\quad +\text{h.c.}\\
\overline{\mathcal{L}}_{4,\mathrm{II}} &= \frac{-1}{512}\int d^2\Theta\, 2\mathcal{E}\,(\overline{\mathcal{D}}^2-8R)\Big(c_4+\frac{2}{3\sqrt{2}}c_4(\Phi+\Phi^\dagger)\Big)\{\mathcal{D},\overline{\mathcal{D}}\}(\Phi+\Phi^\dagger)\{\mathcal{D},\overline{\mathcal{D}}\}(\mathcal{D}\Phi\mathcal{D}\Phi)\overline{\mathcal{D}}^2\Phi^\dagger\\
&\quad +\text{h.c.}\\
\overline{\mathcal{L}}_{4,\mathrm{III}} &= \frac{-1}{256\sqrt{2}}\int d^2\Theta\, 2\mathcal{E}\,(\overline{\mathcal{D}}^2-8R)\Big(\frac{19}{6}c_4+\frac{76}{9\sqrt{2}}c_4(\Phi+\Phi^\dagger)\Big)\mathcal{D}\Phi\mathcal{D}\Phi\overline{\mathcal{D}}\Phi^\dagger\overline{\mathcal{D}}\Phi^\dagger\\
&\qquad\qquad \times\{\mathcal{D},\overline{\mathcal{D}}\}\{\mathcal{D},\overline{\mathcal{D}}\}(\Phi+\Phi^\dagger)+\text{h.c.}\\
\overline{\mathcal{L}}_{4,\mathrm{IV}} &= \frac{1}{512\sqrt{2}}\int d^2\Theta\, 2\mathcal{E}\,(\overline{\mathcal{D}}^2-8R)\Big(-c_3-\frac{11}{3}c_4+\frac{1}{\sqrt{2}}(-\frac{2}{3}c_2-\frac{88}{9}c_4)(\Phi+\Phi^\dagger)\Big)\\
&\qquad\qquad \times\{\mathcal{D},\overline{\mathcal{D}}\}\mathcal{D}\Phi\mathcal{D}\Phi\overline{\mathcal{D}}\Phi\overline{\mathcal{D}}\Phi^\dagger\{\mathcal{D},\overline{\mathcal{D}}\}\Phi+\text{h.c.}\\
\overline{\mathcal{L}}_{4,\mathrm{V}} &= -\frac{1}{128}\int d^2\Theta\, 2\mathcal{E}\,(\overline{\mathcal{D}}^2-8R)\Big(-\frac{1}{16}-\frac{1}{3}c_3-\frac{9}{4}c_4+\frac{1}{\sqrt{2}}(-\frac{1}{24}c_2-\frac{8}{9}c_3-\frac{21}{2}c_4)(\Phi+\Phi^\dagger)\Big)\\
&\qquad\qquad \times\mathcal{D}\Phi\mathcal{D}\Phi\overline{\mathcal{D}}\Phi^\dagger\overline{\mathcal{D}}\Phi^\dagger\{\mathcal{D},\overline{\mathcal{D}}\}\Phi\{\mathcal{D},\overline{\mathcal{D}}\}\Phi^\dagger+\text{h.c.}
\end{aligned}\tag{5.116}$$

When expressed in components fields, $\overline{\mathcal{L}}_4^{\mathrm{SUGRA}}$ will give rise to the appropriate higher derivatives of the complex scalar A, as well as those terms in (5.58)-(5.63) involving the auxiliary field F and its derivatives. As in $\overline{\mathcal{L}}_1^{\mathrm{SUGRA}}$, $\overline{\mathcal{L}}_2^{\mathrm{SUGRA}}$ and $\overline{\mathcal{L}}_3^{\mathrm{SUGRA}}$, we also find terms involving the auxiliary fields of supergravity. Now, however, there arise terms which are cubic or higher order in M, as well as terms involving *derivatives* of b_μ and M. We note that such terms were also present in the supergravity extension $\overline{\mathcal{L}}_4^{\mathrm{SUGRA}}$ in the conformal Galileon case discussed in [62]. A complete analysis of these higher polynomial and derivative terms involving the supergravity auxiliary fields, both in the conformal and heterotic Galileon cases, is an interesting avenue of research to explore. However, this is not necessary for our present purposes, as we will see shortly.

5.10 The Cosmological Limit

Recall that the heterotic Galileons are derived in the limit where the four-dimensional momenta and the auxiliary field F are all small compared the mass α associated with the curvature of the fifth-dimension. To continue in the gravitational case, it is extremely useful to work in a limit in which the four-dimensional spacetime curvature scalar $\mathcal{R}$ is restricted to be small compared to α^2. That is,

$$\mathcal{R} \ll \alpha^2 < M_{CY}^2 < M_P^2 \ . \tag{5.117}$$

This scenario, which we referred to as the "cosmological limit" in [62], allows one to drop the majority of terms appearing in the supergravity extended Lagrangian.

Let us first consider the worldvolume Lagrangian (5.113), constructed from $\overline{\mathcal{L}}_1^{\mathrm{SUGRA}}$, $\overline{\mathcal{L}}_2^{\mathrm{SUGRA}}$ and $\overline{\mathcal{L}}_3^{\mathrm{SUGRA}}$ only. Taking this limit in (5.113), the "cosmological" supergravity Lagrangian is found to be

$$\begin{aligned}
\frac{\overline{\mathcal{L}}_{1+2+3}^{\mathrm{cosmo}}}{e} \;=\;& -\frac{1}{2}M_P^2\mathcal{R} + \frac{\partial W}{\partial A}F + \frac{\partial W^*}{\partial A^*}F^* - \frac{\partial^2 K}{\partial A \partial A^*}(\nabla A \cdot \nabla A^* - FF^*) \\
&+ \left(-\frac{1}{\sqrt{2}}c_3 - \frac{\sqrt{2}}{3}c_4 - 2c_4(A+A^*)\right)\Big((\partial A)^2(\nabla^2 A^*) + (\partial A^*)^2(\nabla^2 A) \\
&\qquad +2F^*\partial F \cdot \partial A + 2F\partial F^* \cdot \partial A^* \Big) \\
&+ 2c_4\Big(2(FF^*)^2 - 4FF^*\nabla A \cdot \nabla A^* - FF^*\big((\nabla A)^2 + (\nabla A^*)^2\big)\Big) \\
&+ \left(\frac{1}{8}c_2 + \frac{1}{3}c_3 - \frac{1}{3}c_4 + \frac{1}{\sqrt{2}}(\frac{2}{3}c_3 - \frac{4}{3}c_4)(A+A^*)\right)\Big(4(\nabla A)^2(\nabla A^*)^2 - 8FF^*\nabla A \cdot \nabla A^* \\
&\qquad +4(FF^*)^2\Big) \ .
\end{aligned} \tag{5.118}$$

We can now extend these results to include the "cosmological" terms from $\overline{\mathcal{L}}_4^{\mathrm{SUGRA}}$. One can show that, in this limit, all terms arising from the elimination of the supergravity auxiliary fields M and b_μ must necessarily be suppressed by powers of M_P and, hence, can be ignored. The relevant terms will consist of two parts. The first part–labelled as $4A$–is made up of the expressions given in (5.58)-(5.63) with the partial derivatives ∂ replaced by

∇ and the metric $\eta_{\mu\nu}$ replaced with $g_{\mu\nu}$. That is, we add to (5.118) the following:

$$
\begin{aligned}
\frac{\overline{\mathcal{L}}_{4A}^{\text{cosmo}}}{e} \;=\;& \Big(-\frac{1}{4}c_4-\frac{1}{6\sqrt{2}}c_4(A+A^*)\Big)\Big(4\nabla_\mu(\nabla A)^2\nabla^\mu(\nabla A^*)^2-8\nabla_\mu(FA_{,\nu})\nabla^\mu(F^*A^{*,\nu})\\
&\qquad +16FF^*\nabla F\cdot\nabla F^*\Big)\\
+\;& \Big(c_4+\frac{2}{3\sqrt{2}}c_4(A+A^*)\Big)\Big((A+A^*)^{,\mu}\big(\nabla_\mu(\nabla A)^2\nabla^2A+\nabla_\mu(\nabla A^*)^2\nabla^2A^*\big)\\
&\qquad -(A+A^*)^{,\mu}\big(\nabla_\mu(FA_{,\nu})F^{*,\nu}+\nabla_\mu(F^*A^*_{,\nu})F^{,\nu}\big)\\
&\qquad -(A+A^*)^{,\mu}\big(\nabla_\mu(F\nabla^2A-\nabla F\cdot\nabla A)F^*+\nabla_\mu(F^*\nabla^2A^*-\nabla F^*\cdot\nabla A^*)F\big)\\
&\qquad -\nabla_\mu\nabla_\nu(A-A^*)\big(\nabla^\mu(FA^{,\nu})F^*-\nabla^\mu(F^*A^{*,\nu})F\big)-4FF^*\nabla F\cdot\nabla F^*\Big)\\
-\;& \frac{32}{3\sqrt{2}}c_4(A-A^*)^{,\nu}(A+A^*)_{,\mu}\big(\nabla^\mu(FA_\nu)F^*-\nabla^\mu(F^*A^*_\nu)F\big)\\
-\;& \frac{32}{3\sqrt{2}}c_4FF^*(A+A^*)_{,\mu}\big(\nabla^\mu(\nabla A)^2+\nabla^\mu(\nabla A^*)^2\big)\\
+\;& \frac{64}{3\sqrt{2}}c_4\Big(F(F^*)^2(A+A^*)_{,\mu}F^{,\mu}+F^*F^2(A+A^*)_{,\mu}F^{*,\mu}\Big)\\
+\;& 2\sqrt{2}\Big(-\frac{19}{6}c_4-\frac{76}{9\sqrt{2}}c_4(A+A^*)\Big)\Big((\nabla A)^2(\nabla A^*)^2-2FF^*\nabla A\cdot\nabla A^*+(FF^*)^2\Big)\\
&\quad \nabla^2(A+A^*)\\
+\;& \frac{1}{\sqrt{2}}\Big(-c_3-\frac{11}{3}c_4+\frac{1}{\sqrt{2}}(-\frac{2}{3}c_3-\frac{88}{9}c_4)(A+A^*)\Big)\\
&\Big(\nabla_\mu\big((\nabla A)^2(\nabla A^*)^2\big)-2\nabla_\mu(FF^*\nabla A\cdot\nabla A^*)+\nabla_\mu(FF^*)^2\Big)(A+A^*)^{,\mu}\\
+\;& \Big(-\frac{1}{16}c_2-\frac{1}{3}c_3-\frac{9}{4}c_4+\frac{1}{\sqrt{2}}(-\frac{1}{24}c_2-\frac{8}{9}c_3-\frac{21}{2}c_4)(A+A^*)\Big)\\
&\Big((\nabla A)^2(\nabla A^*)^2-2FF^*\nabla A\cdot\nabla A^*+(FF^*)^2\Big)\nabla A\cdot\nabla A^*
\end{aligned}
\tag{5.119}
$$

One finds, however, that in addition to these terms, the presence of curvature leads to *two additional terms* arising from the supergravity extension of $\overline{\mathcal{L}}^{\text{SUSY}}_{4,\,\text{2ndterm}}$ in (5.60) that are not suppressed in the cosmological limit. These constitute the second part of the $\overline{\mathcal{L}}_4^{\text{SUGRA}}$ contribution to the cosmological limit and are given by

$$
\begin{aligned}
&\frac{\overline{\mathcal{L}}_{4B}^{\text{cosmo}}}{e}\\
=\;& \Big(c_4+\frac{2}{3\sqrt{2}}c_4(A+A^*)\Big)\Big(\frac{17}{4}\mathcal{R}FF^*\nabla^2(A+A^*)-\frac{9}{8}FF^*\mathcal{R}_{\mu\nu}\nabla^\mu(A+A^*)\nabla^\nu(A+A^*)\Big).
\end{aligned}
\tag{5.120}
$$

We conclude that in the cosmological limit defined by (5.117), the diffeomorphically invariant four-dimensional $N = 1$ supersymmetric Lagrangian is given by the sum

$$\frac{\overline{\mathcal{L}}^{\text{cosmo}}}{e} = \frac{\overline{\mathcal{L}}^{\text{cosmo}}_{1+2+3+4(A+B)}}{e} \ . \tag{5.121}$$

Appendix A

B-L MSSM Spectrum in the Case of Simultaneous Wilson Lines

The LSP Spectrum:

An important property of the initial SUSY parameter space in determining low-energy phenomenology is the identity of the LSP. Recall that when R-parity is violated, no restrictions exist on the identity of the LSP; for example, it can carry color or electric charge. Our main scan provides an excellent opportunity to examine the possible LSP's and the probability of their occurrence . To this end, a histogram of possible LSP's is presented in Figure A.1–with the possible LSP's indicated along the horizontal axis, and $\log_{10}$ of the number of valid points with a given LSP on the vertical axis. The notation here is a bit condensed, but is specified in more detail in Table A.1. The notation is devised to highlight the phenomenology of the different LSP's, specifically their decays[1], which are also presented in Table A.1.

The most common LSP in our main scan is the lightest neutralino, $\tilde{\chi}_1^0$. However, not all $\tilde{\chi}_1^0$ states are created equal. LHC production modes for the lightest neutralino depend significantly on the composition of the neutralino–a bino LSP cannot be directly produced at the LHC, but the other neutralino LSP's can. This is the basis we use for the division of these states. The state $\tilde{\chi}_{\tilde{B}}^0$ designates a mostly rino or mostly blino neutralino, $\tilde{\chi}_{\tilde{W}}^0$ a mostly wino neutralino and $\tilde{\chi}_{\tilde{H}}^0$ a mostly Higgsino neutralino. Here, the subscript mostly indicates the greatest contribution to that state. As an unrealistic example, if $\tilde{\chi}_1^0$ is 34% wino, 33% bino and 33% Higgsino, it is still labeled $\tilde{\chi}_{\tilde{W}}^0$. The chargino LSP's are similarly separated into wino-like and Higgsino-like charginos, and the stops and sbottom divisions are as in earlier work, references [146, 145]. Note that this notation for the stops, $\tilde{t}_{ad}$ and $\tilde{t}_r$, are only used to describe stop LSP's. For non-LSP stops, we use the conventional notation

[1] Recall that when R-parity is violated, as it is in this scenario, the LSP can decay to lighter non-supersymmetric states.

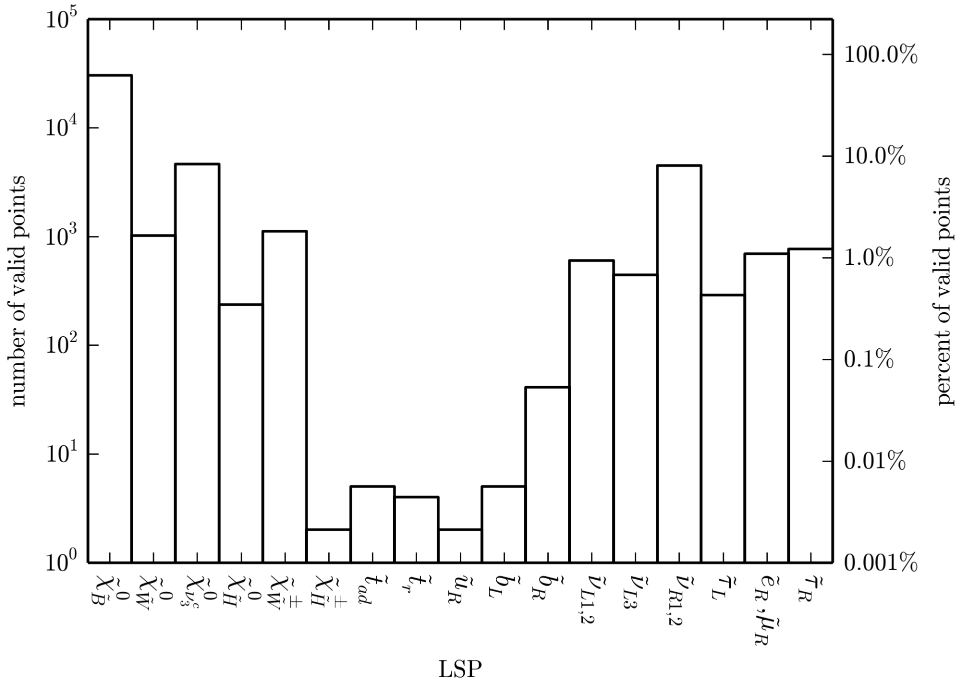

Figure A.1: A histogram of the LSP's in the main scan showing the percentage of valid points with a given LSP. Sparticles which did not appear as LSP's are omitted. The y-axis has a log scale. The dominant contribution comes from the lightest neutralino, as one might expect. The notation for the various states, as well as their most likely decay products, are given in Table A.1. Note that we have combined left-handed first and second generation sneutrinos into one bin, and that each generation makes up about 50% of the LSP's. The same is true for the first and second generation right-handed sleptons and sneutrinos.

Symbol	Description	Decay
$\tilde{\chi}^0_{\tilde{B}}$ $\tilde{\chi}^0_{\tilde{W}}$ $\tilde{\chi}_{\nu^c}$ $\tilde{\chi}^0_{\tilde{H}}$	A bino-like neutralino, mostly rino ($\tilde{W}_R$) or mostly blino ($\tilde{B}'$). Mostly wino neutralino. Mostly third-generation right-handed neutrino. Mostly Higgsino neutralino.	$\ell^{\pm}W^{\mp}$, νZ, νh
$\tilde{\chi}^{\pm}_{\tilde{W}}$ $\tilde{\chi}^{\pm}_{\tilde{H}}$	Mostly wino charginos. Mostly Higgsino charginos.	$\nu W^{\pm}$, $\ell^{\pm}Z$, $\ell^{\pm}h$
$\tilde{g}$	Gluino.	$t\bar{t}\nu$, $t\bar{b}\ell^-$
$\tilde{t}_{ad}$	Left- and right-handed stop admixture.	ℓ^+b
$\tilde{t}_r$	Mostly right-handed stop (over 99%).	$t\nu$, τ^+b
$\tilde{q}_R$	Right-handed first and second generation squarks.	ℓ^+j, νj
$\tilde{b}_L$	Mostly left-handed sbottom.	$b\nu$
$\tilde{b}_R$	Mostly right-handed sbottom.	$b\nu$, ℓ^-t
$\tilde{\nu}_{L_{1,2}}$ $\tilde{\nu}_{L_3}$	First and second generation left-handed sneutrinos. LSP's are split evenly among these two generations. Third generation left-handed sneutrino.	$b\bar{b}$, W^+W^-, ZZ, $t\bar{t}$, $\ell'^+\ell^-$, hh, $\nu\nu$
$\tilde{\nu}_{R_{1,2}}$	First and second generation right-handed sneutrinos.	$\nu\nu$
$\tilde{\tau}_L$	Third generation left-handed stau.	$t\bar{b}$, W^-h, $e\nu$, $\mu\nu$, $\tau\nu$
$\tilde{e}_R, \mu_R$	First and second generation right-handed sleptons. LSP's are split evenly between these two generations.	$e\nu$, $\mu\nu$
$\tilde{\tau}_R$	Third generation right-handed stau.	$t\bar{b}$, $e\nu$, $\mu\nu$, $\tau\nu$

Table A.1: The notation used for the states in Figure A.1 and their probable decays. More decays are possible in certain situations depending on what is kinematically possible and the parameter space. Gluino decays are especially dependent on the NLSP, here assumed to be a neutralino. Here, the word "mostly" means it is the greatest contribution to the state. The symbol ℓ represents any generation of charged leptons. The left-handed sneutrino decay into $\ell'^+\ell^-$ indicates a lepton flavor violating decay–that is, ℓ'^+ and ℓ^- do not have the same flavor. Note that j is a jet–indicating a light quark.

$\tilde{t}_1$ and $\tilde{t}_2$.

To make Figure A.1 more readable, we have made an effort to combine bins that have similar characteristics. The first and second generation left-handed sneutrinos are combined into one bin, where about 50% of the LSP's are first generation sneutrinos. The same holds true for the first and second generation right-handed sleptons, while the first generation right-handed sneutrino is always chosen to be lighter than the second generation right-handed sneutrino. This similarity between the first and second generation sleptons is expected, since their corresponding Yukawa couplings are not large enough to distinguish them through the RG evolution. For both sleptons and squarks, more LSP's exist for the third-generation–as expected from the effects of the third-generation Yukawa couplings, which tend to decrease sfermion masses in the RGE evolution.

The myriad of possible LSP's leads to a rich collider phenomenology. This phenomenology is not the main focus of this study, but it is worthwhile to briefly review it here. In models where R-parity violation is parameterized by bilinear R-parity breaking, such as the $B-L$ MSSM, SUSY particles are still pair produced and cascade decay to the LSP. At this point, the bilinear R-parity violating terms allow the LSP to decay. While only a few studies have been done on the phenomenology of the minimal $B-L$ MSSM [93, 94, 146, 145], there have been several works on the phenomenology of explicit bilinear R-parity violation, which has some similarities to this model. See [165, 111, 102, 103] for general discussions. Table A.1 provides some basic information on the most probable decay modes of each of the possible LSP's. Note that ℓ signifies a charged lepton of any generation and j a jet–implying a light quark. Some interesting aspects of Table A.1 were discussed in [161].

The Non-LSP Spectrum:

To get a sense of the non-LSP spectrum, we produce histograms of the masses of the sparticles associated with the valid points in the main scan. In the following histograms, there will be quite a few pairs of fields that will be highly degenerate; these will be represented by only one curve. This includes $SU(2)_L$ sfermion partners, which are only split by small electroweak terms. First generation squarks are also degenerate with second generation squarks with the same isospin, due to phenomenological constraints. A consequence of this is that all first and second generation left-handed squarks are highly degenerate.

Figure A.2 shows histograms of the squark masses. Because they come in $SU(2)_L$ doublets and the first- and second-family squarks must be degenerate, all four of the first- and second-family left-handed squarks have nearly identical mass and the histograms coincide. The degeneracy of first- and second-family squarks is also evident in the right-handed squark masses. The first and second family right-handed down squarks are generally lighter than their up counterparts because of the effect of the $U(1)_{3R}$ charge in the RGEs. Figure A.3 shows histograms of the masses of the sneutrinos and sleptons. The third-family sleptons

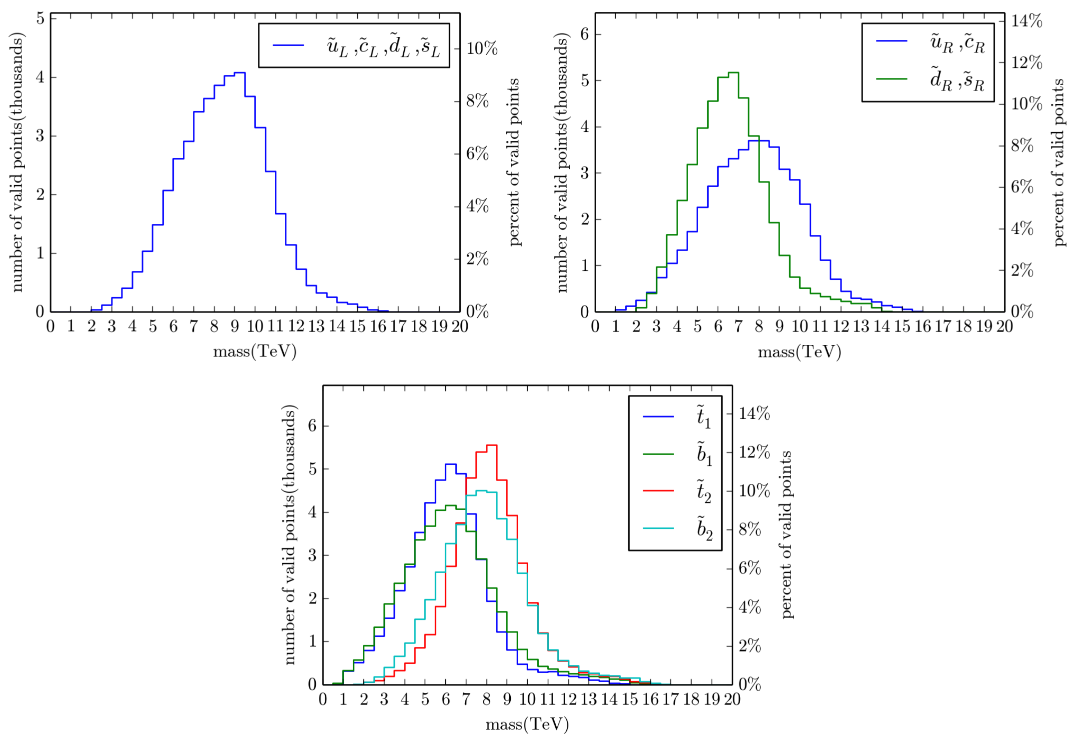

Figure A.2: Histograms of the squark masses from the valid points in the main scan. The first- and second-family left-handed squarks are shown in the top-left panel. Because they come in $SU(2)_L$ doublets, and the first- and second-family squarks must be degenerate, all four of these squarks have nearly identical mass and the histograms coincide. The first- and second-family right-handed squarks are shown in the top-right panel. The right-handed down squarks are generally lighter than their up counterparts because of the effect of the $U(1)_{3R}$ charge in the RGEs. The third family squarks are shown in the bottom panel.

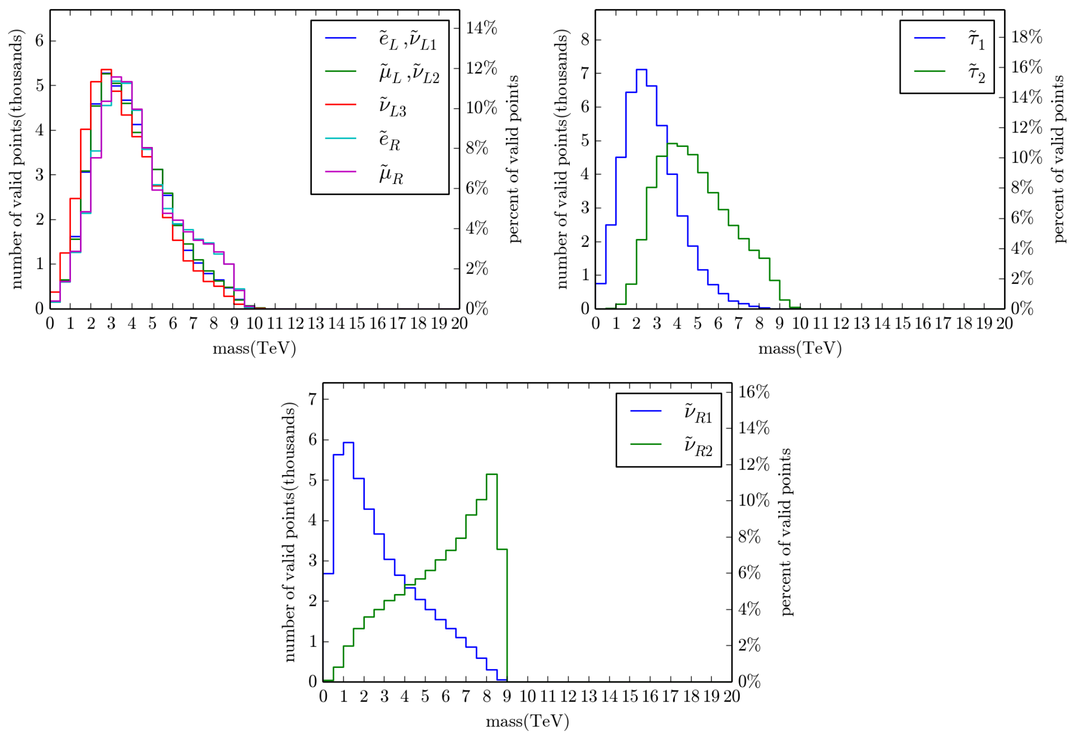

Figure A.3: Histograms of the sneutrino and slepton masses associated with the valid points in the main scan. First- and second-family entries are in the top-left panel, along with the third family left-handed sneutrino. Staus are in the top-right panel with mass-ordered labeling. In the bottom panel, the first- and second-family right-handed sneutrinos are labeled such that $\tilde{\nu}_{R1}$ is always lighter than $\tilde{\nu}_{R2}$.

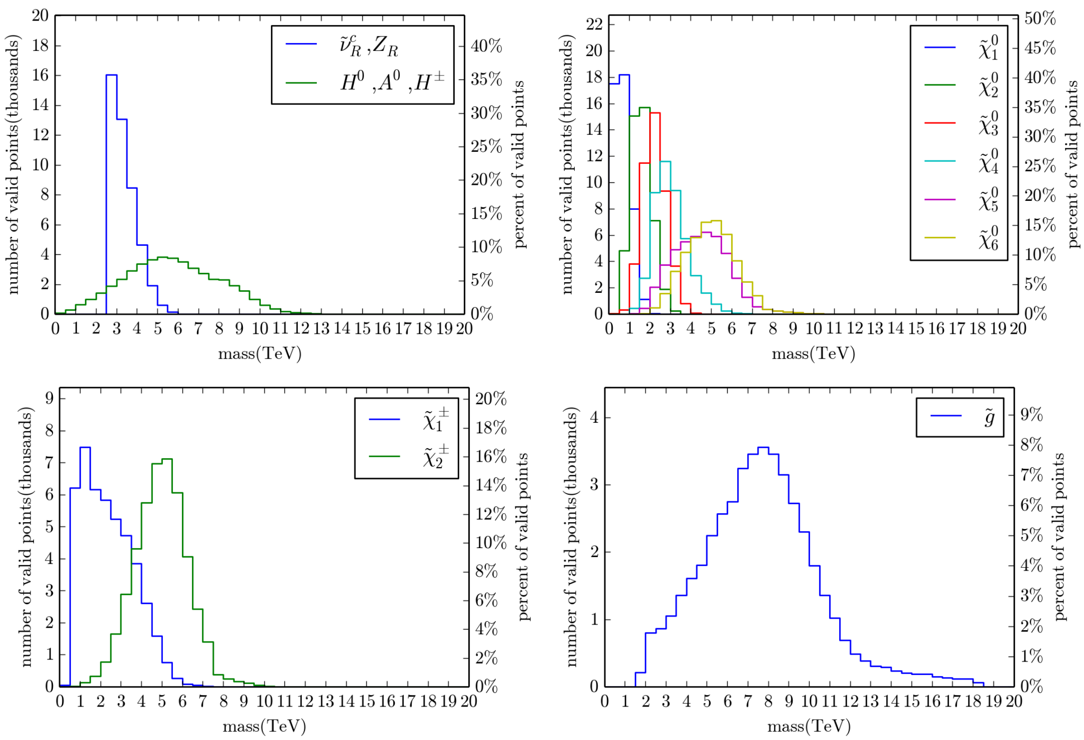

Figure A.4: The CP-even component of the third-family right-handed sneutrino, heavy Higgses, neutralinos, charginos and the gluino in the valid points from our main scan. The CP-even component of the third-generation right-handed sneutrino is degenerate with Z_R. The $\tilde{\chi}_5^0$ and $\tilde{\chi}_5^0$ are typically Higgsinos.

and left-handed sneutrinos tend to be the lighter because of the influence of the τ Yukawa coupling. The right-handed sneutrinos are labeled such that $\tilde{\nu}_{R_1}$ is always lighter than $\tilde{\nu}_{R_2}$. Figure A.4 presents histograms of the CP-even component of the third-generation right-handed sneutrino, the heavy Higgses, the neutralinos, the charginos, and the gluino. The CP-even component of the third-generation right-handed sneutrino is degenerate with Z_R. It is always heavier than 2.5 TeV because we have imposed the collider bound on Z_R. The neutralinos and charginos are labeled from lightest to heaviest as is canonical in SUSY models. The $\tilde{\chi}^0_5$ and $\tilde{\chi}^0_6$ are typically Higgsinos. We emphasize that all of the above histograms are calculated using our main scan; that is, for the choice of $M = 2700$ GeV and $f = 3.3$. We remind the reader that these values were chosen in [161] so as to maximize the number of valid points and repeated in this section so as to enable simple comparison with the split Wilson mass results. However, the mass scale of these histograms is heavily dependent on the choice of M. Smaller (larger) values for M will move the above distributions distinctly toward lighter (heavier) sparticle masses.

Plots of the physical particle spectra for two valid points are presented in Figure A.5. These two points are selected from the pool of valid points from the main scan based on the simple criteria that they are the valid points with the largest right-side-up and upside-down hierarchy respectively; that is, the largest splittings between the $B-L$ and SUSY scales in the two possible hierarchies. Plots of the high-scale boundary values for two sample valid

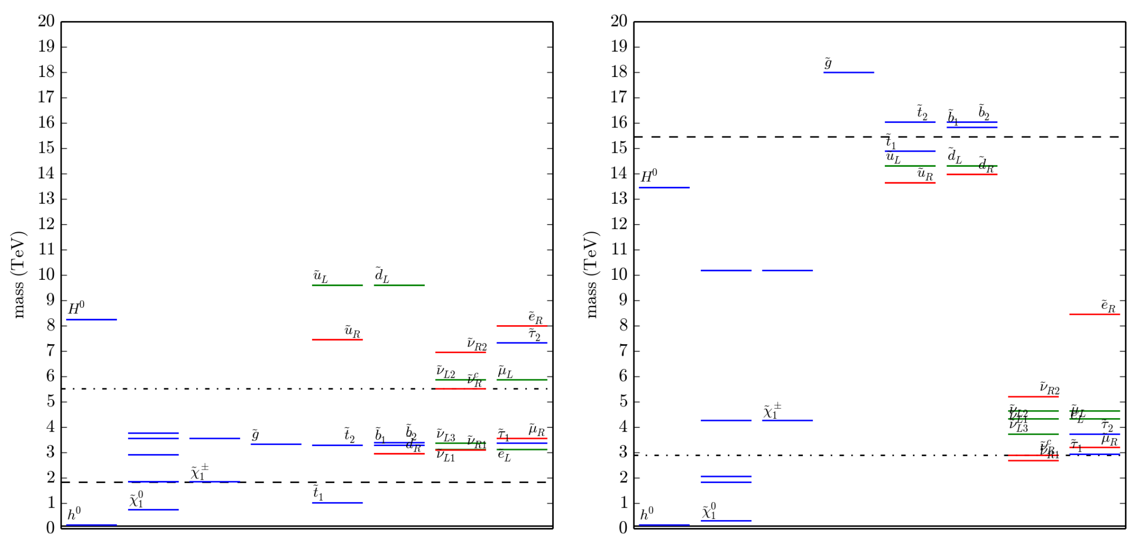

Figure A.5: Two sample physical spectra with a right-side-up hierarchy and upside-down hierarchy. The $B-L$ scale is represented by a black dot-dash-dot line. The SUSY scale is represented by a black dashed line. The electroweak scale is represented by a solid black line. The label $\tilde{u}_L$ is actually labeling the nearly degenerate $\tilde{u}_L$ and $\tilde{c}_L$ masses. The labels $\tilde{u}_R$, $\tilde{d}_L$ and $\tilde{d}_R$ are similarly labeling the nearly degenerate first- and second- family masses.

points from our main scan are presented in Figure A.6. While these look like Figs. A.5, they do not correspond to physical masses but, rather, mass parameters at $\langle M_U \rangle$. These two valid points are selected from the pool of valid points from the main scan based on a simple criterion. The two plots show the valid points with the largest and smallest amount of splitting in the initial values of the scalar soft mass parameters. The amount of splitting is defined as the standard deviation of the initial values of the 20 scalar soft mass parameters.

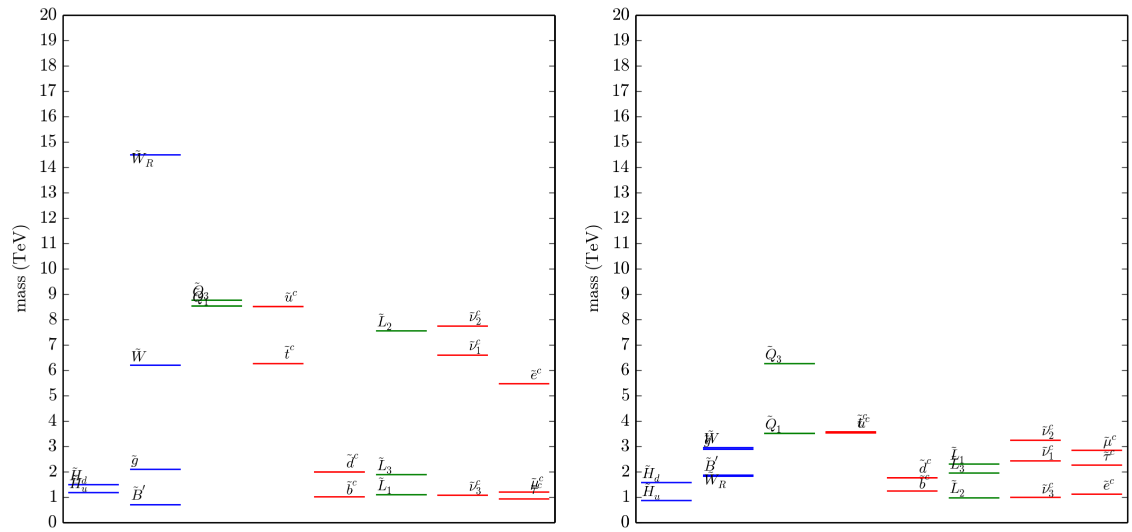

Figure A.6: Example high-scale boundary conditions at $\langle M_U \rangle$ for the two valid points with the largest and smallest amount of splitting. The label $\tilde{Q}_1$ is actually labeling the nearly degenerate $\tilde{Q}_1$ and $\tilde{Q}_2$ soft masses. The labels $\tilde{u}^c$ and $\tilde{d}^c$ are similarly labeling the nearly degenerate first and second family masses.

Appendix B

Lowering the B-L Scale

In this Appendix, we present the details of the renormalization group equations that allow us to specify the desired B-L breaking scale, and then run in energy-momentum up to the unification scale $\langle M_U \rangle$ to determine the associated initial values for both $m^2_{\tilde{\nu}^c_{R,3}}(t_U)$ and $m^2_{H_u}(t_U)$. To do this, we rely heavily on the description of the RGE's of the B-L MSSM presented in [161], as well as on the phenomenological analyses of the low-energy physics discussed in those papers.

B.1 RG Running of the Sneutrino Mass

In the upside-down hierarchy, the RGEs describing the running of $m^2_{\tilde{\nu}^c_{R,3}}$ are[1]

$$\begin{aligned} 16\pi^2 \frac{d}{dt} m^2_{\tilde{\nu}^c_{R,3}}(t) = &-3g^2_{BL}(t)M^2_{B-L}(t) - 2g^2_R(t)M^2_R(t) \\ &+\frac{3}{4}g^2_{BL}(t)S_{B-L}(t) - g^2_R(t)S_R(t)\,, \quad t_{SUSY} < t < t_U \end{aligned} \tag{B.1}$$

$$16\pi^2 \frac{d}{dt} m^2_{\tilde{\nu}^c_{R,3}}(t) = \left(\frac{3}{4}g^2_{BL}(t) + \frac{1}{2}g^2_R(t)\right) m^2_{\tilde{\nu}^c_{R,3}}(t)\,, \quad t_{BL} < t < t_{SUSY} \tag{B.2}$$

where we define $t = ln(\frac{M}{M_Z})$. Here, M_a, g_a are the associated gaugino masses and gauge couplings for $a = BL, 3R$, and the S_a-terms are defined as

$$S_{B-L} = \mathrm{Tr}\left(2m^2_{\tilde{Q}} - m^2_{\tilde{u}^c_R} - m^2_{\tilde{d}^c_R} - 2m^2_{\tilde{L}} + m^2_{\tilde{\nu}^c_R} + m^2_{\tilde{e}^c_R}\right) \tag{B.3}$$

$$S_R = m^2_{H_u} - m^2_{H_d} + \mathrm{Tr}\left(-\frac{3}{2}m^2_{\tilde{u}^c_R} + \frac{3}{2}m^2_{\tilde{d}^c_R} - \frac{1}{2}m^2_{\tilde{\nu}^c_R} + \frac{1}{2}m^2_{\tilde{e}^c_R}\right) \tag{B.4}$$

[1]Here, we amend the equation for the running in the region $t_{BL} < t < t_{SUSY}$ from the expression given in [161].

The RGEs for the M_a and S_a are given in [161], and can be solved to yield the following analytic expressions.

$$\begin{aligned} S_a(t) &= \frac{g_a^2(t)}{g_a^2(t_U)} S_a(t_U) && \text{(B.5)} \\ M_a(t) &= \frac{g_a^2(t)}{g_a^2(t_U)} M_a(t_U) && \text{(B.6)} \end{aligned}$$

The running of the gauge couplings g_a can be found by solving the RGEs

$$\begin{aligned} \frac{d}{dt}\alpha_a^{-1} &= -\frac{b_{a,S}}{2\pi}, \qquad a = BL, R, \qquad t_{SUSY} < t < t_U \\ \frac{d}{dt}\alpha_a^{-1} &= -\frac{b_a}{2\pi}, \qquad a = BL, R, \qquad t_{BL} < t < t_{SUSY} \\ \frac{d}{dt}\alpha_1^{-1} &= -\frac{b_1}{2\pi}, \qquad t_Z < t < t_{SUSY} && \text{(B.7)} \end{aligned}$$

with the boundary conditions

$$\alpha_{BL}(t_{BL}) = \frac{2}{5}\frac{\alpha_1(t_{BL})}{\cos^2\theta_R}, \quad \alpha_R(t_{BL}) = \frac{3}{5}\frac{\alpha_1(t_{BL})}{\sin^2\theta_R}, \quad \alpha_1(t_Z) = 0.0170 \tag{B.8}$$

The beta functions for the various regimes are $b_{BL,S} = 6, b_{R,S} = 7$ and $b_{BL} = \frac{33}{8}, b_R = \frac{53}{12}, b_1 = \frac{41}{10}$.

We can solve the RGEs given in equations (B.1) and (B.2) to arrive at the following expression for $m^2_{\tilde{\nu}^c_{R,3}}$ at a given scale. We find that

$$\begin{aligned} & m^2_{\tilde{\nu}^c_{R,3}}(t) \\ =\; & m^2_{\tilde{\nu}^c_{R,3}}(t_U) + \frac{3}{4} b^{-1}_{BL,S} M^2_{B-L}(t_U)\left(\frac{g^4_{BL}(t_U) - g^4_{BL}(t)}{g^4_{BL}(t_U)}\right) + \frac{1}{2} b^{-1}_{R,S} M^2_R(t_U)\left(\frac{g^4_R(t_U) - g^4_R(t)}{g^4_R(t_U)}\right) \\ & -\frac{3}{8} b^{-1}_{BL,S} S_{B-L}(t_U)\left(\frac{g^2_{BL}(t_U) - g^2_{BL}(t)}{g^2_{BL}(t_U)}\right) + \frac{1}{2} b^{-1}_{R,S} S_R(t_U)\left(\frac{g^2_R(t_U) - g^2_R(t)}{g^2_R(t_U)}\right) \end{aligned} \tag{B.9}$$

for $t_{SUSY} < t < t_U$, and

$$\begin{aligned} & m^2_{\tilde{\nu}^c_{R,3}}(t) \\ =\; & m^2_{\tilde{\nu}^c_{R,3}}(t_{SUSY}) \left[\frac{\alpha^{-1}_{BL}(t_U) - \frac{b^{SUSY}_{BL}}{2\pi}(t_{SUSY} - t_U) - \frac{b_{BL}}{2\pi}(t - t_{SUSY})}{\alpha^{-1}_{BL}(t_U) - \frac{b^{SUSY}_{BL}}{2\pi}(t_{SUSY} - t_U)}\right]^{\frac{1}{4\pi}\frac{3}{4}(-\frac{b_{BL}}{2\pi})^{-1}} \\ & \times \left[\frac{\alpha^{-1}_R(t_U) - \frac{b^{SUSY}_R}{2\pi}(t_{SUSY} - t_U) - \frac{b_R}{2\pi}(t - t_{SUSY})}{\alpha^{-1}_R(t_U) - \frac{b^{SUSY}_R}{2\pi}(t_{SUSY} - t_U)}\right]^{\frac{1}{4\pi}\frac{1}{2}(-\frac{b_R}{2\pi})^{-1}} \\ =\; & m^2_{\tilde{\nu}^c_{R,3}}(t_{SUSY}) \left(\frac{g^2_{BL}(t)}{g^2_{BL}(t_{SUSY})}\right)^{\frac{3}{8b_{BL}}} \left(\frac{g^2_R(t)}{g^2_R(t_{SUSY})}\right)^{\frac{1}{4b_R}} \end{aligned} \tag{B.10}$$

for $t_{BL} < t < t_{SUSY}$.

Given that we know $m^2_{\tilde{\nu}^c_{R,3}}(t)$ at $t = t_{BL}$, we would like to determine the corresponding value of $m^2_{\tilde{\nu}^c_{R,3}}(t)$ at $t = t_U$. Rearranging equations (B.9) and (B.10), we find that

$$\begin{aligned}
& m^2_{\tilde{\nu}^c_{R,3}}(t_U) \\
= \; & -\frac{3}{4} b^{-1}_{BL,S} M^2_{B-L}(t_U) \left(\frac{g^4_{BL}(t_U) - g^4_{BL}(t_{SUSY})}{g^4_{BL}(t_U)} \right) - \frac{1}{2} b^{-1}_{R,S} M^2_R(t_U) \left(\frac{g^4_R(t_U) - g^4_R(t_{SUSY})}{g^4_R(t_U)} \right) \\
& + \frac{3}{8} b^{-1}_{BL,S} S_{B-L}(t_U) \left(\frac{g^2_{BL}(t_U) - g^2_{BL}(t_{SUSY})}{g^2_{BL}(t_U)} \right) - \frac{1}{2} b^{-1}_{R,S} S_R(t_U) \left(\frac{g^2_R(t_U) - g^2_R(t_{SUSY})}{g^2_R(t_U)} \right) \\
& + m^2_{\tilde{\nu}^c_{R,3}}(t_{BL}) \left(\frac{g^2_{BL}(t_{SUSY})}{g^2_{BL}(t_{BL})} \right)^{\frac{3}{8 b_{BL}}} \left(\frac{g^2_R(t_{SUSY})}{g^2_R(t_{BL})} \right)^{\frac{1}{4 b_R}}
\end{aligned} \tag{B.11}$$

However, we must now use the fact that $S_{B-L}(t_U)$ and $S_R(t_U)$ contain $m^2_{\tilde{\nu}^c_{R,3}}(t_U)$. To accomplish this, we redefine the above expressions in terms of two new objects, $S_{B-L}(t_U)'$ and $S_R(t_U)'$, given by

$$\begin{aligned}
S_{B-L} &= \mathrm{Tr}\left(2m^2_{\tilde{Q}} - m^2_{\tilde{u}^c_R} - m^2_{\tilde{d}^c_R} - 2m^2_{\tilde{L}} + m^2_{\tilde{e}^c_R} \right) + m^2_{\tilde{\nu}^c_{R,1}} + m^2_{\tilde{\nu}^c_{R,2}} + m^2_{\tilde{\nu}^c_{R,3}} \\
&= S'_{B-L} + m^2_{\tilde{\nu}^c_3} \qquad \text{(B.12)} \\
S_R &= m^2_{H_u} - m^2_{H_d} + \mathrm{Tr}\left(-\frac{3}{2} m^2_{\tilde{u}^c_R} + \frac{3}{2} m^2_{\tilde{d}^c_R} + \frac{1}{2} m^2_{\tilde{e}^c_R} \right) - \frac{1}{2} m^2_{\tilde{\nu}^c_{R,1}} - \frac{1}{2} m^2_{\tilde{\nu}^c_{R,2}} - \frac{1}{2} m^2_{\tilde{\nu}^c_{R,3}} \\
&= S'_R - \frac{1}{2} m^2_{\tilde{\nu}^c_{R,3}} \qquad \text{(B.13)}
\end{aligned}$$

respectively. For simplicity, we have suppressed the fact that all terms in (B.12) and (B.13) are evaluated at $t = t_U$. Doing this, and re-arranging terms to extract $m^2_{\tilde{\nu}^c_{R,3}}(t_U)$, we arrive at the expression

$$\begin{aligned}
m^2_{\tilde{\nu}^c_{R,3}}(t_U) = & \left(1 - \frac{3}{8} b^{-1}_{BL,S} \left(\frac{g^2_{BL}(t_U) - g^2_{BL}(t_{SUSY})}{g^2_{BL}(t_U)} \right) - \frac{1}{4} b^{-1}_{R,S} \left(\frac{g^2_R(t_U) - g^2_R(t_{SUSY})}{g^2_R(t_U)} \right) \right)^{-1} \\
& \Bigg\{ -\frac{3}{4} b^{-1}_{BL,S} M^2_{B-L}(t_U) \left(\frac{g^4_{BL}(t_U) - g^4_{BL}(t_{SUSY})}{g^4_{BL}(t_U)} \right) - \frac{1}{2} b^{-1}_{R,S} M^2_R(t_U) \left(\frac{g^4_R(t_U) - g^4_R(t_{SUSY})}{g^4_R(t_U)} \right) \\
& + \frac{3}{8} b^{-1}_{BL,S} S'_{B-L}(t_U) \left(\frac{g^2_{BL}(t_U) - g^2_{BL}(t_{SUSY})}{g^2_{BL}(t_U)} \right) - \frac{1}{2} b^{-1}_{R,S} S'_R(t_U) \left(\frac{g^2_R(t_U) - g^2_R(t_{SUSY})}{g^2_R(t_U)} \right) \\
& + m^2_{\tilde{\nu}^c_{R,3}}(t_{BL}) \left(\frac{g^2_{BL}(t_{SUSY})}{g^2_{BL}(t_{BL})} \right)^{\frac{3}{8 b_{BL}}} \left(\frac{g^2_R(t_{SUSY})}{g^2_R(t_{BL})} \right)^{\frac{1}{4 b_R}} \Bigg\}
\end{aligned} \tag{B.14}$$

B.2 Cosmological Constraint

Recall from (4.18) and (4.32) that, in order to construct our inflaton and match the necessary cosmological data, it is required that

$$m^2_{H_u}(t_U) + m^2_{\tilde{L}_3}(t_U) + m^2_{\tilde{\nu}^c_{R,3}}(t_U) \quad = \quad 3(1.58 \times 10^{13}\text{GeV})^2\,. \tag{B.15}$$

We have previously satisfied this condition in our computational framework by not randomly generating $m^2_{H_u}(t_U)$ but, instead, randomly generating the other two masses and using (B.15) to calculate the required value of $m^2_{H_u}(t_U)$. In the context of our present discussion, we must take this expression into account when we enforce a specific B-L scale. Since this relation involves $m_{\tilde{\nu}^c_3}$, and m_{H_u} enters (B.14) via the S-terms, we can see that equations (B.14) and (B.15) are intertwined and must be solved simultaneously. To do this, we can re-express these equations in the form

$$\begin{aligned} m^2_{\tilde{\nu}^c_{R,3}}(t_U) &= A + Bm^2_{H_u}(t_U) \\ m^2_{\tilde{\nu}^c_{R,3}}(t_U) + m^2_{H_u}(t_U) &= C \ \ , \end{aligned} \tag{B.16}$$

where

$$\begin{aligned}
A \quad &= \quad \left(1 - \frac{3}{8b_{BL,S}}\left(1 - \frac{g^2_{BL}(t_{SUSY})}{g^2_{BL}(t_U)}\right) - \frac{1}{4b_{R,S}}\left(1 - \frac{g^2_{R}(t_{SUSY})}{g^2_{R}(t_U)}\right)\right)^{-1} \\
&\quad\ \left\{ - \frac{3}{4b_{BL,S}}M^2_{B-L}(t_U)\left(1 - \frac{g^4_{BL}(t_{SUSY})}{g^4_{BL}(t_U)}\right) - \frac{1}{2b_{R,S}}M^2_R(t_U)\left(1 - \frac{g^4_{R}(t_{SUSY})}{g^4_{R}(t_U)}\right)\right. \\
&\quad\ + \frac{3}{8b_{BL,S}}S'_{B-L}(t_U)\left(1 - \frac{g^2_{BL}(t_{SUSY})}{g^2_{BL}(t_U)}\right) - \frac{1}{2b_{R,S}}S''_R(t_U)\left(1 - \frac{g^2_{R}(t_{SUSY})}{g^2_{R}(t_U)}\right) \\
&\quad\ \left. + m_{\tilde{\nu}^c_{R,3}}(t_{BL})\left(\frac{g^2_{BL}(t_{SUSY})}{g^2_{BL}(t_{BL})}\right)^{\frac{3}{8b_{BL}}}\left(\frac{g^2_{R}(t_{SUSY})}{g^2_{R}(t_{BL})}\right)^{\frac{1}{4b_R}}\right\} \\
B \quad &= \quad \left(1 - \frac{3}{8b_{BL,S}}\left(1 - \frac{g^2_{BL}(t_{SUSY})}{g^2_{BL}(t_U)}\right) - \frac{1}{4b_{R,S}}\left(1 - \frac{g^2_{R}(t_{SUSY})}{g^2_{R}(t_U)}\right)\right)^{-1} \\
&\quad\ \left\{ - \frac{1}{2b_{R,S}}\left(1 - \frac{g^2_{R}(t_{SUSY})}{g^2_{R}(t_U)}\right)\right\} \\
C \quad &= \quad 3(1.58 \times 10^{13}\text{GeV})^2 - m^2_{\tilde{L}_3}(t_U)
\end{aligned} \tag{B.17}$$

with

$$S''_R \quad = \quad S'_R + m^2_{H_u}\ . \tag{B.18}$$

The equations in (B.16) are then soluble by inverting the matrix expression

$$\begin{pmatrix} 1 & -B \\ 1 & 1 \end{pmatrix} \begin{pmatrix} m^2_{\tilde{\nu}^c_{R,3}}(t_U) \\ m^2_{H_u}(t_U) \end{pmatrix} = \begin{pmatrix} A \\ C \end{pmatrix} \tag{B.19}$$

to give

$$\begin{pmatrix} m^2_{\tilde{\nu}^c_{R,3}}(t_U) \\ m^2_{H_u}(t_U) \end{pmatrix} = \frac{1}{1+B} \begin{pmatrix} 1 & B \\ -1 & 1 \end{pmatrix} \begin{pmatrix} A \\ C \end{pmatrix} = \frac{1}{1+B} \begin{pmatrix} A+BC \\ -A+C \end{pmatrix} \tag{B.20}$$

and inserting A, B and C in (B.17). In particular, for $m^2_{\tilde{\nu}^c_{R,3}}(t_U)$ we find

$$\begin{aligned}
&m^2_{\tilde{\nu}^c_{R,3}}(t_U) = \\
&\frac{1}{1+\left(1-\frac{3}{8b_{BL,S}}\left(1-\frac{g^2_{BL}(t_{SUSY})}{g^2_{BL}(t_U)}\right)-\frac{1}{4b_{R,S}}\left(1-\frac{g^2_R(t_{SUSY})}{g^2_R(t_U)}\right)\right)^{-1}\left\{-\frac{1}{2b_{R,S}}\left(1-\frac{g^2_R(t_{SUSY})}{g^2_R(t_U)}\right)\right\}} \\
&\left[\left(1-\frac{3}{8b_{BL,S}}\left(1-\frac{g^2_{BL}(t_{SUSY})}{g^2_{BL}(t_U)}\right)-\frac{1}{4b_{R,S}}\left(1-\frac{g^2_R(t_{SUSY})}{g^2_R(t_U)}\right)\right)^{-1}\right. \\
&\left\{-\frac{3}{4b_{BL,S}}M^2_{B-L}(t_U)\left(1-\frac{g^4_{BL}(t_{SUSY})}{g^4_{BL}(t_U)}\right)-\frac{1}{2b_{R,S}}M^2_R(t_U)\left(1-\frac{g^4_R(t_{SUSY})}{g^4_R(t_U)}\right)\right. \\
&+\frac{3}{8b_{BL,S}}S'_{B-L}(t_U)\left(1-\frac{g^2_{BL}(t_{SUSY})}{g^2_{BL}(t_U)}\right)-\frac{1}{2b_{R,S}}S''_R(t_U)\left(1-\frac{g^2_R(t_{SUSY})}{g^2_R(t_U)}\right) \\
&\left.+m_{\tilde{\nu}^c_{R,3}}(t_{BL})\left(\frac{g^2_{BL}(t_{SUSY})}{g^2_{BL}(t_{BL})}\right)^{\frac{3}{8b_{BL}}}\left(\frac{g^2_R(t_{SUSY})}{g^2_R(t_{BL})}\right)^{\frac{1}{4b_R}}\right\} \\
&+\left(1-\frac{3}{8b_{BL,S}}\left(1-\frac{g^2_{BL}(t_{SUSY})}{g^2_{BL}(t_U)}\right)-\frac{1}{4b_{R,S}}\left(1-\frac{g^2_R(t_{SUSY})}{g^2_R(t_U)}\right)\right)^{-1} \\
&\left.\times\left\{-\frac{1}{2b_{R,S}}\left(1-\frac{g^2_R(t_{SUSY})}{g^2_R(t_U)}\right)\right\}\times\left(3(1.58\times 10^{13}\text{GeV})^2-m^2_{\tilde{L}_3}(t_U)\right)\right].
\end{aligned} \tag{B.21}$$

The solutions to $m^2_{H_u}$ and $m^2_{\tilde{\nu}^c_{R,3}}$ given by equation (B.20) are implemented in our computational framework as follows:

1. The scalar soft mass parameters $\{m^2_{\tilde{Q}_1}, m^2_{\tilde{Q}_2}, m^2_{\tilde{Q}_3}, m^2_{\tilde{u}^c_{R,1}}, m^2_{\tilde{u}^c_{R,2}}, m^2_{\tilde{u}^c_{R,3}}, m^2_{\tilde{d}^c_{R,1}}, m^2_{\tilde{d}^c_{R,2}}, m^2_{\tilde{d}^c_{R,3}}, m^2_{\tilde{e}^c_{R,1}}, m^2_{\tilde{e}^c_{R,2}}, m^2_{\tilde{e}^c_{R,3}}\ m^2_{\tilde{L}_1}, m^2_{\tilde{L}_2}, m^2_{\tilde{L}_3}, m^2_{\tilde{\nu}^c_{R,1}}, m^2_{\tilde{\nu}^c_{R,2}}, m^2_{H_d}\}$ and the soft gaugino masses $\{M_3, M_2, M_{B-L}, M_R\}$ are thrown statistically at the unification mass scale M_U.

2. The SUSY breaking scale M_{SUSY} is initially approximated by the absolute value of M_3.

3. The desired value M_{BL} of the B-L scale is inputted by choosing $m^2_{\tilde{\nu}^c_{R,3}}(M_{BL})$ using (4.29).

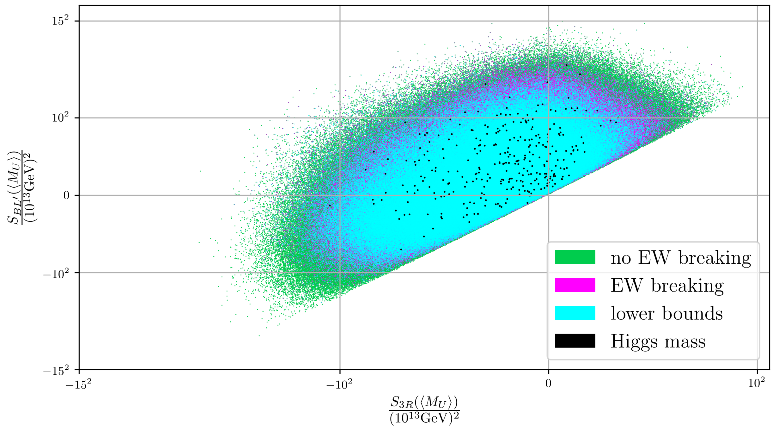

Figure B.1: Results from generating 50 million sets of initial data where the B-L scale is chosen from a log-uniform distribution between 10^6 GeV and 10^{14} GeV. We find that 6,123,522 points break B-L but not electroweak symmetry, and 1,997,972 points break B-L and electroweak symmetry. Of the latter 1,040,259 points are consistent with current LHC bounds on sparticle searches. Finally, we have 305 points which satisfy all these conditions and are within the 2σ window of the measured Higgs mass.

4. Using this value of the B-L scale, the initial guess for the M_{SUSY} and the previously generated soft-breaking masses, we determine the values of $m^2_{\tilde{\nu}^c_{R,3}}$ and $m^2_{H_u}$ at M_U using equation (B.20).

5. Having a complete set of initial soft mass data, the SUSY scale is iteratively solved for using the relation

$$\sqrt{m_{\tilde{t}_1}(M_{SUSY})m_{\tilde{t}_2}(M_{SUSY})} = M_{SUSY}\,. \tag{B.22}$$

   In each iteration, the value of M_{SUSY} changes. Hence, one must re-solve for $m^2_{\tilde{\nu}^c_{R,3}}$ and $m^2_{H_u}$ at M_U using equation (B.20) and the updated value of M_{SUSY}. This process continues until the iterative solution for (B.22) converges within an allowed range.

6. We finally check to see if $m^2_{\tilde{\nu}^c_{R,3}}(M_U) < m^2_{\tilde{\nu}^c_{R,1}}(M_U)$, $m^2_{\tilde{\nu}^c_{R,2}}(M_U)$, a condition which defines the third family right-handed sneutrino. If this is not satisfied, we discard this set of initial data and then return to the first step.

7. The complete set of soft masses, the final value of M_{SUSY} and the inputted value of the B-L breaking scale are then used to carry out the remaining physical checks on the scale of electroweak breaking, the Higgs mass and the sparticle mass bounds in the manner described in [161].

In the main text of this thesis, we will use this formalism to generate physically acceptable valid black points whose B-L scale is in the range 10^{10} GeV $\leq M_{BL} \leq 10^{12}$ GeV. This range comfortably accommodates our theory of reheating. Be that as it may, it is of interest to see whether the B-L scale can be substantially reduced to much lower values. With that in mind, in this Appendix we will implement the above procedure and generate 50 million initial throws of the soft masses with the inputted scale of $U(1)_{B-L}$ breaking randomly generated from a log-uniform distribution between 10^6 GeV and 10^{14} GeV. Carrying out our checks, we find that this ultimately leads to 305 sets of initial data which satisfy all phenomenological constraints 1), 2) and 3) presented earlier. These physically valid black points are shown in Figure B.1. The distribution of the B-L breaking scale for the black points in Figure B.1 is given in Figure B.2and verifies that our approach has indeed allowed us to extend the range of the B-L scale to lower values.

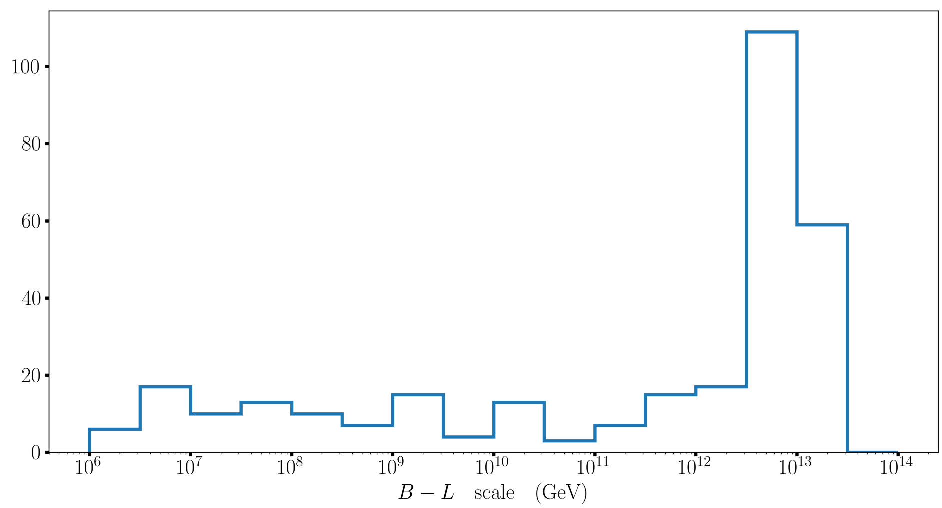

Figure B.2: Distribution of the B-L breaking scale for the 305 black points displayed in Figure B.1.

B.3 Fine-Tuning

As we have seen, in order to ensure that the scale of B-L breaking have a desired value, the mass of the third family right-handed sneutrino has to be adjusted against the other masses. To quantify the degree of fine-tuning necessary, we re-examine equation (B.14).

Re-arranging this equation as an expression for M_{BL}, we find

$$
\begin{aligned}
&\frac{1}{2}\frac{\left(\frac{g_{BL}^2(t_{SUSY})}{g_{BL}^2(t_{BL})}\right)^{\frac{3}{8b_{BL}}}\left(\frac{g_R^2(t_{SUSY})}{g_R^2(t_{BL})}\right)^{\frac{1}{4b_R}}}{\left(1-\frac{3}{8b_{BL,S}}\left(1-\frac{g_{BL}^2(t_{SUSY})}{g_{BL}^2(t_U)}\right)-\frac{1}{4b_{R,S}}\left(1-\frac{g_R^2(t_{SUSY})}{g_R^2(t_U)}\right)\right)}M_{BL}^2 \\
=\;& \left(1-\frac{3}{8b_{BL,S}}\left(1-\frac{g_{BL}^2(t_{SUSY})}{g_{BL}^2(t_U)}\right)-\frac{1}{4b_{R,S}}\left(1-\frac{g_R^2(t_{SUSY}}{g_R^2(t_U)}\right)\right)^{-1} \\
&\Big\{-\frac{3}{4b_{BL,S}}M_{B-L}^2(t_U)\left(1-\frac{g_{BL}^4(t_{SUSY})}{g_{BL}^4(t_U)}\right)-\frac{1}{2b_{R,S}}M_R^2(t_U)\left(1-\frac{g_R^4(t_{SUSY})}{g_R^4(t_U)}\right) \\
&+\frac{3}{8b_{BL,S}}S'_{B-L}(t_U)\left(1-\frac{g_{BL}^2(t_{SUSY})}{g_{BL}^2(t_U)}\right)-\frac{1}{2b_{R,S}}S'_R(t_U)\left(1-\frac{g_R^2(t_{SUSY})}{g_R^2(t_U)}\right)\Big\} \\
&-m_{\tilde{\nu}^c_{R,3}}^2(t_U)\,. \qquad \text{(B.23)}
\end{aligned}
$$

This can be schematically expressed as

$$
\frac{1}{2}fFM_{BL}^2 = FX - m_{\tilde{\nu}^c_{R,3}}^2(t_U)\,, \qquad \text{(B.24)}
$$

where

$$
\begin{aligned}
f &= \left(\frac{g_{BL}^2(t_{SUSY})}{g_{BL}^2(t_{BL})}\right)^{\frac{3}{8b_{BL}}}\left(\frac{g_R^2(t_{SUSY})}{g_R^2(t_{BL})}\right)^{\frac{1}{4b_R}} \\
F &= \left(1-\frac{3}{8b_{BL,S}}\left(1-\frac{g_{BL}^2(t_{SUSY})}{g_{BL}^2(t_U)}\right)-\frac{1}{4b_{R,S}}\left(1-\frac{g_R^2(t_{SUSY}}{g_R^2(t_U)}\right)\right)^{-1} \qquad \text{(B.25)} \\
X &= \Big\{-\frac{3}{4b_{BL,S}}M_{B-L}^2(t_U)\left(1-\frac{g_{BL}^4(t_{SUSY})}{g_{BL}^4(t_U)}\right)-\frac{1}{2b_{R,S}}M_R^2(t_U)\left(1-\frac{g_R^4(t_{SUSY})}{g_R^4(t_U)}\right) \\
&\quad+\frac{3}{8b_{BL,S}}S'_{B-L}(t_U)\left(1-\frac{g_{BL}^2(t_{SUSY})}{g_{BL}^2(t_U)}\right)-\frac{1}{2b_{R,S}}S'_R(t_U)\left(1-\frac{g_R^2(t_{SUSY})}{g_R^2(t_U)}\right)\Big\}
\end{aligned}
$$

Equation (B.24) shows us precisely where the delicate cancellation necessary to produce a low B-L breaking scale arises. To quantify the degree of fine-tuning, we can plot the ratio

$$
\frac{FX}{\frac{1}{2}FfM_{BL}^2} = \frac{X}{\frac{1}{2}fM_{BL}^2} \qquad \text{(B.26)}
$$

against the M_{BL} for those sets of initial data which survive all the phenomenological checks previously outlined. The quantity (B.26) is the Barbieri-Giudice (B-G) sensitivity [16] for the B-L breaking scale. The results of doing this for the 305 "black points" in Figure B.1 are shown in Figure B.3.

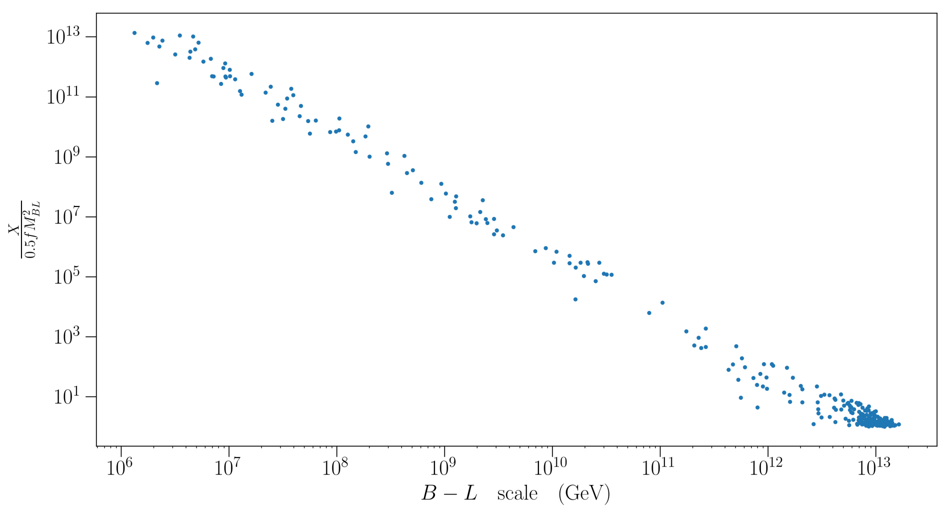

Figure B.3: Log-log plot of $\frac{X}{\frac{1}{2}fM_{BL}^2}$ against the B-L scale, for the valid black points shown in Figure B.1 from the scan of 50 million sets of initial conditions. The quantity $\frac{X}{\frac{1}{2}fM_{BL}^2}$ expresses the degree of fine-tuning required to achieve the associated value of the B-L scale.

Appendix C

Diagonalization of Mass Matrices

In the B-L MSSM we have three families of quark and lepton chiral superfields

$$
\begin{aligned}
& Q \sim (\mathbf{3}, \mathbf{2}, 0, 1/3)\,,\ u_R^c \sim (\bar{\mathbf{3}}, \mathbf{1}, -1/2, -1/3)\,,\ d_R^c \sim (\mathbf{3}, \mathbf{1}, 1/2, -1/3) \\
& L \sim (\mathbf{1}, \mathbf{2}, 0, -1)\,,\ e_R^c(\mathbf{1}, \mathbf{1}, 1/2, 1)\,,\ \nu_R^c(\mathbf{1}, \mathbf{1}, -1/2, 1)\,,
\end{aligned}
\tag{C.1}
$$

as well as a pair of Higgs-Higgs conjugate doublet superfields

$$
H_u \sim (\mathbf{1}, \mathbf{2}, 1/2, 0)\,,\ H_d \sim (\mathbf{1}, \mathbf{2}, -1/2, 0)\,,
\tag{C.2}
$$

where we have presented the transformation properties under the gauge group $SU(3)_C \times SU(2)_L \times U(1)_{3R} \times U(1)_{B-L}$. The superpotential for the B-L MSSM is given by

$$
W = y_u Q H_u u_R^c - y_d Q H_d d_R^c - y_e L H_d e_R^c + y_\nu L H_u \nu_R^c + \mu H_u H_d\,,
\tag{C.3}
$$

where we assume that the Yukawa parameters are family diagonal and real, and do not display the family index. This gives rise to the Lagrangian

$$
\begin{aligned}
\mathcal{L}_W &= -W\big|_{\theta^2} + \text{h.c} \\
&\supset -y_t \left(H_u^0 t_L t_R^c - H_u^+ b_L t_R^c\right) - y_\tau \left(\tilde{\tau}_L \psi_d^0 \tau_R^c - \tilde{\nu}_{3,L} \psi_d^- \tau_R^c\right) \\
&\quad -y_{\nu_3} \left(H_u^0 \nu_{L,3} \nu_{R,3}^c - H_u^+ \tau_L \nu_{R,3}^c + \tilde{\nu}_{L,3} \psi_u^0 \nu_{R,3}^c + \tilde{\nu}_{R,3}^c \psi_u^0 \nu_{L,3} - \tilde{\nu}_{R,3}^c \psi_u^+ \tau_L\right) \\
&\quad -\mu \left(\psi_u^+ \psi_d^- - \psi_u^0 \psi_d^0\right) + \text{h.c.}\,,
\end{aligned}
\tag{C.4}
$$

as well as the purely scalar F-term potential $V_F = \sum_i \left|\frac{\partial W}{\partial \phi_i}\right|^2$.

We also have the soft-mass terms for the $SU(2)$, $U(1)_{3R}$ and $U(1)_{B-L}$ gauginos given by

$$\begin{aligned}\mathcal{L}_{soft} &= -\frac{1}{2}M_2\left(\tilde{W}^1\tilde{W}^1+\tilde{W}^2\tilde{W}^2+\tilde{W}^3\tilde{W}^3\right)-\frac{1}{2}M_{3R}\tilde{W}_R\tilde{W}_R-\frac{1}{2}M_{B-L}\tilde{B}\tilde{B}+\text{h.c.}\\ &= -M_2\tilde{W}^+\tilde{W}^- -\frac{1}{2}M_2\tilde{W}^3\tilde{W}^3-\frac{1}{2}M_{3R}\tilde{W}_R\tilde{W}_R-\frac{1}{2}M_{B-L}\tilde{B}\tilde{B}+\text{h.c.}\,, \qquad \text{(C.5)}\end{aligned}$$

where

$$\tilde{W}^{\pm} = \frac{1}{\sqrt{2}}(\tilde{W}^1 \mp \tilde{W}^2)\,. \qquad \text{(C.6)}$$

Additionally, the following terms arise from the gauge super-covariant derivative:

$$\begin{aligned}\mathcal{L}_{kinetic} &= -\frac{1}{\sqrt{2}}g_2\left(\sqrt{2}H_u^{0*}\tilde{W}^-\psi_u^+ - H_u^{0*}\tilde{W}^3\psi_u^0+\tilde{\nu}_{L,3}^*\tilde{W}^3\nu_{L,3}+\sqrt{2}\tilde{\nu}_{L,3}^*\tilde{W}^+\tau_L\right)\\ &\quad -\sqrt{2}g_R\left(q_{R_u}H_u^{0*}\tilde{W}_R\psi_u^0+q_{R_\nu}\tilde{\nu}_{R,3}^{c*}\tilde{W}_R\nu_{R,3}^c\right)\\ &\quad -\sqrt{2}g_{BL}\left(q_{BL_L}\tilde{\nu}_{L,3}^*\tilde{B}\nu_{L,3}+q_{BL_\nu}\tilde{\nu}_{R,3}^{c*}\tilde{B}\nu_{R,3}^c\right)+\text{h.c.} \qquad \text{(C.7)}\end{aligned}$$

The inflaton, $\phi = (H_u^0+\tilde{\nu}_{L,3}+\tilde{\nu}_{R,3}^c)/\sqrt{3}$, attains a time-dependent expectation value during both the inflationary and post-inflationary periods. In doing so, it gives rise to fermion mixing terms in the Lagrangian. We now determine the mass eigenstates and eigenvalues due to this mixing.

C.1 Chargino Mixing

Dropping terms which have any neutrino Yukawa coupling y_ν, the effective mass Lagrangian for the "charginos" is given by

$$\begin{aligned}\mathcal{L}_{mass,C} &= -g_2\langle H_u^{0*}\rangle\tilde{W}^-\psi_u^+ - g_2\langle\tilde{\nu}_{L,3}^*\rangle\tilde{W}^+\tau_L+y_\tau\langle\tilde{\nu}_{L,3}\rangle\tau_R^c\psi_d^-\\ &\quad -\mu\psi_u^+\psi_d^- - M_2\tilde{W}^+\tilde{W}^-+\text{h.c.} \qquad \text{(C.8)}\end{aligned}$$

Of course, the expectation values need to be expressed in terms of the RMS value of the inflaton field using

$$\langle H_u^0\rangle = \langle\tilde{\nu}_{L,3}\rangle = \langle\tilde{\nu}_{R,3}^c\rangle = \frac{1}{\sqrt{6}}\sqrt{\langle\psi^2\rangle}\,. \qquad \text{(C.9)}$$

However, for clarity, we will continue to express the expectation values in terms of the original fields until it becomes necessary to evaluate them. We can re-express (C.8) as

$$\mathcal{L}_{mass,C} = -\frac{1}{2}\vec{\Psi}^T M_C\vec{\Psi}+\text{h.c.}\,, \qquad \text{(C.10)}$$

where

$$\vec{\Psi}^T = \left(\tilde{W}^+, \tilde{\psi}_u^+, \tau_R^c, \tilde{W}^-, \psi_d^-, \tau_L\right) \tag{C.11}$$

and

$$M_C = \begin{pmatrix} 0 & X^T \\ X & 0 \end{pmatrix}, \quad X = \begin{pmatrix} M_2 & g_2 \langle H_u^{0*} \rangle & 0 \\ 0 & \mu & -y_\tau \langle \tilde{\nu}_{L,3} \rangle \\ g_2 \langle \tilde{\nu}_{L,3}^* \rangle & 0 & 0 \end{pmatrix} \tag{C.12}$$

The mass eigenstates of this system can be found by diagonalizing the 3-by-3 matrix X, using the two 3-by-3 unitary matrices U and V defined by

$$U^* X V^{-1} = \begin{pmatrix} m_{\tilde{C}_1} & & \\ & m_{\tilde{C}_2} & \\ & & m_{\tilde{C}_3} \end{pmatrix}, \tag{C.13}$$

$$\begin{pmatrix} \tilde{C}_1^+ \\ \tilde{C}_2^+ \\ \tilde{C}_3^+ \end{pmatrix} = V \begin{pmatrix} \tilde{W}^+ \\ \psi_u^+ \\ \tau_R^c \end{pmatrix}, \quad \begin{pmatrix} \tilde{C}_1^- \\ \tilde{C}_2^- \\ \tilde{C}_3^- \end{pmatrix} = U \begin{pmatrix} \tilde{W}^- \\ \psi_d^- \\ \tau_L \end{pmatrix}. \tag{C.14}$$

It is easier to find the matrices U and V from the expressions

$$U^* X X^\dagger U^T = V X^\dagger X V^{-1} = \begin{pmatrix} m_{\tilde{C}_1}^2 & & \\ & m_{\tilde{C}_2}^2 & \\ & & m_{\tilde{C}_3}^2 \end{pmatrix}. \tag{C.15}$$

As it stands, the expressions one gets for the mass eigenvalues and mixing matrices U, V involve solving for the roots of a cubic equation and give very cumbersome expressions. We can simplify the situation by working in the limit in which the μ-term is negligible and can be dropped – a reasonable approximation during the period of reheating, where $\sqrt{\langle \psi^2 \rangle}$ is initally around 10^{14} GeV and the gaugino mass M_2 is always of $\mathcal{O}(10^{13}\text{GeV})$. As $\sqrt{\langle \psi^2 \rangle}$ decreases, the μ-term does become comparable to (and indeed larger than) terms such as $g_2\sqrt{\langle \psi^2 \rangle}$ that we have kept. However, this will occur after the bulk of reheating has occurred, and thus will have an insignificant effect, so we will simply drop μ in our subsequent calculations.

The Small μ Limit

When terms involving μ are dropped, the system to be diagonalized (presented in (C.12)) simplifies tremendously. We are able to decouple the τ_R^c, ψ_d^- states as there is no longer any mixing between ψ_d^- and ψ_u^+. Indeed, examining the effective mass Lagrangian in equation (C.8), we see that

$$\mathcal{L}_{mass} \quad \supset \quad y_\tau \langle \tilde{\nu}_{L,3} \rangle \, \tau_R^c \psi_d^- + \text{h.c.} \,, \tag{C.16}$$

which looks like a Dirac mass for the fermion

$$\Psi_{Dirac} = \begin{pmatrix} \psi_d^- \\ \tau_R \end{pmatrix} \,, \tag{C.17}$$

with mass $y_\tau \langle \tilde{\nu}_{L,3} \rangle$. We can then simplify the system given in equations (C.11), (C.12) to

$$\vec{\Psi}^T = \left(\tilde{W}^+, \tilde{\psi}_u^+, \tilde{W}^-, \tau_L \right) \,, \tag{C.18}$$

$$M_C = \begin{pmatrix} 0 & X^T \\ X & 0 \end{pmatrix} \,, \quad X = \begin{pmatrix} M_2 & g_2 \langle H_u^{0*} \rangle \\ g_2 \langle \tilde{\nu}_{L,3}^* \rangle & 0 \end{pmatrix} \,. \tag{C.19}$$

Expressing the matrix X schematically as

$$X = \begin{pmatrix} x_1 & x_2 \\ x_2 & 0 \end{pmatrix} \tag{C.20}$$

where $x_1 = M_2$, $x_2 = g_2 \sqrt{\langle \psi \rangle} / \sqrt{6}$, it follows that

$$X X^\dagger = X^\dagger X = \begin{pmatrix} (x_1)^2 + (x_2)^2 & x_1 x_2 \\ x_1 x_2 & (x_1)^2 + (x_2)^2 \end{pmatrix} \,. \tag{C.21}$$

The eigenvalues of (C.21) are then given by

$$m^2_{\tilde{C}_1} = \frac{1}{2} \left((x_1)^2 + 2(x_2)^2 - \sqrt{(x_1)^4 + 4(x_1)^2 (x_2)^2} \right) \,, \tag{C.22}$$

$$m^2_{\tilde{C}_2} = \frac{1}{2} \left((x_1)^2 + 2(x_2)^2 + \sqrt{(x_1)^4 + 4(x_1)^2 (x_2)^2} \right) \,. \tag{C.23}$$

The matrices U and V become

$$U = V = \frac{1}{\sqrt{4(x_2)^2 + (x_1 - \sqrt{(x_1)^2 + 4x_2^2})^2}} \begin{pmatrix} x_1 - \sqrt{(x_1)^2 + 4x_2^2} & 2x_2 \\ x_1 + \sqrt{(x_1)^2 + 4x_2^2} & 2x_2 \end{pmatrix} . \tag{C.24}$$

It follows that the associated mass eigenstates are

$$\begin{pmatrix} \tilde{C}_1^+ \\ \tilde{C}_2^+ \end{pmatrix} = V \begin{pmatrix} \tilde{W}^+ \\ \tilde{\psi}_u^+ \end{pmatrix} , \qquad \begin{pmatrix} \tilde{C}_1^- \\ \tilde{C}_2^- \end{pmatrix} = U \begin{pmatrix} \tilde{W}^- \\ \tau_L \end{pmatrix} \tag{C.25}$$

with masses $m_{\tilde{C}_1}$, $m_{\tilde{C}_2}$.

Decays of the inflaton into the charginos arise from the vertices

$$\mathcal{L}_{decay,C} = -\frac{g_2}{\sqrt{6}} \psi \tilde{W}^- \psi_u^+ - \frac{g_2}{\sqrt{6}} \psi \tilde{W}^+ \tau_L + \text{h.c.} \tag{C.26}$$

Assuming that the states with mass $m_{\tilde{C}_2}$ are too heavy to be produced, we will be interested in the decays to $\tilde{C}_1^+$, $\tilde{C}_1^-$ only. Rotating the vertices above, we find that

$$\mathcal{L}_{decay,C} = -\frac{g_2}{\sqrt{6}} \psi \left(U_{1W}^* V_{1u}^* + U_{1\tau}^* V_{1W}^* \right) \tilde{C}_1^+ \tilde{C}_1^- \tag{C.27}$$

where

$$\begin{aligned} U_{1W} = V_{1W} &= \frac{x_1 - \sqrt{(x_1)^2 + 4x_2^2}}{\sqrt{4(x_2)^2 + (x_1 - \sqrt{(x_1)^2 + 4x_2^2})^2}} , \\ U_{1\tau} = V_{1u} &= \frac{2x_2}{\sqrt{4(x_2)^2 + (x_1 - \sqrt{(x_1)^2 + 4x_2^2})^2}} . \end{aligned} \tag{C.28}$$

For later use, we note that in the limit that $x_2 \ll x_1$, the above matrix elements have the form

$$\begin{aligned} U_{1W} = V_{1W} &= -\frac{x_2}{x_1} + \frac{3}{2}\left(\frac{x_2}{x_1}\right)^3 + \mathcal{O}\left(\frac{x_2}{x_1}\right)^5 , \\ U_{1\tau} = V_{1u} &= 1 - \frac{1}{2}\left(\frac{x_2}{x_1}\right)^2 + \frac{11}{8}\left(\frac{x_2}{x_1}\right)^4 + \mathcal{O}\left(\frac{x_2}{x_1}\right)^6 . \end{aligned} \tag{C.29}$$

The decay rate for the process $\psi \to \tilde{C}_1^+ \tilde{C}_1^-$ can be determined to be

$$\Gamma = \left(\frac{(|\alpha|^2 + |\beta|^2)(m_\psi^2 - 2m_{\tilde{C}_1}^2) - (\alpha\beta^* + \beta\alpha^*)(2m_{\tilde{C}_1}^2)}{16\pi m_\psi^3} \right) (m_\psi^2 - 4m_{\tilde{C}_1}^2)^{1/2} \tag{C.30}$$

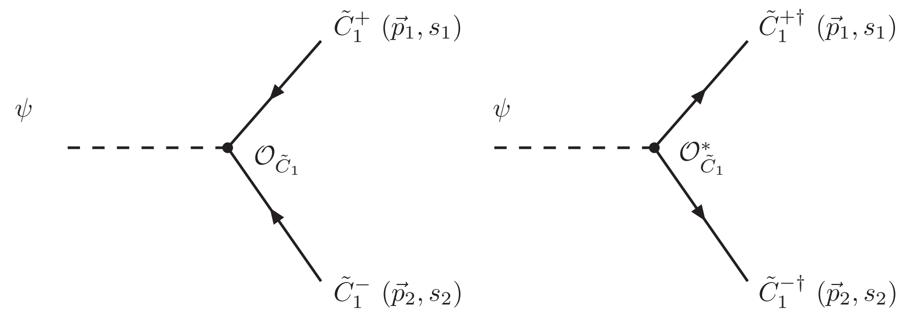

Figure C.1: Diagrams which contribute to the decay $\psi \to \tilde{C}_1^+ \tilde{C}_2^-$. Here, the coupling $\mathcal{O}_{\tilde{C}_1} = -\frac{g_2}{\sqrt{6}}(U_{1W}^* V_{1u}^* + U_{1\tau}^* V_{1W}^*)$.

where

$$|\alpha|^2 = |\beta|^2 = \frac{g_2^2}{6}|U_{1W}V_{1u} + U_{1\tau}V_{1W}|^2\,. \tag{C.31}$$

Since α, β are real, we can simplify this further to get

$$\Gamma = \gamma^2 \frac{(m_\psi^2 - 4m_{\tilde{C}_1}^2)^{3/2}}{8\pi m_\psi^2}\,, \tag{C.32}$$

where

$$\gamma = \frac{g_2}{\sqrt{6}}(U_{1W}V_{1u} + U_{1\tau}V_{1W})\,, \tag{C.33}$$

$$m_{\tilde{C}_1}^2 = \frac{1}{2}\left((x_1)^2 + 2(x_2)^2 - \sqrt{(x_1)^4 + 4(x_1)^2(x_2)^2}\right)\,. \tag{C.34}$$

C.2 Neutralino Mixing

Again, ignoring terms which come with a factor of a neutrino Yukawa coupling y_ν, the effective mass Lagrangian for the "neutralinos" is given by

$$\begin{aligned}\mathcal{L}_{mass,N} \quad = \quad & \mu\psi_u^0\psi_d^0 - \frac{1}{2}M_2\tilde{W}^0\tilde{W}^0 - \frac{1}{2}\tilde{W}_R\tilde{W}_R - \frac{1}{2}M_{B-L}\tilde{B}\tilde{B} \\ & +\frac{1}{\sqrt{2}}g_2\left\langle H_u^{0*}\right\rangle\tilde{W}^0\psi_u^0 - \frac{1}{\sqrt{2}}g_2\left\langle\tilde{\nu}_{L,3}^*\right\rangle\tilde{W}^0\nu_{L,3} \\ & -\sqrt{2}g_R q_{R_u}\left\langle H_u^{0*}\right\rangle\tilde{W}_R\psi_u^0 - \sqrt{2}g_R q_{R_\nu}\left\langle\tilde{\nu}_{R,3}^{c*}\right\rangle\tilde{W}_R\nu_{R,3}^c \\ & -\sqrt{2}g_{BL}q_{BL_L}\left\langle\tilde{\nu}_{L,3}^*\right\rangle\tilde{B}\nu_{L,3} - \sqrt{2}g_{BL}q_{BL_\nu}\left\langle\tilde{\nu}_{R,3}^{c^*}\right\rangle\tilde{B}\nu_{R,3}^c \\ & +\text{h.c.}\end{aligned} \tag{C.35}$$

Here, q_{G_x} denotes the $U(1)_G$ charge of the field $x = H_u, \nu_R^c, L$, where $G = R, B-L$. We can express this as

$$\mathcal{L}_{mass,N} \quad = \quad -\frac{1}{2}\vec{\psi}^{\,T}M_N\vec{\psi} + \text{h.c.}\,, \tag{C.36}$$

where

$$\vec{\psi}^{\,T} = \left(\tilde{B}, \tilde{W}_R, \tilde{W}^0, \psi_d^0, \psi_u^0, \nu_{L,3}, \nu_{R,3}^c\right) \tag{C.37}$$

and

$$M_N = \\ \begin{pmatrix} M_{B-L} & 0 & 0 & 0 & 0 & -\sqrt{2}g_{BL}\left\langle\tilde{\nu}_{L,3}^*\right\rangle & \sqrt{2}g_{BL}\left\langle\tilde{\nu}_{R,3}^{c*}\right\rangle \\ 0 & M_R & 0 & 0 & \frac{g_R}{\sqrt{2}}\left\langle H_u^{0*}\right\rangle & 0 & -\frac{g_R}{\sqrt{2}}\left\langle\tilde{\nu}_{R,3}^{c*}\right\rangle \\ 0 & 0 & M_2 & 0 & -\frac{g_2}{\sqrt{2}}\left\langle H_u^{0*}\right\rangle & \frac{g_2}{\sqrt{2}}\left\langle\tilde{\nu}_{L,3}^*\right\rangle & 0 \\ 0 & 0 & 0 & 0 & -\mu & 0 & 0 \\ 0 & \frac{g_R}{\sqrt{2}}\left\langle H_u^{0*}\right\rangle & -\frac{g_2}{\sqrt{2}}\left\langle H_u^{0*}\right\rangle & -\mu & 0 & 0 & 0 \\ -\sqrt{2}g_{BL}\left\langle\tilde{\nu}_{L,3}^*\right\rangle & 0 & \frac{g_2}{\sqrt{2}}\left\langle\tilde{\nu}_{L,3}^*\right\rangle & 0 & 0 & 0 & 0 \\ \sqrt{2}g_{BL}\left\langle\tilde{\nu}_{R,3}^{c*}\right\rangle & -\frac{g_R}{\sqrt{2}}\left\langle\tilde{\nu}_{R,3}^{c*}\right\rangle & 0 & 0 & 0 & 0 & 0 \end{pmatrix}. \tag{C.38}$$

For simplicity, let us schematically re-express this to give

$$M_N = \begin{pmatrix} x_1 & 0 & 0 & 0 & 0 & x_2 & x_3 \\ 0 & x_4 & 0 & 0 & x_5 & 0 & x_6 \\ 0 & 0 & x_7 & 0 & x_8 & x_9 & 0 \\ 0 & 0 & 0 & 0 & x_{10} & 0 & 0 \\ 0 & x_5 & x_8 & x_{10} & 0 & 0 & 0 \\ x_2 & 0 & x_9 & 0 & 0 & 0 & 0 \\ x_3 & x_6 & 0 & 0 & 0 & 0 & 0 \end{pmatrix} \tag{C.39}$$

The Small μ Limit

In this limit, the ψ_d^0 state decouples from the mixing. Hence, we only have a six-dimensional system to analyze. This is given by

$$\vec{\psi}^{\,T} = \left(\tilde{B}, \tilde{W}_R, \tilde{W}^0, \psi_u^0, \nu_{L,3}, \nu_{R,3}^c\right) \ , \tag{C.40}$$

$$M_N = \begin{pmatrix} x_1 & 0 & 0 & 0 & x_2 & x_3 \\ 0 & x_4 & 0 & x_5 & 0 & x_6 \\ 0 & 0 & x_7 & x_8 & x_9 & 0 \\ 0 & x_5 & x_8 & 0 & 0 & 0 \\ x_2 & 0 & x_9 & 0 & 0 & 0 \\ x_3 & x_6 & 0 & 0 & 0 & 0 \end{pmatrix} . \tag{C.41}$$

Let us make some further simplifying assumptions in order to find the eigenvalues and eigenvectors of this system.

- Take $x_1 = x_4 = x_7 = M \sim 1.58 \times 10^{13}$ GeV.
- Take $-x_2 = x_3 = x_5 = -x_6 = -x_8 = x_9 = u \sim g\sqrt{\langle \psi^2 \rangle}$, where $g \sim 0.57$

The mass matrix N then takes the form

$$M_N = \begin{pmatrix} M & 0 & 0 & 0 & -u & u \\ 0 & M & 0 & u & 0 & -u \\ 0 & 0 & M & -u & u & 0 \\ 0 & u & -u & 0 & 0 & 0 \\ -u & 0 & u & 0 & 0 & 0 \\ u & -u & 0 & 0 & 0 & 0 \end{pmatrix} . \tag{C.42}$$

The eigenvalues and eigenvectors of this system can now be evaluated and are given in table 4.2. We find that the lightest eigenstates, that is, those into which the inflaton can decay, are given in terms of the states in (C.40) by

$$\tilde{N}_1 = \frac{1}{\sqrt{3}}\,(0,0,0,1,1,1)^T \ ,$$
$$\tilde{N}_{2a} = \left(-u, 2u, -u, -\frac{1}{2}(M+\sqrt{M^2+12u^2}), 0, \frac{1}{2}(M+\sqrt{M^2+12u^2})\right)^T \Bigg/ \sqrt{M^2+12u^2+M\sqrt{M^2+12u^2}} \ ,$$
$$\tilde{N}_{2b} = \left(\sqrt{3}u, 0, -\sqrt{3}u, -\sqrt{u^2+\frac{1}{6}(M^2+M\sqrt{M^2+12u^2})}, 2\sqrt{u^2+\frac{1}{6}(M^2+M\sqrt{M^2+12u^2})}, -\sqrt{u^2+\frac{1}{6}(M^2+M\sqrt{M^2+12u^2})}\right)^T \Bigg/ \sqrt{M^2+12u^2+M\sqrt{M^2+12u^2}} \ . \tag{C.43}$$

For completeness, the heavier eigenstates are

$$\tilde{N}_3 = \frac{1}{\sqrt{3}}\,(1,1,1,0,0,0)^T \ ,$$
$$\tilde{N}_{4a} = \left(\sqrt{u^2+\frac{1}{6}(M^2+M\sqrt{M^2+12u^2})}, -2\sqrt{u^2+\frac{1}{6}(M^2+M\sqrt{M^2+12u^2})}, \sqrt{u^2+\frac{1}{6}(M^2+M\sqrt{M^2+12u^2})}\ , -\sqrt{3}u, 0, \sqrt{3}u\right)^T \Bigg/ \sqrt{M^2+12u^2+M\sqrt{M^2+12u^2}} \ ,$$
$$\tilde{N}_{4b} = \left(-\sqrt{3}\sqrt{u^2+\frac{1}{6}(M^2+M\sqrt{M^2+12u^2})}, 0, \sqrt{3}\sqrt{u^2+\frac{1}{6}(M^2+M\sqrt{M^2+12u^2})}, -u, 2u, -u\right)^T \Bigg/ \sqrt{M^2+12u^2+M\sqrt{M^2+12u^2}} . \tag{C.44}$$

The mass matrix can be diagonalized using the matrix N, where

$$N \ = \ \left(\tilde{N}_1, \tilde{N}_{2a}, \tilde{N}_{2b}, \tilde{N}_3, \tilde{N}_{4a}, \tilde{N}_{4b},\right)^T \tag{C.45}$$

such that

$$N^* M_N N^{-1} \ = \ \mathrm{diag}\left(0, \frac{1}{2}(M-\sqrt{M^2+12u^2}), \frac{1}{2}(M-\sqrt{M^2+12u^2}), M, \frac{1}{2}(M+\sqrt{M^2+12u^2}), \frac{1}{2}(M+\sqrt{M^2+12u^2})\right) \tag{C.46}$$

Without the VEVs, the last six terms in (C.35) are

$$\begin{aligned}\mathcal{L}_{decay,N} &= \frac{1}{\sqrt{2}}g_2 H_u^{0*}\tilde{W}^0\psi_u^0 - \frac{1}{\sqrt{2}}g_2\tilde{\nu}_{L,3}^*\tilde{W}^0\nu_{L,3} - \sqrt{2}g_R q_{R_u} H_u^{0*}\tilde{W}_R\psi_u^0 \\ &\quad -\sqrt{2}g_R q_{R_\nu}\tilde{\nu}_{R,3}^{c*}\tilde{W}_R\nu_{R,3}^c - \sqrt{2}g_{BL}q_{BL_L}\tilde{\nu}_{L,3}^*\tilde{B}\nu_{L,3} - \sqrt{2}g_{BL}q_{BL_\nu}\tilde{\nu}_{R,3}^{c^*}\tilde{B}\nu_{R,3}^c \\ &\quad +\text{h.c.} \\ &= \frac{1}{\sqrt{6}}\psi\Big(\frac{1}{\sqrt{2}}g_2\tilde{W}^0\psi_u^0 - \frac{1}{\sqrt{2}}g_2\tilde{W}^0\nu_{L,3} - \sqrt{2}g_R q_{R_u}\tilde{W}_R\psi_u^0 - \sqrt{2}g_R q_{R_\nu}\tilde{W}_R\nu_{R,3}^c \\ &\qquad -\sqrt{2}g_{BL}q_{BL_L}\tilde{B}\nu_{L,3} - \sqrt{2}g_{BL}q_{BL_\nu}\tilde{B}\nu_{R,3}^c\Big) + \text{h.c.} \qquad (C.47)\end{aligned}$$

Rotating the Lagrangian to the lightest mass eigenstates $\tilde{N}_1$, $\tilde{N}_{2a}$ and $\tilde{N}_{2b}$, we find that the term $\psi\tilde{N}_1\tilde{N}_1$ is absent, and hence the decay $\psi \to \tilde{N}_1\tilde{N}_1$ is not allowed. Furthermore, we find that

$$\begin{aligned}\mathcal{L}_{decay,N} &\supset \frac{1}{\sqrt{6}}\Big(\frac{g_2}{\sqrt{2}}(N^*_{(2a)0}N^*_{1u} - N^*_{(2a)0}N^*_{1L}) - \frac{g_R}{\sqrt{2}}(N^*_{(2a)R}N^*_{1u} - N^*_{(2a)R}N^*_{1\nu}) \\ &\qquad -\sqrt{2}g_2(N^*_{(2a)B}N^*_{1\nu} - N^*_{(2a)B}N^*_{1L})\Big)\psi\tilde{N}_1\tilde{N}_{2a} \\ &\quad +\frac{1}{\sqrt{6}}\Big(\frac{g_2}{\sqrt{2}}(N^*_{(2b)0}N^*_{1u} - N^*_{(2b)0}N^*_{1L}) - \frac{g_R}{\sqrt{2}}(N^*_{(2b)R}N^*_{1u} - N^*_{(2b)R}N^*_{1\nu}) \\ &\qquad -\sqrt{2}g_2(N^*_{(2b)B}N^*_{1\nu} - N^*_{(2b)B}N^*_{1L})\Big)\psi\tilde{N}_1\tilde{N}_{2b} \\ &\quad +\text{h.c.} \\ &= 0\,, \qquad (C.48)\end{aligned}$$

since $N_{iu} = N_{iL} = N_{i\nu} = \frac{1}{\sqrt{3}}$. It follows that there is no decay of ψ to $\tilde{N}_1\tilde{N}_{2a}$ or to $\tilde{N}_1\tilde{N}_{2b}$. Searching the Lagrangian for the remaining kinematically allowed decay terms, we find

$$\begin{aligned}\mathcal{L}_{decay,N} &\supset \frac{1}{\sqrt{6}}\Big(\frac{g_2}{\sqrt{2}}N^*_{(2a)0}\left(N^*_{(2a)u} - N^*_{(2a)L}\right) - \frac{g_R}{\sqrt{2}}N^*_{(2a)R}\left(N^*_{(2a)u} - N^*_{(2a)\nu}\right) \\ &\quad -\sqrt{2}g_{BL}N^*_{(2a)B}\left(N^*_{(2a)\nu} - N^*_{(2a)L}\right)\Big)\psi\tilde{N}_{2a}\tilde{N}_{2a} + \frac{1}{\sqrt{6}}\Big((2a)\to(2b)\Big)\psi\tilde{N}_{2b}\tilde{N}_{2b} \\ &\quad +\frac{1}{\sqrt{6}}\Big(\frac{g_2}{\sqrt{2}}N^*_{(2a)0}\left(N^*_{(2b)u} - N^*_{(2b)L}\right) - \frac{g_R}{\sqrt{2}}N^*_{(2a)R}\left(N^*_{(2b)u} - N^*_{(2b)\nu}\right) \\ &\quad -\sqrt{2}g_{BL}N^*_{(2a)B}\left(N^*_{(2b)\nu} - N^*_{(2b)L}\right)\Big)\psi\tilde{N}_{2a}\tilde{N}_{2b} + \frac{1}{\sqrt{6}}\Big((2a)\leftrightarrow(2b)\Big)\psi\tilde{N}_{2a}\tilde{N}_{2b} \\ &= \mathcal{O}_a\psi\tilde{N}_{2a}\tilde{N}_{2a} + \mathcal{O}_b\psi\tilde{N}_{2b}\tilde{N}_{2b} + \mathcal{O}_c\psi\tilde{N}_{2a}\tilde{N}_{2b}\,. \qquad (C.49)\end{aligned}$$

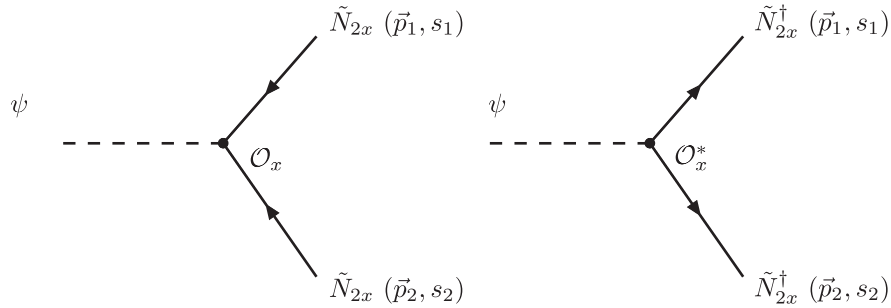

Figure C.2: Feynman diagrams which contribute to the processes $\psi \to \tilde{N}_{2a}\tilde{N}_{2a}$ and $\psi \to \tilde{N}_{2b}\tilde{N}_{2b}$.

This allows the inflaton decays $\psi \to \tilde{N}_{2a}\tilde{N}_{2a}$, $\psi \to \tilde{N}_{2b}\tilde{N}_{2b}$ and $\psi \to \tilde{N}_{2a}\tilde{N}_{2b}$. The first two decay rates take the same form

$$\begin{aligned}&\Gamma_d(\psi \to \tilde{N}_{2x}\tilde{N}_{2x})\\ =\ & \frac{1}{32\pi m_\psi^2}\Big((|\alpha|^2 + |\beta|^2)(m_\psi^2 - 2m_{\tilde{N}_2}^2) - 2(\alpha\beta^* + \beta\alpha^*)m_{\tilde{N}_2}^2\Big)(m_\psi^2 - 4m_{\tilde{N}_2}^2)^{1/2}\end{aligned} \tag{C.50}$$

where $\alpha = \beta = i\mathcal{O}_a$ and $i\mathcal{O}_b$ for $x = a, b$ respectively. The decay rate to $\tilde{N}_{2a}\tilde{N}_{2b}$ takes the form

$$\begin{aligned}&\Gamma_d(\psi \to \tilde{N}_{2a}\tilde{N}_{2b})\\ =\ & \frac{1}{16\pi m_\psi^2}\Big[(|\alpha|^2 + |\beta|^2)(m_\psi^2 - 2m_{\tilde{N}_2}^2) - 2(\alpha\beta^* + \beta\alpha^*)m_{\tilde{N}_2}^2\Big](m_\psi^2 - 4m_{\tilde{N}_2}^2)^{1/2}\end{aligned} \tag{C.51}$$

with $\alpha = \beta = i\mathcal{O}_c$. The above expressions simplify to give equations (4.122) and (4.123).

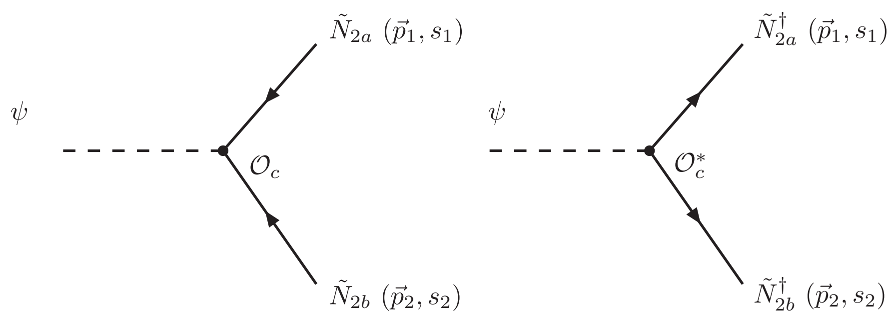

Figure C.3: Feynman diagrams which contribute to the processes $\psi \to \tilde{N}_{2a}\tilde{N}_{2b}$.

Appendix D

Higher-Derivative SUGRA Lagrangians

D.1 Constructing Higher-Derivative SUGRA Lagrangians

We give a brief explanation of how the supergravity Lagrangians written in terms of superfields can be expressed in component fields. The formalism used here is based on work presented in [130], [22, 87, 88] and [171]. Recall that a chiral superfield Φ has the following Θ expansion

$$\Phi = A + \sqrt{2}\Theta\psi + \Theta\Theta F \ . \tag{D.1}$$

The components of Φ can be obtained by acting with $\mathcal{D}$ and then taking the lowest component, which we denote by "$|$". For example,

$$F = -\tfrac{1}{4}\mathcal{D}^2\Phi|, \tag{D.2}$$

is the Θ^2 component of Φ.

Within the context of $N = 1$ supergravity, we are interested in constructing invariant superfield Lagrangians. This can be accomplished as follows. An integral over chiral superspace, $\int d^2\Theta\, \mathcal{E} X$, requires the integrand X to be a chiral superfield. Multiplication by the chiral density $\mathcal{E}$ means that under local supersymmetry, the entire integral transforms into a total space derivative. The product $\mathcal{E}X$ continues to be chiral and has an exact expansion in the local superspace coordinate Θ^α. As explained above, we can construct a chiral superfield X out of any Lorentz scalar $\mathcal{O}$ by acting on it with the chiral projector $\overline{\mathcal{D}}^2 - 8R$. The integral $\int d^2\Theta\mathcal{E}X$ then projects out the Θ^2 component of $\mathcal{E}X$. However, we have seen in (D.2) that the Θ^2 component of a chiral superfield can be obtained by first acting with $-\frac{1}{4}\mathcal{D}^2$ and then taking the lowest component. Choosing $X = (\overline{\mathcal{D}}^2 - 8R)\mathcal{O}$, it follows that

$$\int d^2\Theta\, \mathcal{E}(\overline{\mathcal{D}}^2 - 8R)\mathcal{O} \;\;=\;\; -\frac{1}{4}\mathcal{D}^2(\mathcal{E}(\overline{\mathcal{D}}^2 - 8R)\mathcal{O})| \;. \tag{D.3}$$

Under the assumption that we ignore all fermions, including the gravitino, this can be written as

$$\begin{aligned}\int d^2\Theta\, \mathcal{E}(\overline{\mathcal{D}}^2 - 8R)\mathcal{O} \;\;&=\;\; -\frac{1}{4}\mathcal{E}|\; \mathcal{D}^2((\overline{\mathcal{D}}^2 - 8R)\mathcal{O})| - \frac{1}{4}\mathcal{D}^2\mathcal{E}|\; ((\overline{\mathcal{D}}^2 - 8R)\mathcal{O})| \\ &=\;\; -\frac{1}{4}\mathcal{E}|\; \mathcal{D}^2((\overline{\mathcal{D}}^2 - 8R)\mathcal{O})| + \mathcal{E}|_{\Theta^2}\; (\overline{\mathcal{D}}^2 - 8R)\mathcal{O})| \;,\end{aligned} \tag{D.4}$$

where

$$\begin{aligned} R \;\;&=\;\; -\tfrac{1}{6}M + \Theta^2(\tfrac{1}{12}\mathcal{R} - \tfrac{1}{9}MM^* - \tfrac{1}{18}b^\mu b_\mu + \tfrac{1}{6}ie_a{}^\mu\mathcal{D}_\mu b^a) \\ \mathcal{E} \;\;&=\;\; \tfrac{1}{2}e - \tfrac{1}{2}\Theta^2 eM^* \end{aligned} \tag{D.5}$$

It follows that one can compute the component field expansion of a supergravity Lagrangian by evaluating the following terms,

$$\mathcal{D}^2\overline{\mathcal{D}}^2\mathcal{O}|\;, -8\mathcal{D}^2(R\mathcal{O})|\;, \overline{\mathcal{D}}^2\mathcal{O}|\;, -8R\mathcal{O}|\;. \tag{D.6}$$

As an example, consider the term

$$\bar{\mathcal{L}}_X \;\;=\;\; -\frac{1}{4}\int d^2\Theta 2\mathcal{E}(\overline{\mathcal{D}}^2 - 8R)\Big[(\Phi + \Phi^\dagger)^{-3}\mathcal{D}\Phi\mathcal{D}\Phi\overline{\mathcal{D}}^2\Phi^\dagger\Big] + \text{h.c.}\;, \tag{D.7}$$

One begins with the higher-derivative superfield expression

$$\mathcal{O}_X = (\Phi + \Phi^\dagger)^{-3}\mathcal{D}\Phi\mathcal{D}\Phi\overline{\mathcal{D}}^2\Phi^\dagger\;. \tag{D.8}$$

Then, the associated Lagrangian is obtained by the appropriate chiral projection and superspace integration. For $\mathcal{O}_X$, which is not hermitian, one writes

$$\bar{\mathcal{L}}_X = -\frac{1}{4}\int d^2\Theta\, 2\mathcal{E}(\overline{\mathcal{D}}^2 - 8R)\mathcal{O}_X + \text{h.c.} \tag{D.9}$$

Having obtained the superfield expression for the $\bar{\mathcal{L}}_X$ Lagrangian, we now apply the preceding formalism to express it in terms of component fields. It follows from the above that one must evaluate the four lowest component terms in (D.6). To exhibit our methods, let us compute $\overline{\mathcal{D}}^2\mathcal{O}|$.

$$
\begin{aligned}
& \overline{\mathcal{D}}^2\big((\Phi+\Phi^\dagger)^{-3}\mathcal{D}\Phi\mathcal{D}\Phi\overline{\mathcal{D}}^2\Phi^\dagger\big)\big| \\
= \;& \overline{\mathcal{D}}^2\big((\Phi+\Phi^\dagger)^{-3}\big)\big|\;\mathcal{D}\Phi\mathcal{D}\Phi\overline{\mathcal{D}}^2\Phi^\dagger\big| + 2\mathcal{D}^\alpha\big((\Phi+\Phi^\dagger)^{-3}\big)\big|\;\mathcal{D}_\alpha\big(\mathcal{D}\Phi\mathcal{D}\Phi\overline{\mathcal{D}}^2\Phi^\dagger\big)\big| \\
+ \;& (\Phi+\Phi^\dagger)^{-3}\big|\;\overline{\mathcal{D}}^2\big(\mathcal{D}\Phi\mathcal{D}\Phi\overline{\mathcal{D}}^2\Phi^\dagger\big)\big| \;. \qquad \text{(D.10)}
\end{aligned}
$$

We calculate these terms by distributing the $\mathcal{D}_\alpha$ and $\overline{\mathcal{D}}_{\dot{\alpha}}$ operators appropriately, and commuting them until we are able to apply the defining expressions for chiral and anti-chiral fields

$$\overline{\mathcal{D}}_{\dot{\alpha}}\Phi = 0 \;, \quad \mathcal{D}_\alpha\Phi^\dagger = 0 \;. \qquad \text{(D.11)}$$

Many terms that arise in the intermediate stages of the calculation involve fermions. For example, expressions which contain $\mathcal{D}_\alpha\Phi| = \sqrt{2}\psi_\alpha$ are fermionic. In keeping with the main text of this thesis, all such terms will be dropped. However, the essential difficulty involved in the computation is the presence of curvature and torsion in supergravity. Hence, anti-commutators of the $\mathcal{D}, \overline{\mathcal{D}}$ operators now give rise to terms which would not have been present in the global supersymmetric case. Explicitly, we have

$$
\begin{aligned}
\Big(\mathcal{D}_C\mathcal{D}_B - (-)^{bc}\mathcal{D}_B\mathcal{D}_C\Big)V^A \;&=\; (-)^{d(c+b)}V^D R_{CBD}{}^A - T_{CB}^{\;\;D}\mathcal{D}_D V^A \\
&=\; \Big(V^e R_{CBe}{}^A + (-)^{(c+b)}V^\delta R_{CB\delta}{}^A + (-)^{(c+b)}V_{\dot{\delta}} R_{CB}{}^{\dot{\delta}A}\Big) \\
&\quad\; - \Big(T_{CB}^{\;\;e}\mathcal{D}_e V^A + T_{CB}^{\;\;\delta}\mathcal{D}_\delta V^A + T_{CB\dot{\delta}}\overline{\mathcal{D}}^{\dot{\delta}}V^A\Big) \;, \qquad \text{(D.12)}
\end{aligned}
$$

where the A, B, C, D indices can be $a, \alpha, \dot{\alpha}$, and the exponents b, c, d take the values 0 or 1 when the indices B, C, D are bosonic or fermionic respectively. $R_{CBD}{}^A$ and $T_{CB}^{\;\;D}$ are superfields which respectively contain components of the curvature and torsion. For $N = 1$ supergravity, these superfields and their component expansions are given, for example, in [171], Chapter 15.

Using these results, we determine that the first two terms in (D.10) are fermionic and, hence, are taken to vanish. The third term is given by

$$(\Phi+\Phi^\dagger)^{-3}\big|\;\overline{\mathcal{D}}^2\big(\mathcal{D}\Phi\mathcal{D}\Phi\overline{\mathcal{D}}^2\Phi^\dagger\big)\big| = (A+A^*)^{-3}\;\overline{\mathcal{D}}^2\big(\mathcal{D}\Phi\mathcal{D}\Phi\overline{\mathcal{D}}^2\Phi^\dagger\big)\big| \;. \qquad \text{(D.13)}$$

We compute the lowest component term on the right-hand-side as follows.

$$
\begin{aligned}
\overline{\mathcal{D}}^2(\mathcal{D}\Phi\mathcal{D}\Phi\overline{\mathcal{D}}^2\Phi^\dagger)| &= \epsilon^{\dot\beta\dot\alpha}\overline{\mathcal{D}}_{\dot\beta}\overline{\mathcal{D}}_{\dot\alpha}(\mathcal{D}\Phi\mathcal{D}\Phi\overline{\mathcal{D}}^2\Phi^\dagger)| \\
&= \left(\overline{\mathcal{D}}_{\dot\alpha}\mathcal{D}\Phi|\ \overline{\mathcal{D}}_{\dot\beta}\mathcal{D}\Phi|\ \overline{\mathcal{D}}^2\Phi^\dagger|\ - \overline{\mathcal{D}}_{\dot\beta}\mathcal{D}\Phi|\ \overline{\mathcal{D}}_{\dot\alpha}\mathcal{D}\Phi|\ \overline{\mathcal{D}}^2\Phi^\dagger|\ \right) \\
&= \epsilon^{\dot\beta\dot\alpha}\epsilon^{\beta\alpha}\left(\overline{\mathcal{D}}_{\dot\alpha}\mathcal{D}_\alpha\Phi|\ \overline{\mathcal{D}}_{\dot\beta}\mathcal{D}_\beta\Phi|\ - \overline{\mathcal{D}}_{\dot\beta}\mathcal{D}_\alpha\Phi|\ \overline{\mathcal{D}}_{\dot\alpha}\mathcal{D}_\beta\Phi|\ \right)\overline{\mathcal{D}}^2\Phi^\dagger| \\
&= \epsilon^{\dot\beta\dot\alpha}\epsilon^{\beta\alpha}\Big((-2i\sigma^a_{\alpha\dot\alpha}e_a{}^\mu\partial_\mu A)(-2i\sigma^b_{\beta\dot\beta}e_b{}^\nu\partial_\nu A) \\
&\quad -(-2i\sigma^a_{\alpha\dot\beta}e_a{}^\mu\partial_\mu A)(-2i\sigma^b_{\beta\dot\alpha}e_b{}^\nu\partial_\nu A)\Big)(-4F^*) \\
&= 16\epsilon^{\dot\beta\dot\alpha}\epsilon^{\beta\alpha}\left(\sigma^a_{\alpha\dot\alpha}\sigma^b_{\beta\dot\beta} - \sigma^a_{\alpha\dot\beta}\sigma^b_{\beta\dot\alpha}\right)e_a{}^\mu e_b{}^\nu\partial_\mu A\,\partial_\nu A\,F^* \\
&= 16\left(\bar\sigma^{a\dot\beta\beta}\sigma^b_{\beta\dot\beta} + \bar\sigma^{a\dot\alpha\beta}\sigma^b_{\beta\dot\alpha}\right)e_a{}^\mu e_b{}^\nu\partial_\mu A\,\partial_\nu A\,F^* \\
&= 16\left(-2\eta^{ab} - 2\eta^{ab}\right)e_a{}^\mu e_b{}^\nu\partial_\mu A\,\partial_\nu A\,F^* \\
&= -64\,(\partial A)^2\,F^*
\end{aligned}
\tag{D.14}
$$

Putting this back into (D.13) and then inserting in (D.10) yields

$$
\overline{\mathcal{D}}^2((\Phi+\Phi^\dagger)^{-3}\mathcal{D}\Phi\mathcal{D}\Phi\overline{\mathcal{D}}^2\Phi^\dagger)| \quad = \quad -64\frac{1}{(A+A^*)^3}\,(\partial A)^2\,F^*\ . \tag{D.15}
$$

The remaining three terms in (D.6) can be evaluated using similar methods.

D.2 Useful Supergravity Identities

Here we present a non-exhaustive list of identities necessary for the computations described in chapter 5.

The superfield results of interest are

$$
\begin{aligned}
&\mathcal{D}_\alpha \mathcal{D}_\beta \mathcal{D}_\gamma \Phi = \tfrac{1}{3}(\{\mathcal{D}_\alpha, \mathcal{D}_\beta\}\mathcal{D}_\gamma - \{\mathcal{D}_\alpha, \mathcal{D}_\gamma\}\mathcal{D}_\beta)\Phi \\
&\mathcal{D}_\alpha \overline{\mathcal{D}}_{\dot\beta} \overline{\mathcal{D}}_{\dot\gamma} \Phi^\dagger = \overline{\mathcal{D}}_{\dot\epsilon}\Phi^\dagger R_{\alpha\dot\beta}{}^{\dot\epsilon}{}_{\dot\gamma} - 2i\sigma^e_{\alpha\dot\beta}\mathcal{D}_e \overline{\mathcal{D}}_{\dot\gamma}\Phi^\dagger \\
&\qquad\qquad -2i\sigma^e_{\alpha\dot\gamma}\left(T_{\dot\beta e}{}^a \mathcal{D}_a \Phi^\dagger + T_{\dot\beta e}{}^\epsilon \mathcal{D}_\epsilon \Phi^\dagger + \overline{\mathcal{D}}^{\dot\epsilon}\Phi^\dagger T_{\dot\beta e}{}^{\dot\epsilon}\right) \\
&\mathcal{D}_\alpha \mathcal{D}_\beta \overline{\mathcal{D}}_{\dot\alpha} \mathcal{D}_\phi \Phi = \mathcal{D}_\alpha \mathcal{D}_\beta \{\overline{\mathcal{D}}_{\dot\alpha}, \mathcal{D}_\phi\}\Phi \\
&\mathcal{D}_\alpha \overline{\mathcal{D}}_{\dot\alpha} \overline{\mathcal{D}}_{\dot\beta} \mathcal{D}_\phi \Phi = 2i\sigma^a_{\phi\dot\beta}\mathcal{D}_\alpha (T_{\dot\alpha a}{}^\epsilon \mathcal{D}_\epsilon \Phi) \\
&\mathcal{D}_\alpha \overline{\mathcal{D}}_{\dot\alpha} \overline{\mathcal{D}}_{\dot\gamma} \overline{\mathcal{D}}_{\dot\delta} \Phi^\dagger = \{\mathcal{D}_\alpha, \overline{\mathcal{D}}_{\dot\alpha}\}\overline{\mathcal{D}}_{\dot\gamma}\overline{\mathcal{D}}_{\dot\delta}\Phi^\dagger - \overline{\mathcal{D}}_{\dot\alpha}\{\mathcal{D}_\alpha, \overline{\mathcal{D}}_{\dot\gamma}\}\overline{\mathcal{D}}_{\dot\delta}\Phi^\dagger + \overline{\mathcal{D}}_{\dot\alpha}\overline{\mathcal{D}}_{\dot\gamma}\{\mathcal{D}_\alpha, \overline{\mathcal{D}}_{\dot\delta}\}\Phi^\dagger \ .
\end{aligned}
\tag{D.16}
$$

When calculating the lowest component of a superfield expression–indicated by " | "–we drop all fermions and present the purely bosonic result. The lowest component expressions for the relevant superfields are given by

$$
\begin{aligned}
&\mathcal{D}_\alpha \Phi\big| = 0 \ , \overline{\mathcal{D}}_{\dot\alpha}\Phi^\dagger\big| = 0 \\
&\mathcal{D}_\alpha \mathcal{D}_\beta \Phi\big| = -2\epsilon_{\alpha\beta}F, \quad \mathcal{D}^2\Phi\big| = -4F \\
&\overline{\mathcal{D}}_{\dot\alpha}\overline{\mathcal{D}}_{\dot\beta}\Phi^\dagger\big| = 2\epsilon_{\dot\alpha\dot\beta}F^*, \quad \overline{\mathcal{D}}^2\Phi^\dagger\big| = -4F^* \\
&\overline{\mathcal{D}}_{\dot\alpha}\mathcal{D}_\alpha \Phi\big| = -T_{\alpha\dot\alpha}{}^a \mathcal{D}_a \Phi\big| = -2i\sigma^a_{\alpha\dot\alpha}e_a{}^\mu \partial_\mu A \\
&\mathcal{D}_\alpha \overline{\mathcal{D}}_{\dot\alpha}\Phi^\dagger\big| = -2i\sigma^a_{\alpha\dot\alpha}e_a{}^\mu\partial_\mu A^* \\
&\mathcal{D}_\alpha \overline{\mathcal{D}}_{\dot\alpha}\overline{\mathcal{D}}_{\dot\beta}\Phi^\dagger\big| = 0 \\
&\mathcal{D}^2\overline{\mathcal{D}}^2\Phi^\dagger\big| = 16e_a{}^\mu \mathcal{D}_\mu \hat{D}^a A^* + \tfrac{32}{3}ib^a\hat{D}^a A^* + \tfrac{32}{3}M^*F^* \\
&\overline{\mathcal{D}}^2\overline{\mathcal{D}}^2\Phi^\dagger\big| = \epsilon^{\dot\alpha\dot\beta}\epsilon^{\dot\gamma\dot\delta}\overline{\mathcal{D}}_{\dot\alpha}\overline{\mathcal{D}}_{\dot\beta}\overline{\mathcal{D}}_{\dot\gamma}\overline{\mathcal{D}}_{\dot\delta}\Phi^\dagger\big| = \tfrac{16}{3}F^*M
\end{aligned}
\tag{D.17}
$$

$$\begin{aligned}
\mathcal{D}_\alpha\mathcal{D}_\beta\overline{\mathcal{D}}_{\dot\alpha}\mathcal{D}_\phi\Phi\big| &= -2i\sigma^a_{\phi\dot\alpha}\big(-T_{\beta a}{}^{\epsilon}\big|\mathcal{D}_\alpha\mathcal{D}_\epsilon\Phi\big| + \mathcal{D}_a\mathcal{D}_\alpha\mathcal{D}_\beta\Phi\big|\big) \\
&= 8i\sigma^a_{\phi\dot\alpha}e_a{}^{\mu}\partial_\mu F - \tfrac{2}{3}F\sigma^a_{\phi\dot\alpha}b_a
\end{aligned}$$

$$\mathcal{D}_\alpha\overline{\mathcal{D}}_{\dot\alpha}\overline{\mathcal{D}}_{\dot\beta}\mathcal{D}_\phi\Phi\big| = \tfrac{2}{3}MF\sigma^a_{\phi\dot\beta}\sigma_{a\alpha\dot\alpha} \tag{D.18}$$

Additionally, we find that

$$\begin{aligned}
\mathcal{D}^2\overline{\mathcal{D}}^2\big(\mathcal{D}\Phi\mathcal{D}\Phi\overline{\mathcal{D}}^2\Phi^\dagger\big)\big| &= -2\overline{\mathcal{D}}_{\dot\beta}\mathcal{D}\Phi\big|\ \overline{\mathcal{D}}^{\dot\beta}\mathcal{D}\Phi\big|\ \mathcal{D}^2\overline{\mathcal{D}}^2\Phi^\dagger\big| - 4\overline{\mathcal{D}}_{\dot\beta}\mathcal{D}\Phi\big|\ \mathcal{D}^\alpha\mathcal{D}\Phi\big|\ \mathcal{D}_\alpha\overline{\mathcal{D}}^{\dot\beta}\Phi^\dagger\big| \\
&+ 4\mathcal{D}^\beta\mathcal{D}\Phi\big|\ \overline{\mathcal{D}}_{\dot\alpha}\mathcal{D}\Phi\big|\ \mathcal{D}_\beta\overline{\mathcal{D}}^{\dot\alpha}\overline{\mathcal{D}}^2\Phi^\dagger\big| - 2\mathcal{D}^\beta\mathcal{D}\Phi\big|\ \mathcal{D}_\beta\mathcal{D}\Phi\big|\ \overline{\mathcal{D}}^2\overline{\mathcal{D}}^2\Phi^\dagger\big| \\
&- 2\mathcal{D}^2\overline{\mathcal{D}}_{\dot\alpha}\mathcal{D}\Phi\big|\ \overline{\mathcal{D}}^{\dot\alpha}\mathcal{D}\Phi\big|\ \overline{\mathcal{D}}^2\Phi^\dagger\big| - 2\overline{\mathcal{D}}_{\dot\alpha}\mathcal{D}\Phi\big|\ \mathcal{D}^2\overline{\mathcal{D}}^{\dot\alpha}\mathcal{D}\Phi\big|\ \overline{\mathcal{D}}^2\Phi^\dagger\big|
\end{aligned} \tag{D.19}$$

and

$$\begin{aligned}
&\mathcal{D}^2\overline{\mathcal{D}}^2\big(\mathcal{D}\Phi\mathcal{D}\Phi\overline{\mathcal{D}}\Phi^\dagger\overline{\mathcal{D}}\Phi^\dagger\big)\big| \\
= \ &4\overline{\mathcal{D}}_{\dot\beta}\mathcal{D}\Phi\big|\ \overline{\mathcal{D}}^{\dot\beta}\mathcal{D}\Phi\big|\ \mathcal{D}^\alpha\overline{\mathcal{D}}\Phi^\dagger\big|\ \mathcal{D}_\alpha\overline{\mathcal{D}}\Phi^\dagger\big| - 4\overline{\mathcal{D}}_{\dot\beta}\mathcal{D}\Phi\big|\ \mathcal{D}^\alpha\mathcal{D}\Phi\big|\ \overline{\mathcal{D}}^{\dot\beta}\overline{\mathcal{D}}\Phi^\dagger\big|\ \mathcal{D}_\alpha\overline{\mathcal{D}}\Phi^\dagger\big| \\
+ \ &4\mathcal{D}^\alpha\mathcal{D}\Phi\big|\ \overline{\mathcal{D}}_{\dot\beta}\mathcal{D}\Phi\big|\ \overline{\mathcal{D}}^{\dot\beta}\overline{\mathcal{D}}\Phi^\dagger\big|\ \mathcal{D}_\alpha\overline{\mathcal{D}}\Phi^\dagger\big| - 4\mathcal{D}^\alpha\mathcal{D}\Phi\big|\ \overline{\mathcal{D}}_{\dot\beta}\mathcal{D}\Phi\big|\ \mathcal{D}_\alpha\overline{\mathcal{D}}\Phi^\dagger\big|\ \overline{\mathcal{D}}^{\dot\beta}\overline{\mathcal{D}}\Phi^\dagger\big| \\
+ \ &4\mathcal{D}^\alpha\mathcal{D}\Phi\big|\ \mathcal{D}_\alpha\mathcal{D}\Phi\big|\ \overline{\mathcal{D}}_{\dot\beta}\overline{\mathcal{D}}\Phi^\dagger\big|\ \overline{\mathcal{D}}^{\dot\beta}\overline{\mathcal{D}}\Phi^\dagger\big|\ .
\end{aligned} \tag{D.20}$$

Bibliography

[1] G. Aad, et al., *Measurement of the Higgs Boson Mass from the $H \to \gamma\gamma$ and $H \to ZZ^* \to 4\ell$ channels with the ATLAS detector using 25 fb^{-1} of pp collision data*, Phys. Rev. D90 (5) (2014) 052004. `arXiv:1406.3827`, `doi:10.1103/PhysRevD.90.052004`.

[2] L. F. Abbott, E. Farhi, M. B. Wise, *Particle Production in the New Inflationary Cosmology*, Phys. Lett. 117B (1982) 29. `doi:10.1016/0370-2693(82)90867-X`.

[3] P. A. R. Ade, et al., *Planck 2015 Results XX: Constraints on inflation*, Astron. Astrophys. 594 (2016) A20. `arXiv:1502.02114`, `doi:10.1051/0004-6361/201525898`.

[4] A. Albrecht, S. Dimopoulos, W. Fischler, E. W. Kolb, S. Raby, P. J. Steinhardt, *New Inflation in Supersymmetric Theories*, Nucl. Phys. B229 (1983) 528–540. `doi:10.1016/0550-3213(83)90347-4`.

[5] A. Albrecht, P. J. Steinhardt, M. S. Turner, F. Wilczek, *Reheating an Inflationary Universe*, Phys. Rev. Lett. 48 (1982) 1437–1440. `doi:10.1103/PhysRevLett.48.1437`.

[6] R. Allahverdi, R. Brandenberger, F.-Y. Cyr-Racine, A. Mazumdar, *Reheating in Inflationary Cosmology: Theory and Applications*, Ann. Rev. Nucl. Part. Sci. 60 (2010) 27–51. `arXiv:1001.2600`, `doi:10.1146/annurev.nucl.012809.104511`.

[7] M. Ambroso, B. Ovrut, *The $B-L$/Electroweak Hierarchy in Heterotic String and M-Theory*, JHEP 10 (2009) 011. `arXiv:0904.4509`, `doi:10.1088/1126-6708/2009/10/011`.

[8] M. Ambroso, B. A. Ovrut, *The Mass Spectra, Hierarchy and Cosmology of B-L MSSM Heterotic Compactifications*, Int. J. Mod. Phys. A26 (2011) 1569–1627. `arXiv:1005.5392`, `doi:10.1142/S0217751X11052943`.

[9] M. A. Amin, M. P. Hertzberg, D. I. Kaiser, J. Karouby, *Nonperturbative Dynamics Of Reheating After Inflation: A Review*, Int. J. Mod. Phys. D24 (2014) 1530003. `arXiv:1410.3808`, `doi:10.1142/S0218271815300037`.

[10] N. D. Antunes, E. J. Copeland, M. Hindmarsh, A. Lukas, *Kinky Brane Worlds*, Phys. Rev. D68 (2003) 066005. arXiv:hep-th/0208219, doi:10.1103/PhysRevD.68.066005.

[11] C. S. Aulakh, R. N. Mohapatra, *Neutrino as the Supersymmetric Partner of the Majoron*, Phys. Lett. 119B (1982) 136–140. doi:10.1016/0370-2693(82)90262-3.

[12] C. S. Aulakh, B. Bajc, A. Melfo, A. Rasin, G. Senjanovic, *$SO(10)$ Theory of R-Parity and Neutrino Mass*, Nucl. Phys. B597 (2001) 89–109. arXiv:hep-ph/0004031, doi:10.1016/S0550-3213(00)00721-5.

[13] C. S. Aulakh, A. Melfo, A. Rasin, G. Senjanovic, *Seesaw and Supersymmetry or Exact R-Parity*, Phys. Lett. B459 (1999) 557–562. arXiv:hep-ph/9902409, doi:10.1016/S0370-2693(99)00708-X.

[14] K. S. Babu, R. N. Mohapatra, *Minimal Supersymmetric Left-Right Model*, Phys. Lett. B668 (2008) 404–409. arXiv:0807.0481, doi:10.1016/j.physletb.2008.09.018.

[15] D. Bailin, A. Love, *Reduced Modular Symmetries of Threshold Corrections and Gauge Coupling Unification*, JHEP 04 (2015) 002. arXiv:1412.7327, doi:10.1007/JHEP04(2015)002.

[16] R. Barbieri, G. F. Giudice, *Upper Bounds on Supersymmetric Particle Masses*, Nucl. Phys. B306 (1988) 63–76. doi:10.1016/0550-3213(88)90171-X.

[17] J. L. F. Barbon, J. R. Espinosa, *On the Naturalness of Higgs Inflation*, Phys. Rev. D79 (2009) 081302. arXiv:0903.0355, doi:10.1103/PhysRevD.79.081302.

[18] V. Barger, P. Fileviez Perez, S. Spinner, *Minimal Gauged $U(1)_{B-L}$ Model with Spontaneous R-Parity Violation*, Phys. Rev. Lett. 102 (2009) 181802. arXiv:0812.3661, doi:10.1103/PhysRevLett.102.181802.

[19] V. Barger, P. Fileviez Perez, S. Spinner, *Three Layers of Neutrinos*, Phys. Lett. B696 (2011) 509–512. arXiv:1010.4023, doi:10.1016/j.physletb.2011.01.015.

[20] B. A. Bassett, S. Tsujikawa, D. Wands, *Inflation Dynamics and Reheating*, Rev. Mod. Phys. 78 (2006) 537–589. arXiv:astro-ph/0507632, doi:10.1103/RevModPhys.78.537.

[21] L. Battarra, M. Koehn, J.-L. Lehners, B. A. Ovrut, *Cosmological Perturbations Through a Non-Singular Ghost-Condensate/Galileon Bounce*, JCAP 1407 (2014) 007. arXiv:1404.5067, doi:10.1088/1475-7516/2014/07/007.

[22] D. Baumann, D. Green, *Supergravity for Effective Theories*, JHEP 03 (2012) 001. arXiv:1109.0293, doi:10.1007/JHEP03(2012)001.

[23] F. Bezrukov, D. Gorbunov, M. Shaposhnikov, *On Initial Conditions for the Hot Big Bang*, JCAP 0906 (2009) 029. arXiv:0812.3622, doi:10.1088/1475-7516/2009/06/029.

[24] F. Bezrukov, A. Magnin, M. Shaposhnikov, S. Sibiryakov, *Higgs Inflation: Consistency and Generalisations*, JHEP 01 (2011) 016. arXiv:1008.5157, doi:10.1007/JHEP01(2011)016.

[25] F. Bezrukov, M. Yu. Kalmykov, B. A. Kniehl, M. Shaposhnikov, *Higgs Boson Mass and New Physics*, JHEP 10 (2012) 140, [,275(2012)]. arXiv:1205.2893, doi:10.1007/JHEP10(2012)140.

[26] F. L. Bezrukov, A. Magnin, M. Shaposhnikov, *Standard Model Higgs Boson Mass from Inflation*, Phys. Lett. B675 (2009) 88–92. arXiv:0812.4950, doi:10.1016/j.physletb.2009.03.035.

[27] F. L. Bezrukov, M. Shaposhnikov, *The Standard Model Higgs Boson as the Inflaton*, Phys. Lett. B659 (2008) 703–706. arXiv:0710.3755, doi:10.1016/j.physletb.2007.11.072.

[28] S. Bielleman, L. E. Ibanez, F. G. Pedro, I. Valenzuela, *Multifield Dynamics in Higgs-otic Inflation*, JHEP 01 (2016) 128. arXiv:1505.00221, doi:10.1007/JHEP01(2016)128.

[29] F. Bonjour, C. Charmousis, R. Gregory, *The Dynamics of Curved Gravitating Walls*, Phys. Rev. D62 (2000) 083504. arXiv:gr-qc/0002063, doi:10.1103/PhysRevD.62.083504.

[30] R. Brandenberger, P. Peter, *Bouncing Cosmologies: Progress and Problems*, Found. Phys. 47 (6) (2017) 797–850. arXiv:1603.05834, doi:10.1007/s10701-016-0057-0.

[31] R. H. Brandenberger, *The Matter Bounce Alternative to Inflationary Cosmology*arXiv:1206.4196.

[32] M. Brandle, A. Lukas, *Five-branes in Heterotic Brane World Theories*, Phys. Rev. D65 (2002) 064024. arXiv:hep-th/0109173, doi:10.1103/PhysRevD.65.064024.

[33] V. Braun, Y.-H. He, B. A. Ovrut, *Supersymmetric Hidden Sectors for Heterotic Standard Models*, JHEP 09 (2013) 008. arXiv:1301.6767, doi:10.1007/JHEP09(2013)008.

[34] V. Braun, Y.-H. He, B. A. Ovrut, T. Pantev, *A Heterotic Standard Model*, Phys. Lett. B618 (2005) 252–258. arXiv:hep-th/0501070, doi:10.1016/j.physletb.2005.05.007.

[35] V. Braun, Y.-H. He, B. A. Ovrut, T. Pantev, *A Standard Model from the $E_8 \times E_8$ Heterotic Superstring*, JHEP 06 (2005) 039. arXiv:hep-th/0502155, doi:10.1088/1126-6708/2005/06/039.

[36] V. Braun, Y.-H. He, B. A. Ovrut, T. Pantev, *The Exact MSSM Spectrum from String Theory*, JHEP 05 (2006) 043. arXiv:hep-th/0512177, doi:10.1088/1126-6708/2006/05/043.

[37] V. Braun, Y.-H. He, B. A. Ovrut, T. Pantev, *Vector Bundle Extensions, Sheaf Cohomology, and the Heterotic Standard Model*, Adv. Theor. Math. Phys. 10 (4) (2006) 525–589. arXiv:hep-th/0505041, doi:10.4310/ATMP.2006.v10.n4.a3.

[38] V. Braun, B. A. Ovrut, T. Pantev, R. Reinbacher, *Elliptic Calabi-Yau Threefolds with $Z_3 \times Z_3$ Wilson Lines*, JHEP 12 (2004) 062. arXiv:hep-th/0410055, doi:10.1088/1126-6708/2004/12/062.

[39] E. Buchbinder, R. Donagi, B. A. Ovrut, *Vector Bundle Moduli and Small Instanton Transitions*, JHEP 06 (2002) 054. arXiv:hep-th/0202084, doi:10.1088/1126-6708/2002/06/054.

[40] E. I. Buchbinder, R. Donagi, B. A. Ovrut, *Vector Bundle Moduli Superpotentials in Heterotic Superstrings and M-theory*, JHEP 07 (2002) 066. arXiv:hep-th/0206203, doi:10.1088/1126-6708/2002/07/066.

[41] E. I. Buchbinder, J. Khoury, B. A. Ovrut, *New Ekpyrotic Cosmology*, Phys. Rev. D76 (2007) 123503. arXiv:hep-th/0702154, doi:10.1103/PhysRevD.76.123503.

[42] Y.-F. Cai, D. A. Easson, R. Brandenberger, *Towards a Nonsingular Bouncing Cosmology*, JCAP 1208 (2012) 020. arXiv:1206.2382, doi:10.1088/1475-7516/2012/08/020.

[43] Y. Cai, R. Deen, B. A. Ovrut, A. Purves, *Reheating in Sneutrino-Higgs Cosmology*arXiv:1804.07848.

[44] P. Candelas, A. M. Dale, C. A. Lutken, R. Schimmrigk, *Complete Intersection Calabi-Yau Manifolds*, Nucl. Phys. B298 (1988) 493. doi:10.1016/0550-3213(88)90352-5.

[45] P. Candelas, C. A. Lutken, R. Schimmrigk, *Complete Intersection Calabi-Yau Manifolds 2: Three Generation Manifolds*, Nucl. Phys. B306 (1988) 113. doi:10.1016/0550-3213(88)90173-3.

[46] B. Carter, R. Gregory, *Curvature Corrections to Dynamics of Domain Walls*, Phys. Rev. D51 (1995) 5839–5846. arXiv:hep-th/9410095, doi:10.1103/PhysRevD.51.5839.

[47] S. Cecotti, S. Ferrara, L. Girardello, *Gravitational Supervertices in $N = 1$, 4-D Superstrings*, Phys. Lett. B198 (1987) 336–342. doi:10.1016/0370-2693(87)90675-7.

[48] S. Chatrchyan, et al., *Observation of a New Boson with Mass Near 125 GeV in pp Collisions at $\sqrt{s} = 7$ and 8 TeV*, JHEP 06 (2013) 081. arXiv:1303.4571, doi:10.1007/JHEP06(2013)081.

[49] E. J. Chun, S. K. Kang, *One Loop Corrected Neutrino Masses and Mixing in Supersymmetric Standard Model without R-Parity*, Phys. Rev. D61 (2000) 075012. arXiv:hep-ph/9909429, doi:10.1103/PhysRevD.61.075012.

[50] E. J. Chun, J. S. Lee, *Implication of Super-Kamiokande Data on R-Parity Violation*, Phys. Rev. D60 (1999) 075006. arXiv:hep-ph/9811201, doi:10.1103/PhysRevD.60.075006.

[51] D. J. H. Chung, E. W. Kolb, A. Riotto, *Production of Massive Particles During Reheating*, Phys. Rev. D60 (1999) 063504. arXiv:hep-ph/9809453, doi:10.1103/PhysRevD.60.063504.

[52] D. Ciupke, *Scalar Potential from Higher Derivative $\mathcal{N} = 1$ Superspace*arXiv:1605.00651.

[53] D. Ciupke, J. Louis, A. Westphal, *Higher-Derivative Supergravity and Moduli Stabilization*, JHEP 10 (2015) 094. arXiv:1505.03092, doi:10.1007/JHEP10(2015)094.

[54] P. Creminelli, A. Nicolis, E. Trincherini, *Galilean Genesis: An Alternative to inflation*, JCAP 1011 (2010) 021. arXiv:1007.0027, doi:10.1088/1475-7516/2010/11/021.

[55] P. Creminelli, L. Senatore, *A Smooth Bouncing Cosmology with Scale Invariant Spectrum*, JCAP 0711 (2007) 010. arXiv:hep-th/0702165, doi:10.1088/1475-7516/2007/11/010.

[56] P. Creminelli, M. Serone, E. Trincherini, *Non-linear Representations of the Conformal Group and Mapping of Galileons*, JHEP 10 (2013) 040. arXiv:1306.2946, doi:10.1007/JHEP10(2013)040.

[57] E. Cremmer, S. Ferrara, C. Kounnas, D. V. Nanopoulos, *Naturally Vanishing Cosmological Constant in $N = 1$ Supergravity*, Phys. Lett. 133B (1983) 61. doi:10.1016/0370-2693(83)90106-5.

[58] S. Davidson, S. Sarkar, *Thermalization after Inflation*, JHEP 11 (2000) 012. arXiv:hep-ph/0009078, doi:10.1088/1126-6708/2000/11/012.

[59] S. P. de Alwis, *Gauge Threshold Corrections and Field Redefinitions*, Phys. Lett. B722 (2013) 176–184. arXiv:1211.5460, doi:10.1016/j.physletb.2013.04.007.

[60] C. de Rham, A. J. Tolley, *DBI and the Galileon Reunited*, JCAP 1005 (2010) 015. arXiv:1003.5917, doi:10.1088/1475-7516/2010/05/015.

[61] R. Deen, B. Ovrut, *$N = 1$ Supergravitational Heterotic Galileons*, JHEP 11 (2017) 026. arXiv:1707.05305.

[62] R. Deen, B. Ovrut, *Supergravitational Conformal Galileons*, JHEP 08 (2017) 014. arXiv:1705.06729, doi:10.1007/JHEP08(2017)014.

[63] R. Deen, B. A. Ovrut, A. Purves, *Supersymmetric Sneutrino-Higgs Inflation*, Phys. Lett. B762 (2016) 441–446. arXiv:1606.00431, doi:10.1016/j.physletb.2016.09.059.

[64] R. Deen, B. A. Ovrut, A. Purves, *The Minimal SUSY $B - L$ Model: Simultaneous Wilson Lines and String Thresholds*, JHEP 07 (2016) 043. arXiv:1604.08588, doi:10.1007/JHEP07(2016)043.

[65] J.-P. Derendinger, R. Sauser, *A Five-brane Modulus in the Effective N=1 Supergravity of M-theory*, Nucl. Phys. B598 (2001) 87–114. arXiv:hep-th/0009054, doi:10.1016/S0550-3213(00)00773-2.

[66] K. R. Dienes, *String Theory and the Path to Unification: A Review of Recent Developments*, Phys. Rept. 287 (1997) 447–525. arXiv:hep-th/9602045, doi:10.1016/S0370-1573(97)00009-4.

[67] K. R. Dienes, A. E. Faraggi, J. March-Russell, *String Unification, Higher Level Gauge Symmetries, and Exotic Hypercharge Normalizations*, Nucl. Phys. B467 (1996) 44–99. arXiv:hep-th/9510223, doi:10.1016/0550-3213(96)00085-5.

[68] A. Djouadi, *The Anatomy of Electro-weak Symmetry Breaking. I: The Higgs boson in the Standard Model*, Phys. Rept. 457 (2008) 1–216. arXiv:hep-ph/0503172, doi:10.1016/j.physrep.2007.10.004.

[69] L. Dolan, J. T. Liu, *Running Gauge Couplings and Thresholds in the Type II Superstring*, Nucl. Phys. B387 (1992) 86–96. arXiv:hep-th/9205094, doi:10.1016/0550-3213(92)90047-F.

[70] R. Donagi, Y.-H. He, B. A. Ovrut, R. Reinbacher, *The Particle Spectrum of Heterotic Compactifications*, JHEP 12 (2004) 054. arXiv:hep-th/0405014, doi:10.1088/1126-6708/2004/12/054.

[71] R. Donagi, B. A. Ovrut, T. Pantev, D. Waldram, *Standard Model Bundles on Non-simply Connected Calabi-Yau Threefolds*, JHEP 08 (2001) 053. arXiv:hep-th/0008008, doi:10.1088/1126-6708/2001/08/053.

[72] R. Donagi, B. A. Ovrut, T. Pantev, D. Waldram, *Standard Models from Heterotic M-theory*, Adv. Theor. Math. Phys. 5 (2002) 93–137. arXiv:hep-th/9912208, doi:10.4310/ATMP.2001.v5.n1.a4.

[73] R. Donagi, B. A. Ovrut, D. Waldram, *Moduli Spaces of Five-Branes on Elliptic Calabi-Yau Threefolds*, JHEP 11 (1999) 030. arXiv:hep-th/9904054, doi:10.1088/1126-6708/1999/11/030.

[74] S. K. Donaldson, *Anti Self-Dual Yang-Mills Connections Over Complex Algebraic Surfaces and Stable Vector Bundles*, Proc. Lond. Math. Soc. 50 (1985) 1–26. doi:10.1112/plms/s3-50.1.1.

[75] H. K. Dreiner, H. E. Haber, S. P. Martin, *Two-Component Spinor Techniques and Feynman Rules for Quantum Field Theory and Supersymmetry*, Phys. Rept. 494 (2010) 1–196. arXiv:0812.1594, doi:10.1016/j.physrep.2010.05.002.

[76] G. R. Dvali, G. Gabadadze, M. Porrati, *4-D Gravity on a Brane in 5-D Minkowski Space*, Phys. Lett. B485 (2000) 208–214. arXiv:hep-th/0005016, doi:10.1016/S0370-2693(00)00669-9.

[77] D. A. Easson, I. Sawicki, A. Vikman, *G-Bounce*, JCAP 1111 (2011) 021. arXiv:1109.1047, doi:10.1088/1475-7516/2011/11/021.

[78] M. B. Einhorn, D. R. T. Jones, *Inflation with Non-minimal Gravitational Couplings in Supergravity*, JHEP 03 (2010) 026. arXiv:0912.2718, doi:10.1007/JHEP03(2010)026.

[79] J. Ellis, M. A. G. Garcia, N. Nagata, D. V. Nanopoulos, K. A. Olive, *Starobinsky-Like Inflation and Neutrino Masses in a No-Scale $SO(10)$ Model*, JCAP 1611 (11) (2016) 018. arXiv:1609.05849, doi:10.1088/1475-7516/2016/11/018.

[80] J. Ellis, M. A. G. GarcÃŋa, D. V. Nanopoulos, K. A. Olive, *Resurrecting Quadratic Inflation in No-Scale Supergravity in Light of BICEP2*, JCAP 1405 (2014) 037. arXiv:1403.7518, doi:10.1088/1475-7516/2014/05/037.

[81] J. Ellis, H.-J. He, Z.-Z. Xianyu, *Higgs Inflation, Reheating and Gravitino Production in No-Scale Supersymmetric GUTs*, JCAP 1608 (08) (2016) 068. arXiv:1606.02202, doi:10.1088/1475-7516/2016/08/068.

[82] J. Ellis, D. V. Nanopoulos, K. A. Olive, *No-Scale Supergravity Realization of the Starobinsky Model of Inflation*, Phys. Rev. Lett. 111 (2013) 111301, [Erratum: Phys. Rev. Lett.111,no.12,129902(2013)]. arXiv:1305.1247, doi:10.1103/PhysRevLett.111.129902,10.1103/PhysRevLett.111.111301.

[83] J. R. Ellis, M. Raidal, T. Yanagida, *Sneutrino Inflation in the Light of WMAP: Reheating, Leptogenesis and Flavor Violating Lepton Decays*, Phys. Lett. B581 (2004) 9–18. arXiv:hep-ph/0303242, doi:10.1016/j.physletb.2003.11.029.

[84] K. Enqvist, J. Sirkka, *Chemical Equilibrium in QCD Gas in the Early Universe*, Phys. Lett. B314 (1993) 298–302. arXiv:hep-ph/9304273, doi:10.1016/0370-2693(93)91239-J.

[85] L. L. Everett, P. Fileviez Perez, S. Spinner, *The Right Side of Tev Scale Spontaneous R-Parity Violation*, Phys. Rev. D80 (2009) 055007. arXiv:0906.4095, doi:10.1103/PhysRevD.80.055007.

[86] F. Farakos, C. Germani, A. Kehagias, *On Ghost-Free Supersymmetric Galileons*, JHEP 11 (2013) 045. arXiv:1306.2961, doi:10.1007/JHEP11(2013)045.

[87] F. Farakos, C. Germani, A. Kehagias, E. N. Saridakis, *A New Class of Four-Dimensional N=1 Supergravity with Non-minimal Derivative Couplings*, JHEP 05 (2012) 050. arXiv:1202.3780, doi:10.1007/JHEP05(2012)050.

[88] F. Farakos, A. Kehagias, *Emerging Potentials in Higher-Derivative Gauged Chiral Models Coupled to N=1 Supergravity*, JHEP 11 (2012) 077. arXiv:1207.4767, doi:10.1007/JHEP11(2012)077.

[89] D. Feldman, P. Fileviez Perez, P. Nath, *R-Parity Conservation via the Stueckelberg Mechanism: LHC and Dark Matter Signals*, JHEP 01 (2012) 038. arXiv:1109.2901, doi:10.1007/JHEP01(2012)038.

[90] S. Ferrara, S. Sabharwal, *Structure of New Minimal Supergravity*, Annals Phys. 189 (1989) 318–351. doi:10.1016/0003-4916(89)90167-X.

[91] S. Ferrara, R. Kallosh, A. Linde, A. Marrani, A. Van Proeyen, *Jordan Frame Supergravity and Inflation in NMSSM*, Phys. Rev. D82 (2010) 045003. arXiv:1004.0712, doi:10.1103/PhysRevD.82.045003.

[92] P. Fileviez Perez, S. Spinner, *Spontaneous R-Parity Breaking and Left-Right Symmetry*, Phys. Lett. B673 (2009) 251–254. arXiv:0811.3424, doi:10.1016/j.physletb.2009.02.047.

[93] P. Fileviez Perez, S. Spinner, *The Minimal Theory for R-Parity Violation at the LHC*, JHEP 04 (2012) 118. arXiv:1201.5923, doi:10.1007/JHEP04(2012)118.

[94] P. Fileviez Perez, S. Spinner, *Supersymmetry at the LHC and The Theory of R-Parity*, Phys. Lett. B728 (2014) 489–495. arXiv:1308.0524, doi:10.1016/j.physletb.2013.12.022.

[95] P. Fileviez Perez, M. B. Wise, *Low Energy Supersymmetry with Baryon and Lepton Number Gauged*, Phys. Rev. D84 (2011) 055015. arXiv:1105.3190, doi:10.1103/PhysRevD.84.055015.

[96] A. Font, L. E. Ibanez, F. Quevedo, *Does Proton Stability Imply the Existence of an Extra* Z_0 *?*, Phys. Lett. B228 (1989) 79–88. doi:10.1016/0370-2693(89)90529-7.

[97] G. Gamberini, G. Ridolfi, F. Zwirner, *On Radiative Gauge Symmetry Breaking in the Minimal Supersymmetric Model*, Nucl. Phys. B331 (1990) 331–349. doi:10.1016/0550-3213(90)90211-U.

[98] D. M. Ghilencea, G. G. Ross, *Precision Prediction of Gauge Couplings and the Profile of a String Theory*, Nucl. Phys. B606 (2001) 101. arXiv:hep-ph/0102306, doi:10.1016/S0550-3213(01)00234-6.

[99] D. K. Ghosh, G. Senjanovic, Y. Zhang, *Naturally Light Sterile Neutrinos from Theory of R-Parity*, Phys. Lett. B698 (2011) 420–424. arXiv:1010.3968, doi:10.1016/j.physletb.2011.03.039.

[100] G. Goon, K. Hinterbichler, M. Trodden, *A New Class of Effective Field Theories from Embedded Branes*, Phys. Rev. Lett. 106 (2011) 231102. arXiv:1103.6029, doi:10.1103/PhysRevLett.106.231102.

[101] G. Goon, K. Hinterbichler, M. Trodden, *Symmetries for Galileons and DBI Scalars on Curved Space*, JCAP 1107 (2011) 017. arXiv:1103.5745, doi:10.1088/1475-7516/2011/07/017.

[102] P. W. Graham, D. E. Kaplan, S. Rajendran, P. Saraswat, *Displaced Supersymmetry*, JHEP 07 (2012) 149. arXiv:1204.6038, doi:10.1007/JHEP07(2012)149.

[103] P. W. Graham, S. Rajendran, P. Saraswat, *Supersymmetric Crevices: Missing Signatures of R-Parity Violation at the LHC*, Phys. Rev. D90 (7) (2014) 075005. arXiv:1403.7197, doi:10.1103/PhysRevD.90.075005.

[104] M. B. Green, J. H. Schwarz, E. Witten, *Superstring Theory Vol. 2: Loop Amplitudes, Anomalies and Phenomenology*, Cambridge, UK: Univ. Pr. (1987) 596 P. (Cambridge Monographs On Mathematical Physics).

[105] P. Griffiths, J. Harris, *Principles of Algebraic Geometry*, Wiley, Wiley Classics Library 2011.

[106] D. J. Gross, J. A. Harvey, E. J. Martinec, R. Rohm, *Heterotic String Theory 1: The Free Heterotic String*, Nucl. Phys. B256 (1985) 253. doi:10.1016/0550-3213(85)90394-3.

[107] A. H. Guth, *Inflationary universe: A possible solution to the horizon and flatness problems*, Physical Review D 23 (2) (1981) 347.

[108] M. J. Hayashi, A. Murayama, *Radiative Breaking of $SU(2)_R \times U(1)_{B-L}$ Gauge Symmetry Induced by Broken $N = 1$ Supergravity in a Left-right Symmetric Model*, Phys. Lett. 153B (1985) 251–256. doi:10.1016/0370-2693(85)90542-8.

[109] K. Hinterbichler, A. Joyce, J. Khoury, G. E. J. Miller, *Dirac-Born-Infeld Genesis: An Improved Violation of the Null Energy Condition*, Phys. Rev. Lett. 110 (24) (2013) 241303. arXiv:1212.3607, doi:10.1103/PhysRevLett.110.241303.

[110] M. Hirsch, M. A. Diaz, W. Porod, J. C. Romao, J. W. F. Valle, *Neutrino Masses and Mixings from Supersymmetry with Bilinear R-Parity Violation: A Theory for solar and atmospheric neutrino oscillations*, Phys. Rev. D62 (2000) 113008, [Erratum: Phys. Rev.D65,119901(2002)]. arXiv:hep-ph/0004115, doi:10.1103/PhysRevD.62.113008,10.1103/PhysRevD.65.119901.

[111] M. Hirsch, W. Porod, *Neutrino Properties and the Decay of the Lightest Supersymmetric Particle*, Phys. Rev. D68 (2003) 115007. arXiv:hep-ph/0307364, doi:10.1103/PhysRevD.68.115007.

[112] P. Horava, E. Witten, *Eleven-Dimensional Supergravity on a Manifold with Boundary*, Nucl. Phys. B475 (1996) 94–114. arXiv:hep-th/9603142, doi:10.1016/0550-3213(96)00308-2.

[113] P. Horava, E. Witten, *Heterotic and Type I String Dynamics from Eleven-Dimensions*, Nucl. Phys. B460 (1996) 506–524, [,397(1995)]. arXiv:hep-th/9510209, doi:10.1016/0550-3213(95)00621-4.

[114] D. Huybrechts, *Complex Geometry: An Introduction*, Springer Berlin Heidelberg, Universitext 2006.

[115] L. E. Ibanez, I. Valenzuela, *The Inflaton as an MSSM Higgs and Open String Modulus Monodromy Inflation*, Phys. Lett. B736 (2014) 226–230. arXiv:1404.5235, doi:10.1016/j.physletb.2014.07.020.

[116] A. Ijjas, P. J. Steinhardt, *Classically Stable Nonsingular Cosmological Bounces*, Phys. Rev. Lett. 117 (12) (2016) 121304. arXiv:1606.08880, doi:10.1103/PhysRevLett.117.121304.

[117] A. Ijjas, P. J. Steinhardt, *Implications of Planck2015 for Inflationary, Ekpyrotic and Anamorphic Bouncing Cosmologies*, Class. Quant. Grav. 33 (4) (2016) 044001. arXiv:1512.09010, doi:10.1088/0264-9381/33/4/044001.

[118] A. Ijjas, P. J. Steinhardt, *Fully Stable Cosmological Solutions with a Non-Singular Classical Bounce*, Phys. Lett. B764 (2017) 289–294. arXiv:1609.01253, doi:10.1016/j.physletb.2016.11.047.

[119] A. Ijjas, P. J. Steinhardt, A. Loeb, *Inflationary Schism*, Phys. Lett. B736 (2014) 142–146. arXiv:1402.6980, doi:10.1016/j.physletb.2014.07.012.

[120] R. Kallosh, A. Linde, D. Roest, *Superconformal Inflationary α-Attractors*, JHEP 11 (2013) 198. arXiv:1311.0472, doi:10.1007/JHEP11(2013)198.

[121] V. Kaplunovsky, J. Louis, *On Gauge couplings in String Theory*, Nucl. Phys. B444 (1995) 191–244. arXiv:hep-th/9502077, doi:10.1016/0550-3213(95)00172-O.

[122] V. S. Kaplunovsky, *One Loop Threshold Effects in String Unification*arXiv:hep-th/9205070.

[123] S. Yu. Khlebnikov, I. I. Tkachev, *Classical Decay of Inflaton*, Phys. Rev. Lett. 77 (1996) 219–222. arXiv:hep-ph/9603378, doi:10.1103/PhysRevLett.77.219.

[124] J. Khoury, J.-L. Lehners, B. A. Ovrut, *Supersymmetric Galileons*, Phys. Rev. D84 (2011) 043521. arXiv:1103.0003, doi:10.1103/PhysRevD.84.043521.

[125] J. Khoury, B. A. Ovrut, N. Seiberg, P. J. Steinhardt, N. Turok, *From Big Crunch to Big Bang*, Phys. Rev. D65 (2002) 086007. arXiv:hep-th/0108187, doi:10.1103/PhysRevD.65.086007.

[126] J. Khoury, B. A. Ovrut, P. J. Steinhardt, N. Turok, *The Ekpyrotic Universe: Colliding Branes and the Origin of the Hot Big Bang*, Phys. Rev. D64 (2001) 123522. arXiv:hep-th/0103239, doi:10.1103/PhysRevD.64.123522.

[127] E. Kiritsis, C. Kounnas, P. M. Petropoulos, J. Rizos, *Universality Properties of $N = 2$ and $N = 1$ Heterotic Threshold Corrections*, Nucl. Phys. B483 (1997) 141–171. `arXiv:hep-th/9608034`, `doi:10.1016/S0550-3213(96)00550-0`.

[128] M. A. Klaput, C. Paleani, *The computation of one-loop heterotic string threshold corrections for general orbifold models with discrete Wilson lines*`arXiv:1001.1480`.

[129] M. Koehn, J.-L. Lehners, B. Ovrut, *Nonsingular Bouncing Cosmology: Consistency of the Effective Description*, Phys. Rev. D93 (10) (2016) 103501. `arXiv:1512.03807`, `doi:10.1103/PhysRevD.93.103501`.

[130] M. Koehn, J.-L. Lehners, B. A. Ovrut, *Higher-Derivative Chiral Superfield Actions Coupled to $N = 1$ Supergravity*, Phys. Rev. D86 (2012) 085019. `arXiv:1207.3798`, `doi:10.1103/PhysRevD.86.085019`.

[131] M. Koehn, J.-L. Lehners, B. A. Ovrut, *Cosmological Super-bounce*, Phys. Rev. D90 (2) (2014) 025005. `arXiv:1310.7577`, `doi:10.1103/PhysRevD.90.025005`.

[132] L. Kofman, A. D. Linde, A. A. Starobinsky, *Reheating after Inflation*, Phys. Rev. Lett. 73 (1994) 3195–3198. `arXiv:hep-th/9405187`, `doi:10.1103/PhysRevLett.73.3195`.

[133] L. Kofman, A. D. Linde, A. A. Starobinsky, *Towards the Theory of Reheating after Inflation*, Phys. Rev. D56 (1997) 3258–3295. `arXiv:hep-ph/9704452`, `doi:10.1103/PhysRevD.56.3258`.

[134] L. M. Krauss, F. Wilczek, *Discrete Gauge Symmetry in Continuum Theories*, Phys. Rev. Lett. 62 (1989) 1221. `doi:10.1103/PhysRevLett.62.1221`.

[135] J. Lauer, D. Lust, S. Theisen, *Four-dimensional Supergravity From Four-dimensional Strings*, Nucl. Phys. B304 (1988) 236–268. `doi:10.1016/0550-3213(88)90626-8`.

[136] A. R. Liddle, D. H. Lyth, Cosmological Inflation and Large-Scale Structure, Cambridge University Press, 2000.

[137] E. Lima, B. A. Ovrut, J. Park, R. Reinbacher, *Nonperturbative Superpotential from Membrane Instantons in Heterotic M-theory*, Nucl. Phys. B614 (2001) 117–170. `arXiv:hep-th/0101049`, `doi:10.1016/S0550-3213(01)00404-7`.

[138] A. D. Linde, *Chaotic Inflation*, Physics Letters B 129 (3-4) (1983) 177–181. `doi:10.1016/0370-2693(83)90837-7`.

[139] A. Lukas, B. A. Ovrut, K. S. Stelle, D. Waldram, *Heterotic M-theory in Five-Dimensions*, Nucl. Phys. B552 (1999) 246–290. `arXiv:hep-th/9806051`, `doi:10.1016/S0550-3213(99)00196-0`.

[140] A. Lukas, B. A. Ovrut, K. S. Stelle, D. Waldram, *The Universe as a Domain Wall*, Phys. Rev. D59 (1999) 086001. arXiv:hep-th/9803235, doi:10.1103/PhysRevD.59.086001.

[141] A. Lukas, B. A. Ovrut, D. Waldram, *On the Four-Dimensional Effective Action of Strongly Coupled Heterotic String Theory*, Nucl. Phys. B532 (1998) 43–82. arXiv:hep-th/9710208, doi:10.1016/S0550-3213(98)00463-5.

[142] A. Lukas, B. A. Ovrut, D. Waldram, *Cosmological Solutions of Horava-Witten theory*, Phys. Rev. D60 (1999) 086001. arXiv:hep-th/9806022, doi:10.1103/PhysRevD.60.086001.

[143] A. Lukas, B. A. Ovrut, D. Waldram, *Nonstandard Embedding and Five-Branes in Heterotic M-theory*, Phys. Rev. D59 (1999) 106005. arXiv:hep-th/9808101, doi:10.1103/PhysRevD.59.106005.

[144] A. Lukas, B. A. Ovrut, D. Waldram, *Heterotic M-theory Vacua with Five-Branes*, Fortsch. Phys. 48 (2000) 167–170. arXiv:hep-th/9903144, doi:10.1002/(SICI)1521-3978(20001)48:1/3<167::AID-PROP167>3.0.CO;2-O.

[145] Z. Marshall, B. A. Ovrut, A. Purves, S. Spinner, *LSP Squark Decays at the LHC and the Neutrino Mass Hierarchy*, Phys. Rev. D90 (1) (2014) 015034. arXiv:1402.5434, doi:10.1103/PhysRevD.90.015034.

[146] Z. Marshall, B. A. Ovrut, A. Purves, S. Spinner, *Spontaneous R-Parity Breaking, Stop LSP Decays and the Neutrino Mass Hierarchy*, Phys. Lett. B732 (2014) 325–329. arXiv:1401.7989, doi:10.1016/j.physletb.2014.03.052.

[147] S. P. Martin, *Some Simple Criteria for Gauged R-Parity*, Phys. Rev. D46 (1992) R2769–R2772. arXiv:hep-ph/9207218, doi:10.1103/PhysRevD.46.R2769.

[148] S. P. Martin, *A Supersymmetry Primer* (1997) 1–98[Adv. Ser. Direct. High Energy Phys.18,1(1998)]. arXiv:hep-ph/9709356, doi:10.1142/9789812839657_0001,10.1142/9789814307505_0001.

[149] A. Masiero, J. W. F. Valle, *A Model for Spontaneous R-Parity Breaking*, Phys. Lett. B251 (1990) 273–278. doi:10.1016/0370-2693(90)90935-Y.

[150] P. Mayr, H. P. Nilles, S. Stieberger, *String Unification and Threshold Corrections*, Phys. Lett. B317 (1993) 53–59. arXiv:hep-th/9307171, doi:10.1016/0370-2693(93)91569-9.

[151] A. Mazumdar, B. Zaldivar, *Quantifying the Reheating Temperature of the Universe*, Nucl. Phys. B886 (2014) 312–327. arXiv:1310.5143, doi:10.1016/j.nuclphysb.2014.07.001.

[152] R. N. Mohapatra, *Mechanism for Understanding Small Neutrino Mass in Superstring Theories*, Phys. Rev. Lett. 56 (1986) 561–563. doi:10.1103/PhysRevLett.56.561.

[153] V. Mukhanov, *Inflation without Selfreproduction*, Fortsch. Phys. 63 (2015) 36–41. arXiv:1409.2335, doi:10.1002/prop.201400074.

[154] B. Mukhopadhyaya, S. Roy, F. Vissani, *Correlation between Neutrino Oscillations and Collider Signals of Supersymmetry in an R-Parity Violating Model*, Phys. Lett. B443 (1998) 191–195. arXiv:hep-ph/9808265, doi:10.1016/S0370-2693(98)01288-X.

[155] A. Nicolis, R. Rattazzi, E. Trincherini, *The Galileon as a Local Modification of Gravity*, Phys. Rev. D79 (2009) 064036. arXiv:0811.2197, doi:10.1103/PhysRevD.79.064036.

[156] H. P. Nilles, *On the Low-energy Limit of String and M-theory* (1998) 709–768arXiv:hep-ph/0004064.

[157] H. P. Nilles, S. Stieberger, *String Unification, Universal One Loop Corrections and Strongly Coupled Heterotic String Theory*, Nucl. Phys. B499 (1997) 3–28. arXiv:hep-th/9702110, doi:10.1016/S0550-3213(97)00315-5.

[158] B. A. Ovrut, *Superstrings and the Auxiliary Field Structure of Supergravity*, Phys. Lett. B205 (1988) 455–458. doi:10.1016/0370-2693(88)90977-X.

[159] B. A. Ovrut, A. Purves, S. Spinner, *Wilson Lines and a Canonical Basis of SU(4) Heterotic Standard Models*, JHEP 11 (2012) 026. arXiv:1203.1325, doi:10.1007/JHEP11(2012)026.

[160] B. A. Ovrut, A. Purves, S. Spinner, *A Statistical Analysis of the Minimal SUSY $B-L$ Theory*, Mod. Phys. Lett. A30 (18) (2015) 1550085. arXiv:1412.6103, doi:10.1142/S0217732315500856.

[161] B. A. Ovrut, A. Purves, S. Spinner, *The Minimal SUSY $B-L$ Model: from the Unification Scale to the LHC*, JHEP 06 (2015) 182. arXiv:1503.01473, doi:10.1007/JHEP06(2015)182.

[162] B. A. Ovrut, H. J. Schnitzer, *A New Approach To Effective Field Theories*, Phys. Rev. D21 (1980) 3369. doi:10.1103/PhysRevD.21.3369.

[163] B. A. Ovrut, J. Stokes, *Heterotic Kink Solitons and their Worldvolume Action*, JHEP 09 (2012) 065. `arXiv:1205.4236`, `doi:10.1007/JHEP09(2012)065`.

[164] C. Patrignani, et al., *Review of Particle Physics*, Chin. Phys. C40 (10) (2016) 100001. `doi:10.1088/1674-1137/40/10/100001`.

[165] W. Porod, M. Hirsch, J. Romao, J. W. F. Valle, *Testing Neutrino Mixing at Future Collider Experiments*, Phys. Rev. D63 (2001) 115004. `arXiv:hep-ph/0011248`, `doi:10.1103/PhysRevD.63.115004`.

[166] A. A. Starobinsky, *Dynamics of Phase Transition in the New Inflationary Universe Scenario and Generation of Perturbations*, Phys. Lett. 117B (1982) 175–178. `doi:10.1016/0370-2693(82)90541-X`.

[167] E. D. Stewart, *Inflation, Supergravity and Superstrings*, Phys. Rev. D51 (1995) 6847–6853. `arXiv:hep-ph/9405389`, `doi:10.1103/PhysRevD.51.6847`.

[168] J. H. Traschen, R. H. Brandenberger, *Particle Production During Out-of-equilibrium Phase Transitions*, Phys. Rev. D42 (1990) 2491–2504. `doi:10.1103/PhysRevD.42.2491`.

[169] M. Trodden, *Baryogenesis and Leptogenesis*, eConf C040802 (2004) L018. `arXiv:hep-ph/0411301`.

[170] K. Uhlenbeck, S. T. Yau, *On the Existence of Hermitan Yang-Mills Connections in Stable Vector Bundles*, Communications on Pure and Applied Mathematics 39 (S1) (1986) S257–S293. `doi:10.1002/cpa.3160390714`.

[171] J. Wess, J. Bagger, *Supersymmetry and Supergravity*, Princeton, USA: Univ. Pr. (1992) 259 p.

[172] E. Witten, *Dimensional Reduction of Superstring Models*, Phys. Lett. 155B (1985) 151. `doi:10.1016/0370-2693(85)90976-1`.

[173] E. Witten, *Strong Coupling Expansion of Calabi-Yau Compactification*, Nucl. Phys. B471 (1996) 135–158. `arXiv:hep-th/9602070`, `doi:10.1016/0550-3213(96)00190-3`.